POLITECNICO DI TORINO

I Faculty of Engineering
Master of Science in Biomedical Engineering

Master Thesis

Hybrid biomimetic nanoconstructs against cancer: preparation and properties

Advisor:
Prof. Valentina Alice Cauda

Author:
Francesca Susa

Luglio 2018

A Laura e Mariuccia

Ringraziamenti

Giunta alla fine della mia tesi di laurea, vorrei dedicare questa pagina a tutti coloro che sono stati indispensabili per la realizzazione di questo lavoro.

La prima persona che vorrei ringraziare è la mia relatrice, Valentina. Grazie per avermi dato la possibilità di lavorare su questo tema, motivo per quale, anni fa, avevo deciso di iscrivermi ad ingegneria biomedica. Grazie per tutto il tempo dedicatomi, per avermi guidata, consigliata e soprattutto per avermi fatta appassionare ancora di più alla ricerca.

Grazie anche a Miguel Manzano che mi ha accolta nell'università di Madrid e per avermi dato la possibilità di lavorare all'estero confrontandomi con una realtà diversa.

Grazie a tutto il personale del TNH Lab, siete un gruppo splendido, è stato un piacere lavorare al vostro fianco. In particolare vorrei ringraziare tutti i dottorandi, Bianca, Marta, Luisa, Andrea e Federica che, nonostante fossi solo una tesista, mi hanno accolta con amicizia nel loro gruppo e sono stati sempre disposti ad aiutarmi e consigliarmi su qualunque cosa avessi bisogno.

Grazie anche a tutti gli altri dottorandi dell'ufficio che mi hanno ospitata e che sono sempre stati pronti a fare due chiacchiere nelle pause pranzo.

Grazie a tutti i dottorandi e personale del dipartimento di chimica inorganica di Madrid, ma un ringraziamento particolare va a Patricia, Irene e Daniel con cui ho potuto lavorare più a stretto contatto.

Il grazie sicuramente più grande va a mia mamma. Grazie per essere sempre stata per me un esempio da seguire, per avermi sempre dato fiducia, consigliata e sostenuta nelle mie scelte.

Grazie a Beba, mia sorella, che nonostante i nostri caratteri opposti c'è stata sempre e sempre ci sarà.

Grazie a mia nonna che mi ha trasmesso la dedizione e la serietà nell'affrontare tutti i compiti della vita.

Grazie a Stefano, perché mi hai sempre sostenuta nelle mie scelte e perché mi hai sempre spronata a vincere le mie indecisioni.

Grazie a tutta la mia famiglia, i miei nonni, zii e cugini e anche a quella che considero la mia "famiglia acquisita", Aristide, Teresa, Alberto e Vittorio.

Grazie a tutti i miei amici perché siete stati preziosi in questi anni per il vostro supporto e il vostro affetto. Un particolare ringraziamento va a Tiziana ed Elisa perché non siete state solo colleghe, ma soprattutto amiche. Ultima ma non per importanza, grazie Martina perché su di te posso sempre contare.

Grazie a tutti, questa tesi è stata realizzata anche grazie a voi.

Riassunto

Con il termine cancro si indicano una serie di patologie genetiche in cui le cellule hanno le caratteristiche di divisione e proliferazione incontrollata e resistenza all'apoptosi, andando quindi a creare masse cellulari abnormi, con l'eccezione dei tumori ematologici che non producono masse ma sono distribuiti nel sangue.

Ogni anno si presentano circa 10 milioni di nuovi casi di neoplasie, trend in crescita nell'ultimo decennio che si suppone nel 2030 porterà ad avere più di 13 milioni di nuovi casi annui. Attualmente i trattamenti maggiormente applicati sono la chirurgia, la radioterapia, la chemioterapia e l'immunoterapia o una combinazione di questi.

La chirurgia consiste nella rimozione fisica della massa tumorale; questa deve necessariamente essere seguita da un'altra delle due terapie per eliminare le, seppur poche, cellule tumorali rimaste. In aggiunta a ciò, non è sempre applicabile se il tumore è eccessivamente esteso o vascolarizzato o il sito difficilmente raggiungibile.

La radioterapia prevede l'irraggiamento del tumore con radiazioni ionizzanti che vanno a danneggiare il DNA e creare uno stress ossidativo tale da indurre la morte cellulare. Prima di raggiungere la morte delle cellule tumorali, però, il paziente deve essere sottoposto a numerose sedute, con conseguente danno anche per le cellule sane adiacenti al tumore.

La chemioterapia è sicuramente la più utilizzata soprattutto nel caso di tumori metastatici. Durante questo trattamento si somministrano sistematicamente uno o più farmaci chemioterapici, che vanno a danneggiare le cellule con un alto indice di divisione e proliferazione, quali sono appunto le cellule tumorali. Tuttavia i chemioterapici non sono selettivamente specifici verso le cellule tumorali, ma vanno anche a danneggiare le cellule sane che hanno un ciclo cellulare molto veloce come quelle del tratto gastrointestinale, del midollo osseo e dei bulbi piliferi, andando a causare gli effetti collaterali più diffusi e conosciuti come nausea, vomito, ulcere, perdita di capelli e sensibilità a malattie e infezioni. Essendo inoltre i farmaci somministrati sistematicamente, solo una piccola parte di questi riesce a penetrare il tumore e ad espletare il suo effetto terapeutico.

L'immunoterapia è ad oggi una delle soluzioni più promettenti, in particolare per i tumori ematologici. Consiste nello stimolare le difese naturali del corpo a combattere il cancro fermandone o rallentandone la crescita e la diffusione ad altri tessuti oppure aiutando il sistema immunitario a distruggere le cellule cancerose. Ci sono vari tipi di immunoterapia: quella basata sugli anticorpi monoclonali, che legano delle molecole di segnalazione sulle cellule tumorali in modo da renderle più riconoscibili al sistema immunitario, non specifica, che stimola le cellule immunitarie in modo aspecifico somministrando interferone e interleuchine, virus-oncolitica, che prevede la somministrazione di virus geneticamente modificati per distruggere le cellule cancerose, T-cellulare, in cui le cellule T del paziente vengono estratte, modificate in laboratorio per far loro riconoscere meglio le cellule tumorali e poi re-iniettate ed infine i vaccini, che istruiscono il sistema immunitario esponendoli ad un antigene. Anche questo tipo di terapia, però, non è priva di effetti collaterali e di rischi e talvolta è perfino priva di efficacia.

Negli ultimi anni si sono cercate nuove strategie per evitare gli effetti collaterali tipici di questi trattamenti e soprattutto per migliorarne l'efficienza. In aiuto alla terapia antitumorale si è sviluppata una branca della nanomedicina, che si sta rivelando essere molto promettente.

I nanomateriali sono quelle particelle che, grazie alle loro dimensioni nanometriche, possono interagire con le cellule alla stessa scala di molti processi biologici; inoltre la loro energia e ampia area superficiale le rendono molto reattive. Il diametro ridotto consente loro di sfruttare l'effetto EPR, ovvero la possibilità di accumularsi all'interno del tumore, grazie alla particolare vascolarizzazione tumorale che presenta un endotelio maggiormente fenestrato rispetto ad un endotelio sano e alla mancanza di drenaggio linfatico.

Tra questi nanomateriali per terapia tumorale una posizione di rilievo viene ricoperta dai nanocarriers e dalle nanoparticelle con proprietà antitumorali intrinseche.

I nanocarriers sono nanoparticelle che hanno la possibilità di incorporare all'interno della loro struttura un farmaco antitumorale, proteggendolo e trasportandolo alle cellule target mediandone poi il rilascio. Un particolare tipo di nanocarrier sono le particelle di silice mesoporosa, dotate di numerosi pori ordinati con un diametro di 3-4 nm. Questa caratteristica conferisce loro un'ampia area superficiale e volume occupato dai pori che consente il caricamento all'interno di una grande quantità di farmaco con il metodo dell'impregnazione. Successivamente questi pori possono essere chiusi con varie metodiche in modo che la particella possa raggiungere il suo target prevenendo il rilascio anticipato in zone inadatte.

Tra le nanoparticelle con proprietà antitumorali intrinseche vi è l'ossido di zinco, che negli ultimi anni ha attirato le attenzioni dei ricercatori. Lo zinco è una elemento già presente normalmente all'interno del corpo umano in tracce e la degradazione di tali particelle provoca la formazione di ioni zinco nella zona, che poi vengono rapidamente metabolizzati dalla cellula. Le particelle di ossido di zinco hanno una tossicità preferenziale per le cellule tumorali, tossicità il cui meccanismo non è ancora completamente compreso. Alcuni studi ipotizzano che specifiche condizioni o stimoli esterni come gli ultrasuoni possano provocare un rilascio di specie radicaliche (ROS, Reactive Oxygen Species) da parte dello ZnO, che crea un forte stress ossidativo nelle cellule con conseguente loro apoptosi. Altri studi hanno ipotizzato invece che il meccanismo di tossicità si basi sul rilascio di ioni zinco durante la degradazione, i quali, andando a saturare il metabolismo dello zinco, creano stress ossidativo nella cellula e quindi la sua morte.

Entrambe queste particelle non sono stabili in ambiente fisiologico e possono aggregare, creando problemi al flusso sanguigno. Nell'ambito di questa tesi si utilizza un doppio strato fosfolipidico per ricoprire le particelle, stabilizzarle, aumentarne la biocompatibilità e renderle invisibili al sistema immunitario, in modo che possano raggiungere il sito del tumore; inoltre, una volta raggiunta la cellula tumorale, il rivestimento in doppio strato fosfolipidico ne facilita l'internalizzazione e ne media il rilascio di farmaco nel caso del nanocarrier.

Lo strato fosfolipidico può essere di varia natura, ma in questa tesi si è utilizzato quello derivato dalla membrana di particolari vescicole extracellulari, chiamate esosomi.

Le vescicole extracellulari (EVs, dall'ingelse Extracellular Vesicles) sono prodotte dalla protrusione verso l'esterno della membrana cellulare o dall'espulsione dalla cellula di vescicole formatesi al suo interno. Le EVs sono costituite quindi da diverse popolazioni, tra cui ectosomi, oncosomi o corpi apoptotici: gli ultimi si formano solo nel caso la cellula stia andando in apoptosi. Gli esosomi invece si distinguono dalle altre vescicole extracellulari per la loro origine: questi infatti non originano dalla protrusione della membrana, ma da corpi multivescicolari che contengono al loro interno vescicole

intraluminali, le quali vengono rilasciate nello spazio extracellulare tramite la fusione con la membrana plasmatica. Gli esosomi hanno un diametro compreso tra 40 e 120 nm e contengono al loro interno molecole di derivazione citoplasmatica e materiale genetico della cellula stessa.

Gli esosomi si trovano in tutti i fluidi biologici e hanno la vitale funzione della comunicazione intercellulare, trasportando proteine e RNA da una cellula emittente verso una cellula ricevente specifica. Sono inoltre coinvolti nella risposta immunitaria e soprattutto nella diffusione di cancro e altre malattie che coinvolgono una mutazione genetica o proteica come le malattie neurodegenerative.

Gli esosomi sono stati selezionati per svolgere la funzione di rivestimento delle nanoparticelle sopramenzionate per molti motivi: il primo è la stabilità che conferiscono alle particelle, permettendo loro di circolare per lungo tempo nel sangue in condizioni fisiologiche e patologiche e consentendone grazie alla loro ridotta dimensione il passaggio attraverso le maggiori barriere corporee, tra le quali anche la barriera ematoencefalica; essendo infine coinvolti nella comunicazione intercellulare, gli esosomi sono già capaci di muoversi verso uno specifico target il quale, nel caso di esosomi estratti da cellule tumorali, risulta essere specifico per altre cellule tumorali.

Nell'ambito di questa tesi gli esosomi vengono estratti da diverse linee di cellule tumorali oppure da siero fetale bovino (FBS) tramite il metodo della centrifugazione frazionata o con un kit di estrazione. Gli esosomi prima dell'accoppiamento vengono tutti caratterizzati tramite la tecnica NTA (Nanoparticle Tracking Analysis), che ne determina concentrazione e taglia, e tramite microscopia elettronica a trasmissione (TEM) che permette di valutarne la morfologia.

Per quanto riguarda l'ossido di zinco, le nanoparticelle vengono invece sintetizzate per via solvotermale, che consente di ottenere cristalli con morfologia sferica di dimensioni tra i 15 e i 20 nm. Vengono poi funzionalizzate con gruppi amino per permettere il legame di molecole di colorante fluorescente (atto550 o atto633) al fine di consentirne l'analisi con il microscopio in fluorescenza.

La prima caratterizzazione che viene applicata all'ossido di zinco è l'analisi della stabilità colloidale tramite Dynamic Light Scattering (DLS), utilizzando diversi mezzi come soluzione disperdente (Figura 1).

In etanolo le particelle sono ben disperse, mentre in PBS e soluzione fisiologica queste iniziano ad aggregare a causa della forza ionica della soluzione. Si effettuano anche delle analisi morfologiche

tramite TEM e microscopia elettronica a scansione a emissione di campo (FESEM) e delle misurazioni della concentrazione tramite NTA.

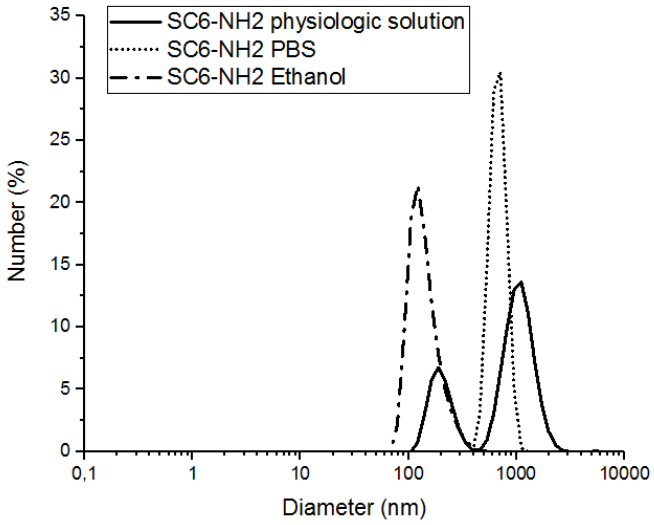

Figura 1: DLS di particelle di ZnO in diversi mezzi

Le nanoparticelle di ZnO sono poi accoppiate con gli esosomi per creare dei nanocostrutti chiamati TNH (TrojaNanoHorse). L'obiettivo della tesi è appunto creare un protocollo ottimale tale da ottimizzare la percentuale di accoppiamento dello ZnO, al fine di avere la maggior parte di questo incapsulato all'interno di esosomi in modo che l'internalizzazione nelle cellule sia potenziata e le particelle di ZnO stabilizzate.

Sono stati fatti numerosi accoppiamenti in cui si è variato un parametro per volta, per poi confrontarlo con i precedenti e selezionare quello migliore. I parametri su cui si è andati ad agire sono stati:

- la temperatura: che è stata fatta variare tra temperatura ambiente, 37°C e 4°C;
- il metodo di agitazione: si sono testati sia un dispositivo, chiamato ruota, che induce un moto rotatorio al recipiente contente esosomi e ZnO (eppendorf), che contiene la soluzione per l'accoppiamento, sia uno shaker orbitale;
- Le quantità di ZnO da aggiungere: un'aliquota è pari ad un numero di particelle uguale a quello dell'aliquota di esosomi. Quindi si è testata una sola aliquota, oppure 3, 5 o 10 volte l'aliquota aggiunte all'inizio dell'accoppiamento tutte insieme, o aggiunte a distanza di tempo l'una dall'altra e la determinazione del numero di run di accoppiamento a cui sottoporre il campione;
- Il volume in cui attuare l'accoppiamento, se più o meno diluito;
- Il tempo di accoppiamento fatto variare tra 90 minuti, 8 e 24 ore;
- L'applicazione di ultrasuoni pre o post accoppiamento;
- Il mezzo di accoppiamento.

Gli accoppiamenti sono stati eseguiti anche con esosomi estratti da diverse linee cellulari, in particolare da cellule tumorali in adesione (KB, carcinoma dell'epidermide della bocca) e cellule tumorali in sospensione (DAUDI, linfoma di burkitt).

Di ogni accoppiamento sono state valutate le percentuali di accoppiamento di zinco e esosomi attraverso il processamento di immagini acquisite con il microscopio in fluorescenza su due canali, come quelle riportate in Figura 2.

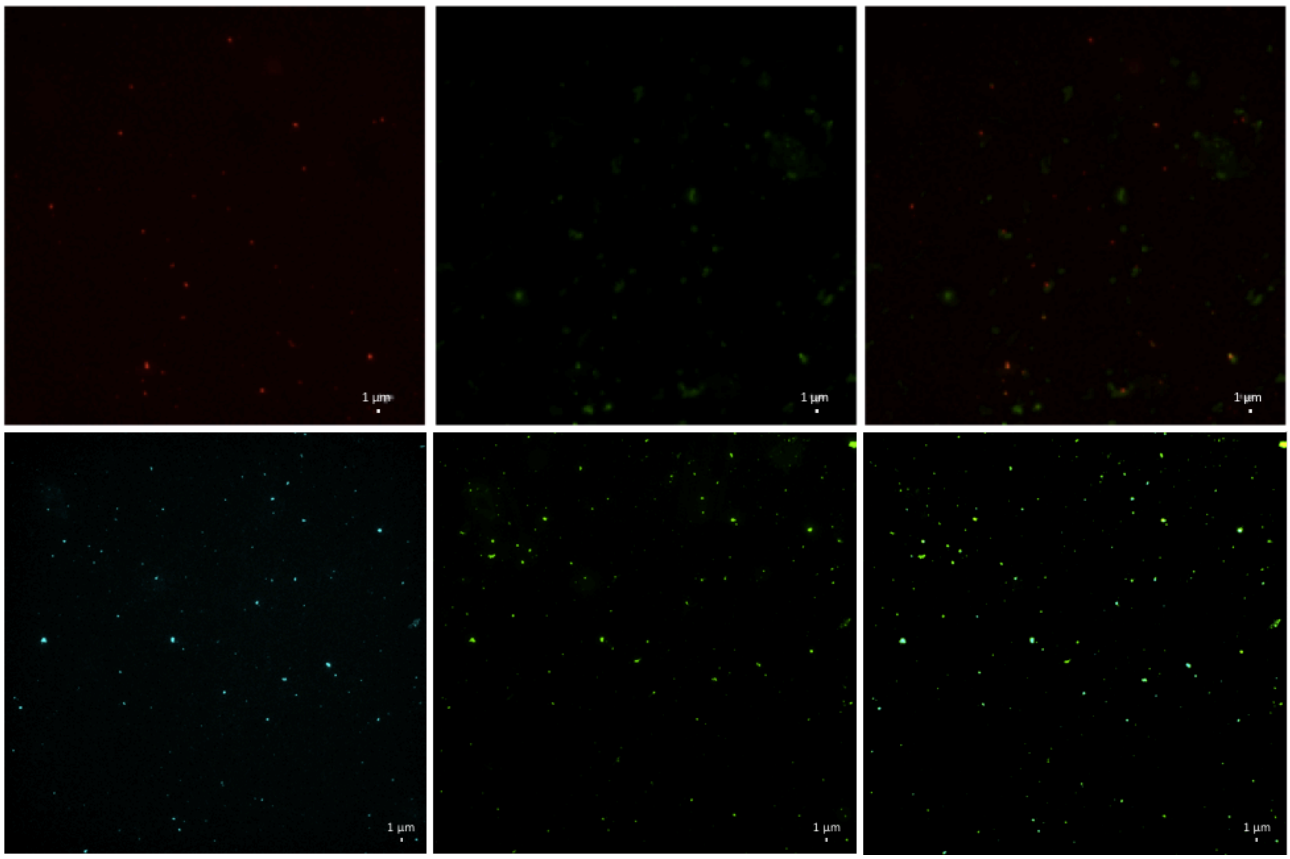

Figura 2: Immagini del TNH al microscopio a fluorescenza, ZnO (sinistra, canale rosso o NIR), esosomi (centro, canale verde), TNH (destra, sovrapposizione). Barra 1 µm.

Alcuni TNH sono stati anche misurati attraverso la tecnica della NTA e confrontati con le particelle e gli esosomi. In Figura 3 sono mostrate la distribuzione di taglia e la concentrazione di ZnO, esosomi e TNH: le dimensioni coincidono con le aspettative, infatti i TNH hanno una dimensione superiore a quella delle particelle non rivestite, il che sta a significare che c'è un rivestimento che crea maggiore spessore. La concentrazione dei TNH è superiore a quella degli esosomi probabilmente perché ci sono o delle nanoparticelle di ZnO libere (senza rivestimento) ma aggregate dovuti al mezzo di sospensione dei TNH (acqua e PBS, mentre nella misura delle nanoparticelle da sole queste si trovano in etanolo).

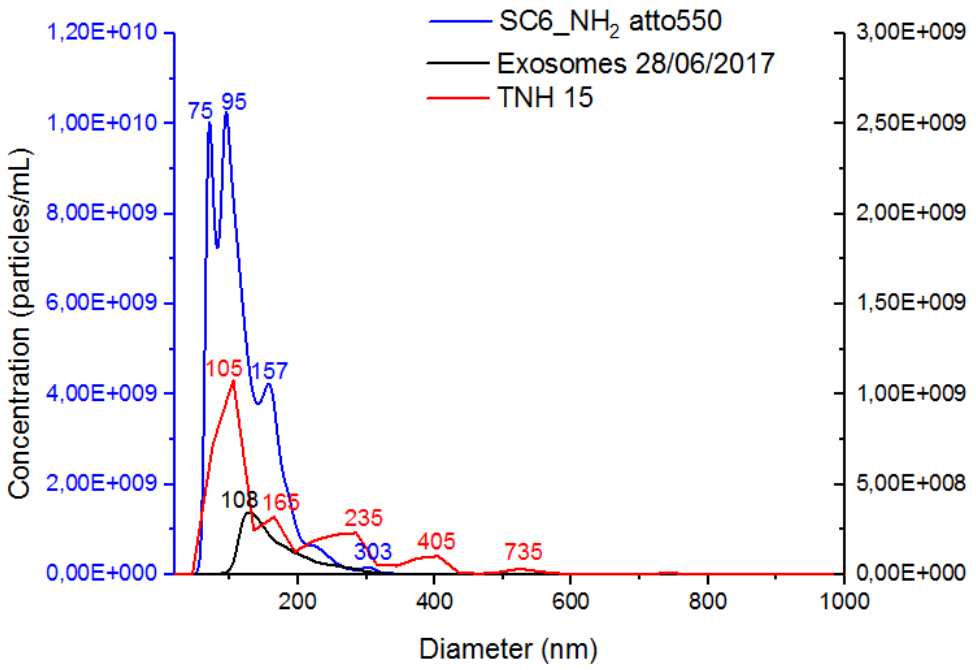

Figura 3: Distribuzione di taglia e concentrazione di un TNH ottenute con il NanoSight

Inoltre di alcuni TNH sono state acquisite delle immagini TEM, soprattutto per valutarne la morfologia e l'integrità dello strato lipidico di copertura, per poi confrontarle con quelle degli esosomi tali e quali. In particolare in Figura 4 sono riportate le immagini di alcuni esosomi (sinistra) e di un TNH (destra). È possibile notare che le dimensioni sono confrontabili, così come la morfologia, ma i TNH presentano all'interno della loro struttura dei puntini più scuri che rappresentano le particelle di ZnO internalizzate.

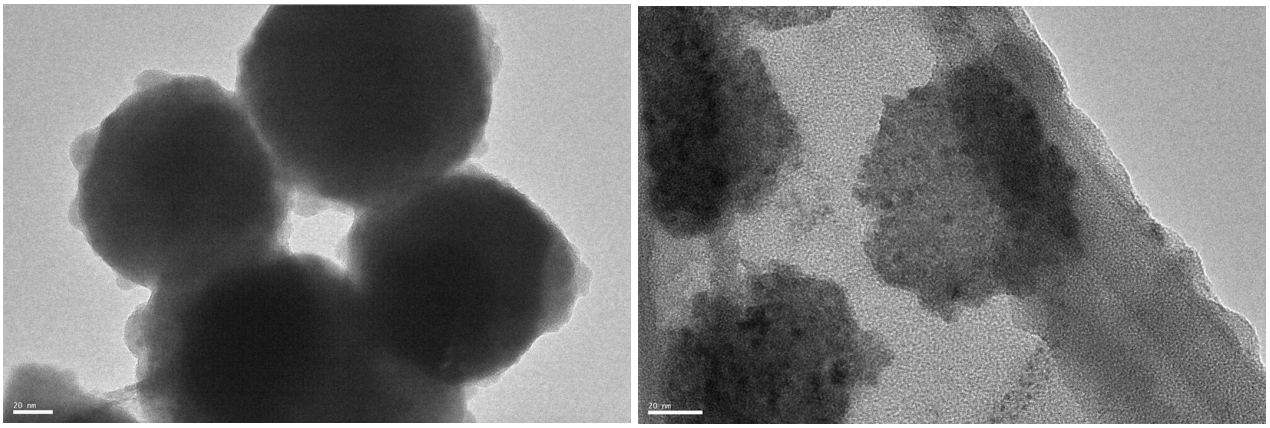

Figura 4: Immagini TEM di esosomi tal quali (sinistra) e TNH (detsra)

Attraverso il TEM si è valutato l'effetto della sonicazione pre e post-accoppiamento. Si può vedere in Figura 5 che i TNH ottenuti sonicando dopo l'accoppiamento (immagine a sinistra) hanno una forma determinata e con dimensioni simili a quelle degli esosomi tali e quali; invece i TNH sonicati prima dell'accoppiamento (immagine a destra) hanno una morfologia ambigua, sono molto grandi, anche oltre

il micron, e sembrano costituiti da esosomi rotti e poi riassemblati insieme, processi non ideali al fine di avere un TNH utilizzabile per l'internalizzazione in cellula.

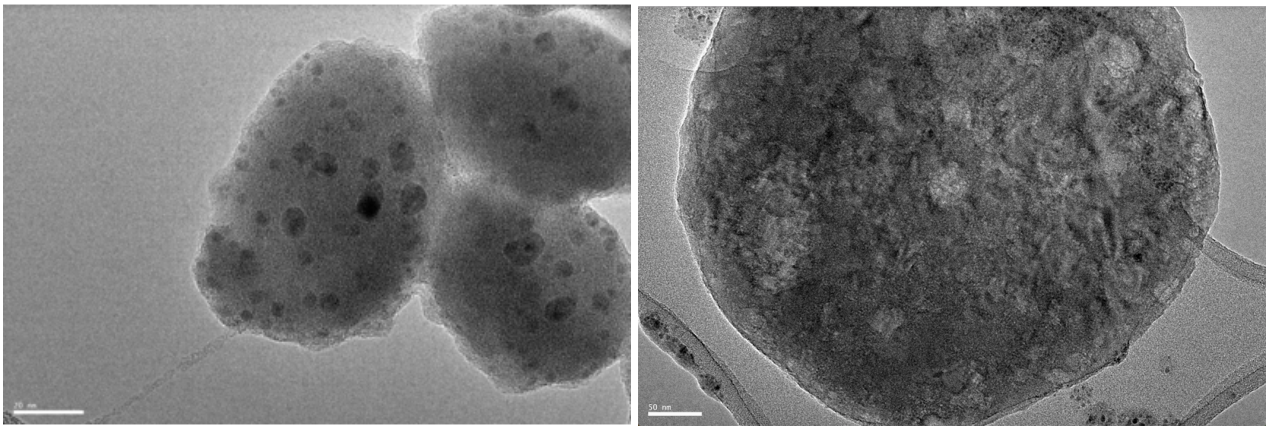

Figura 5: TEM di un TNH sonicato post accoppiamento (sinistra) e pre accoppiamento (destra)

Un discorso a parte deve essere fatto per la selezione del mezzo di sospensione ottimale tra acqua e PBS (1:1) e acqua e soluzione fisiologica (1:1). Infatti questo influisce soprattutto sulla stabilità delle nanoparticelle e degli esosomi, il che si riflette poi sulle percentuali di accoppiamento. In particolare le nanoparticelle di ZnO in PBS hanno una carica superficiale negativa, mentre in soluzione fisiologica questa è positiva. Una carica positiva delle nanoparticelle è preferibile in quanto le membrane cellulari, e quindi anche gli esosomi, possiedono già una carica negativa dovuta alla presenza di proteine di membrana, come anche rilevato tramite misure di potenziale Z. Le due cariche opposte tendono quindi ad attrarsi e ad aumentare l'internalizzazione o per lo meno l'adesionedello ZnO negli esosomi. Secondariamente sono stati analizzati i surnatanti provenienti dal secondo run di due diversi accoppiamenti, uno in PBS e uno in fisiologica, ma sottoposti alle stesse condizioni. Si è valutato lo stato degli esosomi e, come si può vedere in Figura 6, l'accoppiamento in PBS lascia numerosi esosomi e la maggior parte di loro hanno una morfologia danneggiata (immagine a sinistra); in soluzione fisiologica invece gli esosomi rimasti vuoti sono molti meno e sembrano anche avere una struttura morfologica migliore (immagine a destra).

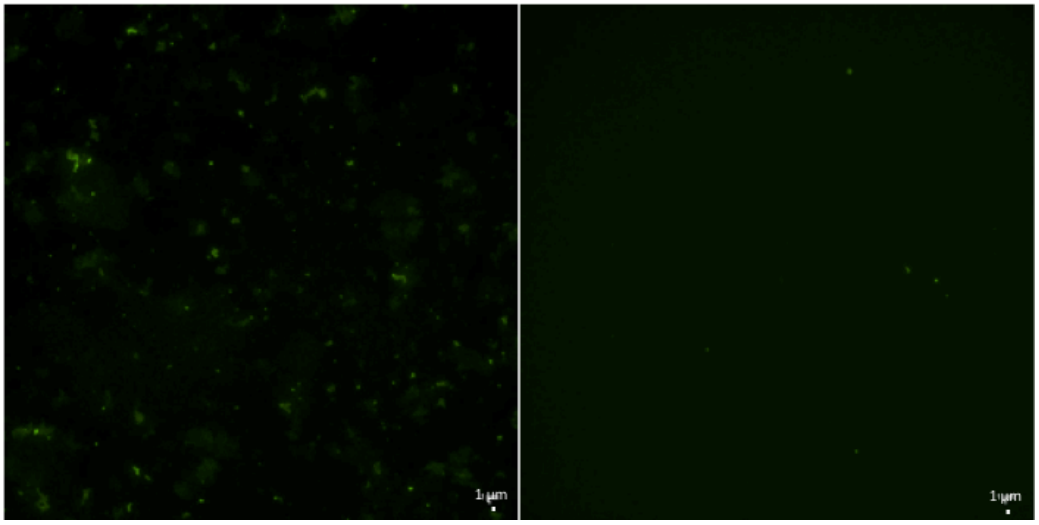

Figura 6: Surnatanti dopo due run di accoppiamento, a sinistra in PBS e a destra in soluzione fisiologica

Alla luce delle considerazioni appena fatte, in Figura 7 sono riassunte le condizioni ottimali di accoppiamento tra nanoparticelle di ZnO e esosomi per ottenere i TNH.

Optimal coupling parameters	
Mixing method	Orbital shaker, 200-250 rpm
Temperature	37 °C
Time	90 minutes each run
Volume	100 µl

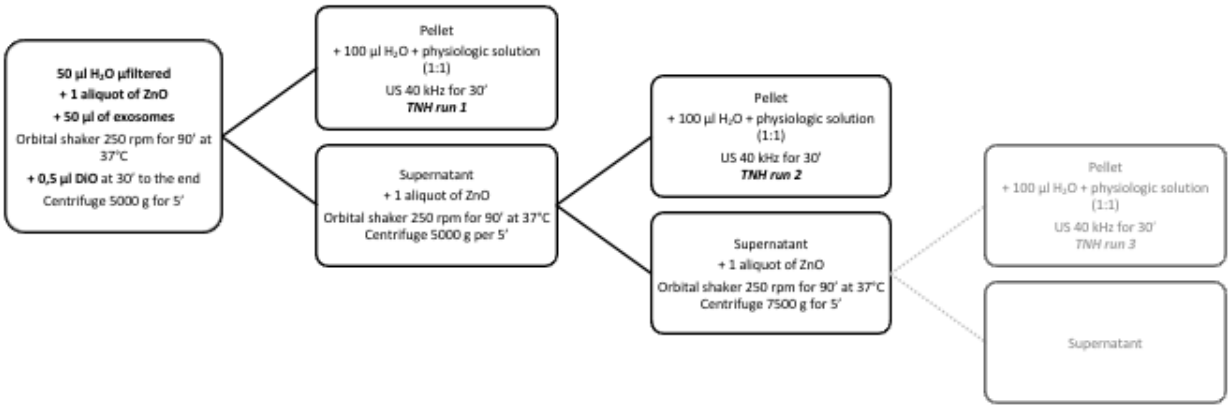

Figura 7: Condizioni ottimali di accoppiamento per i TNH

Una parte della tesi si è occupata di trovare un ulteriore metodo indiretto per la validazione dell'effettiva internalizzazione dell'ossido di zinco negli esosomi. Questo metodo va ad adsorbire tramite interazioni deboli un fluoroforo sulle particelle, ricoperte o meno da un doppio strato lipidico, e si valuta il rilascio del colorante in una cuvetta con una soluzione acquosa separata dalla soluzione di nanoparticelle da una membrana di dialisi, che permette il passaggio del colorante, ma non delle

particelle. La soluzione viene analizzata tramite uno spettrofluorimetro: ci si aspetta di vedere un rilascio maggiore di colorante laddove le particelle non sono rivestite da una membrana.

Il fluoroforo utilizzato è la calceina, che si adsorbe tramite interazioni deboli alle nanoparticelle di ZnO. In soluzione acquosa la calceina viene rilasciata e passa attraverso la membrana di dialisi: tramite lo spettrofluorimetro si ottiene una curva di rilascio, che è il risultato massimo ottenibile. In seguito si fanno gli stessi test su particelle rivestite con DOPC (un lipide commerciale) e esosomi. Si ottengono curve di rilascio con cinetiche molto inferiori a quelle delle particelle non rivestite, ma un certo rilascio graduale è comunque presente, probabilmente dovuto al fatto che sono rimaste delle particelle con calceina libere in soluzione poichè non tutte le particelle riescono ad essere rivestite. Successivamente le membrane lipidiche vengono disassemblate tramite l'aggiunta di etanolo e poi la membrana sciacquata nella cuvetta per rilasciare tutta la calceina. Le particelle rivestite da DOPC presentano un'impennata nella curva di rilascio, facendo intendere che la maggior parte della calceina era rimasta su nanoparticelle di ZnO sigillate all'interno delle membrane lipidiche. Per quelle rivestite da esosomi invece i risultati sono molto peggiori: a seguito dell'aggiunta di etanolo infatti non ci sono variazioni nella curva di rilascio. Ciò è probabilmente dovuto al fatto che l'etanolo fissa i materiali biologici e, differentemente dai DOPC, gli esosomi sono di origine biologica e hanno nella membrana diverse proteine: ciò è causa della fissazione degli esosomi sulla membrana di dialisi, intrappolando al loro interno la calceina che non può essere rilasciata. Sarà quinid necessario approfondire questi studi utilizzando altri agenti in grado di disassemblare le membrane lipidiche, come tensioattivi, es. Triton. In Figura 8 sono rappresentate le curve di rilascio delle tre condizioni appena descritte.

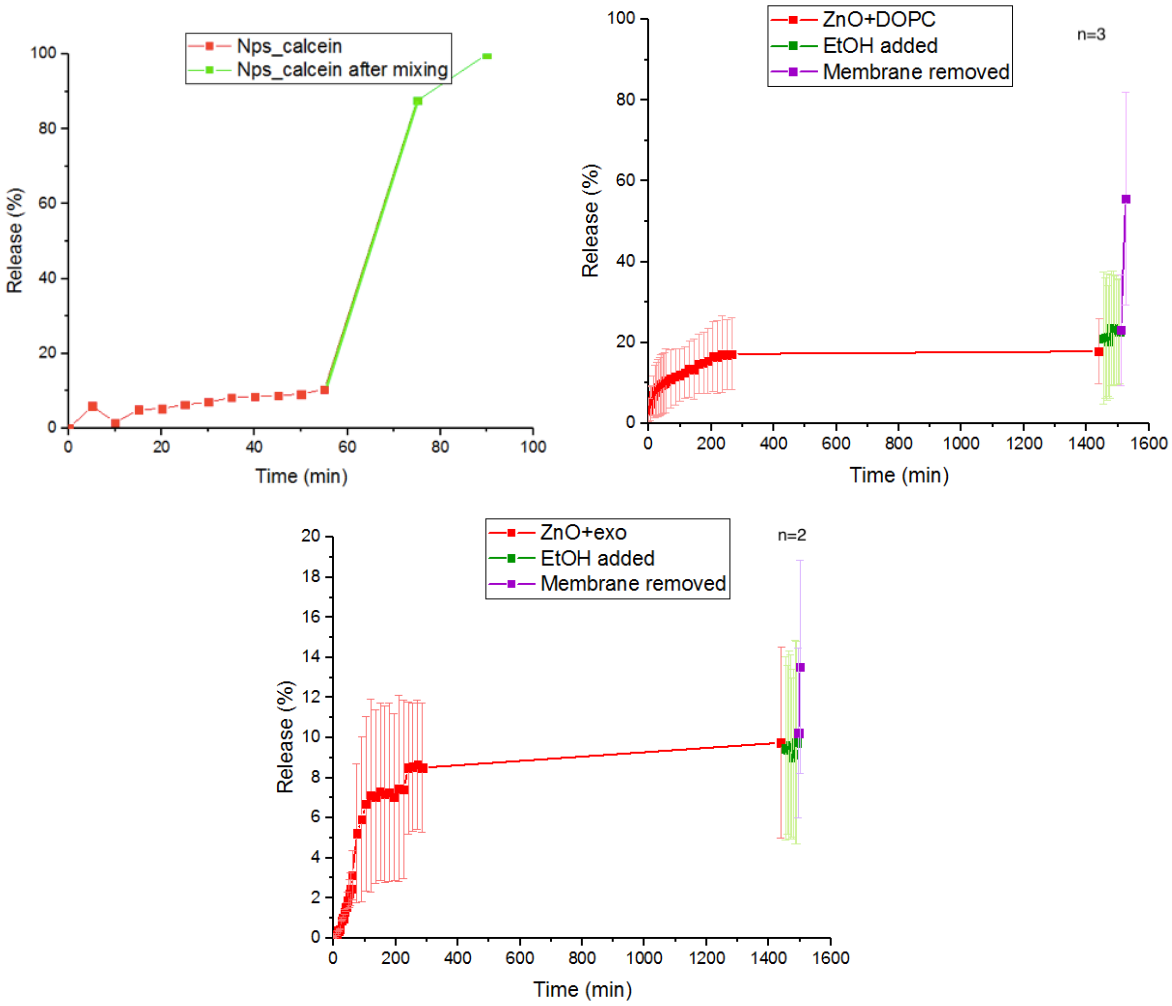

Figura 8: Curve di rilascio di calceina rispettivamente di ZnO non rivestito, ZnO rivestito da DOPC e ZnO rivestito da esosomi

Le nanoparticelle di silice mesoporosa sono state sintetizzate tramite metodo Stöber, modificato con un processo sol-gel assistito da tensioattivi. Sono poi state caratterizzate analizzandone la stabilità colloidale tramite DLS in due diversi mezzi di sospensione: etanolo in cui le particelle sono ben disperse e PBS dove le particelle iniziano ad aggregare dopo pochi secondi, come mostrato in Figura 9. Inoltre, viene fatta un'analisi morfologica attraverso il TEM, un'analisi spettroscopica attraverso la spettroscopia a infrarossi e termogravimetrica per valutare la bontà della sintesi.

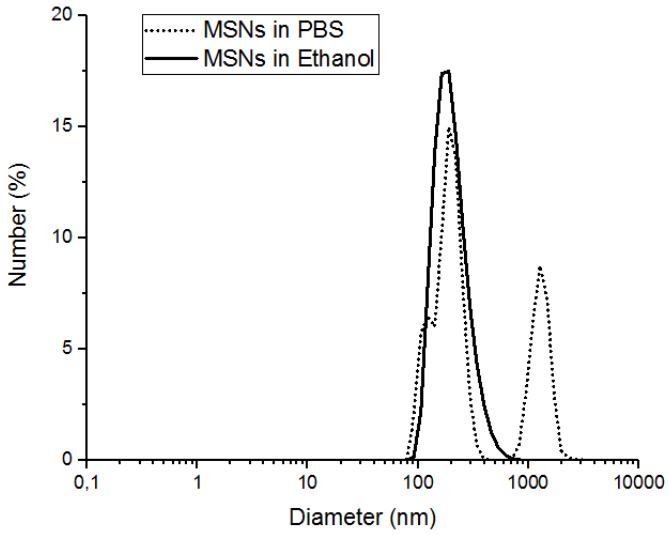

Figura 9: DLS delle nanoparticelle di silice mesoporosa in etanolo e PBS

Data la bassa stabilità delle particelle in ambiente fisiologico, nell'ambito di questa tesi anche la silice mesoporosa viene rivestita con gli esosomi. L'accoppiamento tra le due parti viene realizzato in due modi: con il metodo sopradescritto per i TNH e con uno che alterna 20 secondi di sonicazione a 10 minuti di centrifugazione per due volte.

I nanocostrutti ottenuti vengono analizzati con la DLS per analizzarne la stabilità (Figura 10). Mentre le particelle non rivestite in PBS aggregano velocemente, quelle rivestite da esosomi rimangono ben sospese e disperse anche in PBS.

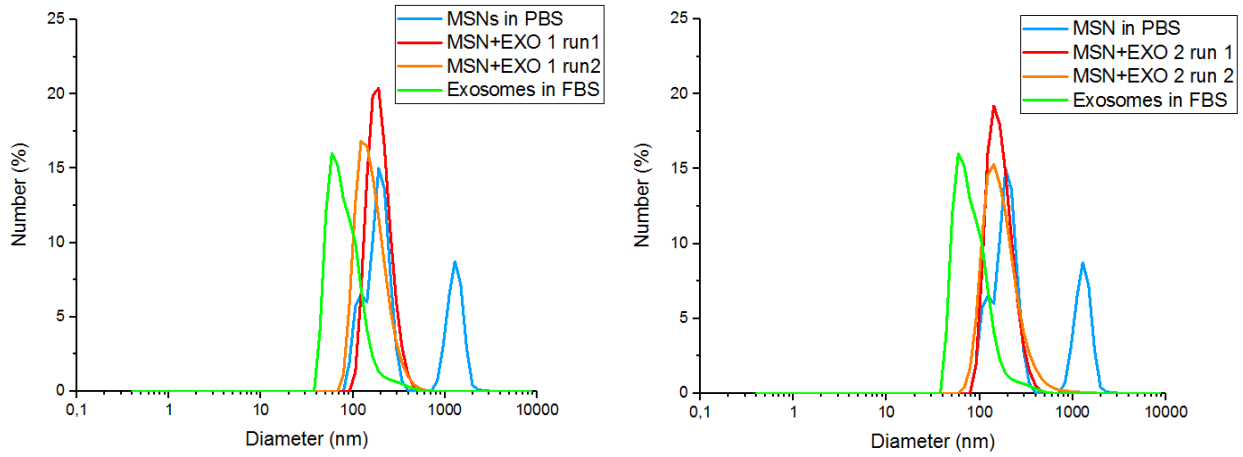

Figura 10: DLS delle particelle di silice mesoporosa rivestite da esosomi e non

A seguito dell'analisi TEM di nanoparticelle tal quali e rivestite si può notare un rivestimento attorno alle nanoparticelle di silice mesoporosa, come riportato in Figura 11.

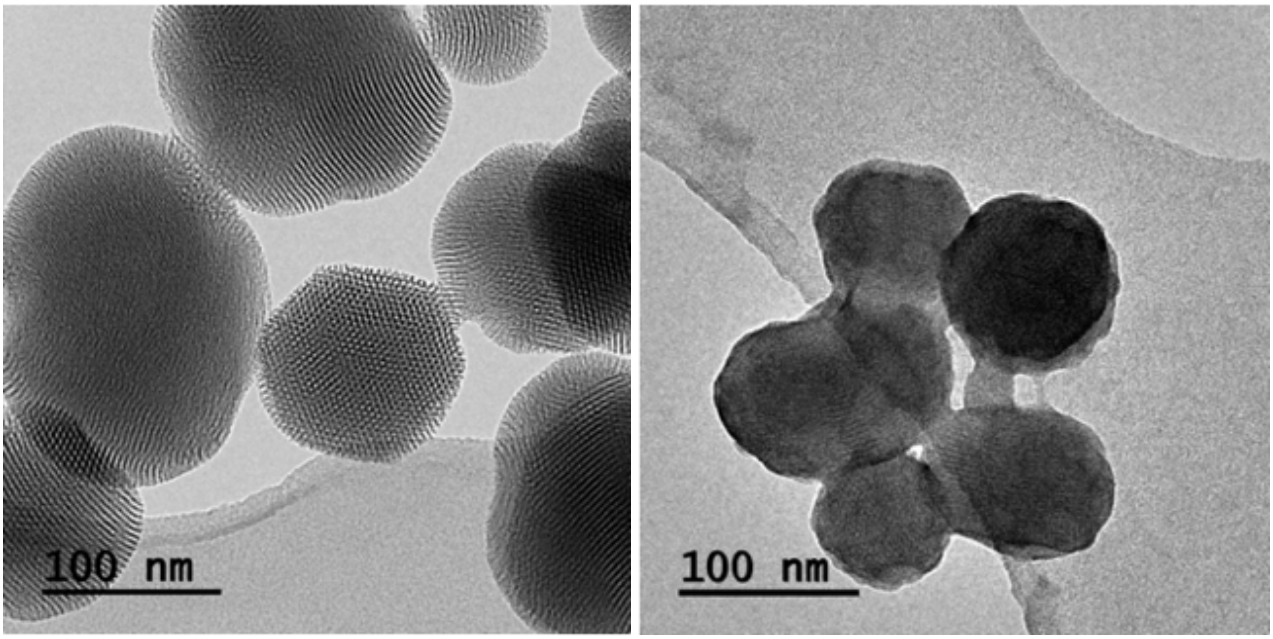

Figura 11: Immagini TEM di nanoparticelle di silice non rivestite (sinistra) e rivestite da esosomi (destra)

In seguito sono stati fatti alcuni test cellulari per valutare l'internalizzazione di queste nanoparticelle rivestite nelle cellule.

Il primo test va a valutare la capacità di ritenzione di molecole all'interno dei pori grazie al rivestimento di esosomi e il loro successivo rilascio all'interno delle cellule. Le nanoparticelle vengono caricate con un fluoroforo, la fluoresceina, poi rivestite con esosomi e infine sono incubate con le cellule. L'aspettativa è quella di vedere un rilascio di fluoresceina limitato solo all'interno delle cellule. I risultati ottenuti tuttavia non sono molto chiari, anche a causa della bassa risoluzione del microscopio a fluorescenza utilizzato. Sicuramente c'è stato un rilascio di fluoresceina, ma non è possibile dire se questo sia limitato all'interno delle cellule o in tutto il medium.

La citometria a flusso mostra la percentuale di cellule che hanno al loro interno delle nanoparticelle. In particolare, in questo caso, sono stati fatti due diversi esperimenti che hanno mostrato risultati interessanti. Le internalizzazioni vengono realizzate in cellule HeLa, ma in un caso vengono utilizzati esosomi estratti da cellule KB, la seconda volta invece esosomi estratti da cellule HeLa. Come mostrato in Figura 12, le percentuali di internalizzazione dei nanocostrutti con esosomi da HeLa è molto maggiore rispetto a quelli con esosomi da KB. Da questi risultati si può evincere che l'internalizzazione viene migliorata di molto se gli esosomi utilizzati sono estratti dalla stessa linea cellulare delle cellule target.

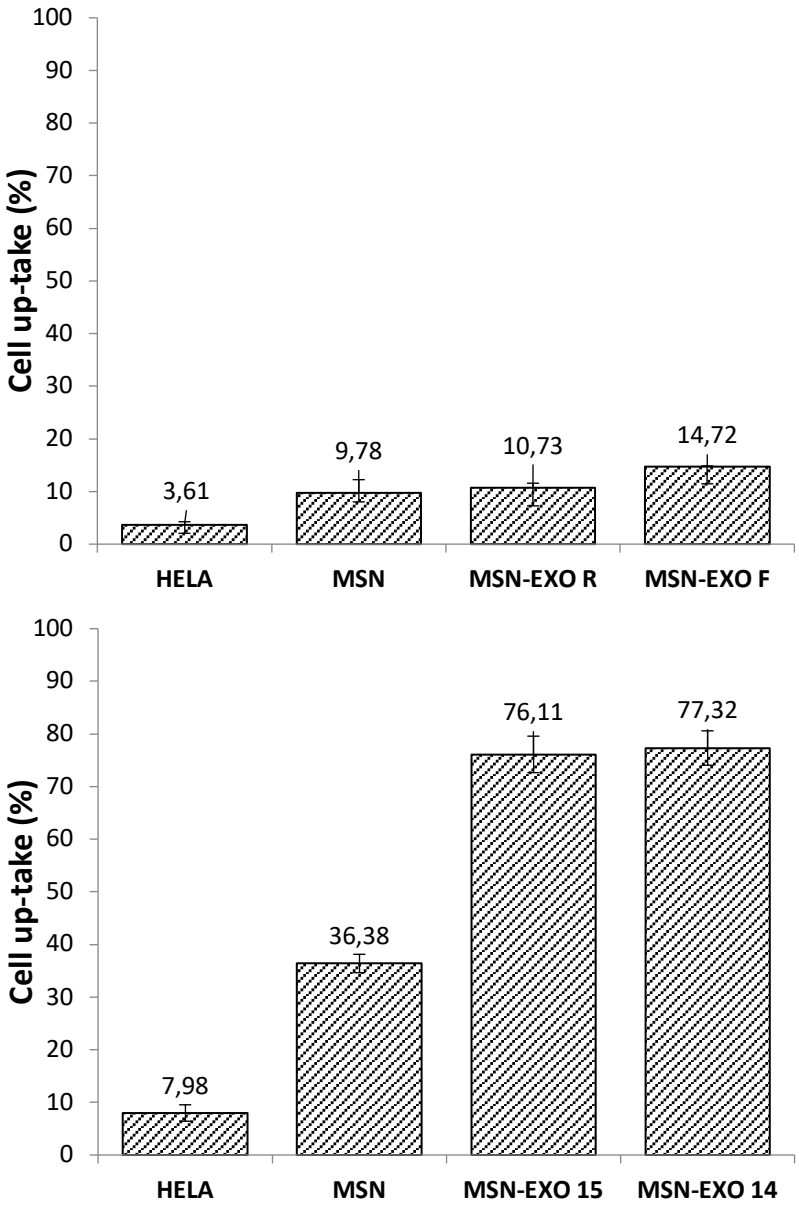

Figura 12: Percentuale di cellule che presentano delle particelleal loro interno. Primo esperimento con esososmi da KB sopra e con esosomi da HeLa sotto

Successivamente sono state fatte delle prove di stabilità dei costrutti tramite la DLS e l'analisi con luce UV.

Dalla Figura 13 si può notare che, nella figura superiore, le particelle non rivestite in PBS aggregano istantaneamente e gli aggregati diventano di dimensione sempre maggiore con il passare dei giorni, fino al settimo, quando il PBS inizia a corrodere e sciogliere la silice mesoporosa. Le particelle rivestite invece presentano una grande stabilità per diversi giorni, mantenendo un aspetto regolare e ben disperso. I risultati mostrati in Figura 14 confermano quelli del test precedente evidenziando l'aggregazione e la precipitazione delle particelle di silice mesoporosa al fondo della cuvetta.

I risultati ottenuti sono promettenti, per quanto riguarda la stabilità in ambiente fisiologico; tuttavia gli esosomi usati per l'accoppiamento sono estratti da FBS, quindi sono molto ricchi di proteine

extracellulari che possono formare una corona proteica attorno alle particelle di silice mesoporosa che sono molto idrofiliche.

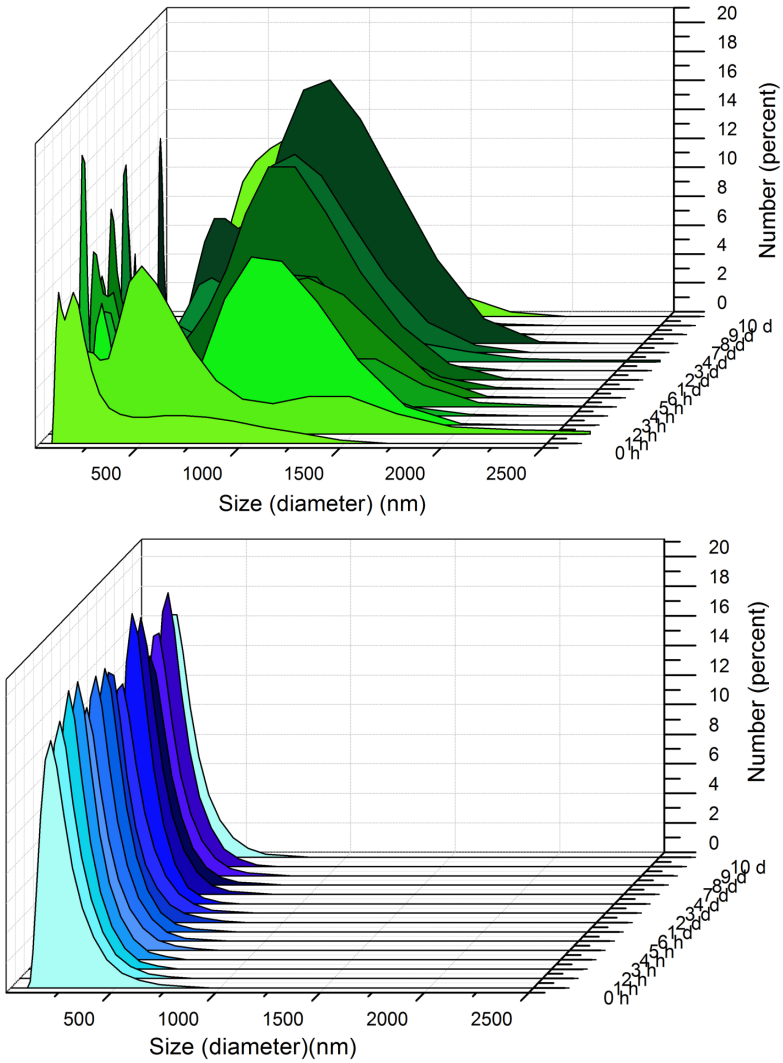

Figura 13: analisi di stabilità in DLS delle particelle non rivestite sopra e dei costrutti di nanoparticelle e esosomi sotto

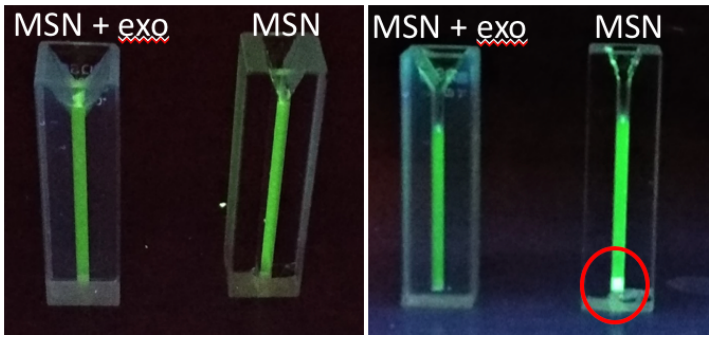

Figura 14: stabilità in cuvetta con luce UV

Sono stati svolti ulteriori test di internalizzazione in cellula tramite microscopio confocale. In Figura 15 sono riportate delle immagini di internalizzazione delle nanoparticelle rivestite da esosomi che sembrano iniziare l'internalizzazione anche dopo sole due ore di incubazione.

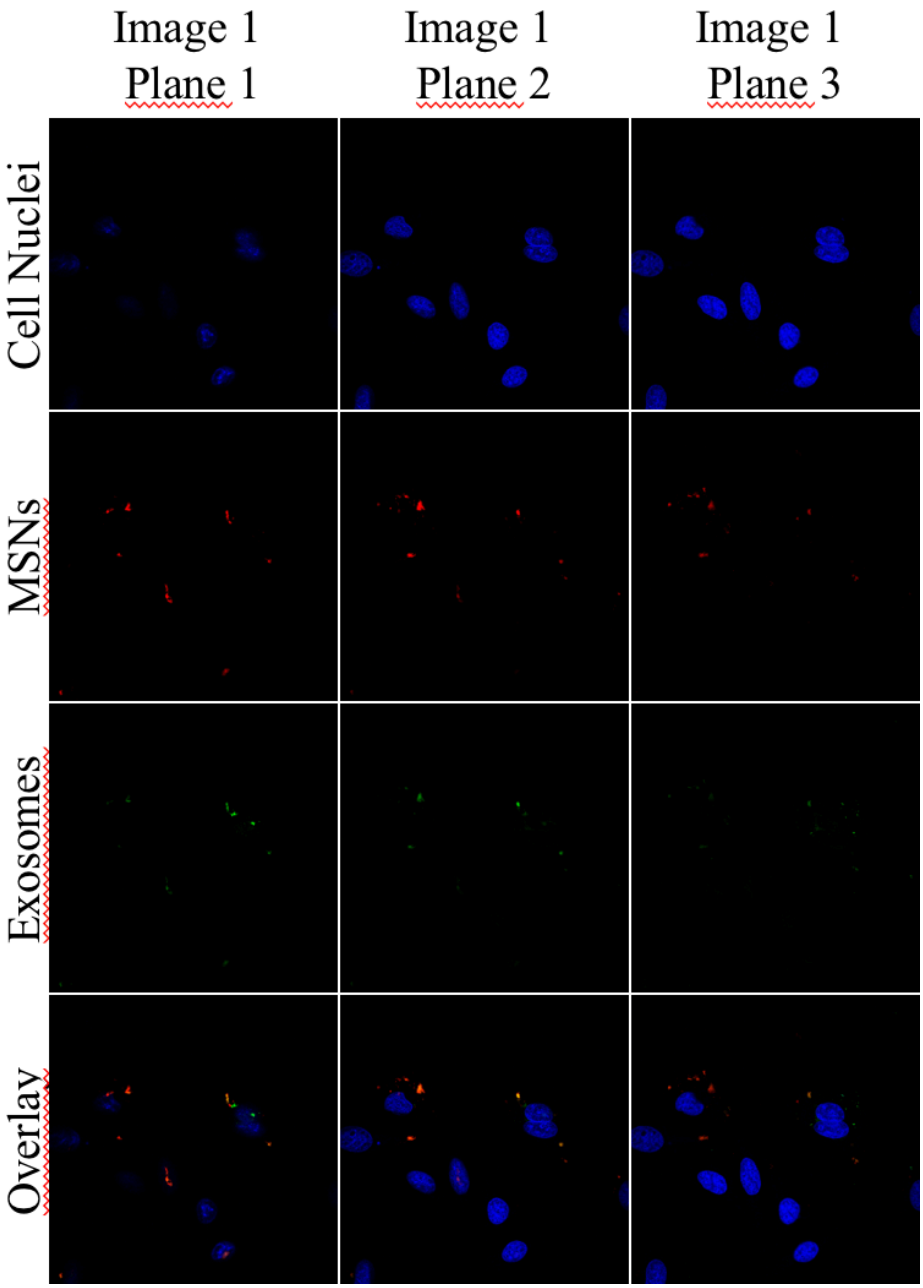

Figura 15: differenti Z-stack della stessa immagine ottenuti tramite microscopia confocale

Un altro test eseguito è il rilascio di fluoresceina in transwell, che tuttavia ha dato risultati opposti a quelli sperati, quindi va ottimizzato il protocollo di questo specifico test.

In conclusione questa tesi può essere considerata un punto di partenza per ulteriori studi per entrambi i due nanocostrutti, il primo basato su una nanoparticella con proprietà antitumorali intrinseche, il secondo su un nanocarrier, rivestiti da esosomi.

Abstract

In the last few years there has been an increasing interest in nanomedicine and in particular in developing nanoparticles to fight cancer. Nanoparticles have gained the attention of researchers because their dimensions allow them to interact directly with cells in the biological processes. Moreover, nanoparticles can be functionalized with proteins, antibodies, or other ligands (i.e. lipid bilayers or polymers) to improve the affinity with cancer cells, as well as their biocompatibility and stability in biological media.

A distinction needs to be made between the two most important classes of nanoconstructs: nanoparticles and nanocarriers. Nanocarriers are used for drug delivery. They are nanosystems able to load, protect and carry to the target cells a drug (for example a chemotherapeutic agent). Nanoparticles in contrast exploit their therapeutic effect based on their intrinsic antitumoral characteristic, i.e. response to an endogenous or exogenous stimulus able to create adverse conditions in the cancer cell, inducing it to death.

In this thesis one type of nanoparticle, constituted by zinc oxide (ZnO), and one type of nanocarrier, mesoporous silica, are developed.

The ZnO nanoparticle (of about 20 nm in diameter) has an intrinsic therapeutic effect, which is still not totally understood in the scientific community. Most of the studies agrees that the cytotoxic effect of ZnO is due to the combination of intracellular Zn^{2+} cations release and the production of ROS (Reactive Oxygen Species) which cause oxidative stresses in the cell and finally the death. In vitro tests have shown an increased cytotoxic effect of ZnO on cancer cells with respect to the healthy counterpart.

The nanocarrier is a mesoporous silica nanoparticle, called MCM-41, having 200 nm in size and with oriented and uniform pores of 4 nm in diameter. Mesoporous silica nanoparticles do not have a therapeutic effect themselves, but they can load different drugs inside their pores.

In this thesis, to promote the stability of both nanoparticles in a physiological environment, increase their biocompatibility and reduce immunogenic effects, both ZnO and MCM-41 nanoparticles are covered by a phospholipidic bilayer derived from extracellular vesicles, in particular exosomes, extracted from living cells. Exosomes are vesicles of 30-200 nm in size, naturally produced by many types of cells as vehicle of intercellular communication and, when autologous, they are not recognized by the immune system.

The purpose of this Master thesis is then to extract exosome from cells and re-use them as a biomimetic, nature-derived coating to stabilize and reduce the immunogenicity of both ZnO and MCM-41 nanoparticles. Most importantly, the natural communication function of exosome can be here conveniently exploited to drive the therapeutic nanoparticles towards the cancer cells. Moreover, when MCM-41 retains the drug into their mesopores, the lipidic bilayer coating of exosome can also help in safely retaining the drug inside the mesoporous silica.

The first part of this thesis concerns the optimization of the coupling process between ZnO nanoparticles and exosomes derived from cancer cells. This coupling creates a new nanoconstruct called TNH (TrojaNanoHorse) and it was carried out in the laboratory of Prof. Valentina Cauda at DISAT within her ERC Starting Grant project. The parameters driving thermodynamically and kinetically this coupling process are systematically studied, in particular considering the coupling time, temperature,

aqueous solvent used, mechanical stirring, and the electrostatic interaction between the ZnO surface, opportunely functionalized, and the exosome lipid bilayer. The efficiency of the coupling is then tested by combining different characterization techniques, such as co-localization optical fluorescence microscopy, transmission electron microscopy (TEM) (this technology with the help of a technician), Dynamic Light Scattering (DLS) coupled with Z-Potential measurements and nanoparticle tracking analysis (NTA) in collaboration with the IRCCS of Candiolo (Turin).

The second part of the Master Thesis is developed at the Universidad Complutense de Madrid in the research group of Prof. Maria Vallet-Regì, also recently granted by an ERC Advanced Grant concerning the development of mesoporous silica nanoparticles against bone-tissue cancers. The Master thesis in this laboratory aims at synthesizing MCM-41 nanoparticles, then developing a coupling protocol between mesoporous silica nanoparticles and exosomes, and study the internalization of this nanoconstruct in cells cultures. Thanks to the broad and systematic study carried out with ZnO-exosomes, the coupling process between mesoporous silica and exosome can be also efficiently studied, however with more difficulties because of MCM-41 greater dimensions and their high hydrophilicity, establishing also a competition mechanism of coupling between exosomes and serum proteins. It turns out that, on the one hand, the exosomes could help to retain the drug inside the pores, on the other hand the formed protein corona improves the biocompatibility and the stability of the whole construct in physiological fluids. Concerning the characterization methods, further skills are acquired, concerning the preparation of biological samples for TEM microscopy, and the use of confocal laser fluorescence microscopy in different optical configurations.

Both the hybrid nanoconstructs studied in this Master thesis show a great potential for cancer treatment, each one in its own way. They could be the starting points for further experiments and studies, deepening the knowledge first in in-vitro cancer cell cultures, studying their internalization process and their mechanisms of causing cell damages. Further studies about their stability in biological fluids and targeting mechanisms can be also envisioned. These nanoconstruct have also the possibility to be patient specific if exosomes are autologous thus leading to personalized therapy and paving the way for the efficient use of nanomedicine approaches.

Table of contents

1 Introduction

Cancer is a group of genetic diseases that involve uncontrolled cell division, replicative immortality and resistance to cell death. Under this conditions tumor cells grow in an abnormal cell mass called tumor, except for hematologic cancer where the cancer cells are distributed throughout the whole blood circulatory system [1].

Cancer is a leading cause of death worldwide, there are 10 million new cases of cancer each year, and an estimation of the World Health Organization evaluate that in 2030 there will be 13.1 million cancer-related deaths [2].

The current treatments for this disease are:

- Surgery, which must be further associated with radio or chemotherapy treatments and it is not always applicable if the tumor is too spread or located in a position difficult to operate;
- Radiotherapy, which consists in using ionising radiations to radiate the tumor, leading to damages in DNA and high oxidative stress. However, many treatments are required before reaching this purpose with a high toxicity for the surrounding healthy cells;
- Chemotherapy, which is the treatment most largely used, consisting in the systemic administration of one or more anticancer drugs. It leads to the death of rapidly dividing cells, so they can affect both cancerous and healthy cells with severe side effects;
- Immunotherapy is a relatively new therapy, thought to be used in the case of hematological tumors. It consists in stimulating the natural defences of the body to fight against the tumor, stopping or slowing its growth and diffusion to other tissue and enhancing the immune system to destroy the tumor. There are various type of immunotherapy: monoclonal antibody therapy, which binds signaling molecules to cancerous cells in oder to make the recognizable by the immune system, aspecific, which stimulates the immune cells by interferon and interleukin, virus-oncolytic, which administrates genetically-modified virus to destry cancer cells, T-cells therapy, where the T-cells of the patients are extracted, modified to better recognize the tumor and re-injected, and vaccines, which expose the immune system to a specific antigen. This therapy, anyway, has some adverse effects and sometimes it is ineffective.

One of the major cause of death related to cancer is the lack of selective delivery of anti-cancer drugs to the cancerous tissues. The toxic side effects limit the maximum tolerated dose of the drug and the efficacy of the therapy. Thus, an improvement of targeted delivery is extremely important to overcome the current limitations in cancer therapy [3].

Nanomedicine is the design and development of therapeutics and diagnostic tools distinguished by the nanoscopic scale of its delivery vehicles and diagnostic agents [4].

Recent developments in nanotechnologies are going to improve the drug delivery, increasing the therapeutic efficiency and at the same time reducing the toxic side effects [3].

The nanoscopic size of nanomaterials allows the interaction with tissues at the same scale of many biological processes, enhancing the intracellular uptake. Furthermore, their dimensions and the increased vascularization of tumors enable the accumulation in the target tissue by the mean of the EPR (Enhanced Permeability and Retention) effect. In addition to this passive targeting, it is possible to functionalize the

surface of these nanomaterials with ligands, proteins or antibodies that have to enhance the uptake by the target cells.

The most studied drug delivery systems are the nanocarriers which have the ability to carry and protect the drug loaded inside. Some polymeric nanoparticles and liposomes have been already approved by the FDA (Food and Drug Administratio) for clinical use [4].

Among the inorganic nanocarriers, mesoporous silica nanoparticles (MSNs) have a large specific surface area and pore volume and they are easy to functionalize. Their tunability of pore size offer a great control in the drug loading percentages and release kinetics. MSNs can deliver the anticancer drug to the tumor in a targeted way and release them on demand increasing the cellular uptake without premature release [2]

At the same time there is a growing interest for nanoparticles with an intrinsic anticancer effect. Their antitumor activity is related to the peculiar features of these nanoparticles, such as the intrinsic antioxidant action, or actions activated by the application of external stimuli, like magnetic or electric fields, light or infrared radiations [5].

Zinc oxide (ZnO) nanoparticles are one of these nanomaterials with antitumor intrinsic activity. The cytotoxicity mechanism of ZnO nanoparticles is not totally understood yet, but it is related to the ROS (Reactive Oxygen Species) production, which causes oxidative stress and cell death. Some studies confer the production of ROS to the semiconductor properties of ZnO [6], while others relate the ROS production to the release of Zn^{2+} ions, generated by the dissolution of ZnO in physiologic environment, which lead to a lack of balance in the zinc homeostasis and subsequent damage of mithocondria [7].

Nevertheless, the cytotoxic mechanism is still unclear, many in vitro cells have shown the preferred toxicity of ZnO towards cancerous cells rather than for healthy ones [8].

In this thesis, to promote the stability of both nanoparticles in a physiological environment, increase their biocompatibility and reduce immunogenic effects, both ZnO and MSNs are covered by a phospholipidic bilayer derived from extracellular vesicles, in particular exosomes, extracted from living cells. Exosomes are vesicles of 30-200 nm in size, naturally produced by many types of cells as vehicle of intercellular communication and, when autologous, they are not recognized by the immune system.

The purpose of this Master thesis is then to extract exosome from cells and re-use them as a biomimetic, nature-derived coating to stabilize and reduce the immunogenicity of both ZnO and MSNs. Most importantly, the natural communication function of exosome can be here conveniently exploited to drive the therapeutic nanoparticles towards the cancer cells. Moreover, when MSNs retain the drug into their mesopores, the lipidic bilayer coating of exosome can also help in safely retaining the drug inside the mesoporous silica.

The first part of this thesis concerns the optimization of the coupling process between ZnO nanoparticles and exosomes derived from cancer cells. This coupling creates a new nanoconstruct called TNH (TrojaNanoHorse). The parameters driving thermodynamically and kinetically this coupling process are systematically studied, in particular considering the coupling time, temperature, aqueous solvent used, mechanical stirring, and the electrostatic interaction between the ZnO surface, opportunely functionalized, and the exosome lipid bilayer. The efficiency of the coupling is then tested by combining different characterization techniques.

The second part of the Master Thesis aims at synthesizing MSNs, then developing a coupling protocol between these nanoparticles and exosomes and study the internalization of this nanoconstruct in cells cultures. Thanks to the broad and systematic study carried out with ZnO-exosome couplings, the coupling process between mesoporous silica and exosome can be also efficiently studied. However more difficulties are encountered because of MSNs great dimensions (around 200 nm) and their high hydrophilicity, establishing also a competition mechanism of coupling between exosomes and serum proteins. It turns out that, on the one hand, the exosomes could help to retain the drug inside the mesopores of the silica, on the other hand the formed protein corona improves the biocompatibility and the stability of the whole construct in physiological fluids.

2 State of art

2.1 Smart drug delivery

The word “cancer” includes a huge variety of genetic diseases with the common features of unregulated cells growth and spreading towards other tissues.

A cancerous formation has some characteristic shared with every kind of tumor:

- Anaplasia, which means that cells have an altered morphological aspect. In particular in the case of benign tumor they have a different size from the healthy counterparts; if the tumor is malignant they appear less differentiated with different morphological features in their dimensions, position and colour of the nucleus.
- Growth rate, cancerous cells have a growth rate faster than the healthy ones. Cells have a reduced cell cycle, especially those called cancerous staminal cells, which are responsible of the proliferation of the tumor.
- Metastasis, during which cancer cells can spread to other tissues. This is the first death cause in cancer patients.

During the normal life of a tissue, there is a balance between tumorigenic and tumor-suppressor species. If this balance fails, there is a predominance of one specie with the result of cancer for tumorigenic species and degenerative diseases for tumor-suppressor species.

In cancer there is an increase of the tumorigenic factors, which leads to a self-production of growth factors by the cancerous cell, an overexpression of receptors on the surface and an increased metabolism. The most important antitumorigenic factor of the cell cycle is the gene p53. It intervenes during the cell cycle to control that the replication is occurring in the right way. If there are mutations in the transcription of DNA, p53 induce the repair of the damage and, if it is impossible, it leads to the apoptosis of the cells preventing the cell become cancerous. In cancer cells, p53 is damaged and it can not exploit its role, so the cell can replicate even if its DNA is altered and avoid apoptosis. Furthermore, cancerous cells can recreate an inflammatory environment around them able to promote their growth and also the angiogenesis.

The current treatment for cancer are surgery, chemotherapy, radiotherapy, immunotherapy or a combination of these methods. The most widely used is chemotherapy, which is the administration to the patient of one or more anticancer drugs. These drugs interfere with the replication of the rapidly dividing and growing cells (like the cancerous staminal cells) and they lead to their death. Unfortunately, these drugs are not selective towards the cancerous cells, but they can damage also healthy tissues with fast proliferation rate, like the cells of the gastrointestinal tract, bone marrow and hair follicles cells. These agents cause severe side effects like gastrointestinal problems, among them, the most common is nausea, vulnerability to diseases due the decreased number of immune cells, and loss of hair. Furthermore, since the amount of drug that reaches cancerous cells is very low, high doses are required increasing the toxicity towards healthy cells and also causing drug resistance.

In the last few years, nanomedicine is revolutionizing cancer diagnosis and treatment, even if there is still a gap between the research or technological advances and clinical applications [9].

Nanomaterials are promising tools for cancer therapy because they can solve the problems of chemotherapy, including non-specific biodistribution, drug resistance, and undesired side effects [10].

Currently there are many studies whose aim is creating antitumor therapies based on nanoparticles like polymers, liposomes, dendrimers, virus, carbon nanotubes, metal nanoparticles that have intrinsic antitumor properties or as nanocarriers [11].

The most important characteristic of nanomaterials is their size. It is in a transitional level between the individual molecule and the bulk materials. When reduced to nanoscale, substances can develop new physicochemical, structural and optical properties increasing the uptake and the interactions with biological tissues. [12]

Nanomaterials has an increased area-to-volume ratio, which leads to a higher chemical reactivity. The interaction with biological systems is driven by the morphological parameters, like size, shape, surface area, surface charge and surface properties. There are different types of nanomaterials studied for developing new cancer therapies, among them there are the nanoparticles and nanocarriers. Concerning the type of materials, in this thesis the focus will be given to metal oxide materials, for both the nanoparticels and the nanocarriers.

Metal oxide nanoparticles for anticancer therapy have an intrinsic anticancer ability or this ability is mediated by external stimuli. They are used to directly kill the cancerous cells both in vitro and in vivo [5].

For example, iron oxide or manganese oxide nanoparticles, used in diagnostic, have also the capacity to generate local hyperthermia (42-45 °C) when stimulated with an external magnetic field. Cancerous cells are selectively killed by this temperature increase because heat is slowly dissipated in tumor tissues due to the lack of a well-organized vascular network. Moreover, hyperthermia causes many changes in cells and leads to a loss of cellular homeostasis [13].

Semiconductors metal oxide nanoparticels, like titanium dioxide or zinc oxide (ZnO) can participate to oxidation-reduction reactions generating ROS during the interaction with UV light or ultrasounds. The ROS generation can thus cause oxidative stress in the cells leading to their death [5][14].

In general, the carriers can be of polymeric, biologic, organic or inorganic origin, but only liposomes and some polymeric formulations have already obtained the approval of the FDA. Metal oxide nanocarriers are nanoscale porous systems with the ability of loading a therapeutic agent inside their structure and delivering it to target cells. They have been deeply investigated in the last years because their great advantages, such as high surface area and loading capacity, better bioavailability, lower toxic side effects and controlled drug release [2].

They also have the ability to protect the drugs improving their properties.

As metal oxide, with a surface rich of hydroxyl groups (OH) both metal oxide nanocarriers and nanoparticels can be fuctionalized with other oprganic or inorganic moieties to improve their biological stability ans target their delivery. In this way, advantages like preventing the accumulation in kidneys, liver and spleen, and combination of the therapeutics to the imaging capabilities, allowing a real-time monitoring, can lead to a theranostic nanosystem [9].

As told above, solid tumors can produce growth factor including VEGF (Vascular Endothelium Growth Factor) which enhance the angiogenesis and the formation of new blood vessels by stimulating

the migration and proliferation of endothelial cells from a close vessel. The new formed vessels are branched, tortuous and enlarged and the cells are not in close contact each other, but there are many pores in the vessel wall. Together with the poor lymphatic drainage, the accumulation of nanomaterials inside the cancerous tissues is enhanced (Enhance Permeation and Retention – EPR- effect, Figure 2.1), thus their therapeutic effect can be exploited very close to the tumor. This is called passive targeting.

With nanomaterials, it is also possibile to exploit the active targeting. This is achieved by functionalizing the surfaces of the nanomaterials with specific ligands, antibodies or proteins that allow a selective recognition of different receptors and antigens overexpressed on tumor cells surfaces, increasing the cytotoxicity for cancer cells and reducing the side effects for the healthy ones [1].

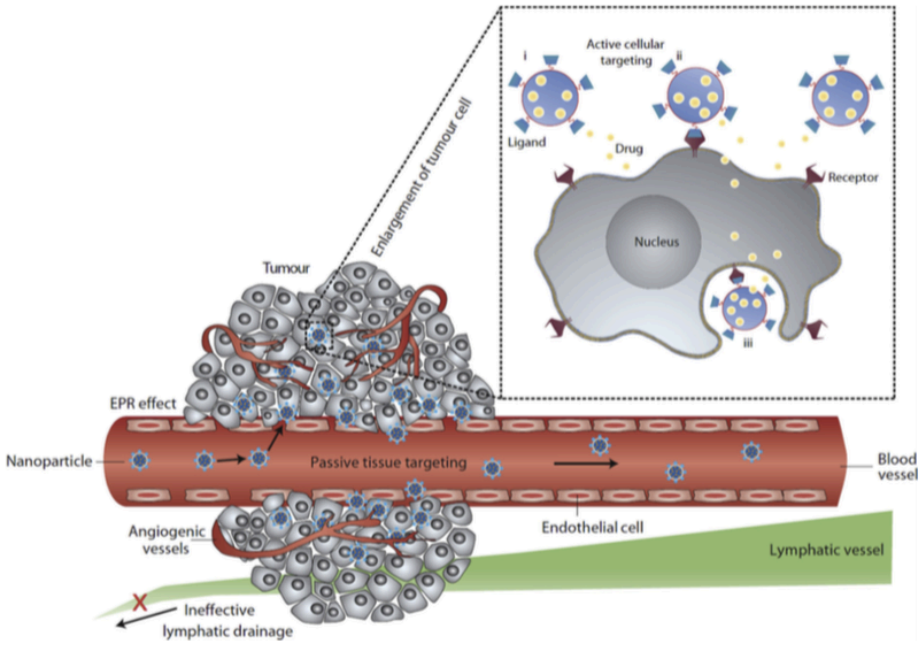

Figure 2.1: EPR effect [1]

There are however still some open challenges to be overcome before the clinical application of these nanomaterials would be successfully reached.

The first challenge is the biocompatibility of the nanosystem under different aspects. If the material is biodegradable it must degrade in non-toxic and possibly resorbable products; while, if it is not degradable it is important to analyze the clearance of the nanoparticles to prevent their accumulation in kidneys, spleen and liver with related toxic/poisoning effects even in the long term [15]. Furthermore, the stability of the nanosystem in physiological environment is of paramount importance: if the nanoparticles are administered in the bloodstream, serum protein and ions are adsorbed on the nanoparticles surface leading to their aggregation and recognition by the immune system. This aspect determines the lifetime of a nanoparticle in the bloodstream, before it is recognized and eliminated by the immune system. This time must be long enough to allow the nanoparticles to reach their target and exploit their function [16]. Therefore, the nanoparticles features must be controlled to guarantee the best biocompatibility.

The maximum size to escape the immune system is 400 nm, but to facilitate the uptake of the nanoparticles by the cells they must be smaller than 200 nm [1].

Furthermore, nanoparticles with hard edges or without a spherical geometry, with strong surface charges and hydrophobic behavious are easily recognized by the immune system and eliminated.

In these cases, it could be useful making a biomimetic coating on the nanoparticles to allow them to escape the immune system and to have a better dispersibility in physiological fluids.

Another challenge to be addressed is the possibility to transfer the production processes on the industrial scale for a further commercialization [15].

2.2 Extracellular vesicles

Extracellular vesicles (EVs) are nano or microsized vesicles, surrounded by a lipid membrane, that are produced by the cells to transport cargoes. There are various types of extracellular vesicles, depending on the release pattern or the biogenesis. There are microvesicles which bud directly from the cells membrane, containing cytoplasmic cargo, with a diameter from 100 nm to 1 μm. Another type of extracellular vesicle is formed by the fusion of multivesicular bodies (MVB) with cell membrane, where the MVB releases smaller vesicles, called exosomes, whose diameter is between 40 and 120 nm. Ectosomes (100 nm-1 μm) are released from the plasma membrane trough protrusions or budding. Dying cells release apoptotic bodies, vesicles (50 nm-2 μm) derived from the disaggregation of the cell. Oncosomes (1-10 μm) are large extracellular vesicles released abundantly by malignant cells and corrupted with tumor progression. [17][18]

The membranes of the EVs are composed by a double lipidic layer similar to the one of the plasma membrane of the cells and rich of various proteins, antigens and receptors which may vary depending on the EVs origin. This feature allows extracellular vesicles to interact with cells and play a central role in many physiological processes (Figure 2.2), for example they are used by the cells to communicate each other, by cancer cells to proliferate, migrate and produce metastasis.

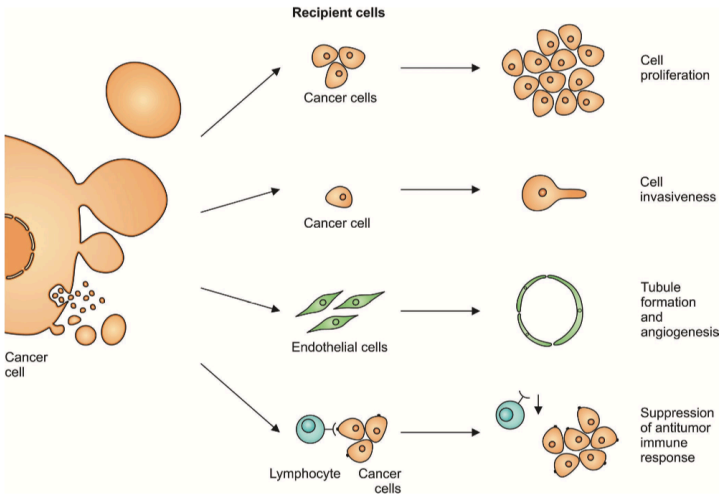

Figure 2.2: Extracellular vesicles and their recipient cells [17]

2.2.1 Exosomes

A peculiar type of extracellular vesicles are the exosomes: they are stored inside an intermediate endocytic compartment called multi vesicular body (MVB), that fuses with the plasma membrane liberating intraluminal vesicles, called exosomes. Their biogenesis is shown in Figure 2.3.

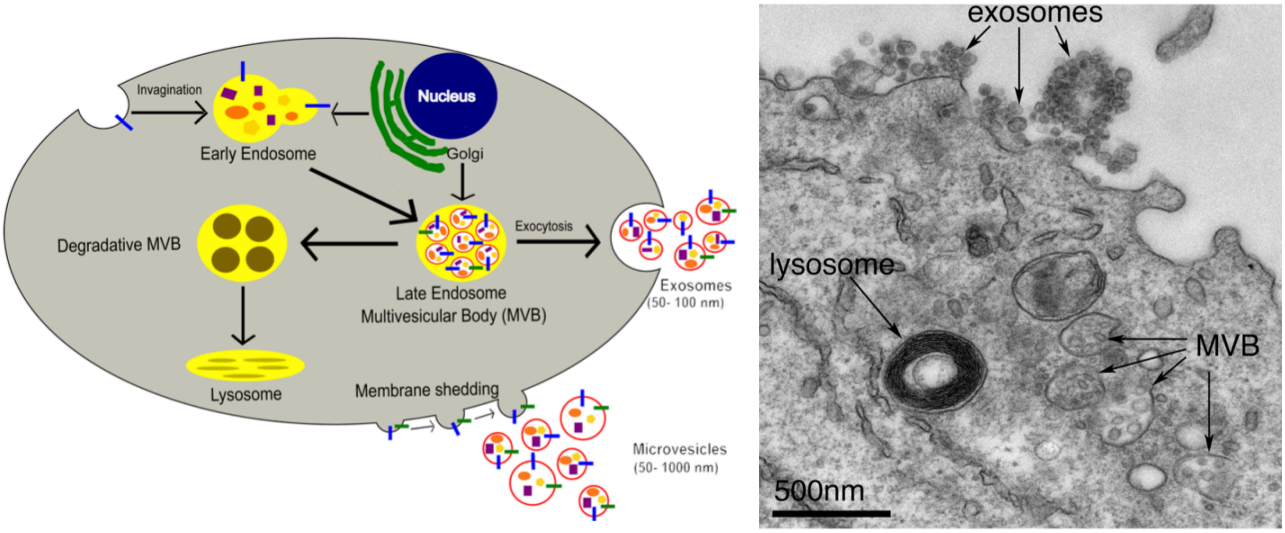

Figure 2.3: Biogenesis of exosomes (left figure from [19]and right figure from [20])

They are secreted by all the cell type and they can be found in all body fluids, blood, lymph, saliva and urine.

They are nanospheres with a bilayered membrane and under Trasmssion Electron Microscopy (whan dried, stained and fixed) they appear like rounded bodies with a cup like morphology (Figure 2.4). [18]

They can contain lipids, proteins and genetic materials derived from the parent cell.

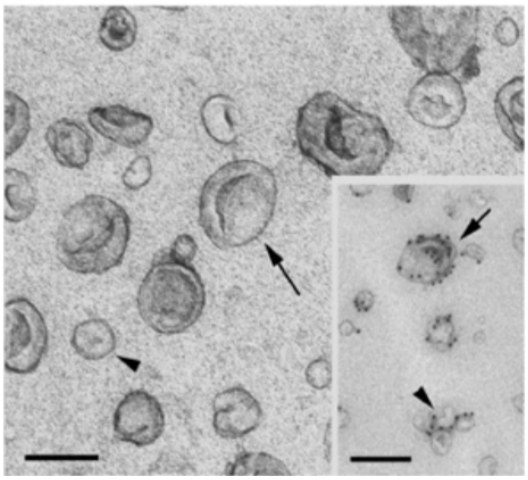

Figure 2.4: Exosomes seen with electron microscopy. Scale bar is 100nm [21]

They have been discovered for the first time 30 years ago, but they were largely ignored for years because they were considered only a mean of cellular waste disposal.

In the last decade the research on exosomes has led to several important discoveries: first, they are thought to be the mean of intercellular communication and macromolecules exchange between cells. Secondly, exosomes contain a cargo inside their membranes: in the previous years it was thought to be constituted only by waste products of the cells, but recently, it is discovered that the cargoes are also made by proteins, lipids, mRNA, miRNA and DNA which are contributing factors in the development of some cell functions or diseases. And finally, the most important factor that enhances the research on this topic, is the use of exosomes as vectors for drug delivery because they are naturally-derived "liposomes". All these reasons lead to an increasing interest of exosomes with a huge amount of literature published in the last ten years. [20]

Exosomes are generated by cells with an endocytic compartment through three steps of the endosomal pathway: the formation of early endosomes by the invagination of the plasma membrane, the inward budding of the early endosomal membrane which fills the endosomal luminal space with exosomes or intraluminal vesicles (this filled endorse are also known as MVBs) and finally the fusion of MVBs with the plasma membrane to release exosomes through exocytosis or with lysosomes for degradation. [19]

In order to release their cargoes inside a cell, exosomes have to fuse with the acceptor cell and this could take place through the direct fusion with the plasma membrane or through the engulfment with the formation of an endocytic organelle, this last process being not totally understood yet.

Exosomes are produced in the late endocytic compartment of the cells and, after their release in the extrallular space, they can diffuse in intercellular fluids. When they reach the target cell, they can be taken up with three potential mechanisms, as shown in Figure 2.5:

- Endocytosis: when exosomes reach the membrane of the target cell, the membrane create an inward protrusion which engulfs the exosomes and they are carried inside endosomes.
- Fusion with plasma membrane: when they reach the plasma membrane, the membrane of the exosome is embodied in the cell membrane and the cargo is released inside the cell
- Through surface ligands: exosomes membrane exposes some proteins which could bind with specific receptors on the target cell surface and, if this happens, exosomes are engulfed by the plasma membrane.

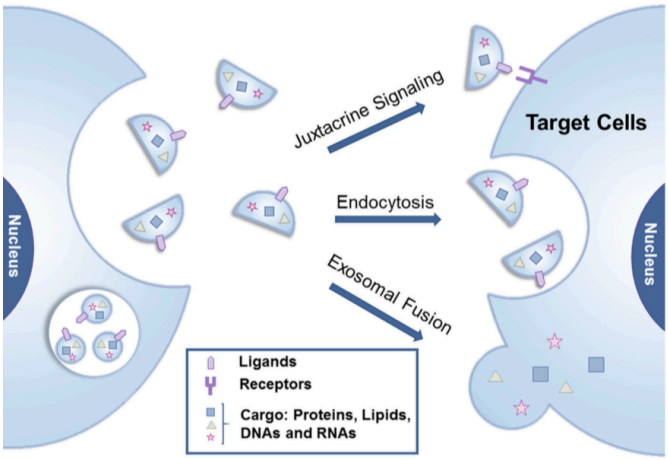

Figure 2.5: mechanisms of uptake of exosomes by recipient cells [22]

Exosomes are secreted by many different types of cells that release them in biological fluids, like synovial fluid, breast milk, urine, saliva amniotic liquid and in blood serum. [23]

Their most important biological function, and the one that makes them interesting for researchers, is the mediation in cells communication in a targeted specific way throughout the body. In particular, they carry proteins related with distant cells communication, but also pathogens like virus and prions and disease markers (like in breast cancer [24]).

The first one is their involvement in the immune response, many immune cells like dendritic cells, macrophages, B and T cells actively produce exosomes [24]. For example, exosomes secreted by antigen presenting cells express on their surfaces major histocompatibility complex (MHC) molecules which activate T-cells to enhance a specific immune response. [23]

They can also influence the expression and the activity of proteins releasing mRNA and miRNA in an acceptor cell. [20]

Furthermore, they are also associated to many common diseases, they are vehicles for the spread of cancer and neurodegenerative diseases because they can contain disease-associated cargoes. Exosomes play a crucial role in cancer. Tumor cells produce an increased amount of exosomes and they induce a pro-tumoral environment carrying genomic and proteomic products to distant sites, promoting angiogenesis, thrombosis and tutor cells proliferation, as well as silencing the immune system response. In this prospect, exosomes can be used to detect the presence of some types of cancer. In neurodegenerative diseases, they are responsible for transferring misfolded proteins to healthy neurons, spreading the disease from cell to cell. [23]

Anyway, exosomes have not only the aim of spreading diseases, but they have also the ability to induce tissue regeneration by carrying growth factors, proteins, miRNA, mRNA and lipids to the site of injury. [23]

The exosomes can be isolated from body fluids, but also by the cell culture medium with several different techniques. The most common is differential centrifugation, which is the protocol used to extract the majority of exosomes used in this thesis.

The International Society for Extracellular Vesicles (ISEV) in 2014 published a paper in which they recommend defining exosomes only the extracellular vesicles presenting certain surface markers (Figure 2.6). On the surface of exosomes there must be TSG101, Alix, flotillin 1, tetraspanins like CD9, CD63 and CD81, integrins and cell adhesion molecules. For what concerns the lipid content, exosomes are enriched of cholesterol, sphingomyelin and hexosyceramids. [25]

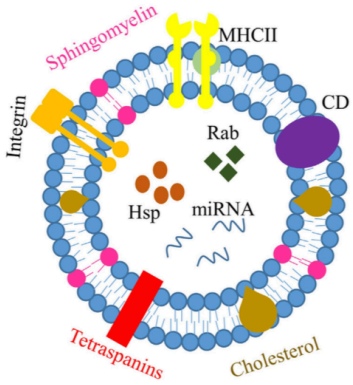

Figure 2.6: Composition of exosomes [23]

THERAPEUTIC FUNCTION OF EXOSOMES

Exosomes can be used as carriers and have the capability of travelling from one cell to another, delivery different cargoes, and they can also easily fuse with plasma membrane releasing their contents inside the cells.

They are extracellular vesicles released from cells, so they express some lipids, ligands and cell adhesion molecules that give them the targeting ability toward specific cells depending on the donor cells type.

Exosomes can be loaded with several small molecules, both hydrophobic and hydrophilic (Figure 2.7). The hydrophilic compounds are internalised inside the aqueous core of the exosomes, while the hydrophobic ones are incorporated inside the lipid bilayer of the membrane. Furthermore, proteins and genetic materials (DNA and RNAs) can be loaded into exosomes through genetic engineering. Moreover, exosomes surface can be modified to better characterize them after the extraction, membranes can be equipped with fluorescence molecules, fluorophore-conjugated antibodies, antibodies which can help the tracking of exosomes in vitro and in vivo as well. [26]

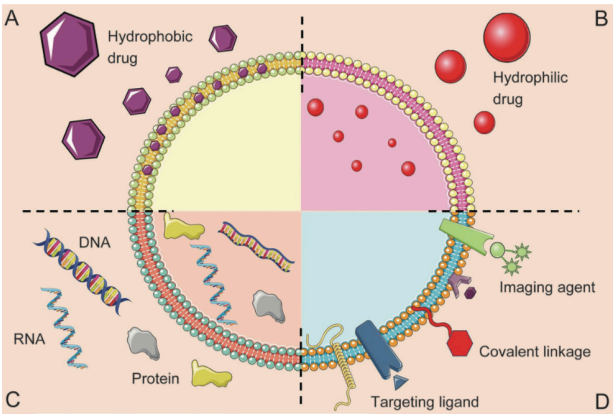

Figure 2.7: Molecules that can be loaded in exosomes [26]

In some genetic diseases there are one or more than one altered genes that could be replaced by the correct ones through gene therapy. The main idea of gene therapy is to deliver DNA, mRNA, miRNA or

siRNA to the cells in order to replace or silence the damaged ones. The most important problem is the delivery of oligonucleotides to target cells, because they could not be injected in vitro into the cells if they are not extractable and they could neither be injected in the bloodstream because elicases quickly degrade them. In the last years, viral vectors, liposomes and other approaches have been investigated to be used for the delivery of oligonucleotides. Even though some of them have reach the clinical evaluation, there are still some problems like immune response, random integration for viral vectors and rapid clearance for liposomes.

A good alternative that is going to be investigated is the use of exosomes and in general of EVs as vectors for gene therapy. They naturally contain and transport genetic materials, so they could be engineered to carry a specific cargo to target cells. [19]

Exosomes could be used also as vehicles for drug delivery and they offer several advantages comparing with the other methods, i.e. a better stability in the blood which allows them to cover long distances in physiologic and pathologic conditions, their small size and their capacity to carry surface molecules enable them to cross several biological barriers, above all the blood brain barrier. Furthermore, they have also an intrinsic ability of targeting. In particular, exosomes extracted from cancer cells have the ability to selectively target those cancer cells and certain tissues to propagate the metastasis. [22]

Exosomes have been studied as drug delivery vehicles in many studies. Some researchers [27] use exosomes as vehicles for an anti-inflammatory substance, curcumin. This substance seems to be protective from lipopolysaccharides-induced brain inflammation in mice models. Exosomes improve the solubility, the circulation time of curcumin and allow the penetration inside the blood brain barrier. Additionally, curcumin-loaded exosomes are selectively internalised by the microglial cells. Other studies load exosomes with different chemotherapeutics drugs, such as doxorubicin [28] and Paclitaxel [29] which are successfully deliver by exosomes to target cells reducing the tumor growth in mice, but also reducing the side effects.

There are several methods to load drugs inside exosomes [22]:

- Incubation is the simplest method. It requires to pose in contact exosomes and the drug under an agitation method;
- Electroporation of a solution of exosomes and drug with short, high-voltage pulses to let the drug penetrate the exosomal membrane. This method has a high efficiency, but could cause the aggregation of exosomes;
- Sonication is another effective method to load drug inside exosomes, based on different protocols of sonication of a mixture containing the two components. This method is also very efficient, but has the disadvantage to destroy most of the exosomes.

There are some challenges that have to be overcome if exosomes have to be use in clinical treatments. The most important one, and the most challenging, is that the number of exosomes produced by cells are not sufficient for production in a clinically applicable scale.

Next, another problem is the efficient loading of exosomes with a cargo without altering their structures and compositions which can lead to the recognition by the immune system and to their degradation.

It is also possible that the drug loaded inside the exosomes can cause the loss of the ability to recognise their target tissue, preventing exosomes to exploit their therapeutic effects. [24]

2.3 Zinc oxide

Zinc Oxide (ZnO) is a semiconductor metal oxide with catalytic, electrical, electronic, piezoelectric and optical properties studied since 70's [30], and in the last years, it is acquiring an increasing interest in the biomedical and nanomedicine fields.

ZnO nanoparticles are synthesized via vapour phase method (chemical vapour deposition, metalorganic chemical vapour, sputtering…) or via liquid phase approaches (sol-gel, hydrothermal or solvothermal syntheses…). Especially, the sol-gel methods, previously used for the synthesis of metal oxide microstrucutres, are adapted for the synthesis of smaller nanoparticles because they have mild process conditions for what concerns temperatures and reagents, low costs and, additionally, they allow a strict control over the morphology and the size of the final products [31].

The precursors for the synthesis of ZnO nanoparticles include inorganic salts and organic zinc compounds (i.e., zinc nitrate or zinc acetate) that can hydrolase in alkaline solutions, forming tetrahedral coordination compounds ($(Zn(OH)_4)^2$). The subsequent hydrolysis and consensation of these intermediate products leads to crystalline zinc oxide. Through this process it is possible to obtain nano- and microspheres, nanowires, nanorods, multipods and flower-like structures[32].

ZnO with micrometric size is classified as a "GRAS" (Generally Recognized As Safe) substance by FDA (Food and Drug Administration). Nevertheless, ZnO with nanometric size has different properties, owing to its dimensions, which enhance the interactions with biological compartments but also a new mechanism of toxicity not present in the bulk material.

ZnO nanoparticles are believed to be nontoxic, biosafe and biocompatible and they are used in everyday life such as drugs and cosmetics [33]. When ZnO nanoparticles are administered in the bloodstream, they can survive for a limited amount of time, after which they are eventually dissolved into mineral ions that can be completely absorbed by the body and become a part of the metabolism [33].

After iron, zinc is the second most abundant trace metal in the human body (more or less 2 g in the whole body) and it has important biological functions in many tissues, often associated with the folding of proteins and it is also an important cofactor for more than 300 metalloenzymes [34]. Zinc plays a role in the protection of biological structures from damages by free-radicals, stabilization the molecular components of the membranes, DNA replication and repair, cell cycle progression and apoptosis, immune response and transmission of the nervous impulse [35].

Zinc plays also a crucial role in the defence against cancer. During a cell cycle, the cell goes through several phases that lead to its duplication. Between different phases there are some checkpoints where p53 gene and caspase enzyme control that the replication is taking place in the correct way and, if not, they activate a repair mechanism to correct the altered DNA. If this mechanism fails, they induce the apoptosis, preventing the altered cell from dividing, which may later develop in a cancerous cell. Zinc has an important role in maintaining the activity of the tumor suppressor gene p53, which regulate the apoptosis of cells with damaged DNA. Furthermore zinc is responsible for the activation of the caspase-6 enzyme, involved in apoptosis [36].

On the other hand, if the extracellular concentration of zinc is in excess, it becomes cytotoxic because it causes the breakdown of the zinc transporters of the cell membrane and the increased intracellular concentration provokes apoptosis or necrosis [37]. This cytotoxic effect caused by high concentration of zinc and the selective targeting toward cancerous cells make zinc an antitumoral agent.

In vitro tests have demonstrated the preferential cytotoxicity of ZnO nanoparticles towards cancerous cells, in particular ZnO shows an increased toxicity against the rapidly dividing cancer cells compared to the healthy ones of the same lineage [38].

The selectivity of ZnO nanoparticles for cancer cells is due to their small diameter which allows the accumulation inside the tumor, by exploiting also the EPR effect. Furthermore, the isoelectric point for ZnO is 9-10, it means that under physiological conditions it has a strong positive charge on its surface. Moreover, compared with healthy cells, cancerous cells have an outer plasma membrane rich of anionic phospholipids, leading to a negative charge on their surface. In this way, it is expected that positively charged ZnO nanoparticles interact electrostatically with the cells membranes promoting the uptake, phagocytosis and thus the toxicity [6].

The cytotoxicity of ZnO is related either to its diossolution and release of Zn^{2+} cations and to the production of ROS (Reactive Oxygen Species) under specific conditions which can lead to cell death when it exceeds the antioxidant capacity of the cell causing oxidative stress and the subsequent damage to cellular proteins, DNA and lipids [38].

The generation of ROS is linked to the semiconductor properties of ZnO [6] when it is enlightened with UV light or by ultrasound application. In presence of a radiation with an energy of more than 3.3 eV, the excitation of electrons from the valence (VB) to conduction band (CB) could generate positive holes and induce hydroxyl radicals formation. In addition, the free electrons in the conduction band can reduce oxygen and generate superoxides. It was also reported in the literature that the presence of crystal defects increases the electron-hole pairs in ZnO NPs even without an additional stimulus [39].

2.4 Mesoporous Silica

MCM-41 is a type of mesoporous silica, belonging to the family of M41S, showing hexagonal arrays of cylindrical mesopores [40] in the range of 2-10 nm in size.

They are produced by self-assembly of silica with a Stöber modified method (Figure 2.8) where the sol-gel process is combined to the presence of self-assembled surfactant to obtain nanoparticles. Surfactants are indeed used as structure directing agents and the silica precursors condensate around these templates. Then the surfactant is removed and it leads the cavities typical of mesoporous silicas [41].

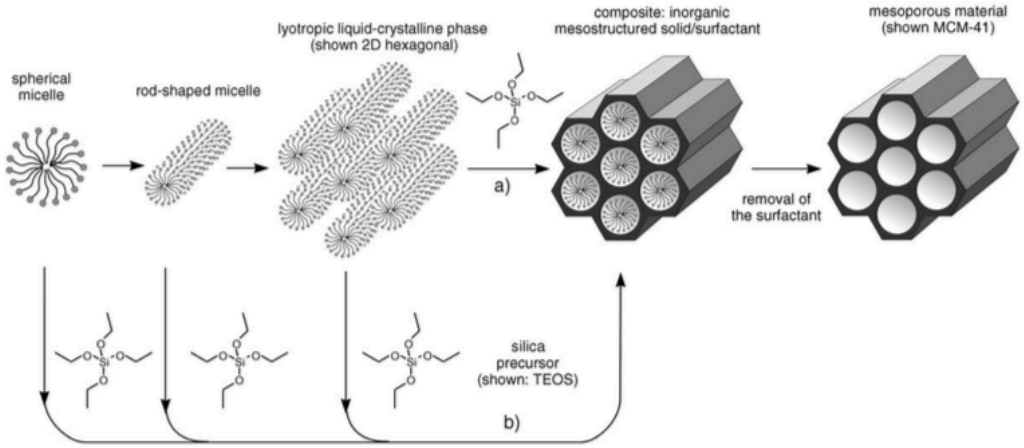

Figure 2.8: Synthesis of MCM-41 [42]

Mesoporous silicas are non-toxic, biocompatible and chemically, thermally and mechanically stable [43] and they also provide a great loading capacity of host molecules inside their pores.

Mesoporous silica nanoparticles (MSNs) can be used as drug delivery systems thanks to their large surface area (700-1000 m^2g^{-1}), high pore volume (0.6-1 cm^3g^{-1}), tuneable size (50-300 nm), shape and pore diameter (2-10 nm), robustness, easy functionalization [44] and narrow mesopores channels which allows the adsorption of biomolecules and drugs with nanometric dimensions inside their ordered pores to be locally released in the site of injury [45].

The molecules can be loaded inside MSNs usually with the impregnation method, by soaking the nanoparticles in a highly concentrated molecule solution [43].

The most important features to be considered in using MSNs as drug delivery systems are:

- The pore diameter, which determines the size of molecules to be loaded. If the dimensions of the molecules are smaller than the pores, they can be hosted inside the cavities, while, if they are larger, they can be adsorbed only on the external surface.
- The surface area, which rules the quantity of retained molecules inside the matrix. When the molecules are smaller than the pores size, only few molecules have the possibility to interact directly with the pore walls, while the rest will not be retained inside the pores.
- The pore volume, which is important in loading large molecules and also when large amount of molecules are required.
- Functionalization of silica walls, which have a high density of silanol groups, can be carried out to modify the interactions with molecules. [45]

The drug delivery process to a solid tumour is made by five steps resumed in the acronym CAPIR: circulation, accumulation, penetration, internalization and release [41].

After the introduction of therapeutic agents inside the pore of the MSNs, it might be possible for them to diffuse out when they are in solution. For this reason, it is necessary to close the pore entrances to avoid the burst release of the therapeutics into the bloodstream before they have reached their target site. in contrast, an uncontrolled delivery can cause severe side effects due to unspecific release [41]. The most common way to reach this aim is grafting stimulus-sensitive gates to the pore entrances or covering

the whole nanoparticle with a cleavable shell that trigger the release after its detachment. The pores open under the action of internal stimuli, pH, redox potential, enzyme concentration, or external one, suche as magnetic and electrical fields, ultrasounds or light [41].

MSNs can be endocytosed by many types of mammalian cell lines, depending on their size, morphology and functionalization, they are well tolerated under a concentration of 100 μg/ml and the products from their degradation become part of the metabolism of the cell. The hemocompatibility of the smaller nanoparticles (100-200 nm) is also demonstrated [44][46].

3 Materials and methods

3.1 Exosomes extraction

Cell culture supernatants usually contain different types of shed membrane fragments and vesicles, so purification protocols are required to ensure that the vesicles extracted are exosomes and not other type of contaminating material [21].

3.1.1 Exosomes extraction from Fetal Bovine Serum

The exosomes from Fetal Bovine Serum (FBS) are extracted during the depletion process of the medium that is used to cultivate cells.

The depletion process is based on ultracentrifugation. The medium containing 20% of FBS is depleted using the MLA-50 rotor of ultracentrifuge OptiMax from Beckman Coulter and the polypropylene tubes (Optiseal, Nominal volume 29.9 ml). The ultracentrifuge is set at 4°C in vacuum. The tubes are loaded with 28 ml of medium each with a sterile syringe and then centrifuged overnight (12 hours) at 100'000 g. Once the centrifuge is finished, the exosomes and more in general, all the extracellular vesicles, are pelleted at the bottom of the centrifuge tube. The tubes contents are then transferred in sterilized 50 ml tubes using a 30 ml syringe, and the pellet resuspended in PBS, aliquoted in volumes of 50 µl in cryo-vials and stored at -80 °C for further use. The depleted medium with 20% FBS without exosomes is sterilized by pouring it into a vacuum-connected 0.22-µm filter on top of a sterile bottle. Finally, the depleted medium is diluted with a medium supplemented with all the nutrients and antibiotics in order to reach the final FBS concentration of 10% required to culture cells and produce exosome from them.

3.1.2 Exosomes extraction from KB, DAUDI and HeLa cells

HeLa cell line is an immortalized type of tumoral cells isolated by cervical cancer.

KB cell line was originally thought to be derived from an epidermal carcinoma of the mouth, but was subsequently found, based on isoenzyme analysis, HeLa marker chromosomes, and DNA fingerprinting, to have been established via HeLa cell contamination.

DAUDI cell line is an Epstein-Barr Virus (EBV) transformed lymphoblastoid line and is a part of the Human Leukocyte Antigen (HLA).

The protocol used for the extraction of exosomes from KB or DAUDI cells is based on a sterile differential ultracentrifugation protocol and is shown in Figure 3.1.

The medium where cells are grown is collected into 50 ml tubes and centrifuged 10 minutes at 130 g at 4°C in order to remove the cells. The surnatant is then transferred in other centrifuge tubes and centrifuged again for 20 minutes at 2'000 g at 4°C to remove dead cells.

The supernatants are collected again and placed into ultracentrifuge polyallomer tubes. They are centrifuged at 10'000 g for 30 minutes at 4°C to remove cell debris. The supernatants are then recollected and recentrifuged at 100'000 g for at least 70 minutes at 4°C. The pellet obtained is a mixture of exosomes and contaminating proteins, it is resuspended in 1 ml of sterile filtrated PBS and the solution is centrifuged at 100'000 g for 60 minutes at 4°C. The pellet, which contains only exosomes and extracellular vesicles, is resuspended in sterile PBS or sterile physiologic solution (0.9% NaCl in water) and then the aliquots are put in cryovials at -80°C for storage.

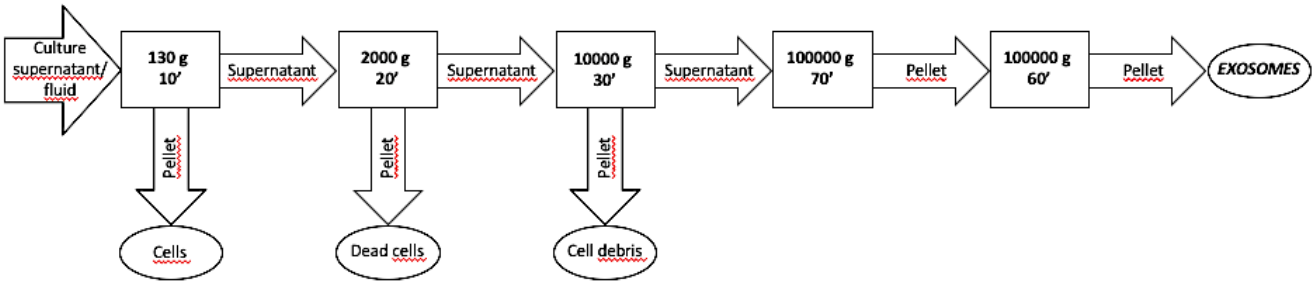

Figure 3.1: KB and DAUDI exosomes purification protocol based on reference [21]

Exosomes from HeLa cells are extracted using the kit for exosomes extraction ExoQuick from BioNova.

3.1.3 Exosomes characterization

Nanoparticle Tracking Analysis (NTA)

Nanoparticle Tracking Analysis uses the properties of light scattering and Brownian motion to obtain the particle size distribution of samples in liquid suspension.

A laser beam crosses a thin and microfluidic sample chamber and the particles suspension and they can be visualized via long working distance, x100 magnification microscope onto which is mounted a video camera.

The camera captures the Brownian motion of the nanoparticles and the software tracks many nanoparticles individually and using the Stokes-Einstein equation calculates their hydrodynamic dimeters.

This measurement provides the particles size and their concentration. There is also the possibility to use the fluorescence mode to have specific results for labelled nanoparticles.

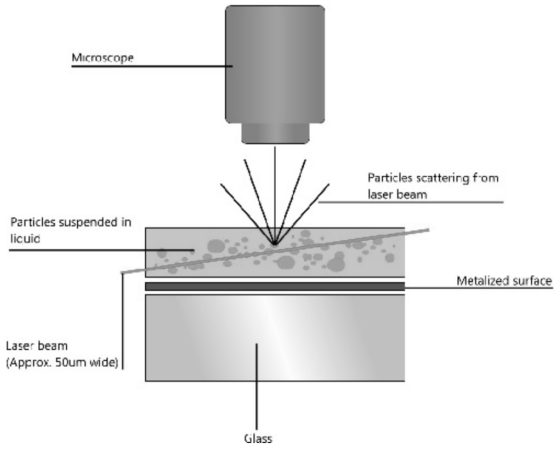

Figure 3.2: Nanoparticle tracking analysis, how it works [47]

The instrument used is NanoSight NS300 (Malvern Panalytical), placed in the IRCCS of Candiolo (Turin). It is based on the NTA technology and allows the measurement of the size and concentration of nanoparticles between 10 and 2000 nm in diameter.

Transmission Electron Microscopy (TEM)

The functioning of TEM is based on an electron beam which, under vacuum, is transmitted through the sample.

The sample of exosomes is prepared diluting the fresh solution with exosomes with a ratio of 1:10 in physiologic solution and depositing it on a holey-carbon copper TEM grid. No staining is applied.

The TEM images are acquired first at 200 kV and then at 80 kV.

3.2 Synthesis and functionalization of zinc oxide nanoparticles

3.2.1 Synthesis of zinc oxide nanoparticles

Zinc Oxide nanoparticles are produced by a microwave-assisted solvotermal synthesis.

This process is carried out using zinc acetate and potassium hydroxide (Sigma Aldrich) in a ratio of 1:2 as precursors and methanol as solvent.

Potassium hydroxide and methanol are mixed in an ultrasonic bath until they form a homogeneous solution. Another solution contained zinc acetate and methanol is mixed by magnetic stirring in the reactor vessel and then is added a little quantity of double distilled water to help the nucleation.

When the potassium hydroxide is completely dissolved the first solution is added to the second in the reactor vessel and the resulting solution is placed into a microwave oven at 60 °C for 30 minutes at a pressure of maximum 10 bar.

The product, i.e. the nanoparticles, is then centrifuged at 5'000 rpm (3500 g) for 10 minutes to remove methanol. 15 ml of ethanol are added to disperse the pellet and then the solution is again centrifuged at 5'000 rpm for 10 minutes. After the two washing steps the pellet is resuspended in fresh ethanol. [48]

Using this protocol, it is possible to obtain single crystal ZnO nanoparticles with spherical morphology, dimensions between 16 and 25 nm and stable in ethanol suspension.

3.2.2 Functionalization of zinc oxide nanoparticles with amino groups

The characterization of TNH is mainly based on fluorescence microscopy, therefore the possibility of attaching fluorescent dyes to ZnO nanoparticles is essential. This possibility is given by the functionalization with amino groups (NH_2).

The functionalization is carried out combining ZnO nanoparticles with APTMS 3-aminopropyltrimethoxysilane (97%, Sigma Aldrich). 100 mg (1.23 mmol) of ZnO nanoparticles dispersed in ethanol are stirred at 78°C in a 100 ml flask under nitrogen gas flow. After 15 minutes 21.4 µl of APTMS (corresponding to 0.123 mmol (22.05 g), corresponding to 10 mol% of total ZnO amount) are added to the solution and then refluxed for 6 hours under nitrogen flow.

Then the functionalized nanoparticles are washed two times to remove the unbound APTMS molecules. [48]

3.2.3 Labelling of zinc oxide nanoparticles with fluorescent dyes

Atto550 / Atto633

The functionalization of ZnO with amino groups allows to label the nanoparticles with dyes in order to detect them with a fluorescence microscopy.

ZnO – NH_2 nanoparticles are coupled with ATTO550-NHS (Thermofischer) or ATTO633-NHS (Thermofischer) ester dyes, at a ratio of 2 μg per mg of nanoparticles. The solution in ethanol is kept in the dark under continuous stirring overnight, then it is washed two times by centrifuging and resuspending the pellet in fresh ethanol to remove unbounded dye molecules. [48]

Calcein

The functionalization of ZnO with calcein allows to have a hydrophilic dye weakly bound to the nanoparticles that could be released in aqueous solution.

A solution 1 μM of calcein is prepared dissolving 3.11 mg of calcein in 5 ml of water. Then the ZnO nanoparticles are labelled placing in an Eppendorf vial 33 μg of ZnO in ethanol and 100 μl of calcein solution and leaving them mixing under magnetic stirring in dark for 1 hour. After that the solution obtained is centrifuged at 10'000 rcf for 5 minutes and the pellet is resuspended in 200 μl of water to remove the excess of calcein.

3.2.4 ZnO Characterization

Dynamic Light Scattering (DLS)

The DLS characterization allows to have an average measure of the nanoparticle size diameter, and the dispersion of the nanoparticles in the solution. It could be carried out in different medium, ethanol, water and PBS.

Measurements are carried out with Zetasizer Nano ZS90.

Z-Potential

This characterization is carried out with the same instrument of the DLS, but with a specific cuvette equipped with two electrodes that produce an electric field which crosses the sample.

Z-potential is a measure of the surface charge of the nanoparticles inside a specific solvent.

Transmission Electron Microscopy (TEM)

TEM images are acquired spotting the sample on a grid as described above and imaged at 200 kV.

Field Emission Scanning Electron Microscopy (FESEM)

FESEM provides topographical and elemental information about the sample. The sample is prepared by spotting the solution of interest on a wafer of silica, left to dry and then put on a stub.

Nanoparticle Tracking Analysis (NTA)

ZnO is also characterized with the NanoSight in order to have the concentration of the solution. This is useful because the coupling between exosomes and ZnO is a ratio 1:1, so there is the need to know the number of nanoparticles/ml.

3.3 Synthesis of labelled Mesoporous Silica nanoparticles (MCM-41)

3.3.1 Synthesis

The MCM41 nanoparticles are synthesized already labelled with two different fluorescent dyes: rhodamine and fluorescein in order to allow the use of fluorescence microscopy. The process for the fluorescein-labelled nanoparticles and the rhodamine-ones is exactly the same.

A solution containing 1 mg of fluorescent dye (rhodamine or fluorescein isothiocyanate), 2.2 µl (3-Aminopropyl)triethoxysilane (APTES) and ethanol is mixed with magnetic stirring for 2 hours.

In a round bottom flask, 1 g of Hexadecyltrimethylammonium bromide (CTAB)(≥ 98%, Sigma Aldrich), 480 ml of milliQ water and 3.5 ml of sodium hydroxide (NaOH, 2M) are mixed with magnetic stirring at 250 rpm in a silicon oil bath at 80 °C for 45 minutes. In this passage CTAB is forming micelles in water environment.

After that, 5 ml of tetraethyl orthosilicate (TEOS) and the solution with the dye are added in the flask through a syringe and an injector with a rate of 250 ml/min and the magnetic stirring continues for two hours. Here the TEOS, which is a silica precursor, deposits around micelles to form the nanoparticles. The stirring time is very important for the dimension of the nanoparticles, beyond two hours nanoparticles become too big.

After two hours the solution is cooled down, then three washing steps are made: they all start with a centrifugation step at 9'000-11'000 rpm for 10-15 minutes, then the supernatant is removed and in the first step milliQ water is added, in second ethanol and in the third 400 ml of extraction solution. The extraction solution is made with 10 g of ammonium nitrate, 50 ml of milliQ water and 950 ml of ethanol.

The solution in the glass flask is heated by a silicon oil bath at 80 °C with a magnetic stirring at 450 rpm overnight in order to remove CTAB.

Another washing step is made with 400 ml of extraction solution and the new solution is left in silicon bath oil at 80 °C with magnetic stirring at 450 rpm for 2 hours.

The obtained solution is cooled down and then there are three washing steps with centrifugation and re-suspension firstly in milliQ water, secondly in ethanol and then in ultra-pure ethanol.

3.3.2 Mesoporous Silica Characterization

Transmission Electron Microscopy (TEM)

The MSNs produced are analyzed with TEM. The nanoparticles are suspended in ethanol, so the solution is spotted on a TEM copper grid with holey carbon film and dried. Just before the measurement, the samples are stained with a solution of 1% of Phosphotugstic Acid (PTA) to label organic materials, in order to know if there is surfactant left. The staining is carried out putting the grids on a drop of PTA solution for 30 seconds on one side and then the same for the other side.

The images are acquired with a JEOL TEM 3000 instrument operated at 300 kV.

DLS and Z-Potential

The measurement of DLS and Z-potential are carried out in two different media: water and PBS.

MCM-41 nanoparticles are centrifuged at 10'000 rpm for 10 minutes to discard ethanol and they are resuspended in water or PBS. The solution is placed inside the cuvettes for the Z-potential and the measure is carried out using a Zetasizer Nano ZS90.

Thermogravimetry (TG)

A thermogravimetric analysis is carried out to verify the high quality of the synthesis. Obtaining MCM-41 nanoparticles of good quality is possible only when the surfactant is almost totally removed from the pores. For this analysis a Perkin-Elmer Pyris Diamond TG/DTA analyser is used. The instrument works like a balance: the sample is placed in an aluminium plaquette, the machine weights

the sample, leads the nanoparticles at 600°C and then it measures the final weight. In this way it's possible to obtain the percentage weight loss which represents the quantity of surfactant left inside the sample.

Infrared spectroscopy analysis

To evaluate the presence of Si-OH and NH_2 groups and Rhodamine, an infrared spectroscopy analysis is carried out.

Fourier Transformed Infrared (FTIR) spectra were obtained in a Nicolet (Thermo Fisher Scientific) Nexus spectrometer equipped with a Smart Golden Gate Attenuated Total Reflectance (ATR) accessory [49].

Physical adsorption of Nitrogen (BET)

BET (Brunauer, Emmett and Teller) analysis is useful to evaluate the specific surface area and the average size and distribution of the pores. The sample is dried with nitrogen purging or in vacuum applying elevated temperatures. Then the volume of gas adsorbed to the surface of the particles is measured at the boiling point of nitrogen (77 K). The amount of the absorbed gas is correlated to the surface area of the particles, including the pore volume and the pore diameter. The calculation is based on BET theory.

3.4 Coupling Exosomes with zinc oxide nanoparticles (TNH)

3.4.1 Coupling

The construction of TNHs passes through the coupling between exosomes and ZnO nanoparticles.

The topic of this thesis is to find the better coupling protocol, for this reason there are many different protocols listed below. All these protocols have some common features.

It is necessary to calculate the right amount of ZnO nanoparticles to be coupled with one vials of exosomes. The coupling ratio between ZnO Nps and exosomes is 1:1 in number, that is in one aliquot of ZnO there are the same number of particles as the number of exosomes in one vial. The number of particles per ml was estimated by NTA assays. The calculations used are:

$$n°of\ exosomes * 50\ \mu l = \text{n° of exosomes in one vial (50 µl)}$$

$$n°of\ exosomes\ in\ one\ vial : amount\ of\ ZnO\ NPs = n° \frac{particles}{ml} ZnO : 1\ ml$$

$$amount\ of\ ZnO\ NPs = \frac{n°of\ exosomes\ in\ one\ vial}{n° \frac{particles}{ml} ZnO}\ [\mu l]$$

The coupling process is carried out following these steps:

- Bidistilled water is filtered with filters with pore's diameter of 2.2 µm
- PBS, or physiologic solution, depending on the suspension medium of exosomes, is filtered with filters with pore's dimeter of 2.2 µm
- A solution of water and PBS (or Physiologic solution) with a ratio of 1:1 is prepared
- One vial (50 µl) of exosomes (from KB or DAUDI cells in PBS or Physiologic solution) is thawed out from -80°C.

- In an eppendorf, as much water as the content of the exosomes vial is added (usually 50 µl)
- One aliquot of ZnO nanoparticles is added in the same eppendorf.
- The thawed content of a vial of exosomes is added in the same eppendorf
- The eppendorf is put under stirring under different conditions
- Before the stirring finishes, 0.5 µl of DiO solution (ratio 1:100, DiO dissolved in DMSO) is added and let under stirring for at least 30 minutes in order to label the exosomes for the fluorescent microscope.
- The solution after different time of stirring is centrifuged and the pellet and the supernatant are separated
- 100 µl of the solution of water and PBS (physiologic solution) is added to the pellet and it is dispersed. This is called Run 1
- The supernatant should be eventually reused to do another step of coupling (Run 2, 3…), by adding one aliquot of ZnO Nps to the supernatant and the process of mixing is repeated.

PBS is a solution usually used to simulate the human body fluids in experimental research. It is a water-based salt solution made of phosphate buffer, sodium chloride and potassium chloride

Physiologic solution is a watery solution of sodium chloride with a ratio of 0.9%.

Table 1: Coupling details of zinc oxide nanoparticles and exosomes

Sample	Exosomes (in PBS)	Run	ZnO nps (SC6-NH_2 atto550)	Coupling conditions	Post-coupling treatment
TNH 12	KB 07/07/2017	Run 1	1 aliquot (1.89 µl)	Orbital shaker 250 rpm, RT, 90'. Centrifuge 16870 g, 5'.	/
		Run 2	1 aliquot (1.89 µl)	Orbital shaker 250 rpm, RT, 90'. Centrifuge 16870 g, 5'.	
TNH 13	KB 28/06/2017	Run 1	1 aliquot (1.73 µl)	Orbital shaker 250 rpm, RT, 90'. Centrifuge 16870 g, 5'.	Centrifuge 16870 g, 5'. Resuspended in 100 µl EMEM. In incubator, 37°C, 24 h
		Run 2	1 aliquot (1.73 µl)	Orbital shaker 250 rpm, RT, 90'. Centrifuge 16870 g, 5'.	/
TNH 14	KB 28/06/2017	Run 1	1 aliquot (1.73 µl)	Wheel, overnight. Centrifuge 18870 g, 5'.	/
TNH 15	KB 28/06/2017	Run 1	1 aliquot (1.73 µl)	Orbital shaker 250 rpm, RT, 90'. Centrifuge 16870 g, 5'.	Combination of Run 1 and Run 2. Stored at 4°C for 4 days.
		Run 2	1 aliquot (1.73 µl)	Orbital shaker 250 rpm, RT, 90'. Centrifuge 16870 g, 5'.	

Sample	Exosomes (in PBS)	Run	ZnO nps (SC6-NH_2 atto550)	Coupling conditions		Post-coupling treatment	
TNH 16	KB 28/06/2017	Run 1	1 aliquot (1.73 µl)	Wheel, 90'. Centrifuge 16870 g, 5'.		/	
		Run 2	1 aliquot (1.73 µl)	Wheel, 90'. Centrifuge 16870 g, 5'.			
TNH 17	KB 28/06/2017	Run 1	1 aliquot (1.73 µl)	Orbital shaker 250 rpm, RT, 90'. Centrifuge 16870 g, 5'.		US 40 kHz, 30'	
		Run 2	1 aliquot (1.73 µl)	Orbital shaker 250 rpm, RT, 90'. Centrifuge 16870 g, 5'.		+ 900 µl EMEM Orbital shaker 250 rpm, 37°C, 24 h	
TNH 18	KB 28/06/2017	Run 1	1 aliquot (1.73 µl)	Orbital shaker 250 rpm, 37°C, 90'. Centrifuge 16870 g, 5'.		US 40 kHz, 30'	
		Run 2	1 aliquot (1.73 µl)	Orbital shaker 250 rpm, 37°C, 90'. Centrifuge 16870 g, 5'.	+ 900 µl EMEM Orbital shaker 250 rpm, 37°C, 24 h	US 40 kHz, 30'	Stored at 4°C for 5 days
TNH 19	KB 28/06/2017	Run 1	1 aliquot (1.73 µl)	Orbital shaker 250 rpm, 4°C, 90'. Centrifuge 16870 g, 5'.		/	
		Run 2	1 aliquot (1.73 µl)	Orbital shaker 250 rpm, 4°C, 90'. Centrifuge 16870 g, 5'.			
TNH 20	KB 07/07/2017	Run 1	1 aliquot (1 µl)	Orbital shaker 250 rpm, 37°C, 8 h. Centrifuge 16870 g, 5'.		US 40 kHz, 30'	
TNH 21	KB 07/07/2017	Run 1	10 aliquots (10 µl)	Orbital shaker 250 rpm, 37°C, 8 h. Centrifuge 16870 g, 5'.		US 40 kHz, 30'	
TNH 22	KB 07/07/2017	Run 1	1 aliquot (1 µl)	Orbital shaker 250 rpm, 37°C, 24 h. Centrifuge 16870 g, 5'.		US 40 kHz, 30'	
TNH 23	DAUDI 24/11/2017	Run 1	1 aliquot (0.94 µl) (dilution 1:5)	Orbital shaker 250 rpm, 37°C, 24 h. Centrifuge 16870 g, 5'.		US 40 kHz, 30'	
TNH 24	DAUDI 24/11/2017 (Physiologic solution)	Run 1	1 aliquot (1.14 µl) (dilution 1:5)	Orbital shaker 250 rpm, 37°C, 24 h. Centrifuge 16870 g, 5'.		US 40 kHz, 30'	

Sample	Exosomes (in PBS)	Run	ZnO nps (SC6-NH_2 atto550)	Coupling conditions	Post-coupling treatment	
TNH 25	KB 07/07/2017	Run 1	3 aliquots (1+1+1 µl)	Orbital shaker 250 rpm, 37°C, 3 h. 1 aliquot of nanoparticles added at t=0, t=1h, t=2h. Centrifuge 16870 g, 5'.	Orbital shaker, 160 rpm, 37°C, 24 h	+ 900 µl PBS Stored at 37°C for 24 h.
		Run 2	3 aliquots (1+1+1 µl)	Orbital shaker 250 rpm, 37°C, 3 h. 1 aliquot of nanoparticles added at t=0, t=1h, t=2h. Centrifuge 16870 g, 5'.	Orbital shaker, 160 rpm, 37°C, 24 h	+ 900 µl PBS Stored at 4°C for 24 h.
TNH 26	KB 07/07/2017	Run 1	1 aliquot (1 µl)	Orbital shaker 250 rpm, 37°C, 24 h. 100 µl water and PBS (1:1) + 900 µl EMEM. Centrifuge 16870 g, 5'.	US 40 kHz, 30' in 1 ml of EMEM.	
TNH 27	KB 07/07/2017	Run 1	5 aliquots (1+1+1+1+ 1 µl)	Orbital shaker 250 rpm, 37°C, 24 h. 100 µl water and PBS (1:1) + 900 µl EMEM. 1 aliquot of nanoparticles added at t=0, t=1h, t=2h, t=3h, t=4h. Centrifuge 16870 g, 5'.	US 40 kHz, 30' in 1 ml of EMEM.	
TNH 28	KB 07/07/2017	Run 1	1 aliquot (1 µl)	US 40 kHz, 37°C, 30'	/	
TNH 29	KB 07/07/2017	Run 1	3 aliquots (1+1+1 µl)	Orbital shaker 250 rpm, 37°C, 3 h. 1 aliquot of nanoparticles added at t=0, t=1h, t=2h. Centrifuge 16870 g, 5'.	US 40 kHz, 37°C, 30'	
TNH 30	KB 07/07/2017	Run 1	1 aliquot (1 µl)	US 59 kHz, 37°C, 30'	/	
TNH 31	KB 07/07/2017	Run 1	1 aliquot (1 µl)	US 1 MHz, 37°C, few seconds	/	
TNH 32	KB 07/07/2017	Run 1	1 aliquot (1 µl)	Orbital shaker 250 rpm, 37°C, 90'. Centrifuge 16870 g, 5'.	US 40 kHz, 37°C, 30'	
TNH 33	KB 07/07/2017	Run 1	1 aliquot (1 µl)	US 40 kHz, 37°C, 30'	/	

Sample	Exosomes (in PBS)	Run	ZnO nps (SC6-NH_2 atto550)	Coupling conditions		Post-coupling treatment	
TNH 34	KB (Physiologic solution) 22/12/2017 (25 µl)	Run 1	1/2 aliquot (2 µl)	Orbital shaker 250 rpm, 37°C, 90'.		/	
				½ centrifuged at 7500 g, 5'.	½ centrifuged at 5000 g, 5'.		
TNH 35	KB (Physiologic solution) 22/12/2017	Run 1	1 aliquot (4 µl)	Orbital shaker 250 rpm, 37°C, 90'. Centrifuge 5000 g, 5'.		/	
		Run 2	1 aliquot (4 µl)	Orbital shaker 250 rpm, 37°C, 90'. Centrifuge 5000 g, 5'.			
		Run 3	1 aliquot (4 µl)	Orbital shaker 250 rpm, 37°C, 90'.			
TNH 36	KB (Physiologic solution) 22/12/2017	Run 1	1 aliquot (4 µl)	Orbital shaker 250 rpm, 37°C, 90'. Centrifuge 5000 g, 5'.		Combination of Run 1 and Run 2 (total volume 200 µl). 100 µl US 40 kHz, 37°C, 30'	Union of Run 1 and Run 2 (total volume 200 µl). 100 µl + 400 µl PBS and centrifuge 2000 g, 5'.
		Run 2	1 aliquot (4 µl)	Orbital shaker 250 rpm, 37°C, 90'. Centrifuge 5000 g, 5'.			
		Run 3	1 aliquot (4 µl)	Orbital shaker 250 rpm, 37°C, 90'.		US 40 kHz, 37°C, 30'. Centrifuge 7500 g, 5'.	
TNH 37	KB (Physiologic solution) 22/12/2017	Run 1	1 aliquot (4 µl)	Orbital shaker 250 rpm, 37°C, 90'. Centrifuge 5000 g, 5'.		/	
		Run 2	1 aliquot (4 µl)	Orbital shaker 250 rpm, 37°C, 90'. Centrifuge 5000 g, 5'.			
		Run 3	1 aliquot (4 µl)	Orbital shaker 250 rpm, 37°C, 90'. Centrifuge 7500 g, 5'.			
TNH 38	DAUDI 24/11/2017	Run 1	1 aliquot (0.72 µl)	Orbital shaker 250 rpm, 37°C, 90'. Centrifuge 5000 g, 5'.		/	
		Run 2	1 aliquot (0.72 µl)	Orbital shaker 250 rpm, 37°C, 90'. Centrifuge 5000 g, 5'.			

Sample	Exosomes (in PBS)	Run	ZnO nps (SC6-NH_2 atto550)	Coupling conditions	Post-coupling treatment
TNH 39	DAUDI 24/11/2017 (Physiologic solution)	Run 1	1 aliquot (0.87 µl)	Orbital shaker 250 rpm, 37°C, 90'. Centrifuge 5000 g, 5'.	/
		Run 2	1 aliquot (0.87 µl)	Orbital shaker 250 rpm, 37°C, 90'. Centrifuge 5000 g, 5'.	
TNH 40	DAUDI 24/11/2017	Run 1	1 aliquot (0.72 µl)	Orbital shaker 250 rpm, 37°C, 90'. Centrifuge 5000 g, 5'.	/
		Run 2	1 aliquot (0.72 µl)	Orbital shaker 250 rpm, 37°C, 90'. Centrifuge 5000 g, 5'.	
TNH 41	DAUDI 24/11/2017 (Physiologic solution)	Run 1	1 aliquot (0.87 µl)	Orbital shaker 250 rpm, 37°C, 90'. Centrifuge 5000 g, 5'.	/
		Run 2	1 aliquot (0.87 µl)	Orbital shaker 250 rpm, 37°C, 90'. Centrifuge 5000 g, 5'.	
TNH 42	DAUDI 24/11/2017	Run 1	1 aliquot D-glucose (1.44 µl)	Orbital shaker 250 rpm, 37°C, 90'. Centrifuge 5000 g, 5'.	/
TNH 43	DAUDI 24/11/2017 (Physiologic solution)	Run 1	1 aliquot D-glucose (1.74 µl)	Orbital shaker 250 rpm, 37°C, 90'. Centrifuge 5000 g, 5'.	/
TNH 47	KB (Physiologic solution) 21/02/2018 (1/2 aliquot)	Run 1	1/2 aliquot (1.5 µl) Atto 633	Orbital shaker 250 rpm, 37°C, 90'. Centrifuge 5000 g, 5'.	/
		Run 2	1/2 aliquot (1.5 µl) Atto 633	Orbital shaker 250 rpm, 37°C, 90'. Centrifuge 7500 g, 5'.	
TNH 48	KB (Physiologic solution) 21/02/2018 (1/2 aliquot)	Run 1	1/2 aliquot (1.5 µl) Atto 633	US 40 kHz, 20". Centrifuge 10000 g, 5'. Supernatant quitted and pellet resuspended in 45 µl physiologic solution. US 40 kHz, 20". Centrifuge 10000 g, 5'.	/

3.4.2 TNH Characterization

Fluorescence Microscopy

Each sample of TNH is characterized through fluorescence microscopy with co-localization method. The aim of this method is evaluating the percentage of coupling between exosomes and ZnO nanoparticles.

The images are acquired using the fluorescence microscope Nikon Eclipse TiE, which is fully automated and inverted wide-field optical microscope, equipped with a super bright wide spectrum Shutter Lambda XL source with a collection of four filter cubes. The system acquires the images with a high resolution (4098x3264 pixels) camera and using four objectives (4, 20, 40, 60x), DIC optics, a motorized stage (including piezo Z control) and a gas and temperature-controlled stage-top incubator for live-cell imaging acquisition.

The system operates with the NIS-element software.

Samples are prepared pipetting out from the solution of interest 3 µl for four times and depositing them drop by drop on the microscope slide, then the drops are covered with a cover-glass slip and it is fixed with common nail varnish.

ZnO are labelled with atto550 and exosomes with DiO, in this way images are acquired with the 60x immersion-oil objective and by exciting the dyes at two different wavelength channels: 550 nm (red, for atto 550) and 488 nm (green for DiO).

The software NIS-element is then used to analyse the co-localization, it counts the spots in red and then the spots in green and after that it makes an overlay of the two images and counts the spots presenting both colours.

The percentage of colocalization is calculated with this formula:

$$\%ZnO\ colocalized = \frac{n°\ NPs\ colocalized}{n°\ NPs\ ZnO}$$

$$\%\ Exosomes\ colocalized = \frac{n°\ NPs\ colocalized}{n°\ exosomes}$$

$$TNH = \frac{n°\ NPs\ colocalized}{n°\ NPs\ ZnO + n°\ exosomes - n°NPs\ colocalized}$$

Nanoparticle Tracking Analysis (NTA)

Some samples of TNH are analysed with NanoSight to have the possibility to compare the size distribution and the concentration of the TNH with the ones of exosomes and ZnO previously acquired.

Transmission Electron Microscopy (TEM)

The sample is prepared diluting the solution of TNH with a ratio of 1:10 in physiologic solution and depositing it on a TEM grid.

Field Emission Scanning Electron Microscopy (FESEM)

The sample is prepared by spotting the solution of interest on a wafer of silica, left to dry and then put on a stub.

3.5 Calcein release

This method is used to verify the effective coupling between ZnO and exosomes. ZnO nanoparticles are labelled with a fluorescent dye, calcein, which does not create strong chemical bonds with of ZnO, but just physically adsorb on its surface and can be easily dissolved in water.

For the experiment is used a common cuvette for the DLS, it is filled with water and it is covered with its top. Between the top and the cuvette is placed a dialysis membrane which separate water from the solution of interest put into the top. The membrane allows the diffusion of calcein in the water below and retains into the top the nanoparticles.

For the measurements a spectrofluorometer (Bruker NS5S) is used with different excitation and collection length depending on the fluorescence reported in Table 2.

Table 2: Excitation and collection lengths for different dyes

Dye	Excitation length (nm)	Collection length (nm)
Calcein	488	500-800
Atto550	550	570-800

Every sample is prepared pouring 4 ml of water in the cuvette, placing the top covered with the dialysis membrane on the cuvette and putting 200 µl the solution of interest in the top through a little hole.

The solution analysed are reported in Table 3.

Table 3: Solution of interest analysed

Solution	Preparation
Calcein (1 µM) in water	Dissolving 3.11 mg of calcein in 5 ml of water
ZnO nps with atto550	Solution of ZnO nanoparticles in ethanol
ZnO Nps labelled with atto550 and with calcein	Solution in water of ZnO nanoparticles labelled with atto550 and calcein
ZnO Nps with calcein coated with DOPC	The preparation steps are the same for the labelling of ZnO with calcein, but after the centrifugation, the pellet is resuspended with 8.25 µg of DOPC and 50 µl of water. Then the solution is centrifuged at 10'000 rcf for 5 minutes and the pellet is dispersed in 200 µl of water.
ZnO Nps with calcein coated with FBS exosomes	A solution is made adding 33 µg of ZnO nanoparticles, 100 µl of calcein solution, 95 µl of PBS and 5 µl of exosomes from FBS in PBS. The solution is left for 90 minutes on an orbital shaker at 250

	rpm. Then it is centrifuged at 16’870 rcf for 5 minutes and the pellet is dispersed in 200 µl of water and PBS (1:1).

In the solutions with DOPC and exosomes, at the end of the measurements, 100 µl of ethanol or Triton X are added to disassemble the lipid membranes and releasing all the calcein left.

3.6 Coupling Exosomes with Mesoporous Silica nanoparticles

3.6.1Coupling

The coupling between MSNs and exosomes is carried out without knowing the exact number of particles because of the lack of a device for nanoparticles tracking analysis (NTA) in the Madrid’s laboratories.

The coupling is carried out following two different protocols: the first one is very similar to the one used for TNH, while the second is used in the laboratory of Madrid to produce Protocells with liposomes and MSNs [50].

The two coupling processes have some steps in common:

- Bi-distilled water is filtered with filters with pore’s dimeter of 2.2 µm
- PBS is filtered with filters with pore’s dimeter of 2.2 µm
- A solution of water and PBS with a ratio of 1:1 is made
- Since the solvent of each type of MSNs is ethanol, they are centrifuged (20’627 rcf, 10’) and dried for one night
- 3 mg of MSNs are weighted and they are resuspended in microfiltered water
- One vial (50 µl) of exosomes is thawed out from -80°C.

Protocol 1:

- The right quantity of nanoparticles is placed in an eppendorf, usually maintaining a ratio of 4:1 with exosomes, unless otherwise specified.
- In the eppendorf exosomes in PBS are added.
- The solution is mixed for 90 minutes on an orbital shaker, at 200 rpm and 37 °C
- If fluorescence is required, to label the exosomes, 1 µl of DiO (1:100) for 50 µl is added 30 minutes before the end of this process
- The solution is centrifuged at 15’000 rpm (20627 rcf) for 10 minutes and the supernatant is removed
- The same volume of the supernatant of water and PBS (1:1) is added to the pellet and it is dispersed.
- It is sonicated at 40 kHz for 30 minutes. This is called Run 1
- The supernatant should be eventually reused to do another step of coupling (Run 2), by adding another aliquot of MSNs to the supernatant and the process of mixing is repeated.

Protocol 2:

- If fluorescence is required, to label the exosomes, 50 µl of exosomes and 1 µl of DiO (1:100) are mixed for 30 minutes on an orbital shaker at 200 rpm and 37°C before starting the coupling.

- The right quantity of nanoparticles is placed in an eppendorf, usually maintaining a ratio of 4:1 with exosomes, unless otherwise specified.
- In the eppendorf exosomes in PBS (with or without DiO) are added.
- The solution is sonicated at 40 kHz for 20 seconds
- It is centrifuged at 15'000 rpm (20627 rcf) for 10 minutes and the supernatant is removed
- The same volume of the supernatant of PBS is added to the pellet and it is dispersed.
- The process of sonication and centrifugation is repeated another time.

Table 4: Coupling details of mesoporous silica nanoparticles and exosomes

Sample	Run	Exosomes (in PBS)	MSNs	DiO	Protocol
MSN+EXO 1	Run 1	25 µl from FBS	25 µl labelled with Rhodamine	No	1
	Run 2	Supernatant from Run 1	6.25 µl labelled with Rhodamine		1
MSN+EXO 2	Run 1	25 µl from FBS	12.5 µl labelled with Rhodamine	No	1
	Run 2	Supernatant from Run 1	12.5 µl labelled with Rhodamine		2
MSN+EXO 3	Run 1	25 µl from FBS	25 µl labelled with Rhodamine	Yes	1
MSN+EXO 4	Run 1	25 µl from FBS	25 µl labelled with Rhodamine	Yes	2
MSN+EXO 5	Run 1	12.5 µl from KB (28/04/2017)	50 µl labelled with Rhodamine	No	1
MSN+EXO 6	Run 1	12.5 µl from KB (28/04/2017)	50 µl labelled with Rhodamine and loaded with fluorescein	No	1
MSN+EXO 7	Run 1	12.5 µl from KB (28/04/2017)	50 µl labelled with Rhodamine	No	2
MSN+EXO 8	Run 1	12.5 µl from KB (28/04/2017)	50 µl labelled with Rhodamine and loaded with fluorescein	No	2

Sample	Run	Exosomes (in PBS)	MSNs	DiO	Protocol
MSN+EXO 9	Run 1	12.5 µl from KB (07/07/2017)	50 µl labelled with Fluorescein	Yes	1
MSN+EXO 10	Run 1	12.5 µl from KB (07/07/2017)	50 µl labelled with Fluorescein	Yes	2
MSN+EXO 11	Run 1	50 µl from FBS	200 µl labelled with Fluorescein	No	1
MSN+EXO 12	Run 1	50 µl from KB (07/07/2017)	100 µl labelled with Rhodamine	Yes	1
MSN+EXO 13	Run 1	150 µl from HeLa cells extracted with kit	300 µl labelled with Rhodamine and loaded with Fluorescein	No	1
MSN+EXO 14	Run 1	25 µl from HeLa cells extracted with kit	100 µl labelled with Fluorescein	Yes	1
MSN+EXO 15	Run 1	25 µl from HeLa cells extracted with kit	100 µl labelled with Fluorescein	Yes	2

3.6.2 MSN+EXO Characterization

DLS and Z-Potential

The samples for DLS and Z-Potential are prepared using MSN+EXO 1 Run 1 and 2 and MSN+EXO 2 Run 1 and 2 (coupling details in Table 4). After that, water and PBS (1:1) added to reach 1 ml for each solution. They are placed inside the cuvettes for the Z-potential and the measure is carried out using a Zetasizer Nano ZS90.

Transmission Electron Microscopy (TEM)

MSN+EXO 1, 2, 5 and 7 are analyzed with TEM. The samples are prepared suspending 20 µl of the sample in 180 µl of PBS and water (1:1) to maintain a concentration of 1:10. Then the solution obtained is spotted on a TEM grid and left to dry. Just before the measurement, the samples are stained with a solution of 1% of Phosphotugstic Acid (PTA) to label organic materials, like exosomes. The staining is carried out putting the grids on a drop of PTA solution for 30 seconds on one side and then the same for the other side.

The images are acquired with a JEOL TEM 3000 instrument operated at 300 kV.

Internalization and release of fluorescein inside HeLa cells

The main idea of this process is verifying the covering of the MSNs with exosomes by loading the nanoparticles with fluorescein and checking its release inside the cells. If this method has positive results it means that the lipid layer is formed around the nanoparticles, it is stable enough until the internalization in the cells and it also enhances the uptake.

MSNs labelled with rhodamine and loaded with fluorescein are prepared adding a solution of fluorescein and PBS with a concentration of 20 mg/ml to 10 mg of MSNs labelled with rhodamine and leaving the solution under magnetic stirring overnight. Then four washing steps (centrifuging at 20627 g for 10 minutes and resuspending the pellet in fresh PBS) are carried out and the nanoparticles are dried, to avoid fluorescein release, in vacuum at 30 °C. Before the use they are resuspended in water with a concentration of 3 mg/ml.

These nanoparticles loaded with fluorescein are used for the coupling with exosomes. The results are two different solution, from the two protocols, called MSN+EXO 6 and MSN+EXO 8, for the coupling details, see Table 4.

MSN+EXO 6 and 8 are centrifuged to eliminate the supernatant of water and PBS and they are resuspended in 1.5 ml of culture medium each. The solutions obtained have a concentration of 100 µg/ml of MSNs.

Four wells have been previously seeded with HeLa cells. When the cells reach the confluency, the culture medium is removed and the medium with the nanoparticles from MSN+EXO 6 and MSN+EXO 8 is added. In particular, 750 µl of medium and nanoparticles is added in each well in order to have two wells with the medium from MSN+EXO 6 and two with the one from MSN+EXO 8. The multiwells plate is placed inside an incubator at 37°C and 5% of CO_2.

After two hours, the medium from two wells (one with the nanoparticles from MSN+EXO 6 and one with the ones from MSN+EXO 8) is removed and it is replaced with the same volume of clear medium. Then the cells are analysed using a fluorescence microscope. The aim is to check the internalization of the MSNs (in red) inside the cells and eventually the release of fluorescein inside and outside the cells.

This process is repeated for the two wells left with the medium with the nanoparticles after 24 h.

In Figure 3.3 is shown the organization of the wells in the culture plate.

Figure 3.3: Organization of wells for the internalization and release of fluorescein inside HeLa cells

750 µl Medium + MSN+EXO 6 2h	750 µl Medium + MSN+EXO 8 2h
750 µl Medium + MSN+EXO 6 24h	750 µl Medium + MSN+EXO 8 24h

Flow cytometry – internalization inside HeLa cells

This method is used to evaluate the selective uptake of MSN+EXO nanoparticles inside the cells.

Before starting the experiment, HeLa cells have been seeded inside 12 wells. Then the culture medium is removed from the wells and it is substituted by fresh medium for the control (cells only), medium with MSNs labelled with fluorescein for the negative control and medium with MSN(labelled with fluorescein)+EXO. All the samples are performed in triplicates.

Two experiments are carried out with the same steps, but for the first one MSN+EXO 9 and 10 are used, and for the second MSN+EXO 14 and 15. In the first one the solutions have a concentration of 50 μg/ml of nanoparticles, while the second of 100 μg/ml.

Control	Control	Control
MSNs (50 μg/ml)	MSNs (50 μg/ml)	MSNs (50 μg/ml)

MSN+EXO 9 (50 μg/ml)	MSN+EXO 9 (50 μg/ml)	MSN+EXO 9 (50 μg/ml)
MSN+EXO 10 (50 μg/ml)	MSN+EXO 10 (50 μg/ml)	MSN+EXO 10 (50 μg/ml)

Control	Control	Control
MSNs (100 μg/ml)	MSNs (100 μg/ml)	MSNs (100 μg/ml)

MSN+EXO 14 (100 μg/ml)	MSN+EXO 14 (100 μg/ml)	MSN+EXO 14 (100 μg/ml)
MSN+EXO 15 (100 μg/ml)	MSN+EXO 15 (100 μg/ml)	MSN+EXO 15 (100 μg/ml)

Figure 3.4: Organization of the different wells in the first experiment (above) and in the second (below)

The wells plates are left in the incubator for the uptake for 2 hours at 37 °C and 5% of CO_2. After this time, the medium is removed from all wells and cells are washed with PBS to eliminate all the medium residual because they can inactivate trypsin. Then 500 μl of trypsin (trypsin EDTA, 0.05%, Sigma Aldrich) are added in each well, and after 5 minutes in incubator, cells should be totally detached from the substrates. Trypsin is neutralized adding 500 μl of medium and the contents of the wells are moved inside 12 eppendorf. They are centrifuged at 1500 rpm (206 rcf) for 5 minutes, the supernatant is removed and the pellet, which contains the cells, is resuspended in 250 μl of PBS and 50 μl of Trypan blue (Trypan blue solution, 0.4%, Thermofischer).

Measurements are carried out with BD FACSCaliber flow cytometer.

Stability

In this part of the thesis two different stability studies for MSNs covered by exosomes are carried out. The first one is conducted using the DLS, while the second is a study of stability in solution with the aid of an UV light.

The aim of the experiment with DLS is to evaluate the preservation of the hydrodynamic diameter of the nanoparticles with and without exosomes during the time and their eventual aggregation, while the purpose of the experiment with UV light is to evaluate the stability in suspension and confirm the eventual aggregation detected with DLS.

For both experiments the same coupling, MSN+ EXO 11, is used. After the process the sample is splitted in two aliquots of 150 μl with a concentration of 100 μg/ml of MSNs.

DLS

The first aliquot is used for the study of the stability through the DLS over time. 850 μl of water and PBS (1:1) are added to the 150 μl from the sample and the solution is placed inside a Z-potential cuvette. In

the same way, another sample is produced with 100 µl of MSNs naked suspended in 900 µl of water and PBS (1:1). As soon as the samples are ready, the measures are taken, placing the cuvettes inside the DLS and acquiring the measure with Zetasizer software. Then a measurement for each sample is acquired every hour for six hours at room temeprature, then after 24 and later each day until the tenth day. The measurements are obtained placing and removing the cuvettes from the instrument without turning them upside down and without shaking.

UV LIGHT

For this experiment the second aliquot is used and the samples are prepared in the same way of the ones for the DLS. The two samples, one with nanoparticles covered by exosomes and one with nanoparticles naked are poured in two cuvettes and they are placed in a dark room. Every hour for the first six hour and then after 24 hours they are enlightened with an UV light to underline the fluorescence (MSNs are labelled with fluorescein) and pictures are taken.

Confocal Microscopy

The experiment through confocal microscope allows to evaluate the internalization inside HeLa cells of the nanoparticles covered or not by exosomes.

After the coupling which produces MSN+EXO 12 (coupling details in Table 4), the samples for the confocal microscope are prepared.

MSN+EXO 12 (150 µl) and 100 µl of MSNs are centrifuged, the supernatants removed and they are resuspended in 2 ml di medium each. In both cases MSNs are labelled with rhodamine.

HeLa cells have been previously seeded in a chambered cell culture slide like the one in Figure 3.5. In each chamber 1 ml of medium with the different nanoparticles is added. In this way there are two chambers with the medium with naked MSNs and two with MSN+EXO 12.

Figure 3.5: Chambered culture slide

The cells are incubated in the chambers for 2 hours with the medium with nanoparticles, then the cells are labelled with DAPI, the chambers are removed and the cells with nanoparticles are fixed with ProLong Diamond Antifade Mountant (Thermofischer)

The confocal microscope used is the Olympus FV1200 (Electron Microscopy Centre, UCM).

Fluorescein release in transwell

The purpose of this experiment is to evaluate the quality of the exosomes cover on the MSNs. MSN are loaded with fluorescein inside, which is going to be released in PBS. The expectation is to see a gradual release from time 0 for the naked nanoparticles and a delayed release for MSNs covered by exosomes.

After the preparation of MSN+EXO 13 (coupling details in Table 4), they are suspended in PBS and the same is done for the MSNs naked. For both the samples MSNs labelled with rhodamine and loaded with fluorescein are used.

The transwell is a multiwell plate with an insert in each well. The insert has a porous membrane at the bottom which prevents the migration of the nanoparticles but allows the diffusion of fluorescein.

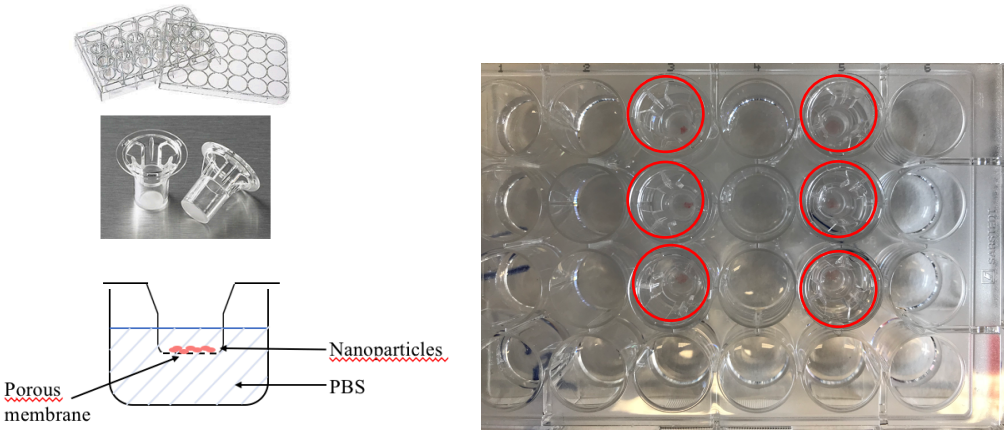

Figure 3.6: Transwell for fluorescein release

600 µl of PBS in each well and 100 µl of the solution with nanoparticles and PBS are poured. The samples are carried out in triplicates to have 3 wells with MSNs naked and 3 with MSN+EXO 13.

Every hour for 8 hours a day for 3 days the contents of the wells are collected, and the intensity of the fluorescein released is measured with a fluorescence microplate reader (Synergy HTX multi-mode microplate reader – BioTek Instruments).

4 Results and Discussion

4.1 Exosomes

In Figure 4.1 and Figure 4.2 there are four examples of the size distribution and concentrations obtained by the NanoSight and related to exosomes extracted from KB cell line and dispersed in either PBS or physiologic solution. Most of the exosomes of the solution have an average diameter around 100 nm, and there are peaks of bigger dimension which represent either larger vesicles or even aggregates.

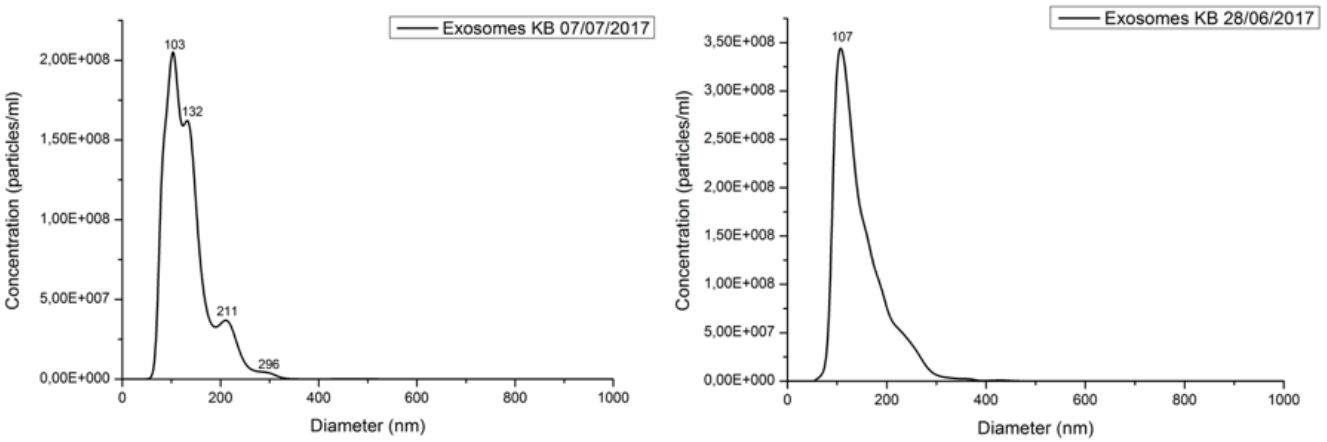

Figure 4.1: Two examples of the size distribution of exosomes from KB cells in PBS, obtained by the NanoSight

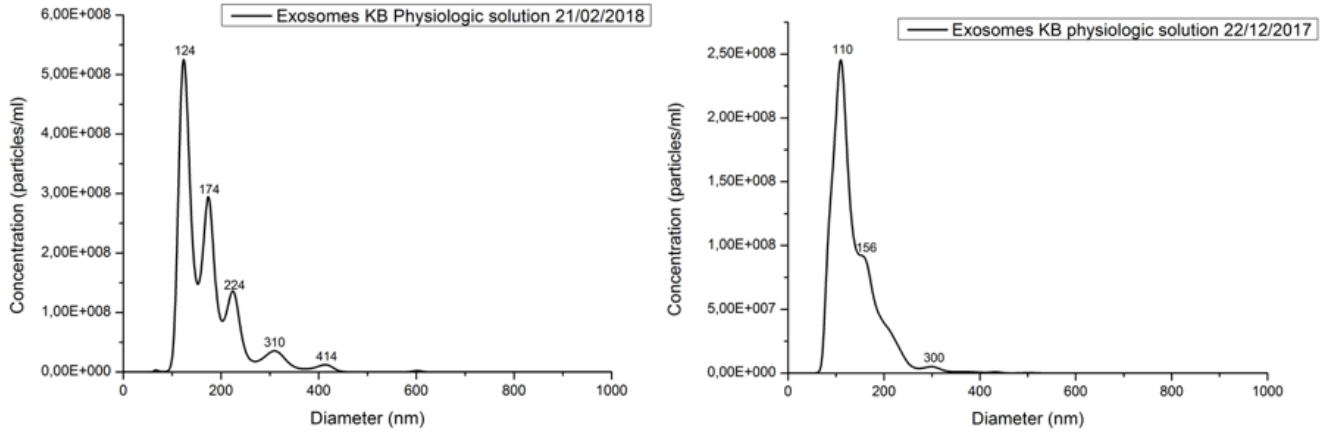

Figure 4.2: Two examples of the size distribution of exosomes from KB cells in physiologic solution, obtained by the NanoSight

Figure 4.3 reports the images of exosomes obtained with FESEM, while Figure 4.4 shows those obtained by TEM. The diameter is similar to the values obtained from the NanoSight.

Exosomes have a spherical shape which can be seen in both TEM and FESEM images, whereas the high voltage used to accelerate the electron beam of the TEM melt the organic materials, if they are not fixed, leading to aggregated structures, as visible for TEM characterization.

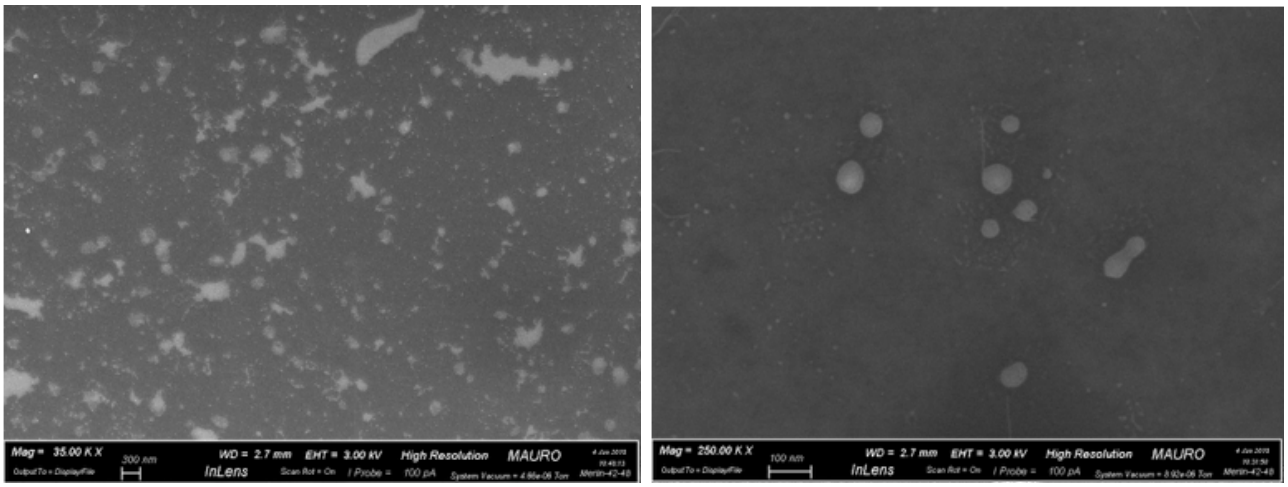

Figure 4.3: Images of exosomes obtained with FESEM

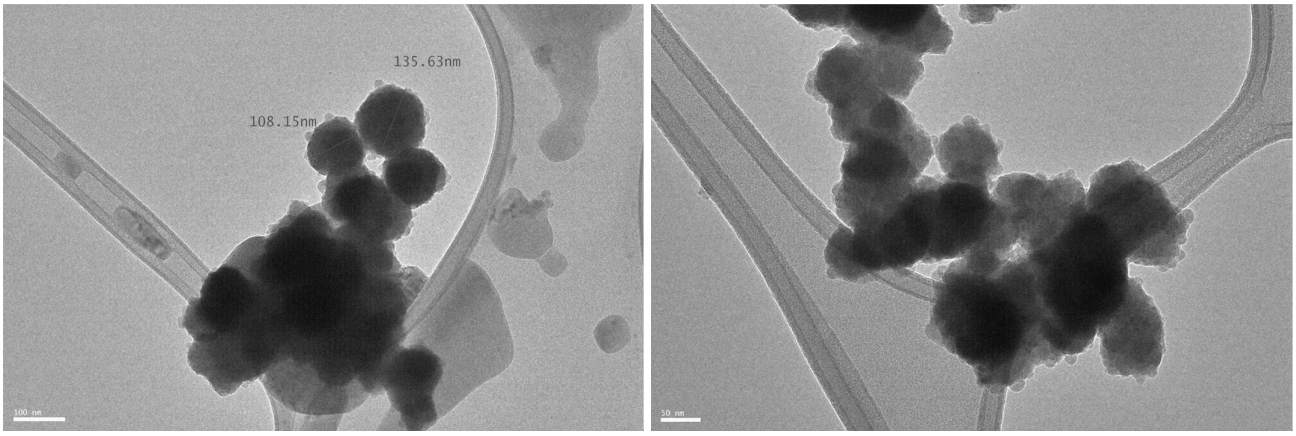

Figure 4.4: TEM images of exosomes

4.2 ZnO nanoparticles

In Figure 4.5, the size distributions and concentrations obtained with the NanoSight are reported. The average dimeter is bigger than the one measured with TEM because this is a measure of the light scattering on the single nanoparticles while it is moving under Brownian motion.

Figure 4.7 reports a TEM image of ZnO nanoparticles. It is possible to see the morphological aspect and the real size of these nanoparticles. They have a geometrical rounded shape, with diameters between 15 and 20 nm.

Furthermore, in Figure 4.6 the behaviour of nanoparticles in different media is shown. ZnO nanoparticles are usually stored in ethanol, where they are very well dispersed. In the other graphs, they are suspended in PBS or physiologic solution and in both these media, nanoparticles aggregates. From the results, it could be hypothesized that nanoparticles in physiologic solution aggregate with a slower rate than in PBS.

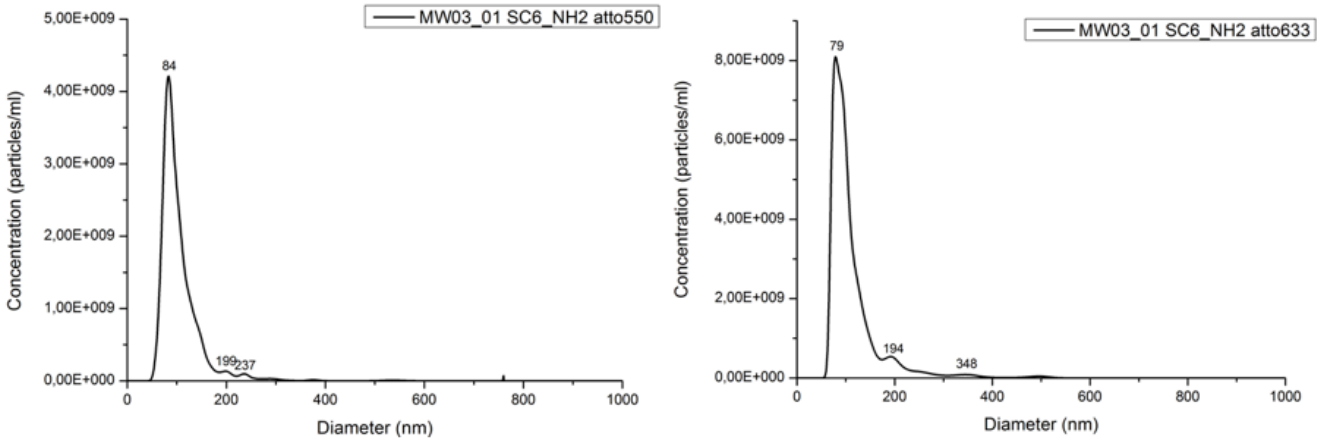

Figure 4.5: NanoSight analysis for ZnO nanoparticles

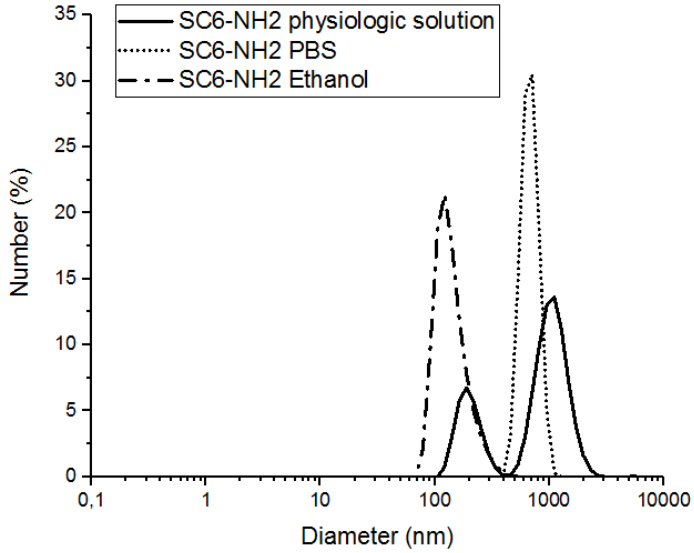

Figure 4.6: DLS of ZnO nanoparticles in different media

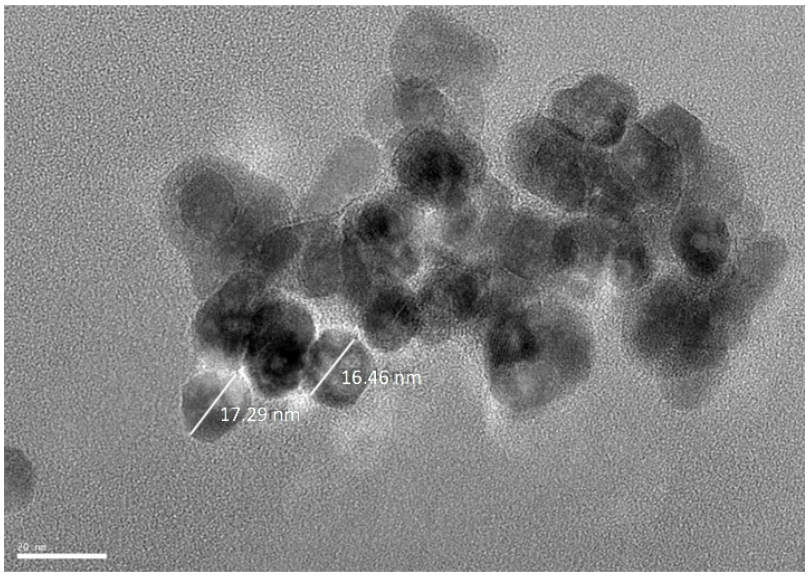

Figure 4.7: TEM image of ZnO nanoparticles

4.3 TNH

4.3.1 Analysis of TNH through fluorescence microscope

In the following list are reported the results of the coupling between exosomes and ZnO to obtain the various TNHs.

The co-localization percentages come from the processing of the images through the software of the fluorescence microscope.

A high percentage of ZnO colocalized is important to have a better internalization of ZnO inside the exosomes. This can further result in the ZnO penetration through the membrane of cancer cells and the accomplishment its therapeutic function. At the same time, less pristine ZnO results in body fluids reducing the risk of aggregation of the nanoparticles and their dissolution in potentially cytotoxic Zn^{2+} cations.

A little less problematic, but also important, is the percentage of exosomes coupled with ZnO. If the majority of the exosomes are coupled implies that the coupling is successful.

- **TNH 12**

	Sample	Conditions	% ZnO colocalized (%)	% Exosomes colocalized (%)	% particles colocalized (%)
TNH 12	Run 1	KB, Orbital Shaker 250 rpm, RT, 90'. Centrifuge 16870 g, 5'	23.47	40.62	17.06
	Run 2	KB, Orbital Shaker 250 rpm, RT, 90'. Centrifuge 16870 g, 5'	18.32	15.77	8.60

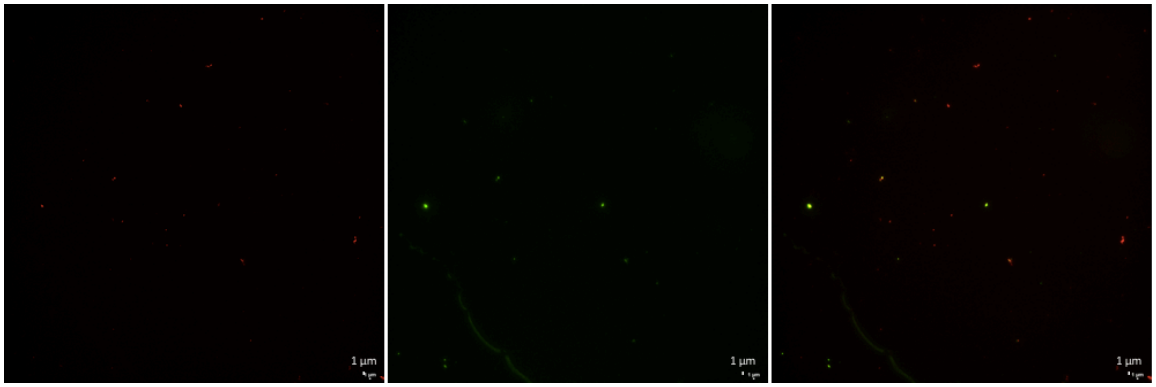

Figure 4.8: TNH 12 run 1, ZnO (left, red channel), exosomes (middle, green channel) and TNH (right, overlay). Scale bar is 1 µm.

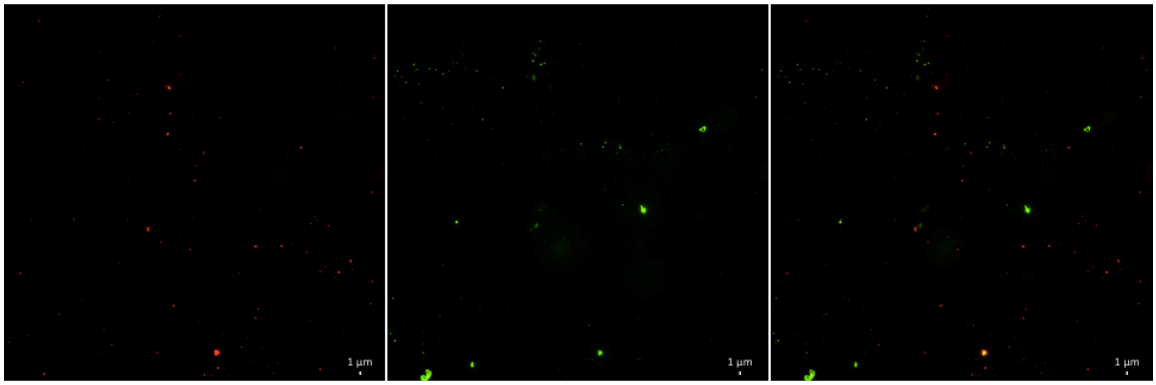

Figure 4.9: TNH 12 run 2, ZnO (left, red channel), exosomes (middle, green channel) and TNH (right, overlay). Scale bar is 1 µm.

TNH 12 is one of the first attempts of coupling. Percentages have to be improved.

- **TNH 13**

	Sample	Conditions	% ZnO colocalized (%)	% Exosomes colocalized (%)	% particles colocalized (%)
TNH 13	Run 1	KB, Orbital Shaker 250 rpm, RT, 90'. Centrifuge 16870 g, 5'	14.04	18.78	7.75
	Run 2	KB, Orbital Shaker 250 rpm, RT, 90'. Centrifuge 16870 g, 5'	19.33	29.97	12.90
	Run 1-24h EMEM	Resuspended in 100 µl EMEM. Incubator 37°C for 24 hours	0.83	0.31	0.23

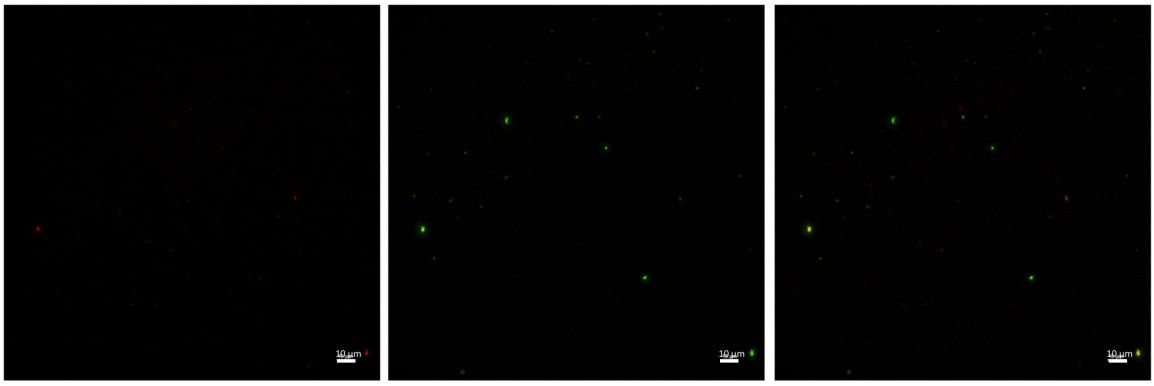

Figure 4.10: TNH 13 run 1, ZnO (left, red channel), exosomes (middle, green channel) and TNH (right, overlay). Scale bar is 10 µm.

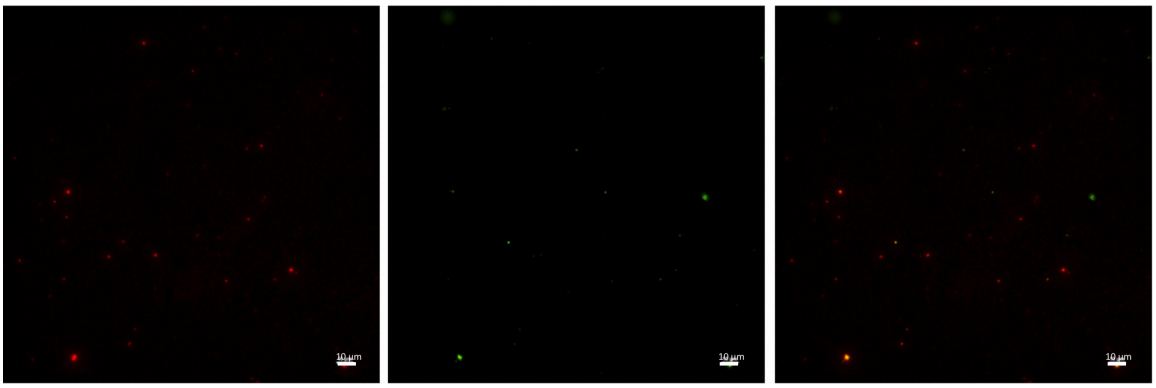

Figure 4.11: TNH 13 run 2, ZnO (left, red channel), exosomes (middle, green channel) and TNH (right, overlay). Scale bar is 10 µm.

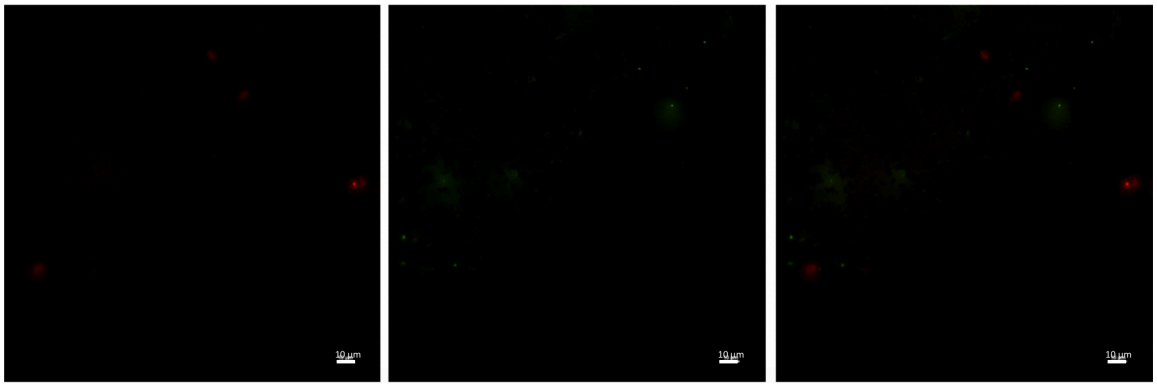

Figure 4.12: TNH 13 run 1 after 24 hours in EMEM, ZnO (left, red channel), exosomes (middle, green channel) and TNH (right, overlay). Scale bar is 10 µm.

In TNH 13 the coupling percentages are not so good, even if there is an improvement during the second run.

After that the first run is suspended in EMEM and left in this condition for 24 hours. The result is that the coupling percentage is strongly decreased and, in addition the red fluorescence is in part bleached.

- **TNH 14**

	Sample	Conditions	% ZnO colocalized (%)	% Exosomes colocalized (%)	% particles colocalized (%)
TNH 14	Run 1	KB, Wheel, RT, overnight. Centrifuge 18870 g, 5’	6.59	37.37	6.13

The coupling for TNH 14 is carried out on a wheel. Probably the low percentages are due to the small volume of the solution of ZnO and exosomes (100 µl) in an eppendorf of 1.5 ml. The continuous turning upside-down on the wheel can cause the spread of exosomes and the nanoparticles on the walls of the Eppendorf, making the coupling difficult and ruining the structure of exosomes.

- **TNH 15**

	Sample	Conditions	% ZnO colocalized (%)	% Exosomes colocalized (%)	% particles colocalized (%)
TNH 15	Run 1	KB, Orbital Shaker 250 rpm, RT, 90'. Centrifuge 16870 g, 5'	34.97	21.82	15.41
	Run 2	KB, Orbital Shaker 250 rpm, RT, 90'. Centrifuge 16870 g, 5'	**65.07**	36.86	33.43
	Run 1 + 2 - 4 d	Combination of Run 1 and Run 2, stored at 4°C for 4 days.	24.70	6.40	5.00

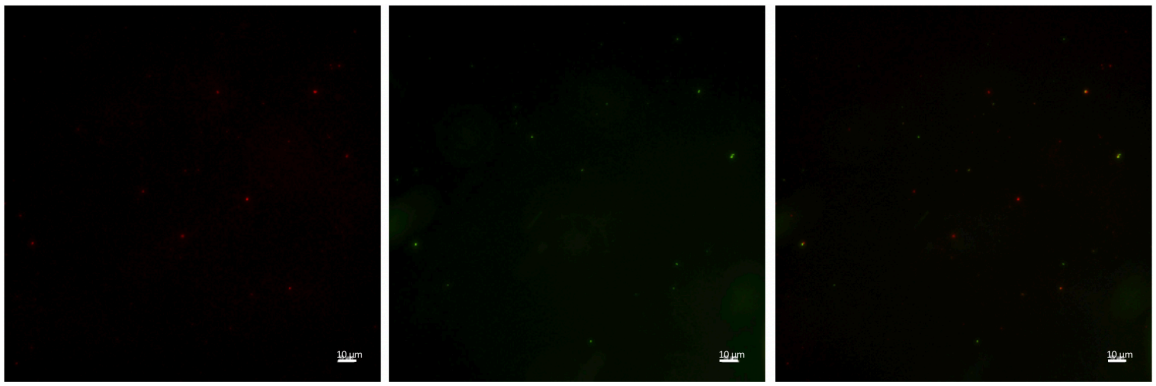

Figure 4.13: TNH 15 run 1, ZnO (left, red channel), exosomes (middle, green channel) and TNH (right, overlay). Scale bar is 10 µm.

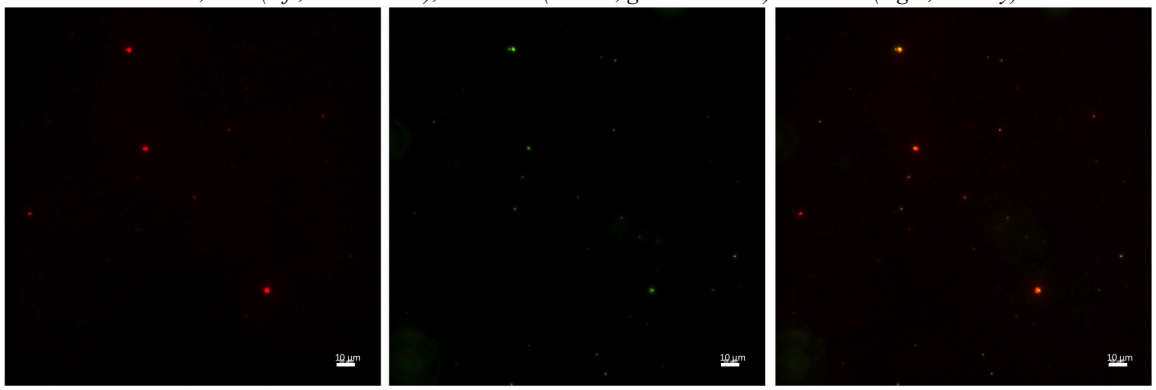

Figure 4.14: TNH 15 run 2, ZnO (left, red channel), exosomes (middle, green channel) and TNH (right, overlay). Scale bar is 10 µm.

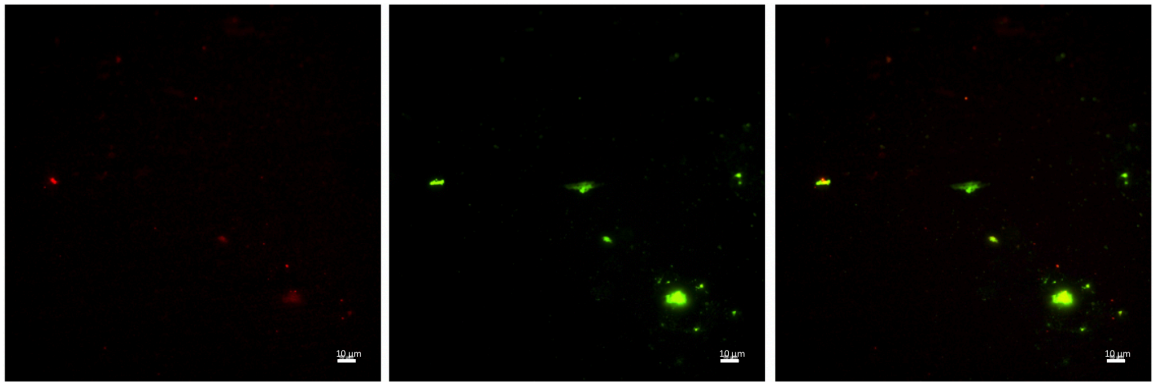

Figure 4.15: TNH 15 run 1+2, at 4°C for 4 days, ZnO (left, red channel), exosomes (middle, green channel) and TNH (right, overlay). Scale bar is 10 µm.

TNH15 shows the same protocol of TNH12 for both run 1 and 2 with very good coupling initially.

At the end it was decided to test the storage (4 days at 4 °C) for both runs by combining them together. However, the resulting coupling percentages lowered. Moreover, several large aggregates are formed, indicating that the storage procedure is not correct for this formulation.

- **TNH 16**

	Sample	Conditions	% ZnO colocalized (%)	% Exosomes colocalized (%)	% particles colocalized (%)
TNH 16	Run 1	KB, Wheel, RT, 90'. Centrifuge 16870 g, 5'	5.49	29.47	4.48
	Run 2	KB, Wheel, RT, 90'. Centrifuge 16870 g, 5'	16.53	13.91	7.87

Figure 4.16:TNH 16 run 1, ZnO (left, red channel), exosomes (middle, green channel) and TNH (right, overlay). Scale bar is 10 µm.

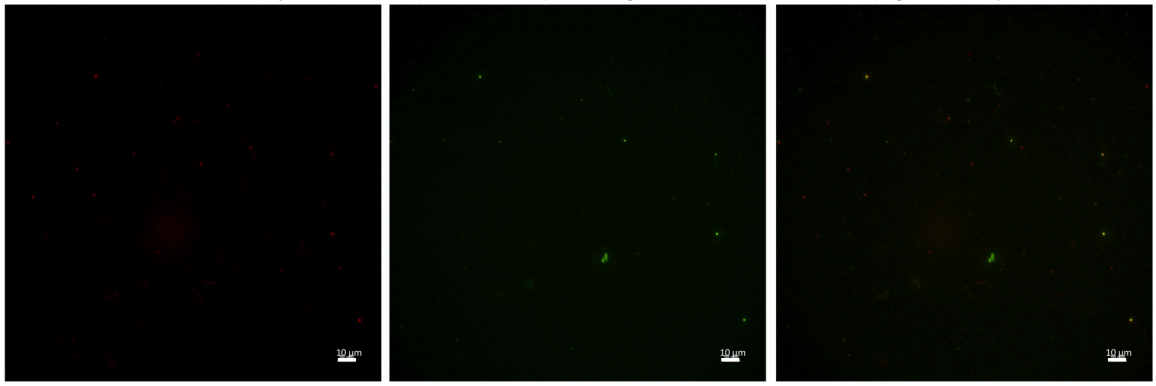

Figure 4.17: TNH 16 run 2, ZnO (left, red channel), exosomes (middle, green channel) and TNH (right, overlay). Scale bar is 10 µm.

TNH 16 is obtained using the wheel as coupling technique. The percentages are low for the same problems explained above for TNH 14.

- **TNH 17**

	Sample	Conditions	% ZnO colocalized (%)	% Exosomes colocalized (%)	% particles colocalized (%)
TNH 17	Run 1	KB, Orbital Shaker 250 rpm, RT, 90'. Centrifuge 16870 g, 5'	15.36	10.90	6.82
	Run 1 – US	US 40 kHz, 30'	15.04	**30.05**	10.87
	Run 2	KB, Orbital Shaker 250 rpm, RT, 90'. Centrifuge 16870 g, 5'	13.51	3.97	3.18
	Run 2– 24h EMEM	+ 900 µl EMEM, orbital shaker 37°C for 24 hours	16.39	17.49	8.74

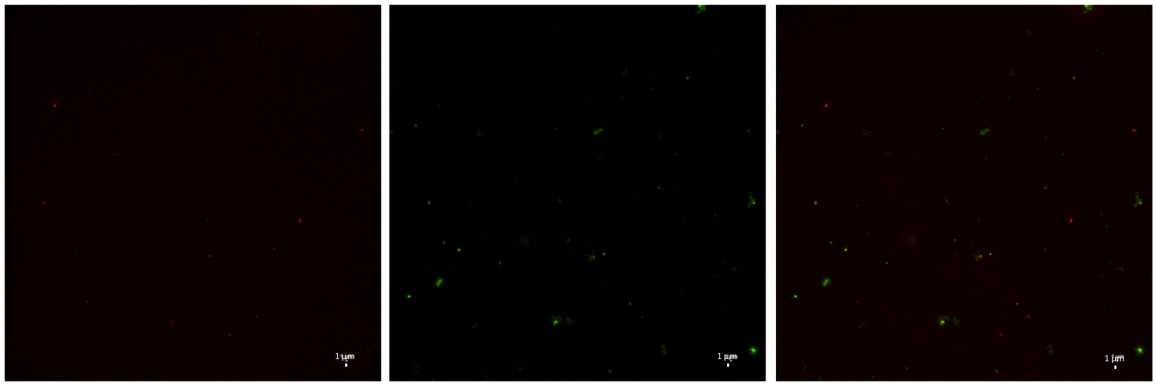

Figure 4.18: TNH 17 run 1, ZnO (left, red channel), exosomes (middle, green channel) and TNH (right, overlay). Scale bar is 1 µm.

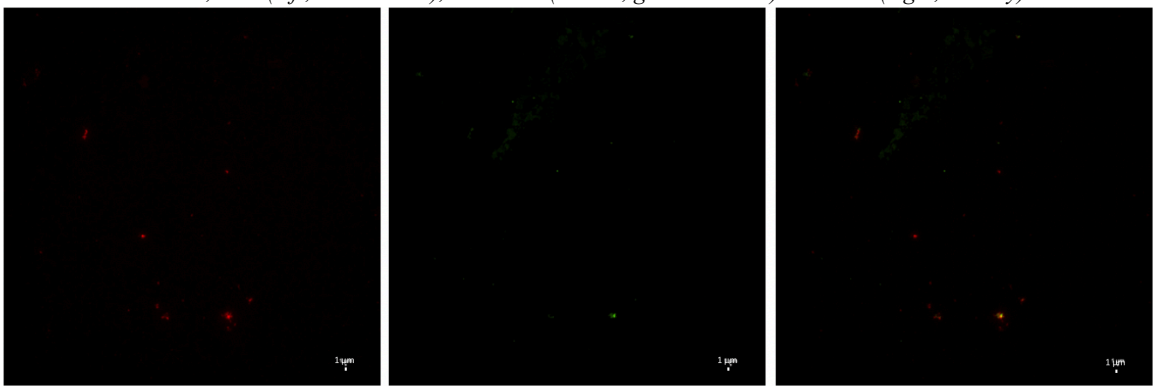

Figure 4.19: TNH 17 run 1 - US, ZnO (left, red channel), exosomes (middle, green channel) and TNH (right, overlay). Scale bar is 1 µm.

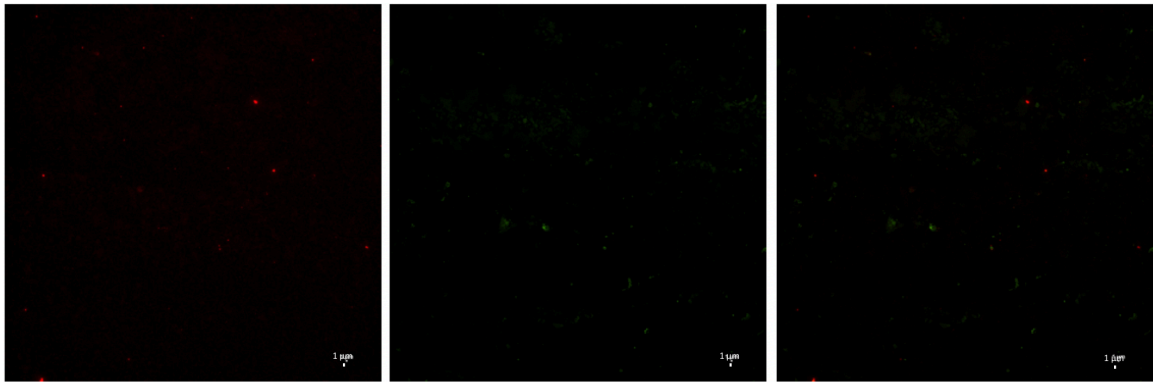

Figure 4.20: TNH 17 run 2, ZnO (left, red channel), exosomes (middle, green channel) and TNH (right, overlay). Scale bar is 1 µm.

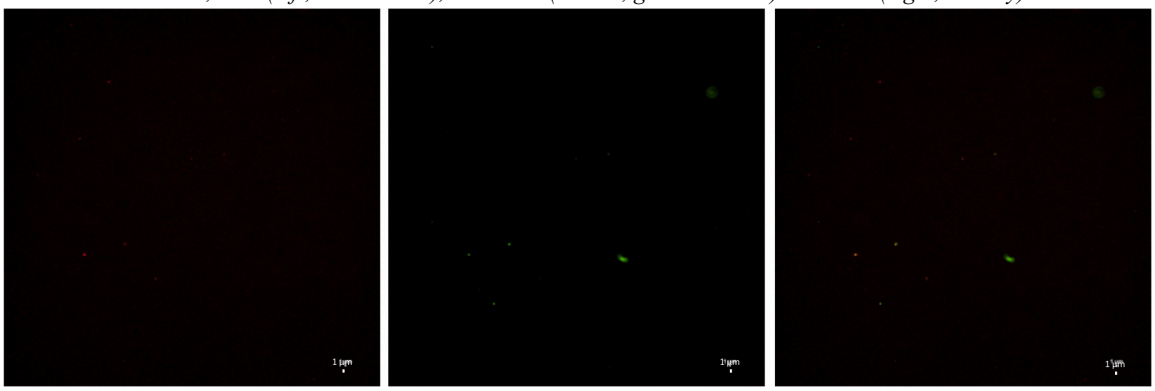

Figure 4.21: TNH 17 run 2 - 24 h in EMEM, 37°C, orbital shaker. ZnO (left, red channel), exosomes (middle, green channel) and TNH (right, overlay). Scale bar is 1 µm.

TNH 17 is prepared using the orbital shaker at room temperature, as the first run of TNH 15. After the first coupling the sample is sonicated for 30 minutes. This process of sonication leads to a better coupling percentage for exosomes, probably because US disassemble the membranes and cause an easily internalization of ZnO nanoparticles. Instead, the percentage of ZnO slightly decreases because there are some aggregates that are disaggregated by US and thus more particles are then visible in the image.

The second run is then resuspended in EMEM and the coupling continue for 24 hours, in this way the percentages increase, but not enough to justify 24 hours of coupling.

- **TNH 18**

	Sample	Conditions	% ZnO colocalized (%)	% Exosomes colocalized (%)	% particles colocalized (%)
TNH 18	Run 1	KB, orbital shaker 250 rpm, 37°C, 90'. Centrifuge 16870 g, 5'	**45.80**	9.07	7.87
	Run 1 – US	US 40 kHz, 30'	**40.08**	11.59	9.86
	Run 2	Orbital shaker 250 rpm, 37°C, 90'. Centrifuge 16870 g, 5'	**48.16**	**41.16**	28.16
	Run 2 – 24h EMEM	+ 900 µl EMEM, orbital shaker, 37°C for 24 hours	**57.62**	**49.88**	31.71

	Run 2 – 24h EMEM US	US 40 kHz, 30’	**66.70**	23.94	21.52
	Run 2-24 EMEM US 5 days	Stored at 4°C for 5 days	19.16	23.65	12.35

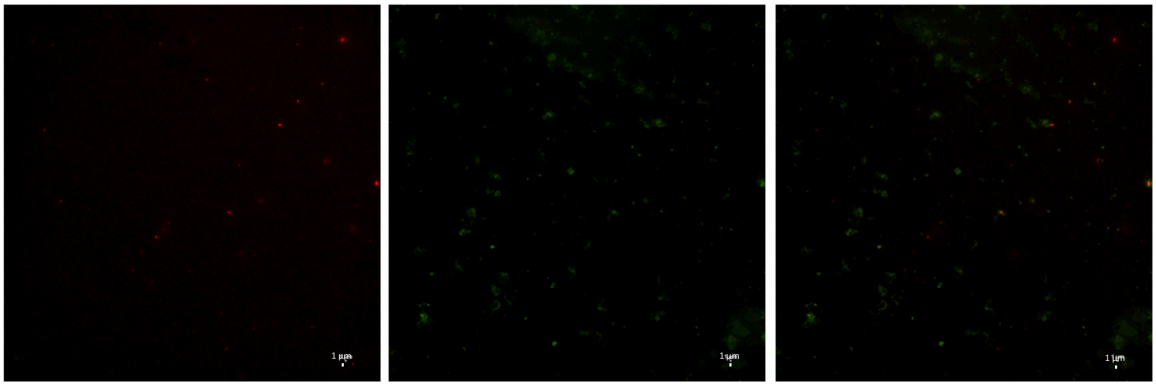

Figure 4.22: TNH 18 run 1, ZnO (left, red channel), exosomes (middle, green channel) and TNH (right, overlay). Scale bar is 1 µm.

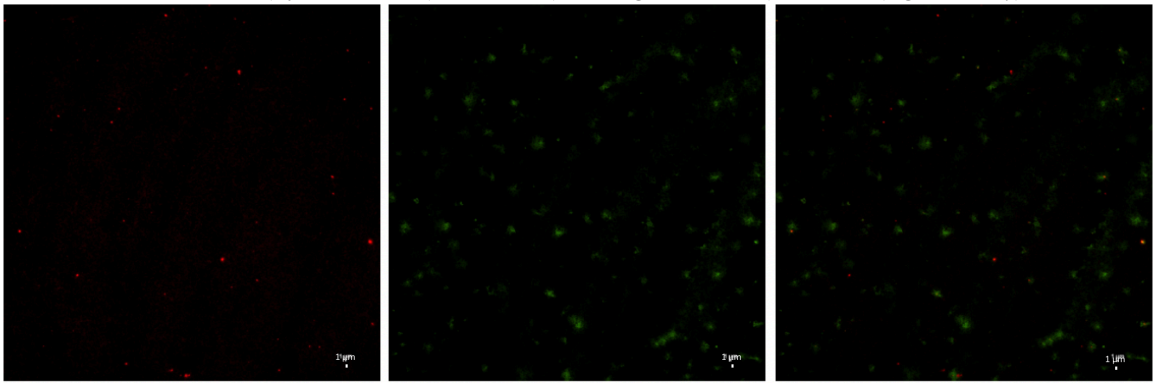

Figure 4.23: TNH 18 run 1 - US, ZnO (left, red channel), exosomes (middle, green channel) and TNH (right, overlay). Scale bar is 1 µm.

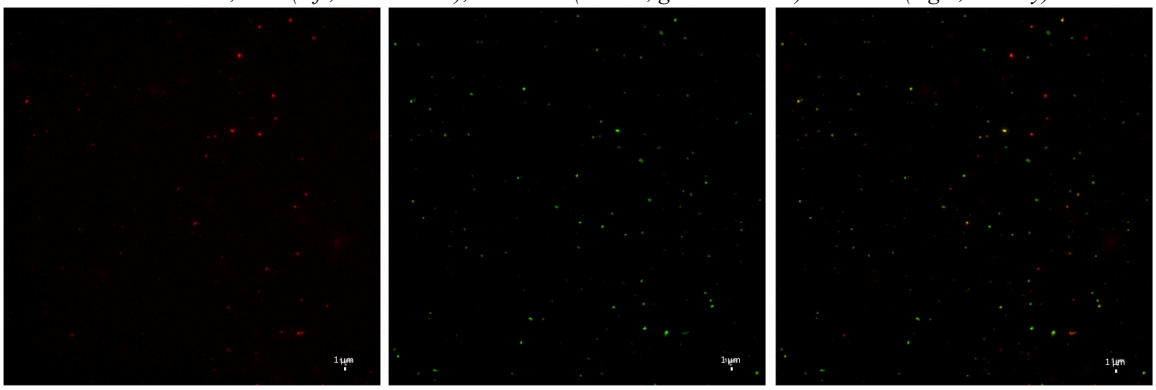

Figure 4.24: TNH 18 run 2, ZnO (left, red channel), exosomes (middle, green channel) and TNH (right, overlay). Scale bar is 1 µm.

Figure 4.25: TNH 18 run 2 - 24 h in EMEM, ZnO (left, red channel), exosomes (middle, green channel) and TNH (right, overlay). Scale bar is 1 μm.

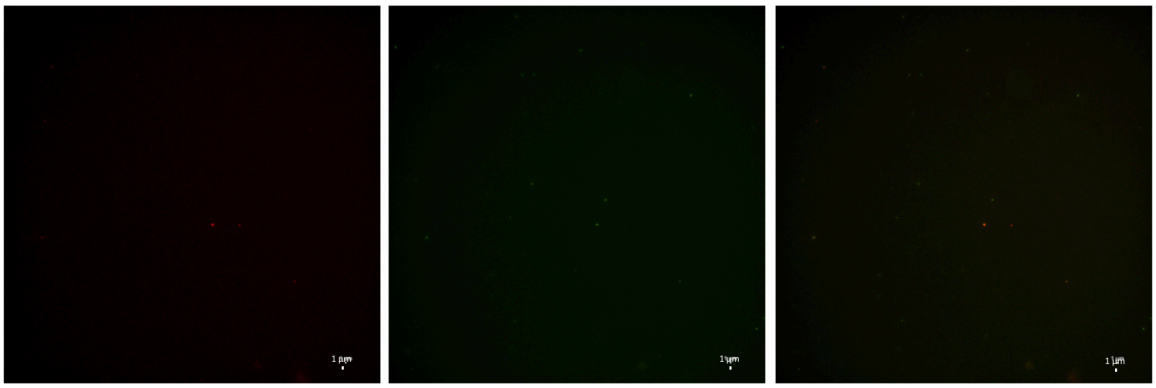

Figure 4.26: TNH 18 run 2 - 24 h in EMEM - US, ZnO (left, red channel), exosomes (middle, green channel) and TNH (right, overlay). Scale bar is 1 μm.

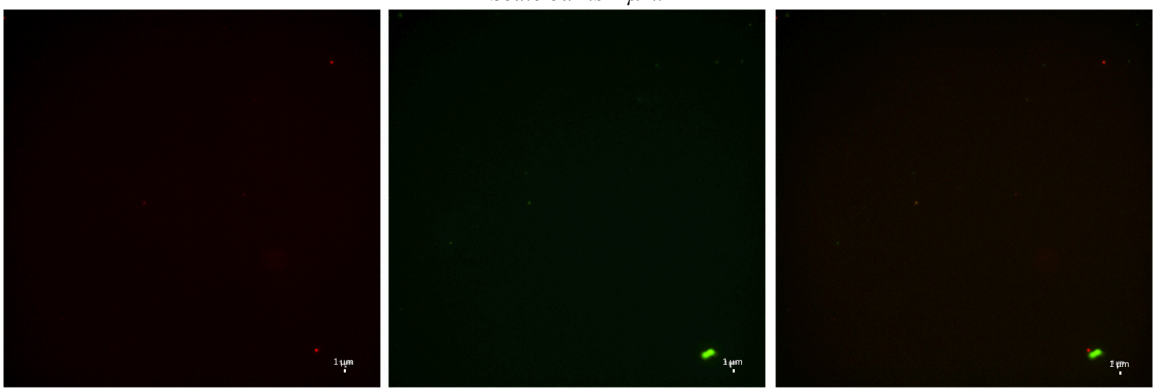

Figure 4.27: TNH 18 run 2 - 24 h in EMEM - US after 5 days at 4°C, ZnO (left, red channel), exosomes (middle, green channel) and TNH (right, overlay). Scale bar is 1 μm.

The coupling of TNH 18 is the same of TNH 15 and TNH 17, but at 37°C. In Run 1 before and after the sonication there are either an increase of the coupling percentage of the exosomes and a decrease of the one of ZnO, for the same reason explained above. After 24 hours in EMEM an increase of the coupling is observed for this sample, but not high enough to justify the time spent for the coupling. The subsequent sonication enhances even more the internalization.

After a storage of 5 days at 4 °C the coupling percentage is drastically reduced, showing again that the TNH storage procedure has to be carefully evaluated in a separated test.

- **TNH 19**

	Sample	Conditions	% ZnO colocalized (%)	% Exosomes colocalized (%)	% particles colocalized (%)
TNH 19	Run 1	KB, orbital shaker 250 rpm, 4°C, 90'. Centrifuge 16870 g, 5'	32.53	31.60	22.62
	Run 2	KB, orbital shaker 250 rpm, 4°C, 90'. Centrifuge 16870 g, 5'	7.62	22.83	5.94

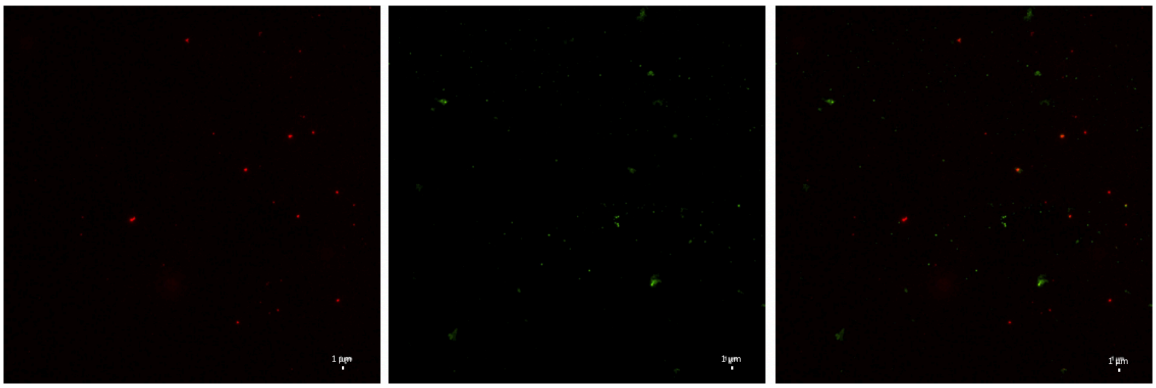

Figure 4.28: TNH 19 run 1, ZnO (left, red channel), exosomes (middle, green channel) and TNH (right, overlay). Scale bar is 1 µm.

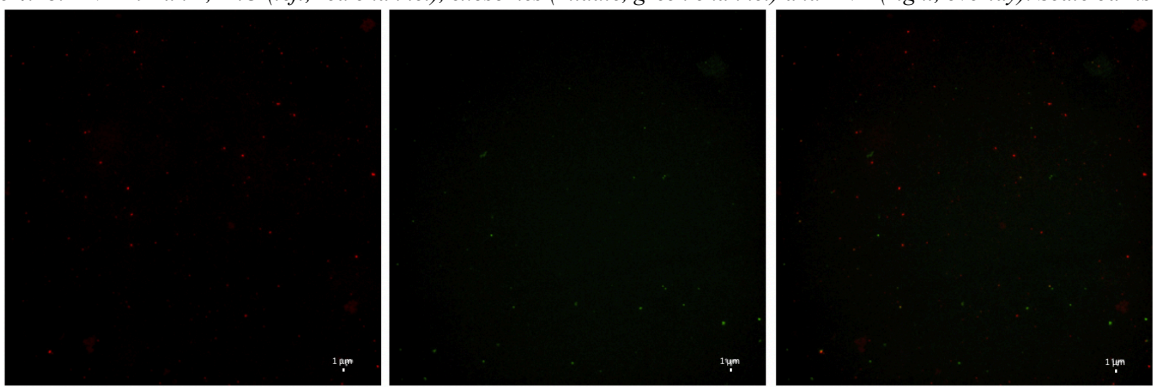

Figure 4.29: TNH 19 run 2, ZnO (left, red channel), exosomes (middle, green channel) and TNH (right, overlay). Scale bar is 1 µm.

TNH 19 is prepared as the previous TNH15, 17 and 18, but here the temperature is maintained at 4°C. At this temperature the exosomes membranes are not fluid enough to allow the penetration of nanoparticles and thus the efficiency of the coupling is low.

- **TNH 20**

	Sample	Conditions	% ZnO colocalized (%)	% Exosomes colocalized (%)	% particles colocalized (%)
TNH 20	Run 1	KB, orbital shaker 250 rpm, 37°C, 8h. Centrifuge 16870 g, 5'	31.31	16.16	12.03
	Run 1 - US	US 40 kHz, 30'	**44.51**	17.49	12.90

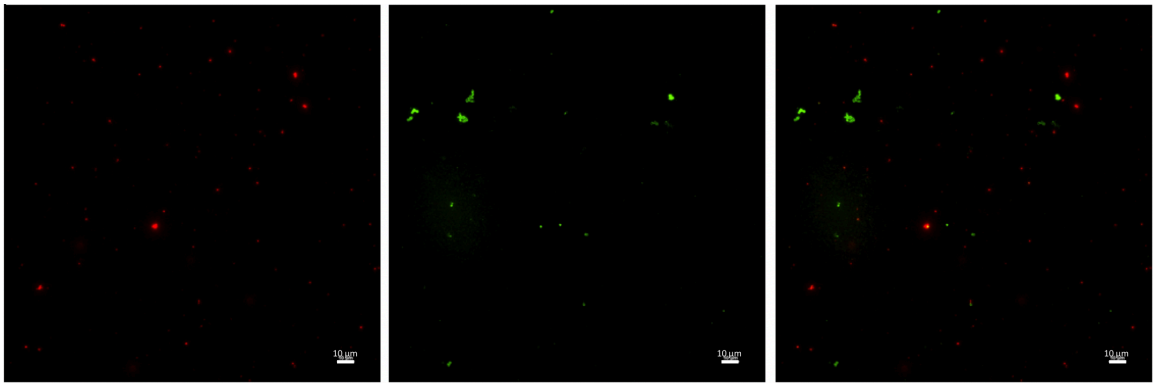

Figure 4.30: TNH 20 run 1, ZnO (left, red channel), exosomes (middle, green channel) and TNH (right, overlay). Scale bar is 10 μm.

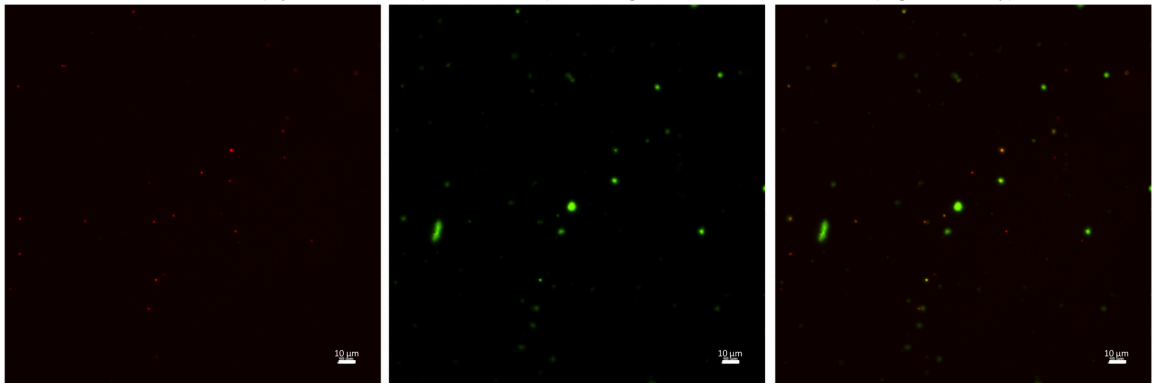

Figure 4.31: TNH 20 run 1 - US, ZnO (left, red channel), exosomes (middle, green channel) and TNH (right, overlay). Scale bar is 10 μm.

The time of coupling for TNH 20 is 8 hours, different from the 90' used previously in the other preparations. The percentages are good, but not as much to motivate such a long time of coupling. Furthermore, it is again demonstrated the improvement of the coupling through the sonication.

- **TNH 21**

	Sample	Conditions	% ZnO colocalized (%)	% Exosomes colocalized (%)	% particles colocalized (%)
TNH 21	Run 1	KB, 10 aliquots of ZnO, orbital shaker 250 rpm, 37°C, 8h. Centrifuge 16870 g, 5'	11.32	18.21	7.25
	Run 1 - US	US 40 kHz, 30'	19.71	17.57	8.85

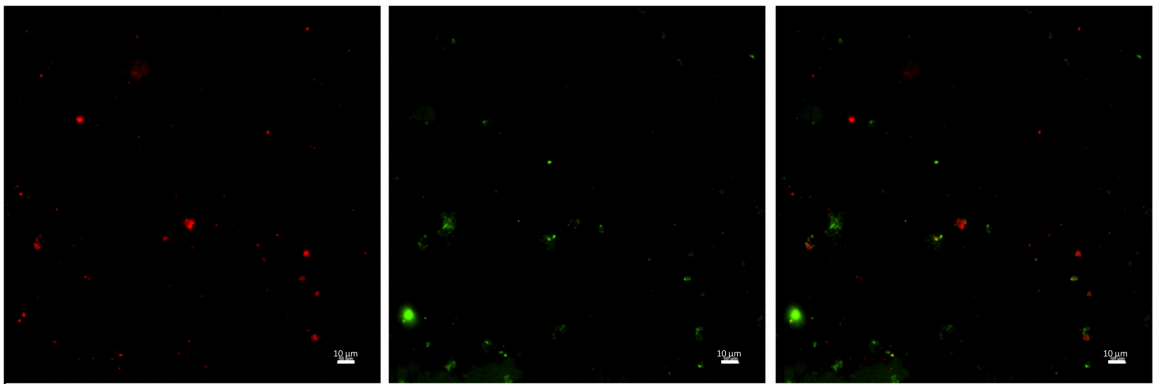

Figure 4.32: TNH 21 run 1, ZnO (left, red channel), exosomes (middle, green channel) and TNH (right, overlay). Scale bar is 10 µm.

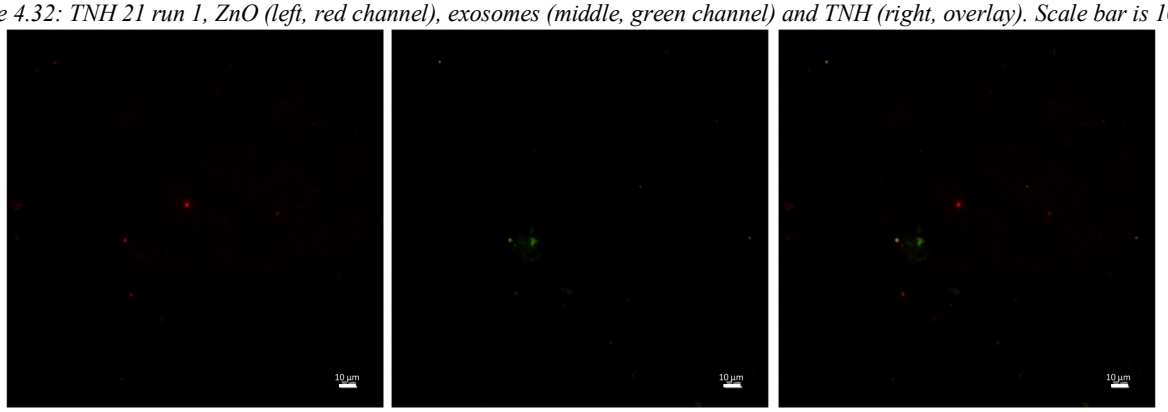

Figure 4.33: TNH 20 run 1 - US, ZnO (left, red channel), exosomes (middle, green channel) and TNH (right, overlay). Scale bar is 10 µm.

To investigate whether the aliquot of ZnO is a limiting factor maintaining low the coupling percentages, it was decided to increase by a factor of ten the amount of ZnO provided for the coupling.

TNH 21 is similar to TNH 20, but 10 times the amounts of ZnO nanoparticles with respect to the aliquot used in the previous couplings, as in TNH20, were added at the beginning. However, this amount of nanoparticles could not be internalized by the exosomes as much quickly to prevent their aggregation. After the post-coupling, sonication the percentages increase a little because of the disaggregation of the aggregates of ZnO.

- **TNH 22**

	Sample	Conditions	% ZnO colocalized (%)	% Exosomes colocalized (%)	% particles colocalized (%)
TNH 22	Run 1	KB, orbital shaker 250 rpm, 37°C, 24h. Centrifuge 16870 g, 5’	37.94	8.09	6.88
	Run 1 - US	US 40 kHz, 30’	**58.23**	23.73	20.33

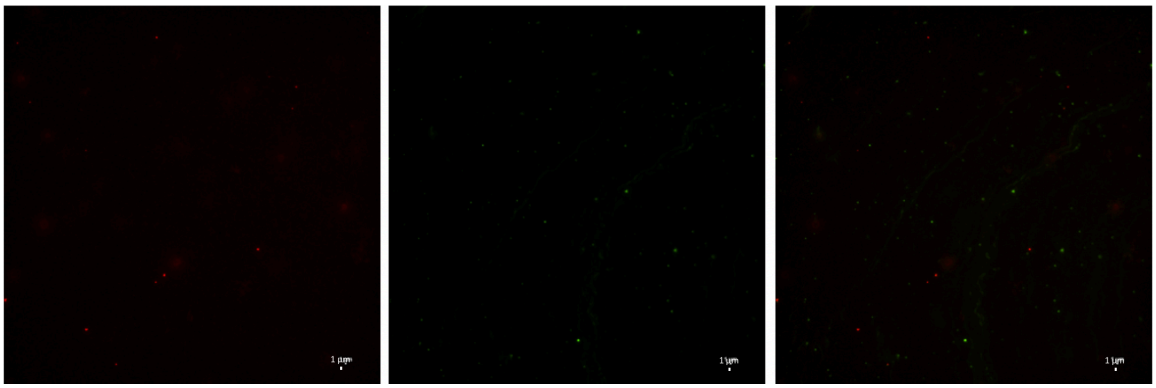

Figure 4.34: TNH 22 run 1 ZnO (left, red channel), exosomes (middle, green channel) and TNH (right, overlay). Scale bar is 1 µm.

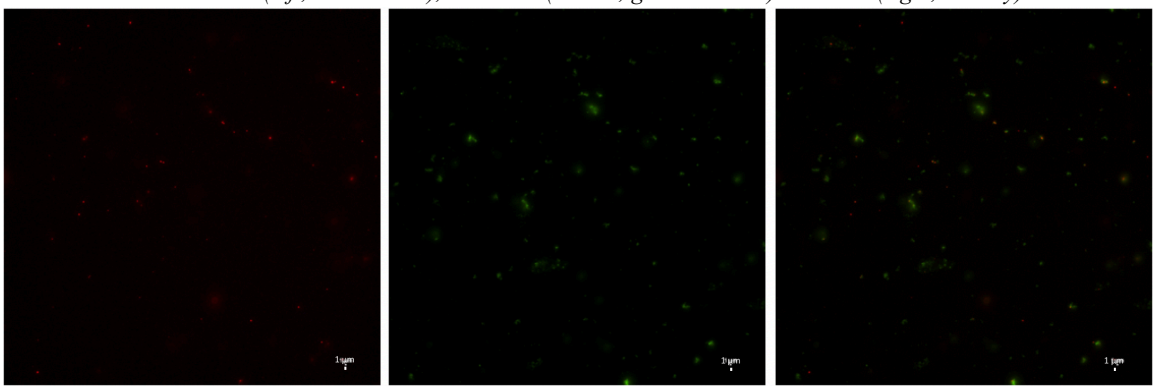

Figure 4.35: TNH 22 run 1 - US, ZnO (left, red channel), exosomes (middle, green channel) and TNH (right, overlay). Scale bar is 1 µm.

TNH 22 time of coupling is 24 hours, instead of 90' or 8 hours of the previous samples. The percentages are good, but not so good to motivate a longer time of coupling. This is also another demonstration of the improvement of the coupling through the sonication.

- **TNH 23**

	Sample	Conditions	% ZnO colocalized (%)	% Exosomes colocalized (%)	% particles colocalized (%)
TNH 23	Run 1	DAUDI in PBS, orbital shaker 250 rpm, 37°C, 24h. Centrifuge 16870 g, 5'	**41.91**	**44.69**	27.92
	Run 1 - US	US 40 kHz, 30'	/	/	/

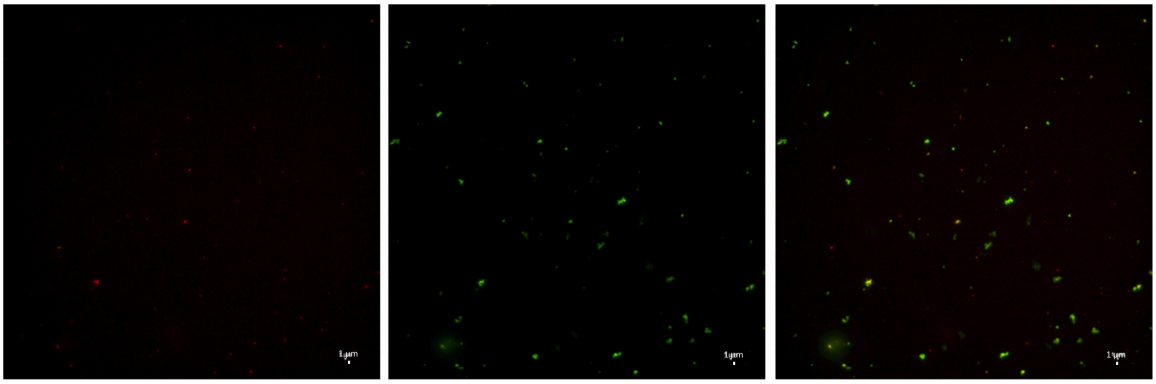

Figure 4.36: TNH 23 run 1, ZnO (left, red channel), exosomes (middle, green channel) and TNH (right, overlay). Scale bar is 1 µm.

TNH 23 is prepared using exosomes extracted from DAUDI cells and dispersed in PBS solution, as the previous ones from KB cells. The rate of coupling is good also after the first run. After the sonication the sample is too diluted to have reliable results.

- **TNH 24**

	Sample	Conditions	% ZnO colocalized (%)	% Exosomes colocalized (%)	% particles colocalized (%)
TNH 24	Run 1	DAUDI (Physiologic solution), orbital shaker 250 rpm, 37°C, 24h. Centrifuge 16870 g, 5’	**58.58**	36.08	29.32
	Run 1 - US	US 40 kHz, 30’	/	/	/

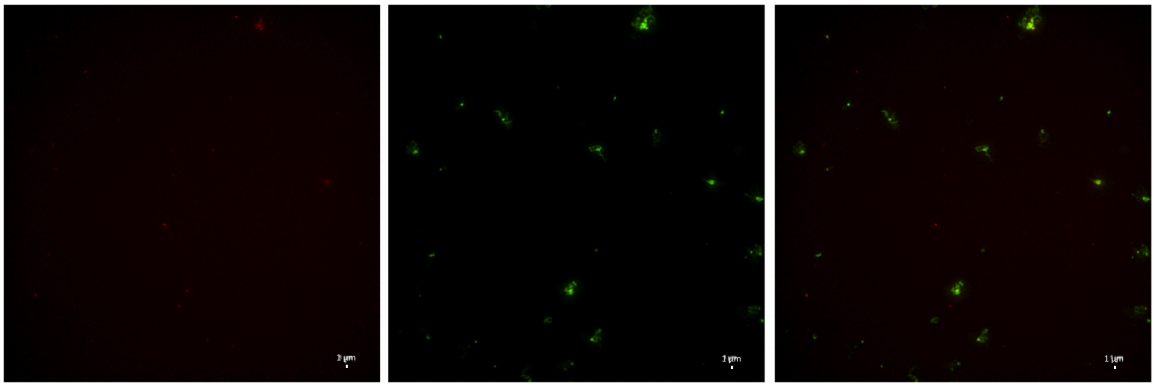

Figure 4.37: TNH 24 run 1, ZnO (left, red channel), exosomes (middle, green channel) and TNH (right, overlay). Scale bar is 1 µm.

TNH 24 is prepared using exosomes extracted from DAUDI cells but in physiologic solution. The rate of coupling is the best ever obtained with exosomes from cancer cells also after the first run. After the sonication the sample is too diluted to have reliable results.

- **TNH 25**

	Sample	Conditions	% ZnO colocalized (%)	% Exosomes colocalized (%)	% particles colocalized (%)
TNH 25	Run 1	KB, orbital shaker 250 rpm, 37°C, 3h, each hour 1 aliquot of ZnO added (until 3 aliquots). Centrifuge 16870 g, 5'	32.91	39.06	21.53
	Run 1 – 24h,	Orbital shaker 160 rpm, 37°C, 24 hours	**61.20**	**48.54**	37.09
	Run 2	Orbital shaker 250 rpm, 37°C, 3h, each hour 1 aliquot of ZnO added (until 3 aliquots). Centrifuge 16870 g, 5'	39.01	**49.80**	26.83
	Run 2 – 24h	Orbital shaker 160 rpm, 37°C, 24 hours	**46.44**	**47.93**	31.73

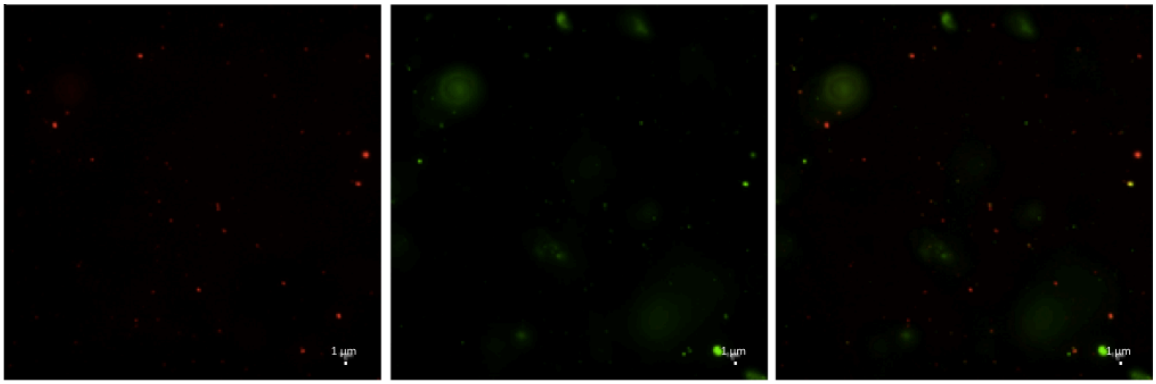

Figure 4.38: TNH 25 run 1, ZnO (left, red channel), exosomes (middle, green channel) and TNH (right, overlay). Scale bar is 1 μm.

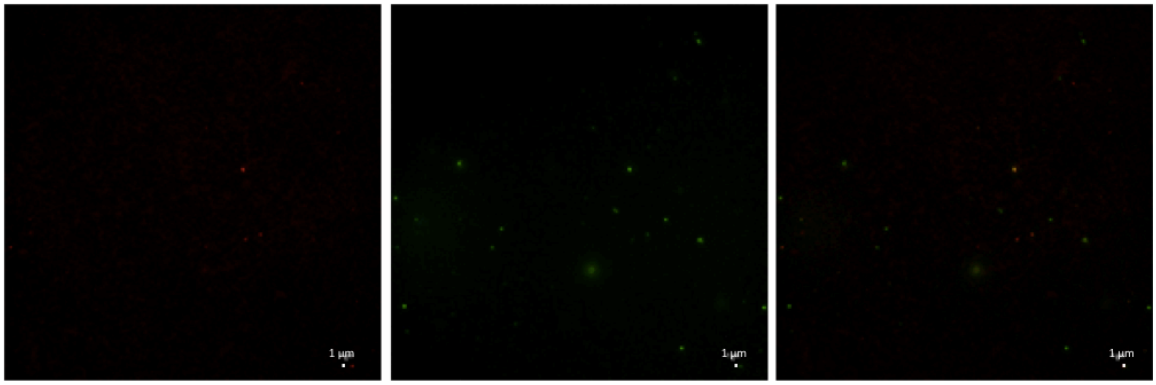

Figure 4.39: TNH 25 run 1 – 24 h 37°C orbital shaker, ZnO (left, red channel), exosomes (middle, green channel) and TNH (right, overlay). Scale bar is 1 μm.

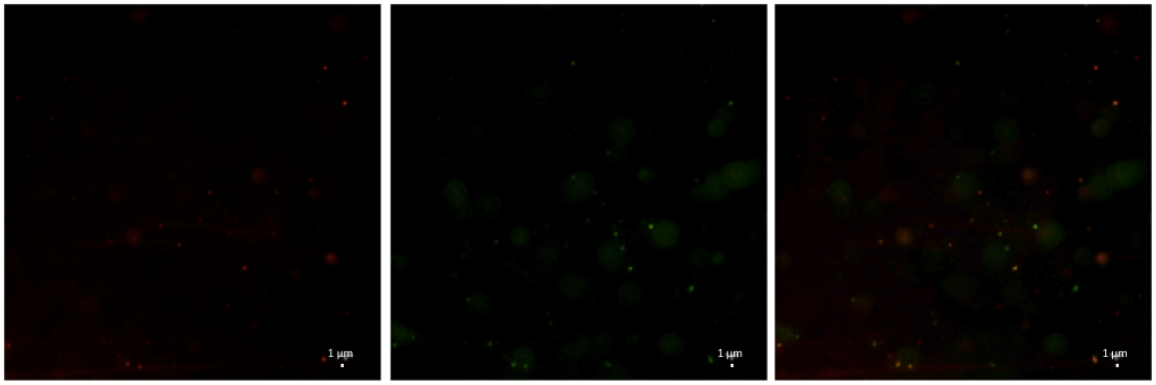

Figure 4.40: TNH 25 run 2, ZnO (left, red channel), exosomes (middle, green channel) and TNH (right, overlay). Scale bar is 1 µm.

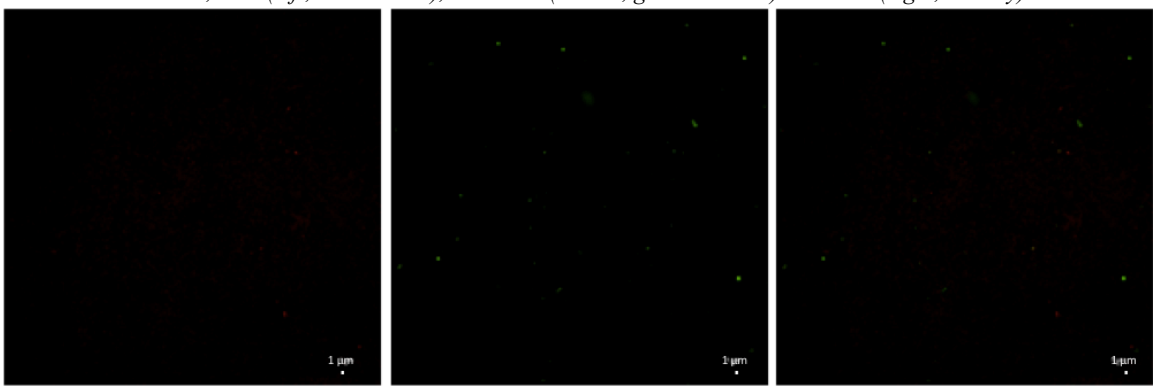

Figure 4.41: TNH 25 run 2 – 24 h 37°C orbital shaker, ZnO (left, red channel), exosomes (middle, green channel) and TNH (right, overlay). Scale bar is 1 µm.

In TNH 25 is carried out a coupling with three aliquots of ZnO nanoparticles in every run. The coupling percentages are good and they increase after 24 hours.

- **TNH 26**

	Sample	Conditions	% ZnO colocalized (%)	% Exosomes colocalized (%)	% particles colocalized (%)
TNH 26	Run 1	KB, orbital shaker 250 rpm, 37°C, 24h in 1 ml of total volume (100 µl of PBS:water (1:1) + 900 µl EMEM). Centrifuge 16870 g, 5’	9.45	6.78	3.75
	Run 1 - US	US 40 kHz, 30’	**39.62**	**39.87**	24.17

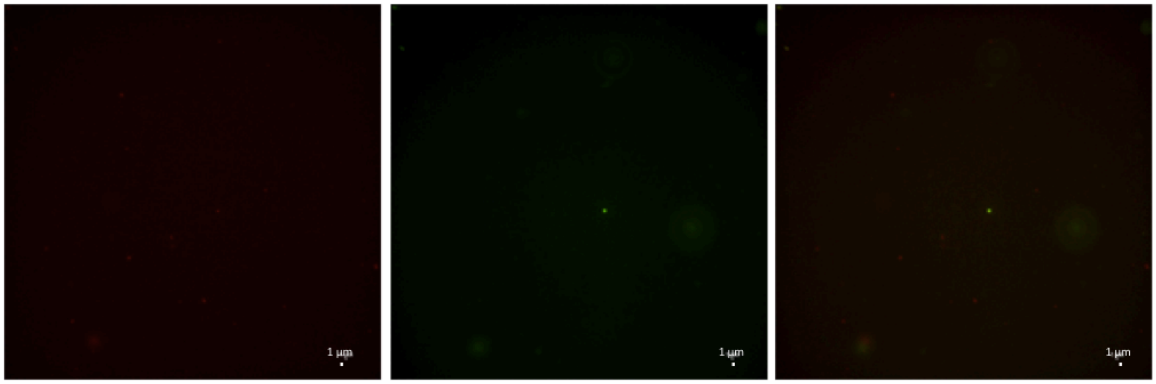

Figure 4.42: TNH 26 run 1, ZnO (left, red channel), exosomes (middle, green channel) and TNH (right, overlay). Scale bar is 1 μm.

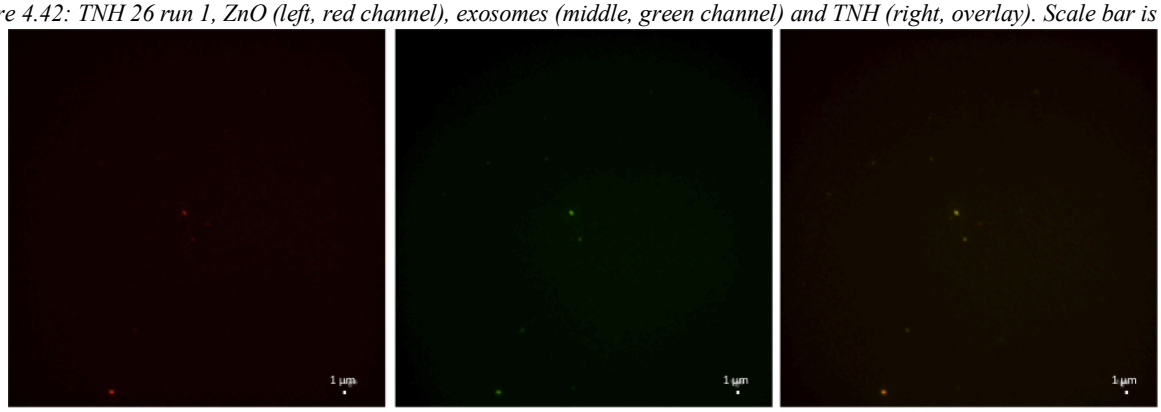

Figure 4.43: TNH 26 run 1-US, ZnO (left, red channel), exosomes (middle, green channel) and TNH (right, overlay). Scale bar is 1 μm.

If the coupling is carried out in a bigger volume (1 ml), like in TNH 26, the coupling percentages are low because there are few impacts between nanoparticles and exosomes. With the sonication they are improved because US cause a strong mixing of the solution increasing the impacts.

- **TNH 27**

	Sample	Conditions	% ZnO colocalized (%)	% Exosomes colocalized (%)	% particles colocalized (%)
TNH 27	Run 1	KB, orbital shaker 250 rpm, 37°C, 24h in 1 ml of total volume (100 µl of PBD:water (1:1) + 900 µl EMEM). Centrifuge 16870 g, 5’	7.91	11.30	4.68
	Run 1 - US	US 40 kHz, 30’	**48.03**	**42.29**	29.55

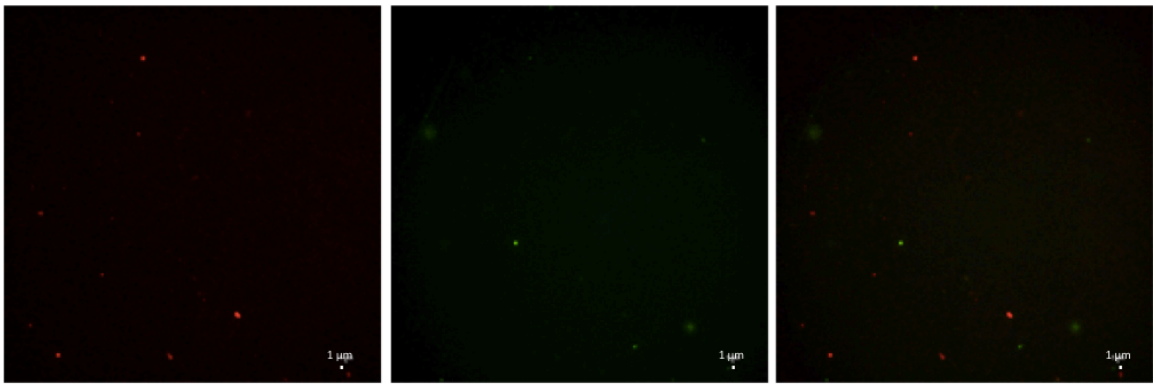

Figure 4.44: TNH 27 run 1, ZnO (left, red channel), exosomes (middle, green channel) and TNH (right, overlay). Scale bar is 1 µm.

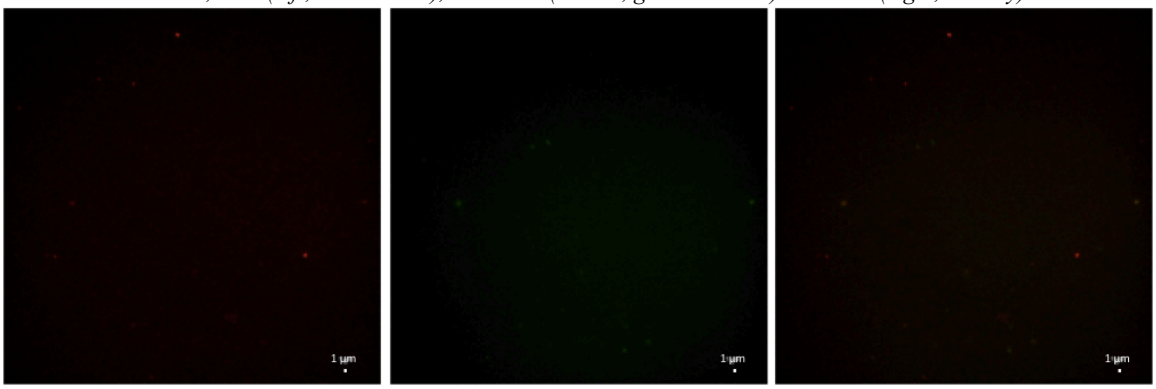

Figure 4.45: TNH 27 run 1 - US, ZnO (left, red channel), exosomes (middle, green channel) and TNH (right, overlay). Scale bar is 1 µm.

In TNH 27 five aliquots of ZnO nanoparticles are added at different times: t=0, t=1h, t=2h, t=3h and t=4h to the exosomes from the beginning of the process. During the first run the coupling is not successful because ZnO in contact with EMEM starts to aggregate. After the sonication such aggregates are disaggregated and the coupling could occur.

- **TNH 28**

	Sample	Conditions	% ZnO colocalized (%)	% Exosomes colocalized (%)	% particles colocalized (%)
TNH 28	Run 1	KB, US 40 kHz, 30’	/	/	/
	Run 1 – 24 h	Storage at 4°C, 24h	**63.76**	**41.09**	32.94

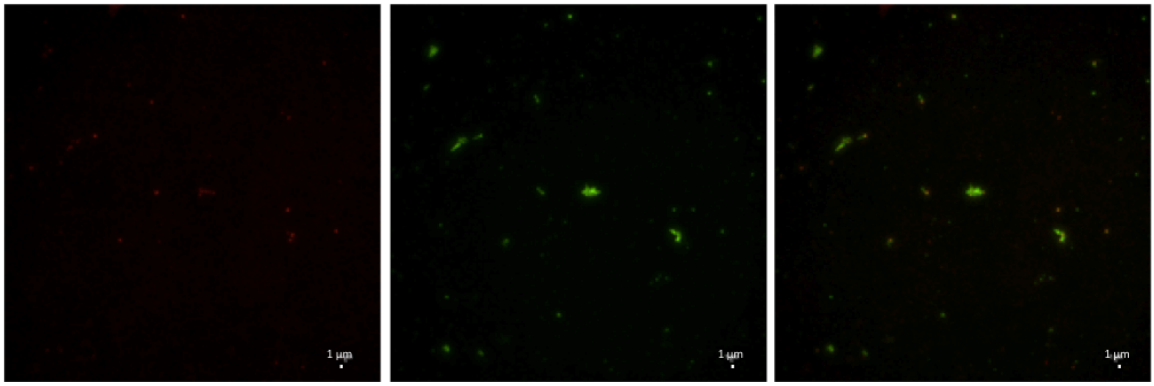

Figure 4.46: TNH 28 run 1 after 24 h, ZnO (left, red channel), exosomes (middle, green channel) and TNH (right, overlay). Scale bar is 1 µm.

The coupling is processed only sonicating the exosomes with ZnO, however the percentages could not be evaluated because of a problem with the microscope, but after 24 hours at 4°C they are still good. The sample was repeated in TNH 33, see below.

- **TNH 29**

	Sample	Conditions	% ZnO colocalized (%)	% Exosomes colocalized (%)	% particles colocalized (%)
TNH 29	Run 1	KB, orbital shaker 250 rpm, 37°C, 3h, each hour 1 aliquot of ZnO added (until 3 aliquots). Centrifuge 16870 g, 5'	21.48	23.71	12.54
	Run 1 - US	US 40 kHz, 30'	**54.97**	31.56	30.49

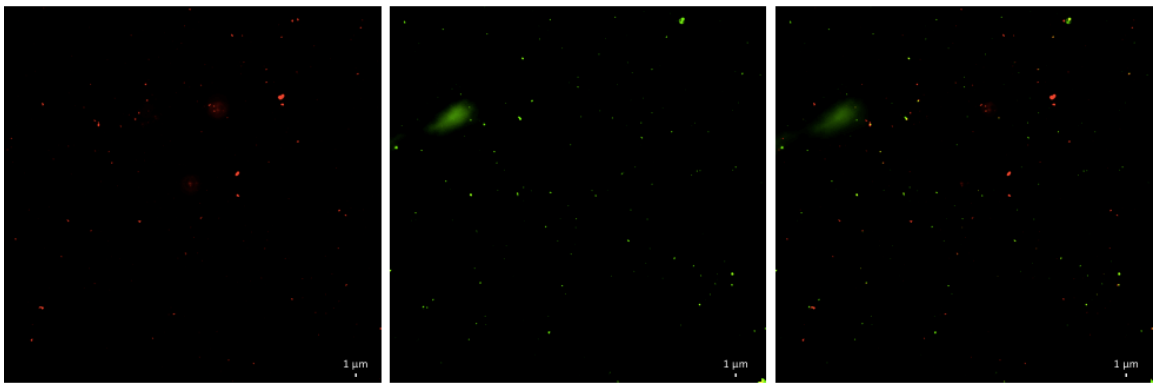

Figure 4.47: TNH 29 run 1, ZnO (left, red channel), exosomes (middle, green channel) and TNH (right, overlay). Scale bar is 1 µm.

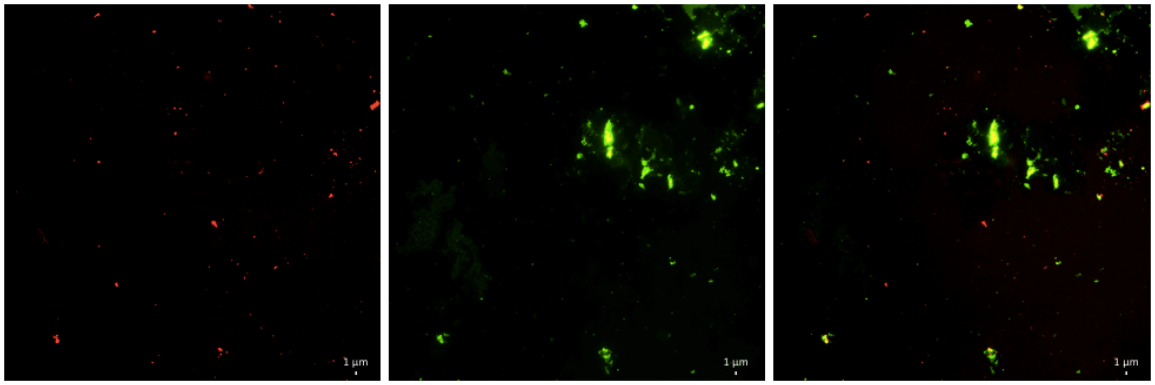

Figure 4.48: TNH 29 run 1-US, ZnO (left, red channel), exosomes (middle, green channel) and TNH (right, overlay). Scale bar is 1 µm.

In TNH 29, three aliquots of nanoparticles are added at time 0, after 1 hour and 2 hours and then the solution is sonicated. In the first run the coupling percentages are low because of the aggregates of nanoparticles, while US disassemble them.

- **TNH 30**

	Sample	Conditions	% ZnO colocalized (%)	% Exosomes colocalized (%)	% particles colocalized (%)
TNH 30	Run 1	US 59 kHz, 30’	/	/	/

ZnO nanoparticles are added to exosomes and they are sonicated at 59 kHz. This US frequency degrades the dyes, so it is impossible to see anything with fluorescence microscope.

- **TNH 31**

	Sample	Conditions	% ZnO colocalized (%)	% Exosomes colocalized (%)	% particles colocalized (%)
TNH 31	Run 1	US 1 MHz, few seconds	10.35	24.08	7.62

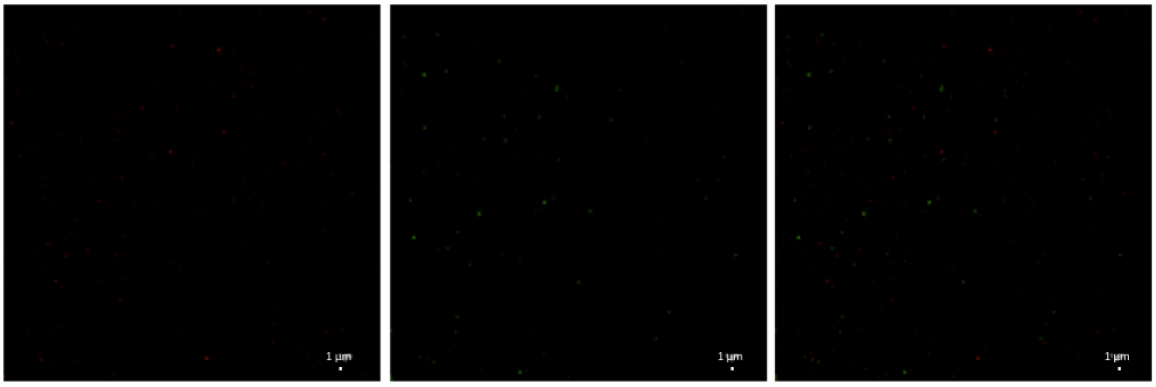

Figure 4.49: TNH 31 run 1, ZnO (left, red channel), exosomes (middle, green channel) and TNH (right, overlay). Scale bar is 1 µm.

In TNH 31, another setting of US is used with the frequency of 1 MHz, but unsuccessfully because of the reduced time of sonication due the rapid increasing of the temperature.

- **TNH 32**

	Sample	Conditions	% ZnO colocalized (%)	% Exosomes colocalized (%)	% particles colocalized (%)
TNH 32	Run 1	KB, orbital shaker 250 rpm, 37°C, 90'. Centrifuge 16870 g, 5'.	/	/	/
	Run 1 - US	US 40 kHz, 30'	20.96	14.69	8.84

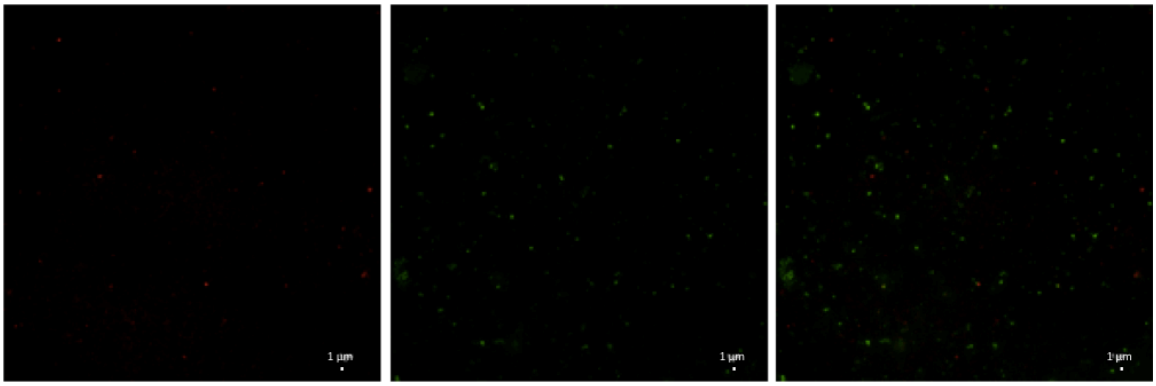

Figure 4.50: TNH 32 run 1 - US, ZnO (left, red channel), exosomes (middle, green channel) and TNH (right, overlay). Scale bar is 1 µm.

Images of the first run of TNH 32 are impossible to acquire because of some problems with the focus of the microscope.

Instead, images of the second run are acquired even if the percentages are not good.

- **TNH 33**

	Sample	Conditions	% ZnO colocalized (%)	% Exosomes colocalized (%)	% particles colocalized (%)
TNH 33	Run 1	KB, US 40 kHz, 30'	**66.48**	**39.97**	31.06

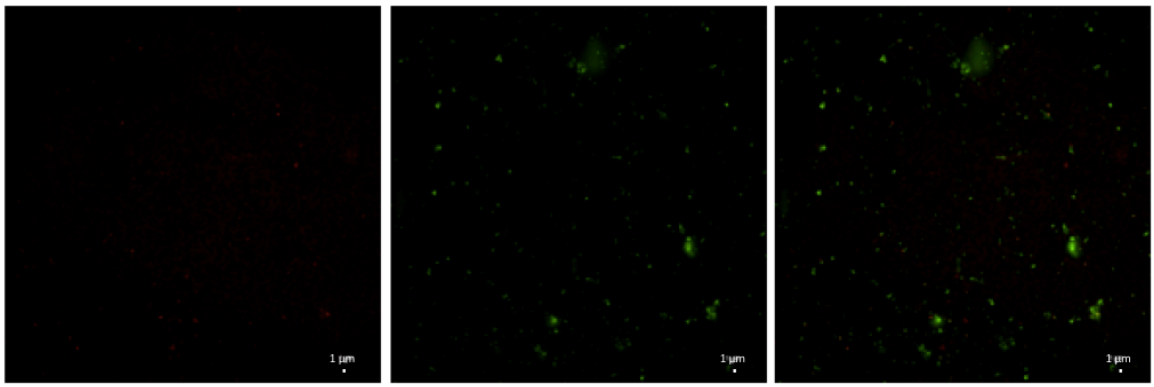

Figure 4.51: TNH 33 run 1, ZnO (left, red channel), exosomes (middle, green channel) and TNH (right, overlay). Scale bar is 1 µm.

TNH 33 is prepared only through sonication. The rate of coupling is very good, but further analysis with TEM (see below, Figure 4.82) shows that exosomes are not intact.

- **TNH 34**

	Sample	Conditions	% ZnO colocalized (%)	% Exosomes colocalized (%)	% particles colocalized (%)
TNH 34	Run 1.1	KB (physiologic solution), orbital shaker 250 rpm, 37°C, 90'. Centrifuge 7500 g, 5'.	**67.73**	**40.08**	34.43
	Run 1.2	KB (physiologic solution), orbital shaker 250 rpm, 37°C, 90'. Centrifuge 5000 g, 5'.	31.61	10.70	8.45

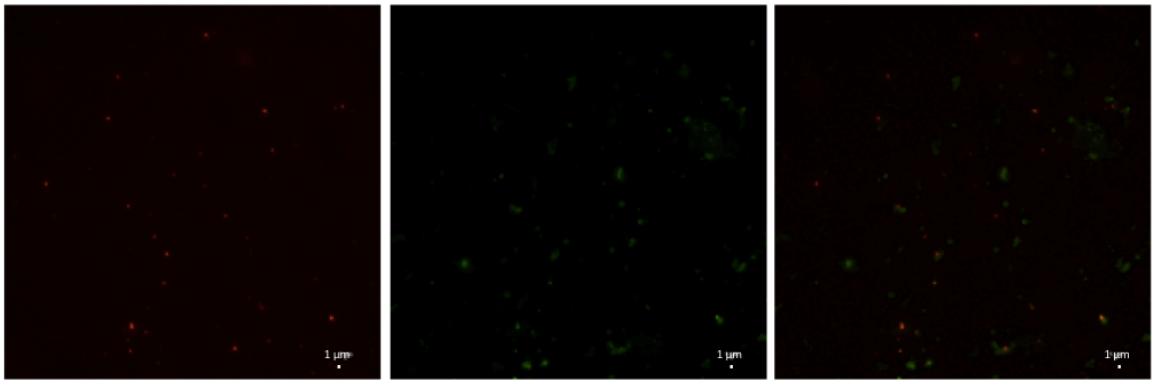

Figure 4.52: TNH 34 run 1.1, ZnO (left, red channel), exosomes (middle, green channel) and TNH (right, overlay). Scale bar is 1 µm

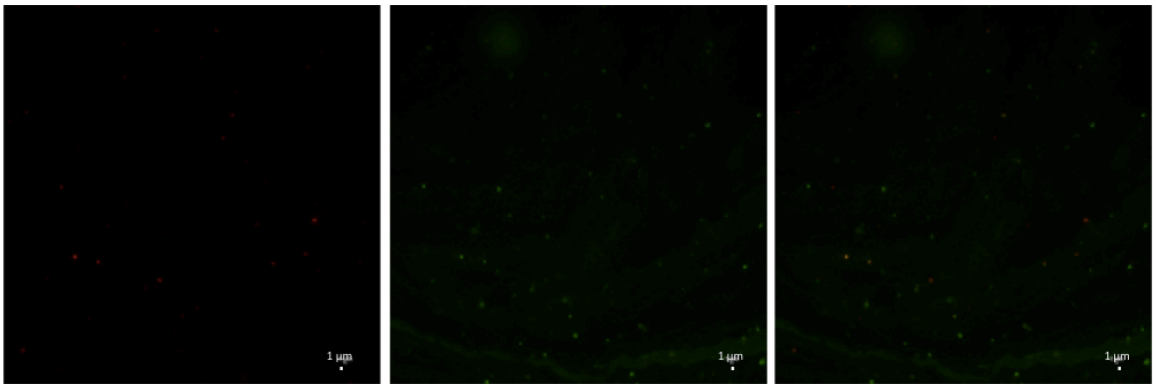

Figure 4.53: TNH 34 run 1.2, ZnO (left, red channel), exosomes (middle, green channel) and TNH (right, overlay). Scale bar is 1 µm

TNH 34 is used to carry out two tests of centrifuge. Many centrifuge steps damage the structure of exosomes and slow centrifuge speed can be also useful to improve the separation of uncoupled ZnO and exosomes (pelleting at higher rates) than the TNH. These proofs demonstrate that also centrifuges at slower rate are enough to pellet TNH without damaging it.

- **TNH 35**

	Sample	Conditions	% ZnO colocalized (%)	% Exosomes colocalized (%)	% particles colocalized (%)
TNH 35	Run 1	KB (physiologic solution), orbital shaker 250 rpm, 37°C, 90'. Centrifuge 5000 g, 5'.	31.09	24.54	13.93
	Run 2	Orbital shaker 250 rpm, 37°C, 90'. Centrifuge 5000 g, 5'.	3.11	12.83	2.53
	Run 3	Orbital shaker 250 rpm, 37°C, 90'. Centrifuge 5000 g, 5'.	1.08	13.08	1.02

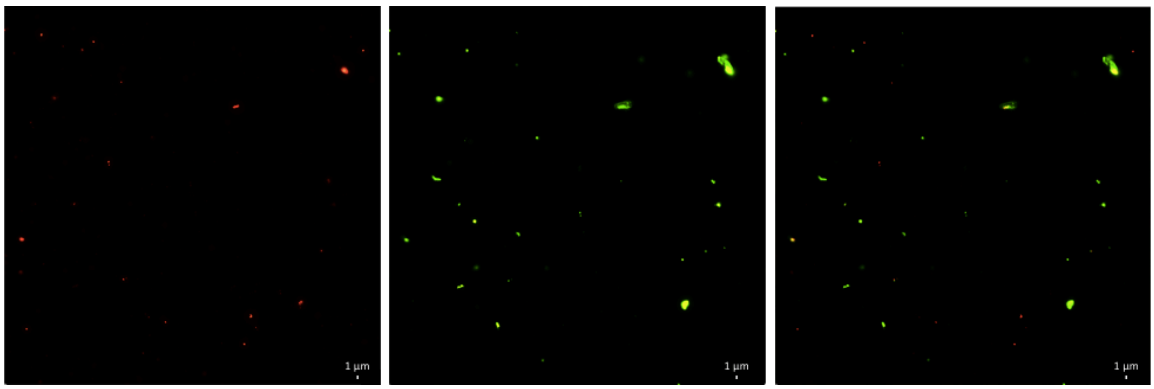

Figure 4.54: TNH 35 run 1, ZnO (left, red channel), exosomes (middle, green channel) and TNH (right, overlay). Scale bar is 1 µm

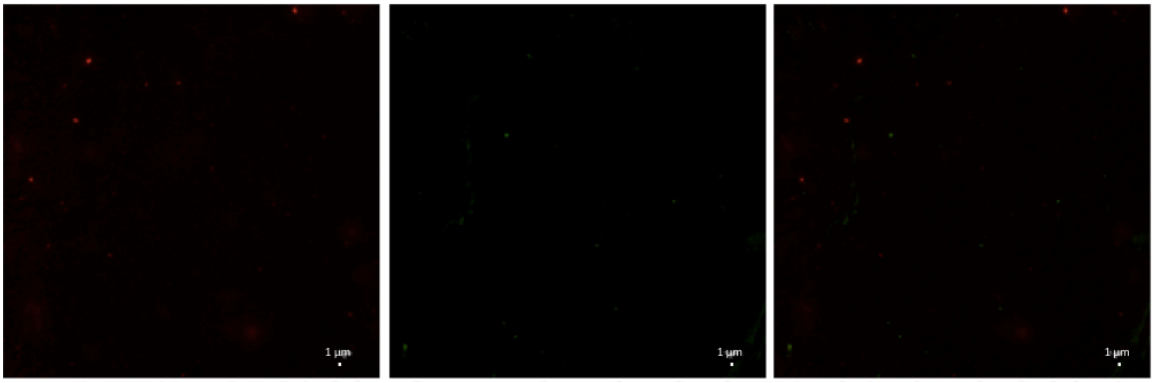

Figure 4.55: TNH 35 run 2, ZnO (left, red channel), exosomes (middle, green channel) and TNH (right, overlay). Scale bar is 1 µm

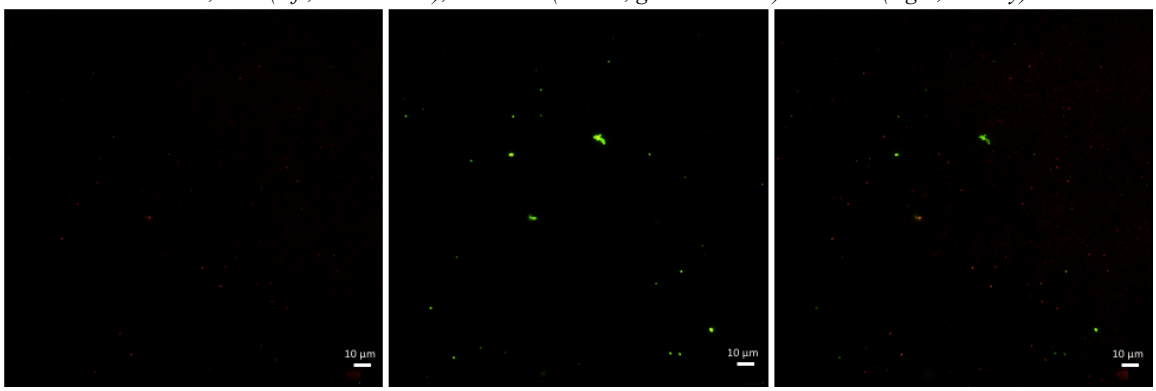

Figure 4.56: TNH 35 run 3, ZnO (left, red channel), exosomes (middle, green channel) and TNH (right, overlay). Scale bar is 10 µm

In TNH 35 it is tried to increase the amount of nanoparticles loaded for one vial of exosomes by adding another run. Results are not so encouraging because in the last run there are few exosomes and many nanoparticles, so the coupling can not occur.

- **TNH 36**

	Sample	Conditions	% ZnO colocalized (%)	% Exosomes colocalized (%)	% particles colocalized (%)
TNH 36	Run 1	KB (physiologic solution), orbital shaker 250 rpm, 37°C, 90'. Centrifuge 5000 g, 5'.	16.84	21.12	10.88
	Run 2	Orbital shaker 250 rpm, 37°C, 90'. Centrifuge 5000 g, 5'.	5.91	9.90	3.48
	Run 1+2 - US	Combination Run 1 and Run 2, US 40 kHz, 30'	25.04	20.34	11.35
	Run 3	Orbital shaker 250 rpm, 37°C, 90'.	6.92	17.68	5.14
	Run 3 - US	US 40 kHz, 30'	4.29	6.61	2.62
	Run 3 – US – 7500 rcf	Centrifuge 7500 g, 5'.	8.02	15.56	4.96

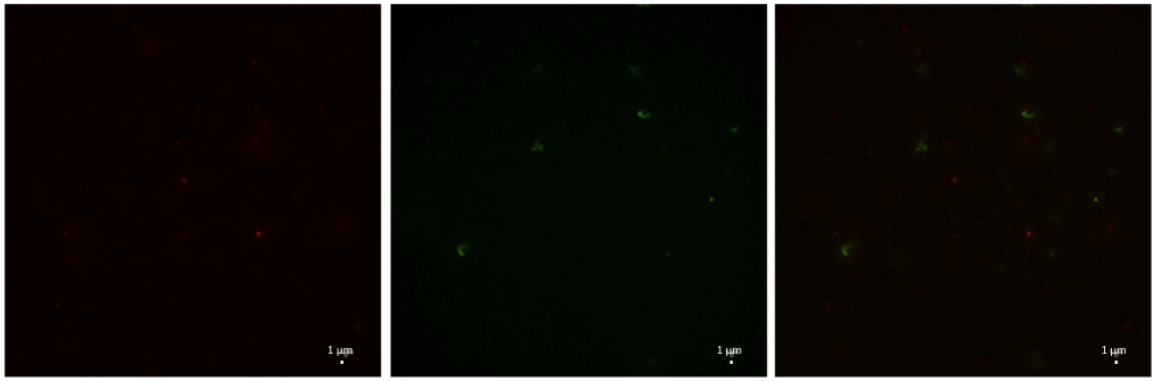

Figure 4.57: TNH 36 run 2, ZnO (left, red channel), exosomes (middle, green channel) and TNH (right, overlay). Scale bar is 1 μm

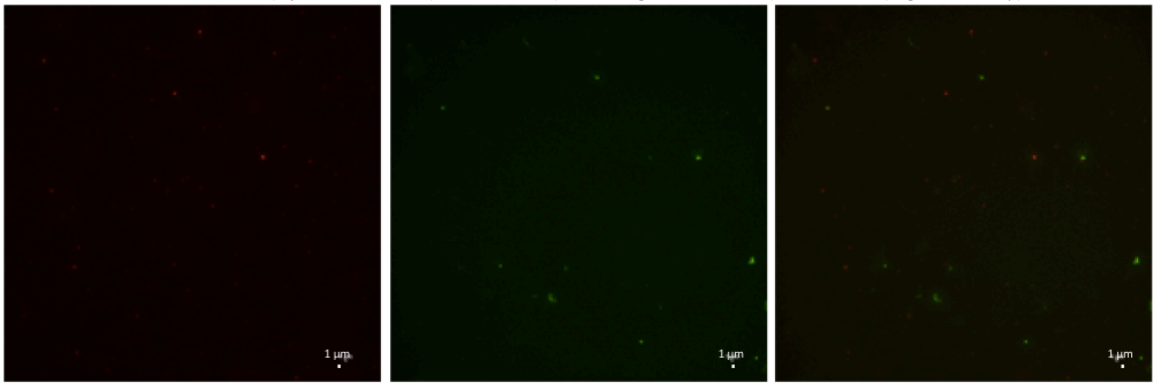

Figure 4.58: TNH 36 run 1+2, ZnO (left, red channel), exosomes (middle, green channel) and TNH (right, overlay). Scale bar is 1 μm

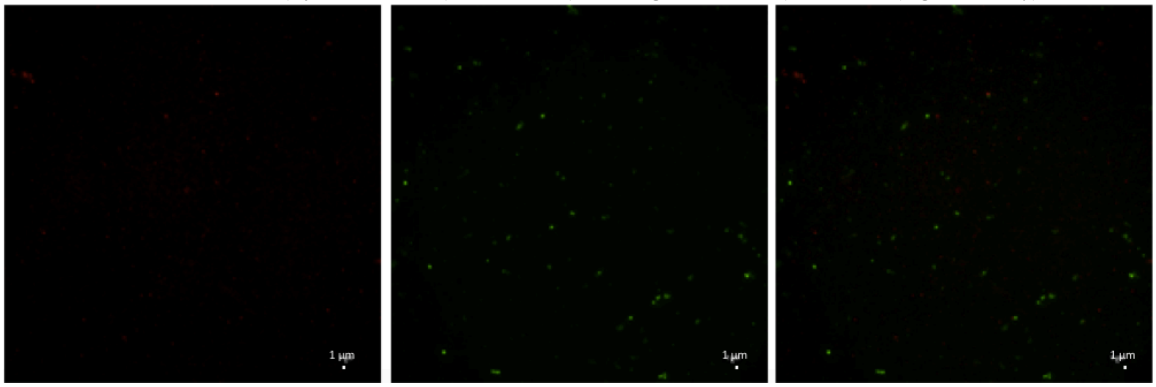

Figure 4.59: TNH 36 run 3, ZnO (left, red channel), exosomes (middle, green channel) and TNH (right, overlay). Scale bar is 1 μm

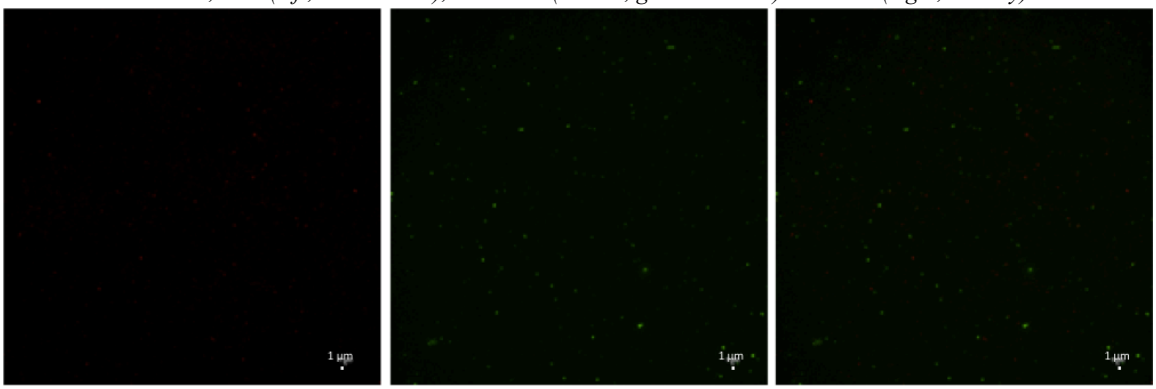

Figure 4.60: TNH 36 run 3 - US, ZnO (left, red channel), exosomes (middle, green channel) and TNH (right, overlay). Scale bar is 1 μm

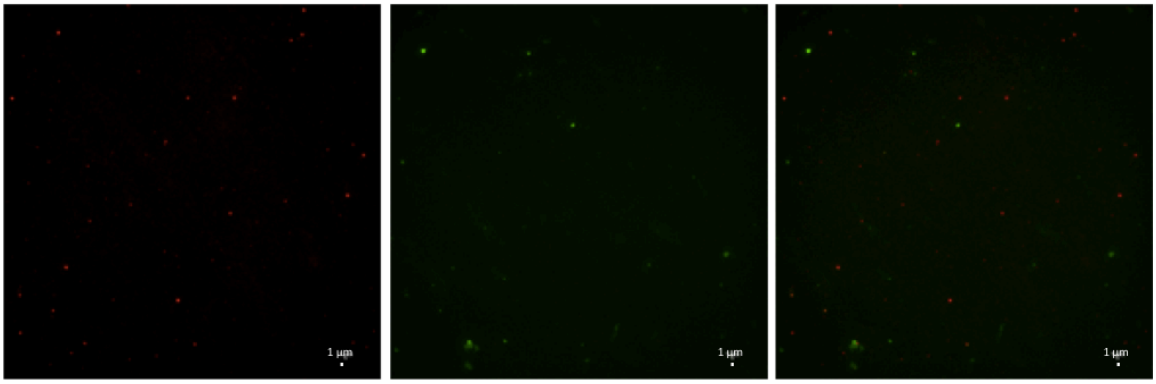

Figure 4.61: TNH 36 run 3 – US centrifuged, ZnO (left, red channel), exosomes (middle, green channel) and TNH (right, overlay). Scale bar is 1 μm

In TNH 36, the protocol used for TNH 35 is repeated and the results are mostly the same, indicating a good repeteability of the two processes.

- **TNH 37**

	Sample	Conditions	% ZnO colocalized (%)	% Exosomes colocalized (%)	% particles colocalized (%)
TNH 37	Run 1	KB (physiologic solution), orbital shaker 250 rpm, 37°C, 90'. Centrifuge 5000 g, 5'.	23.42	11.03	8.11
	Run 2	Orbital shaker 250 rpm, 37°C, 90'. Centrifuge 5000 g, 5'.	38.96	**46.78**	25.92
	Run 3	Orbital shaker 250 rpm, 37°C, 90'. Centrifuge 7500 g, 5'.	26.45	29.90	15.67

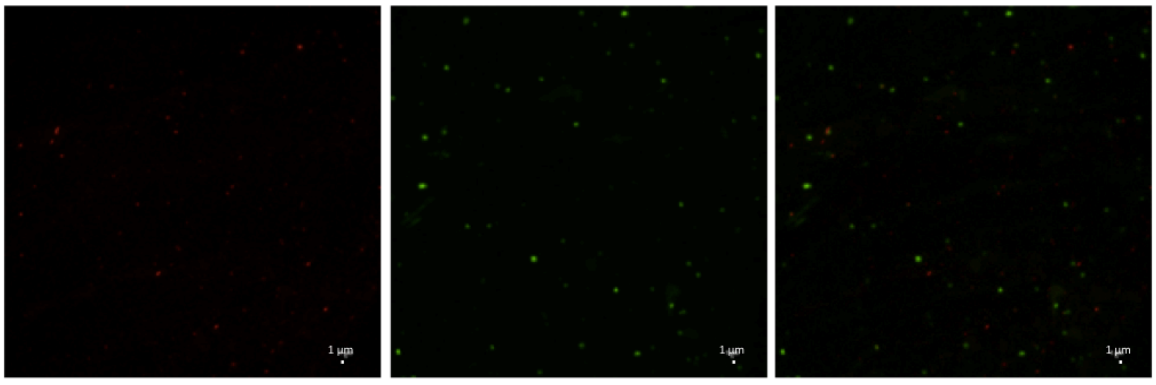

Figure 4.62: TNH 37 run 1, ZnO (left, red channel), exosomes (middle, green channel) and TNH (right, overlay). Scale bar is 1 μm.

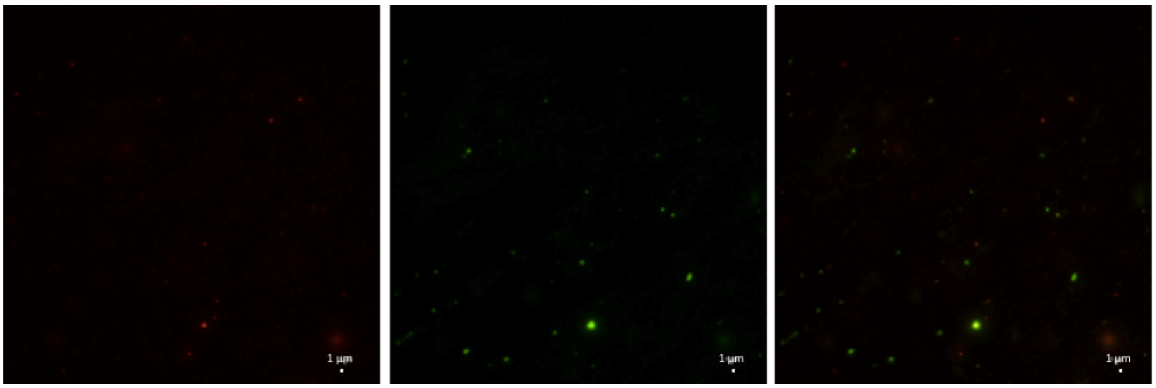

Figure 4.63: TNH 37 run 2, ZnO (left, red channel), exosomes (middle, green channel) and TNH (right, overlay). Scale bar is 1 µm.

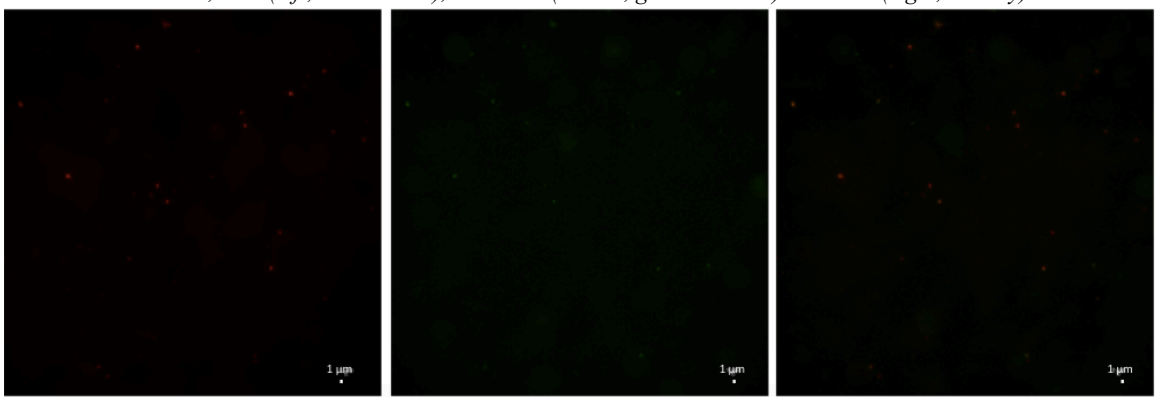

Figure 4.64: TNH 37 run 3, ZnO (left, red channel), exosomes (middle, green channel) and TNH (right, overlay). Scale bar is 1 µm

Repeating for the third time the protocol used for TNH 35 and TNH 36, in TNH 37 there are better percentages of coupling. Unfortunately, there is no reproducibility in these three tests taken together.

- **TNH 38**

	Sample	Conditions	% ZnO colocalized (%)	% Exosomes colocalized (%)	% particles colocalized (%)
TNH 38	Run 1	DAUDI orbital shaker 250 rpm, 37°C, 90'. Centrifuge 5000 g, 5'.	**62.63**	**41.87**	32.51
	Run 2	Orbital shaker 250 rpm, 37°C, 90'. Centrifuge 5000 g, 5'.	**54.83**	**45.36**	33.23

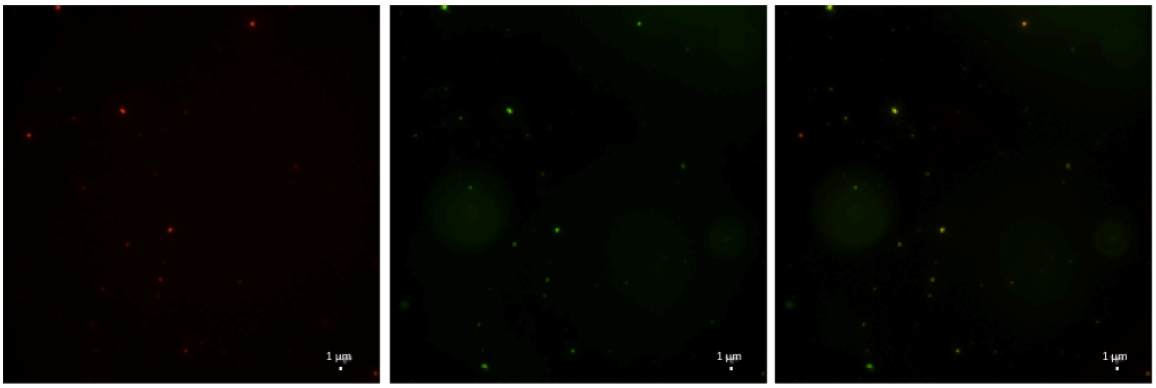

Figure 4.65: TNH 38 run 1, ZnO (left, red channel), exosomes (middle, green channel) and TNH (right, overlay). Scale bar is 1 µm.

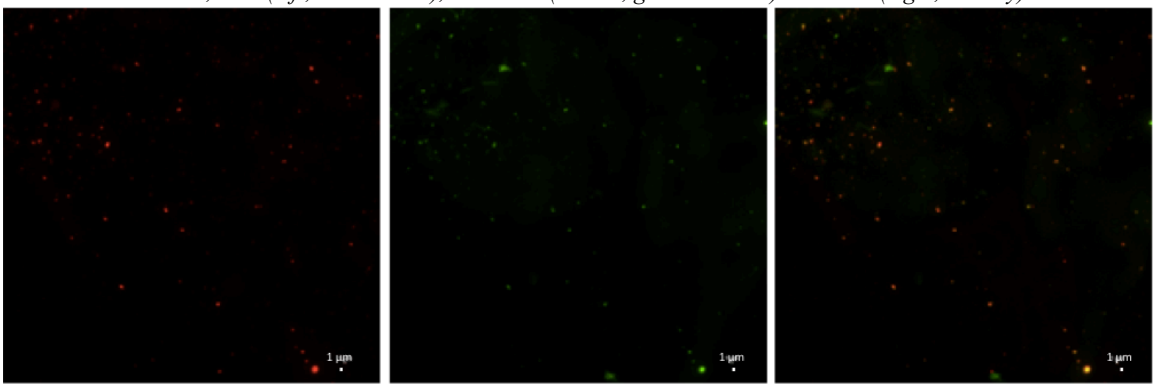

Figure 4.66: TNH 38 run 2, ZnO (left, red channel), exosomes (middle, green channel) and TNH (right, overlay). Scale bar is 1 µm

In TNH 38 exosomes from DAUDI in PBS are used and comparing them with the ones from KB in PBS, percentages are much better.

- **TNH 39**

	Sample	Conditions	% ZnO colocalized (%)	% Exosomes colocalized (%)	% particles colocalized (%)
TNH 39	Run 1	DAUDI (physiologic solution) orbital shaker 250 rpm, 37°C, 90'. Centrifuge 5000 g, 5'.	**42.22**	**44.24**	25.55
	Run 2	Orbital shaker 250 rpm, 37°C, 90'. Centrifuge 5000 g, 5'.	**65.61**	35.55	30.15

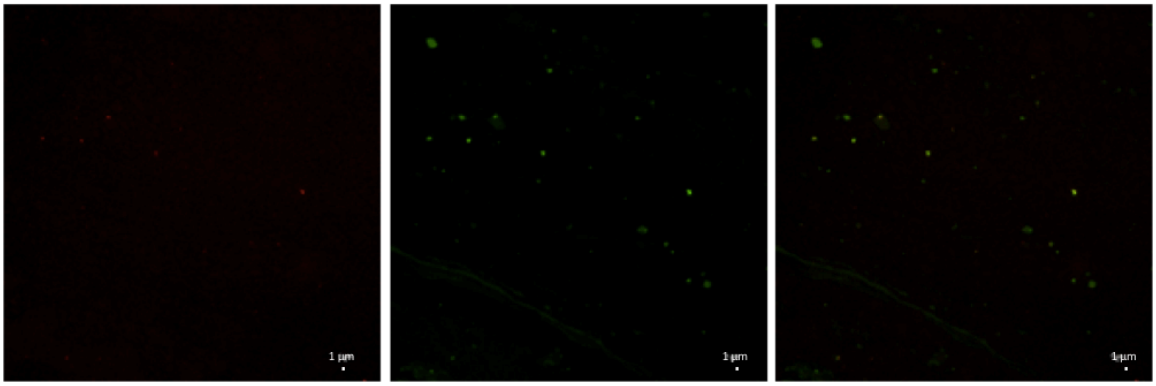

Figure 4.67: TNH 39 run 1, ZnO (left, red channel), exosomes (middle, green channel) and TNH (right, overlay). Scale bar is 1 µm.

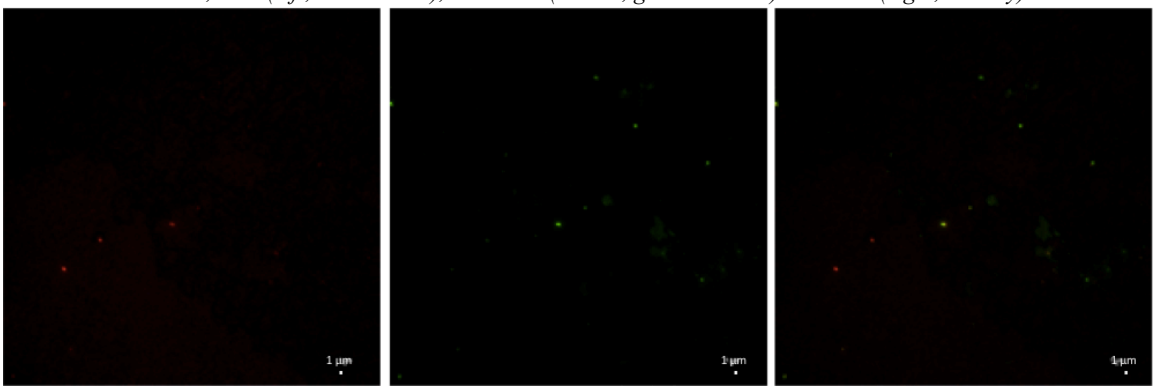

Figure 4.68: TNH 39 run 2, ZnO (left, red channel), exosomes (middle, green channel) and TNH (right, overlay). Scale bar is 1 µm

In TNH 39 exosomes from DAUDI in physiologic solution are used and comparing them with the ones from KB in physiologic solution, percentages are much better.

- **TNH 40**

	Sample	Conditions	% ZnO colocalized (%)	% Exosomes colocalized (%)	% particles colocalized (%)
TNH 40	Run 1	DAUDI orbital shaker 250 rpm, 37°C, 90'. Centrifuge 5000 g, 5'.	25.92	20.65	11.40
	Run 2	Orbital shaker 250 rpm, 37°C, 90'. Centrifuge 5000 g, 5'.	**61.10**	**43.33**	34.40

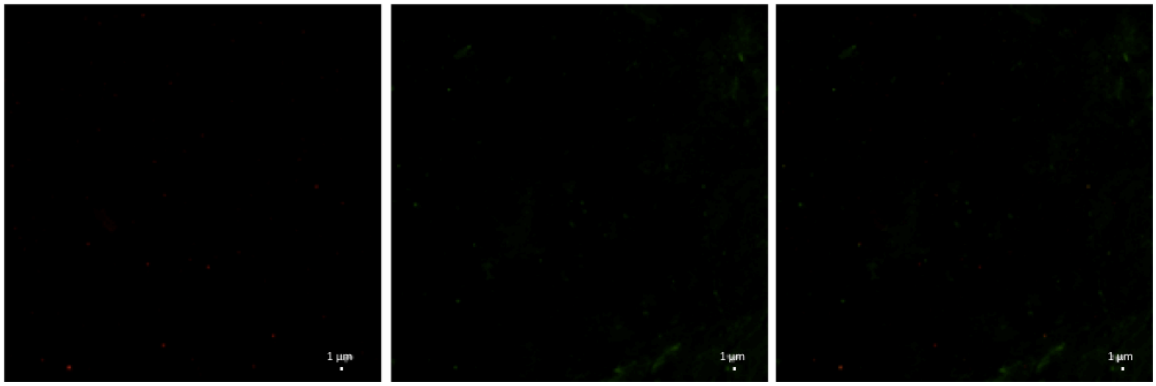

Figure 4.69: TNH 40 run 1, ZnO (left, red channel), exosomes (middle, green channel) and TNH (right, overlay). Scale bar is 1 µm.

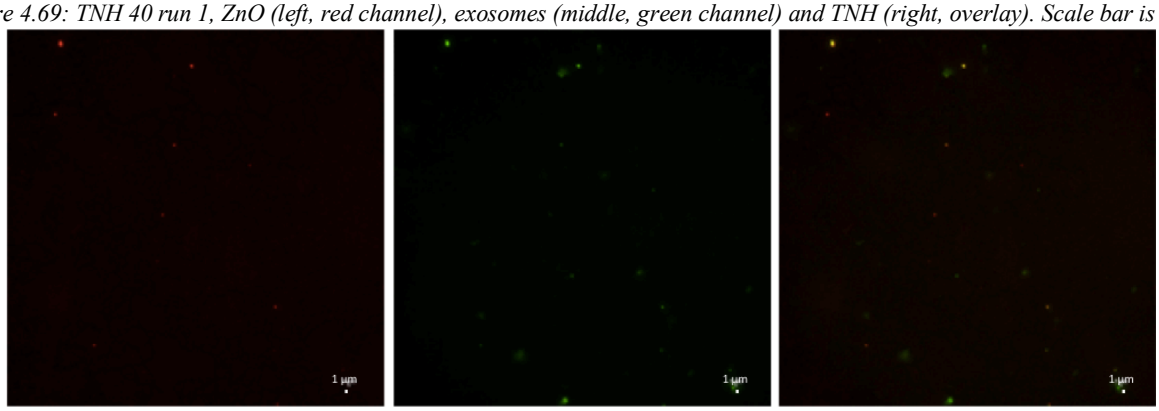

Figure 4.70: TNH 40 run 2 ZnO (left, red channel), exosomes (middle, green channel) and TNH (right, overlay). Scale bar is 1 µm.

TNH 40 is the same coupling of TNH 38, and the trend is confirmed.

- **TNH 41**

	Sample	Conditions	% ZnO colocalized (%)	% Exosomes colocalized (%)	% particles colocalized (%)
TNH 41	Run 1	DAUDI (physiologic solution) orbital shaker 250 rpm, 37°C, 90'. Centrifuge 5000 g, 5'.	**64.69**	16.66	15.19
	Run 2	Orbital shaker 250 rpm, 37°C, 90'. Centrifuge 5000 g, 5'.	**47.42**	20.13	16.45

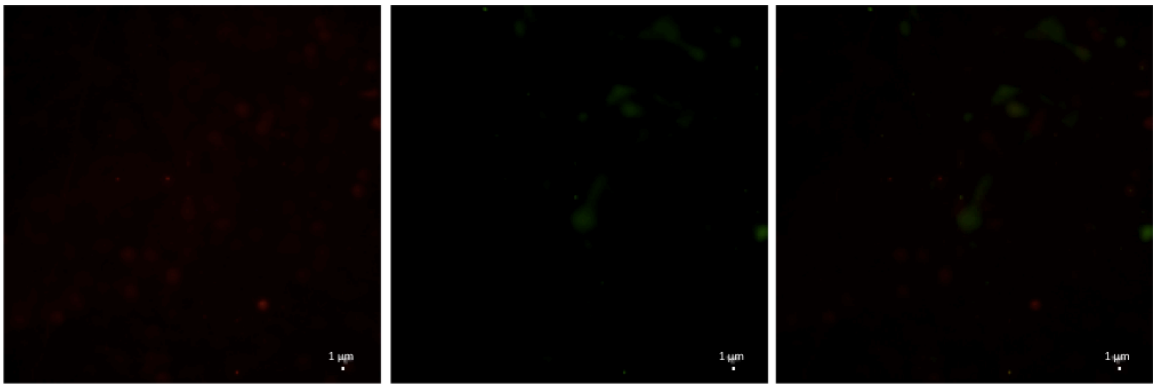

Figure 4.71: TNH 41 run 1, ZnO (left, red channel), exosomes (middle, green channel) and TNH (right, overlay) in that order. Scale bar1

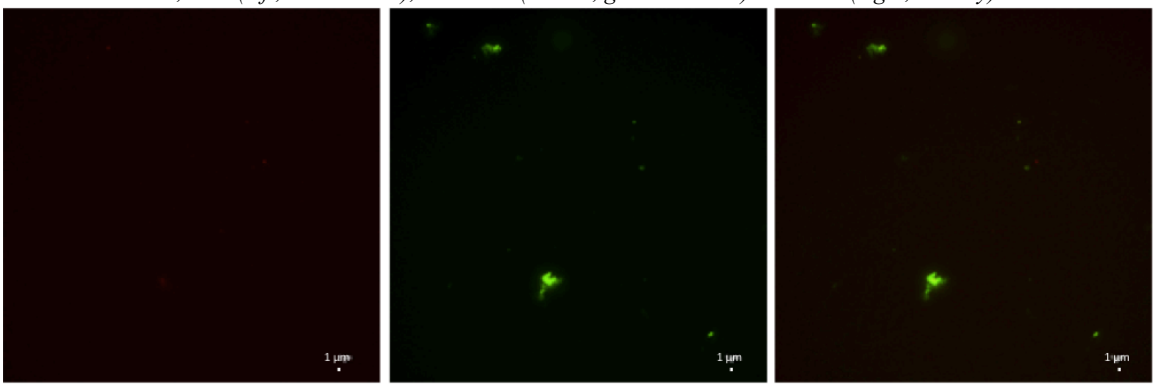

Figure 4.72: TNH 41 run 2, ZnO (left, red channel), exosomes (middle, green channel) and TNH (right, overlay) in that order. Scale bar 1 μm.

TNH 41 is the same coupling of TNH 39, and the trend is confirmed.

- **TNH 42**
  This coupling is prepared using ZnO functionalized with glucose in order to have an easier internalization into the exosomes. However, the addition of glucose in the solution causes the proliferation of fungal hyphae, visible also without the microscope, which damage the solution.

- **TNH 43**
  In TNH 43 there is the same situation of TNH 42, therefore the TNH was not evaluated further.

- **TNH 47**

	Sample	Conditions	% ZnO colocalized (%)	% Exosomes colocalized (%)	% particles colocalized (%)
TNH 47	Run 1	KB (physiologic solution) orbital shaker 250 rpm, 37°C, 90'. Centrifuge 5000 g, 5'.	**58.92**	27.19	22.70
	Run 2	Orbital shaker 250 rpm, 37°C, 90'. Centrifuge 7500 g, 5'.	21.85	14.68	9.56

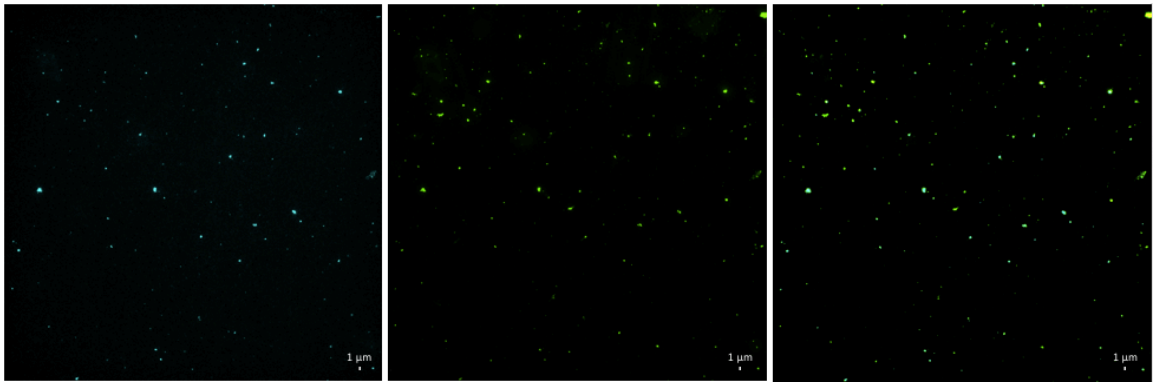

Figure 4.73: TNH 47 run 1, ZnO (left, NIR channel), exosomes (middle, green channel) and TNH (right, overlay) in that order. Scale bar 1 µm.

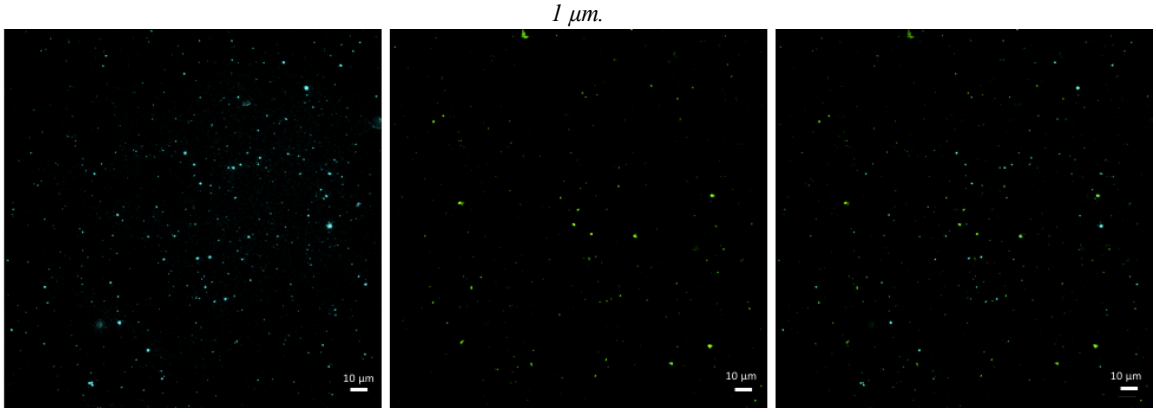

Figure 4.74: TNH 47 run 2, ZnO (left, NIR channel), exosomes (middle, green channel) and TNH (right, overlay) in that order. Scale bar 10 µm.

TNH 47 can be compared with TNH 34, 35, 36, 37. The percentages are more similar to the ones obtained for TNH 34 and 37 where there is a good coupling efficiency.

- **TNH 48**

	Sample	Conditions	% ZnO colocalized (%)	% Exosomes colocalized (%)	% particles colocalized (%)
TNH 48	Run 1	KB (physiologic solution) US 40 kHz, 20". Centrifuge 10000 g, 5'. Pellet resuspended in physiologic solution, US 40 kHz, 20". Centrifuge 10000 g, 5'.	23.77	6.98	5.57

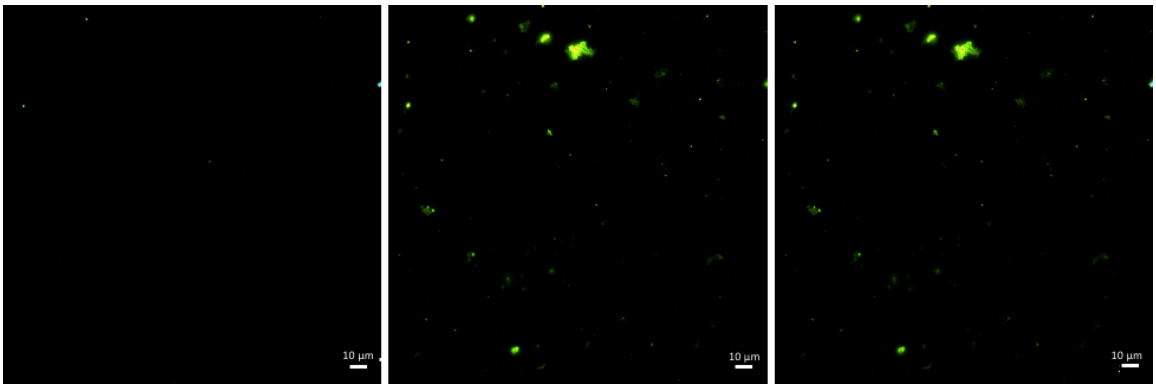

Figure 4.75: TNH 48 run 1, ZnO (left, NIR channel), exosomes (middle, green channel) and TNH (right, overlay) in that order. Scale bar 10 µm.

TNH 48 is prepared with the protocol used for MSNs in Madrid. Comparing TNH 48 with TNH 47 run 1, it is possible to evaluate the efficiency of the two methods. In TNH 48 the coupling percentages are lower than in TNH 47 and exosomes seem to be damaged probably because they suffer the sonication before the coupling as told before for TNH 33 and shown in Figure 4.82.

4.3.2 Nanoparticle Tracking Analysis (NTA)

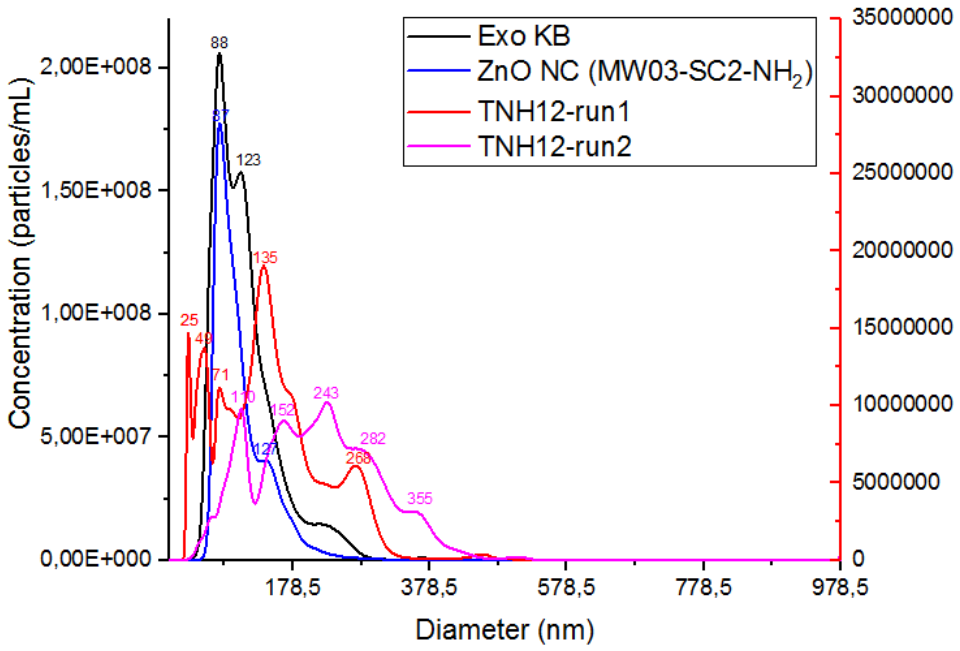

Figure 4.76: Size distribution and concentrations of TNH 12 obtained with NanoSight compared with pristine ZnO and exosomes.

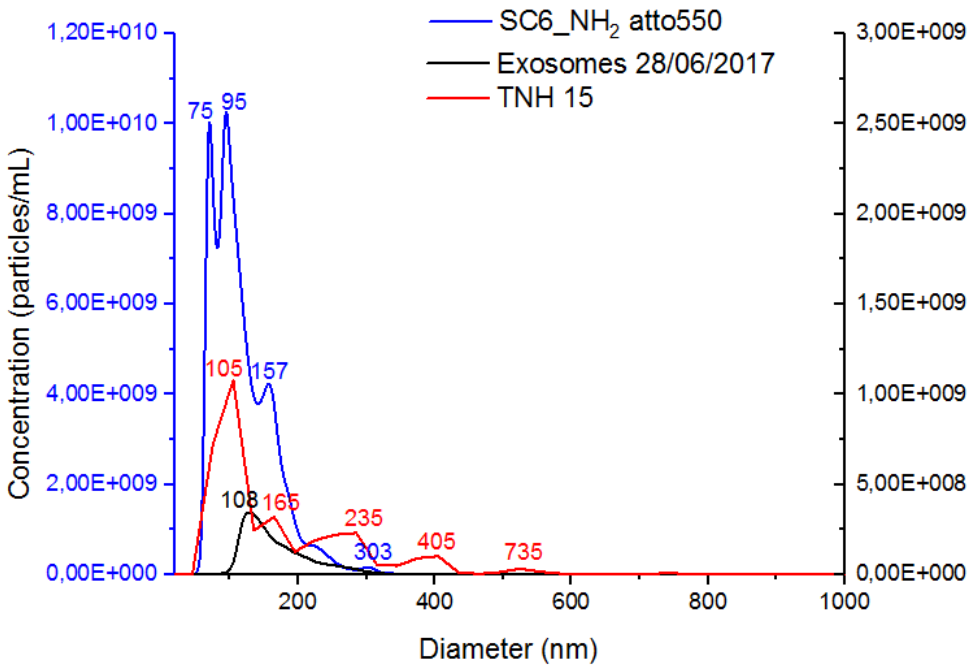

Figure 4.77: Size distribution and concentrations of TNH 15 obtained with NanoSight compared with pristine ZnO and exosomes.

As told before in the discussion of the results from the fluorescence microscope, TNH 15 has better coupling percentages than TNH 12. This result is confirmed by the measurements at the NanoSight. Figure 4.76 and Figure 4.77 report size and distribution of TNH 12 and TNH 15, respectively, compared with ZnO nanoparticles and exosomes.

The comparison between the size distribution of TNH 12 and TNH 15 underlines the differences seen also with the fluorescence microscope. TNH 12 has a floating distribution of size, there are particles around 135 nm and over which can be considered as TNH, but there are also smaller particles than the ZnO nanoparticles which probably are membrane debris, hint that the exosomes are damaged and that they might not participate in covering the ZnO nanoparticles.

In contrast, TNH 15 has a more regular distribution curve of sizes, most of them has a diameter around 105 and 165 nm which are reasonably bigger than the naked ZnO nanoparticles and the exceed can be considered as a phospholipid layer cover. In TNH 15 the concentration of exosomes is lower than the one of the TNH. This is probably because during the coupling some ZnO nanoparticles aggregate . It is important to take into account that the size dispersion curve at NTA of the ZnO nanoparticles is obtained in ethanol, while the one of the TNH is in PBS and water (1:1) so, as shown in the previous chapter of the ZnO results, nanoparticles can easily aggregate in PBS.

4.3.3 Discussions of results of TNH

In the tables below there are the resume of the obtained results.

- **Effect of the temperature**

Table 5: Temperature effect on coupling

	Exosomes aliquot		Conditions	Coupling %		
				% ZnO	% Exosomes	% TNH
TNH 12	KB 07/07/17	Run 1	90', Room Temperature	23.47	40.62	17.06
		Run 2	90', Room Temperature	18.32	15.77	8.60
TNH 13	KB 28/06/17	Run 1	90', Room Temperature	14.04	18.78	7.75
		Run 2	90', Room Temperature	19.33	29.97	12.90
TNH 15	KB 28/06/17	Run 1	90', Room Temperature	34.97	21.81	15.41
		Run 2	90', Room Temperature	65.07	36.86	33.43
TNH 17	KB 28/06/17	Run 1	90', Room Temperature	15.36	10.90	6.82
		Run 2	90', Room Temperature	13.51	3.97	3.18
TNH 18	KB 28/06/17	Run 1	90', 37°C	45.80	9.07	7.87
		Run 2	90', 37°C	48.16	41.16	28.16
TNH 20	KB 07/07/17	Run 1	90', 37°C	31.31	16.16	12.03
TNH 22	KB 07/07/17	Run 1	90', 37°C	37.94	8.09	6.88
TNH 19	KB 28/06/17	Run 1	90', 4°C	32.53	31.60	22.62
		Run 2	90', 4°C	7.62	22.83	5.94

Temperature	Run 1			Run 2		
	% ZnO	% Exo	% TNH	% ZnO	% Exo	% TNH
RT	21.96	23.03	11.76	29.06	21.64	14.53
37°C	36.54	21.80	15.69	48.16	41.16	28.16
4°C	32.53	31.60	22.62	7.62	22.83	5.94

One of the most important parameters is the temperature during the coupling. Ideally, during the coupling, the lipid membrane of the exosomes engulfs the ZnO nanoparticles, so the membrane must be fluid to allow the entrance of ZnO. At 4°C, with the analysis at fluorescence microscope, exosomes are very small and well dispersed, but the membrane is more stable than at higher temperature and this does not allow ZnO to penetrate inside the membrane.

At higher temperatures, i.e. room temperature and 37°C, the coupling percentages are better, but the best coupling efficiency occurs at 37°C, which is the physiologic temperature.

- **Effect of the mixing method**

Table 6: Mixing method effect on coupling

	Exosomes aliquot		Conditions	Coupling %		
				% ZnO	% Exosomes	% TNH
TNH 12	KB 07/07/17	Run 1	90', RT, orbital shaker	23.47	40.62	17.06
		Run 2	90', RT, orbital shaker	18.32	15.77	8.60
TNH 13	KB 28/06/17	Run 1	90', RT, orbital shaker	14.04	18.78	7.75
		Run 2	90', RT, orbital shaker	19.33	29.97	12.90
TNH 15	KB 28/06/17	Run 1	90', RT, orbital shaker	34.97	21.81	15.41
		Run 2	90', RT, orbital shaker	65.07	36.86	33.43
TNH 17	KB 28/06/17	Run 1	90', RT, orbital shaker	15.36	10.90	6.82
		Run 2	90', RT, orbital shaker	13.51	3.97	3.18
TNH 14	KB 28/06/17	Run 1	90', RT, wheel	6.59	37.37	6.13
TNH 16	KB 28/06/17	Run 1	90', RT, wheel	5.49	29.47	4.48
		Run 2	90', RT, wheel	16.53	3.97	3.18

Mixing Method	Run 1			Run 2		
	% ZnO	% Exo	% TNH	% ZnO	% Exo	% TNH
Orbital shaker	21.96	23.03	11.76	29.06	21.64	14.53
Wheel	6.04	33.42	5.31	16.53	13.91	7.87

The two mixing method are the orbital shaker and the wheel. The most suitable instrument is surely the orbital shaker. On the wheel, probably, exosomes stick on the Eppendorf walls and this prevents the coupling and also caused their damage.

- **Effect of the volume**

Table 7: Volume effect on coupling

	Exosomes aliquot		Conditions	Coupling %		
				% ZnO	% Exosomes	% TNH
TNH 22	KB 07/07/17	Run 1	24h, 37°C	37.94	8.09	6.88
TNH 26	KB 07/07/17	Run 1	24h, 37°C, 100µl+ 900µl EMEM	9.45	6.78	3.75

Mixing Method	Run 1			Run 2		
	% ZnO	% Exo	% TNH	% ZnO	% Exo	% TNH
100 µl	37.94	8.09	6.88	-	-	-
1000 µl	9.45	6.78	3.75	-	-	-

The best volume is 100 µl for one aliquot of exosomes (50 µl) because probably a bigger volume caused less collisions and so a less internalization.

- **Effect of the time**

Table 8: Time effect on coupling

	Exosomes aliquot		Conditions	Coupling %		
				% ZnO	% Exosomes	% TNH
TNH 18	KB 28/06/17	Run 1	90', 37°C	45.80	9.07	7.87
		Run 2	90', 37°C	48.16	41.16	28.16
TNH 20	KB 07/07/17	Run 1	8h, 37°C	31.31	16.16	12.03
TNH 22	KB 07/07/17	Run 1	24h, 37°C	37.94	8.09	6.88

Temperature	Run 1			Run 2		
	% ZnO	% Exo	% TNH	% ZnO	% Exo	% TNH
90'	45.80	9.07	7.87	48.16	41.16	28.16
8h	31.31	16.16	12.03	-	-	-
24h	37.94	8.09	6.88	-	-	-

The best coupling time is different runs of 90 minutes. Several hours of coupling do not increase remarkably the coupling percentage. Furthermore, exosomes have a limited lifetime at 37 °C before starting to be damaged, so if less time is required for coupling, there is more time for the circulation in vivo to exploit their role.

- **ZnO quantity**

Table 9: ZnO quantity effect on the coupling

NANOPARTICLES ADDED ALL TOGETHER AT THE BEGINNING						
	Exosomes aliquot		Conditions	Coupling %		
				% ZnO	% Exosomes	% TNH
TNH 20	KB 07/07/17	Run 1	8h, 37°C	31.31	16.16	12.03
TNH 21	KB 07/07/17	Run 1	8h, 37°C, x10 NPs	11.32	18.21	7.25

CONSECUTIVE ADDITION OF NANOPARTICLES						
	Exosomes aliquot		Conditions	Coupling %		
				% ZnO	% Exosomes	% TNH
TNH 18	KB 28/06/17	Run 1	90', 37°C	45.80	9.07	7.87
		Run 2	90', 37°C	48.16	41.16	28.16
TNH 25	KB 07/07/17	Run 1	3h, 37°C, x3 NPs (added at t0,1h and 2h)	32.91	39.06	21.53
		Run 2	3h, 37°C, x3 NPs (added at t0,1h and 2h)	39.01	49.80	26.83
TNH 29	KB 07/07/17	Run 1	3h, 37°C, x3 NPs (added at t0,1h and 2h)	21.48	23.71	12.54

CONSECUTIVE ADDITION OF NANOPARTICLES IN HIGHER VOLUMES						
	Exosomes aliquot		**Conditions**	**Coupling %**		
				% ZnO	**% Exosomes**	**% TNH**
TNH 26	KB 07/07/17	Run 1	24h, 37°C, 100µl+ 900µl EMEM	9.45	6.78	3.75
TNH 27	KB 07/07/17	Run 1	24h, 37°C, 100µl+ 900µl EMEM, x 5 nps added every hour	7.91	11.30	4.37

One of the most important problem of the coupling is the quantity of ZnO used. There is a threshold of ZnO amount under which it is not toxic for the cells, and it must be reached to achieve a toxic effect for cancer cells. Obviously if more ZnO needs to be used, also more exosomes are required. It is not so easy to obtain a huge amount of exosomes even from various extractions, thus the quantity of ZnO for each aliquot must be optimized.

The need to use a lot of nanoparticles faces with the tendency of ZnO to aggregate in PBS and physiologic solution. This is the reason why the best method to increase the amount of ZnO in the coupling is doing different runs, using for the next one the supernatant of the previous one and adding to this an aliquot of ZnO.

Adding at the beginning many nanoparticles causes the aggregation of them and the impossibility to couple with exosomes. However, adding in multistep the NPs in the same run does not even seems to solve the problem, posing a limit for the exosomes to load the nanoparticles. Again, the best results were obtained using different runs.

- **Effect of the suspension medium of exosomes**

Table 10: Suspension medium effect on the coupling

	Exosomes aliquot		**Conditions**	**Coupling %**		
				% ZnO	**% Exosomes**	**% TNH**
TNH 23	DAUDI PBS	Run 1	24h, 37°C	41.90	44.69	27.92
TNH 24	DAUDI Physiologic solution	Run 1	24h, 37°C	58.58	36.08	29.32
TNH 40	DAUDI PBS	Run 1	90', 37°C	25.92	20.65	11.40
		Run 2	90', 37°C	61.10	43.33	34.40
TNH 39	DAUDI Physiologic solution	Run 1	90', 37°C	42.22	44.24	25.55
		Run 2	90', 37°C	65.61	35.55	30.15
TNH 18	KB PBS	Run 1	90', 37°C	45.80	9.07	7.87
TNH 34	KB Physiologic solution	Run 1	90', 37°C	67.73	40.08	34.43

The exosomes used for the coupling come from different cell lines, but they are also suspended in different medium: PBS and physiologic solution. The coupling percentages of the exosomes in physiologic solution seem to be better that the one in PBS, irrespectively from the exosome origin.

Further characterizations are carried out to understand which medium is most suitable for exosomes, but also for the nanoparticles. The first one, shown in Table 11, is the nanoparticles tracking analysis, from which the concentration and the average diameter is obtained. Exosomes from DAUDI cells are from the extraction of 24th of November 2017, while the ones from KB are from the extraction of 21st of February 2018.

Table 11: Characterization of exosomes from different cell line and in different medium

Sample	Concentration (part/ml)	Diameter (nm)
Exo DAUDI PBS	2.98 $E10^9$	159
Exo DAUDI physiologic solution	3.59 $E10^9$	87
Exo KB PBS	5.13 $E10^{10}$	170
Exo KB physiologic solution	2.79 $E10^{10}$	181

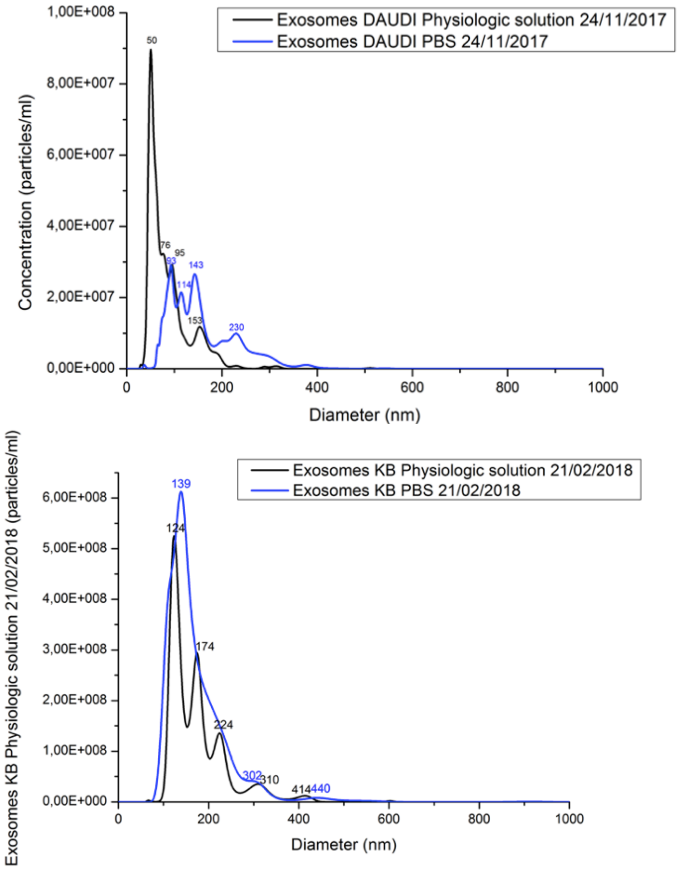

Figure 4.78: Characterization of exosomes from different cell line and in different medium at NanoSight

However, the most important results come from Table 12 and Figure 4.79 where the effects of medium on the ZnO nanoparticles are analysed. The Z-potential results show that in physiologic solution the nanoparticles have a positively charged the surface, while in PBS they are negatively charged. This is very important for the interaction between exosomes (whose membrane is negative) and ZnO, because the positive charge of nanoparticles in physiologic solution can promote an electrostatic interaction, enhancing the coupling.

The DLS analysis in Figure 4.79, showed that both PBS and physiologic solution cause the aggregation of the nanoparticles. However, in physiologic solution the process was recorded to be slower than in PBS (data not shown).

Table 12: Z-potential values for ZnO nanoparticles in PBS and physiologic solution

Sample	Z-potential (mV)
ZnO in PBS	-15.5
ZnO in Physiologic solution	12.3

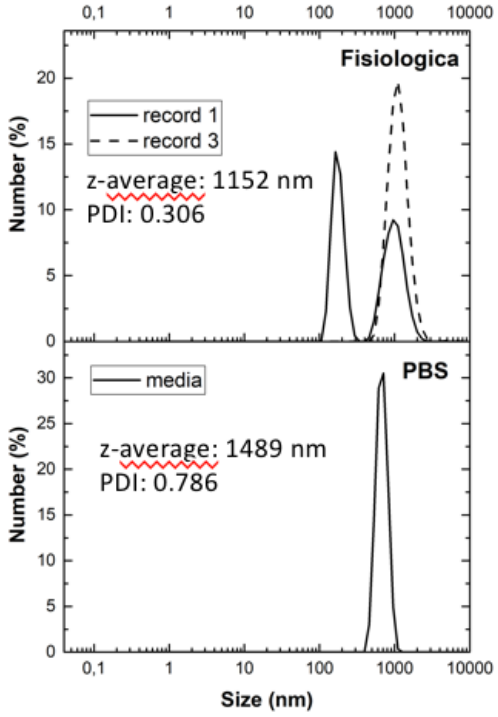

Figure 4.79: DLS of ZnO nanoparticles in PBS and Physiologic solution

A clear proof of this hypothesis is shown in Figure 4.80, presenting two images of the supernatants after two runs of coupling. The supernatant of the exosomes in PBS (left image) is still full of vesicles which seem to be a little damaged, while in the right image are presented the exosomes in physiologic

solution: there are only few exosomes left and they are spherical and small, so they are not corrupted. This means that in physiologic more exosomes are involved in the coupling with ZnO.

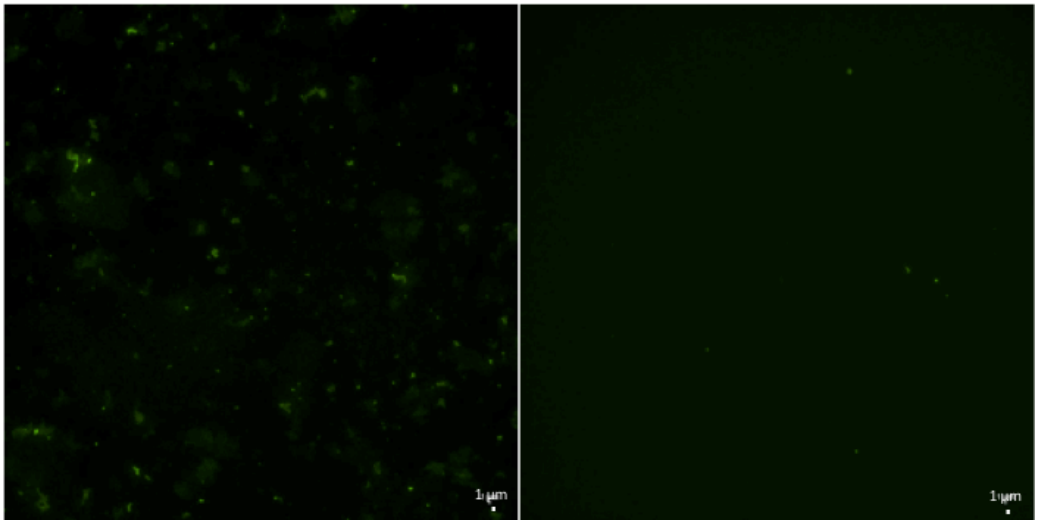

Figure 4.80: Supernatants after two runs of coupling in PBS of TNH 38-run2 (left) and in Physiologic solution f TNH 39-run2 (right)

Table 13 reports the data of TNH 38, 39, 40 and 41 from the fluorescence microscope to better explain the results of the supernatants shown above. The second run of TNH 39 (physiologic solution) has a better coupling percentage than TNH 38 (PBS) for what concerns the ZnO nanoparticles, this could be a proof of the hypothesis above. For what concern the percentages of exosomes, in the second run of TNH 39 it is a little worse than the one of TNH 38, but it is better after the first run and it must be remembered that the exosomes are better dispersed in physiologic solution while in PBS there are many aggregates, so less exosomes to be counted.

As shown in Table 13 and in Table 10, the coupling percentages are better for the exosomes in physiologic solution than in PBS, this could be the reason why there are less exosomes inside the supernatants after the couplings.

Table 13: comparison between TNH 38 and TNH 39

Sample		% ZnO colocalized	% exosomes colocalized	% particles colocalized
TNH 38 (PBS)	Run 1	**62.63**	41.87	32.51
	Run 2	54.83	45.36	33.23
TNH 39 (physiologic solution)	Run 1	42.22	44.24	25.55
	Run 2	**65.61**	35.55	30.15

- **Effect of the sonication**

Table 14: US effect on the coupling

	Exo aliquot		Cond	Coupling %			Cond US	Coupling %		
				% ZnO	% Exo	% TNH		% ZnO	% Exo	% TNH
TNH 17	KB 28/06/17	Run 1	90', RT	15.36	10.90	6.82	30', 40kHz	15.04	30.05	10.87
TNH 18	KB 28/06/17	Run 1	90', 37°C	45.80	9.07	7.87	30', 40kHz	40.08	11.59	9.86
TNH 20	KB 07/07/17	Run 1	8h, 37°C	31.31	16.16	12.03	30', 40kHz	44.51	17.49	12.90
TNH 21	KB 07/07/17	Run 1	8h, 37°C, x10 nps	11.32	18.21	7.25	30', 40kHz	19.71	17.57	8.85
TNH 22	KB 07/07/17	Run 1	24h, 37°C	37.94	8.09	6.88	30', 40kHz	58.23	23.73	20.33
TNH 26	KB 07/07/17	Run 1	24h, 37°C, 100µl + 900µl EMEM	9.45	6.78	3.75	30', 40kHz	39.62	39.87	24.17
TNH 27	KB 07/07/17	Run 1	24h, 37°C, 100µl + 900µl EMEM, x 5 nps added every hour	7.91	11.30	4.37	30', 40kHz	48.03	42.29	21.54
TNH 29	KB 07/07/17	Run 1	3h, 37°C, x3 nps (added at t0,1h and 2h)	21.48	23.71	12.54	30', 40kHz	54.97	31.56	30.49

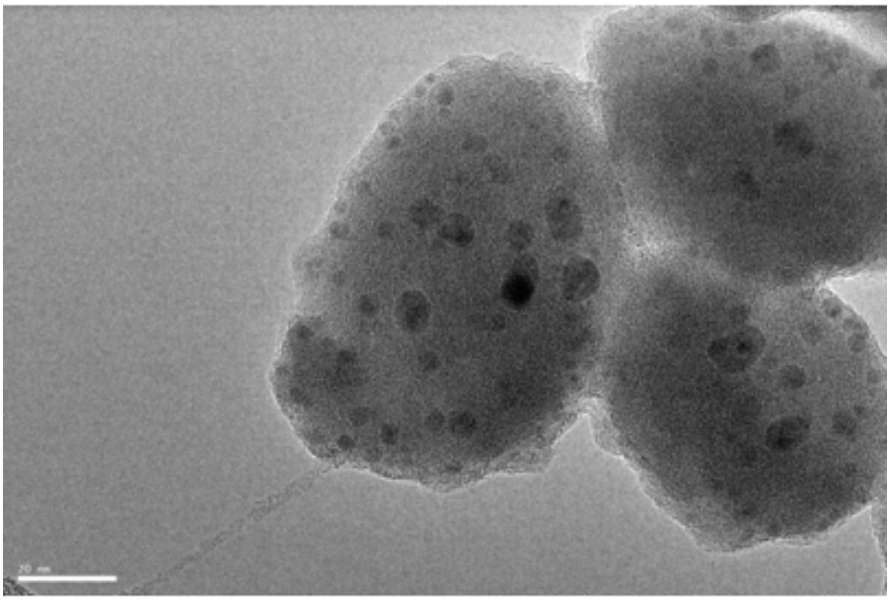

Figure 4.81: TEM image of TNH 20 after sonication

The sonication after the couplings on the orbital shaker causes in almost all the samples (see the green highlighted lines) an improvement of the coupling percentages with respect to the previous conditions, as shown in Table 14. Furthermore, the structure of exosomes is maintained as shown in TEM image (Figure 4.81).

Table 15: effect of the sonication before the coupling

	Exosomes aliquot		**Conditions**	**Coupling %**		
				% ZnO	**% Exosomes**	**% TNH**
TNH 33	KB 07/07/17	Run 1	US 30', 40 kHz at 37°C	66.48	39.97	31.06

The sonication of exosomes and ZnO, without doing the coupling before, gives very good percentages, but as shown in Figure 4.82, exosomes seem to be broken and then reassembled, in this way there are very big aggregates of about 500 nm which are not suitable for the internalization inside cells.

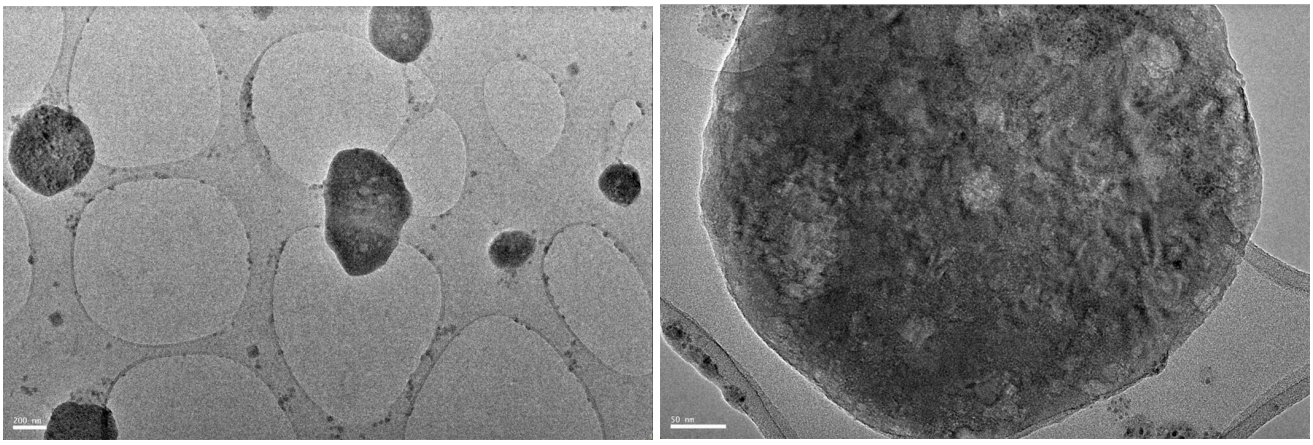

Figure 4.82: TEM images of TNH 33

Limit of resolution of the microscope

A problem that comes out from the fluorescence microscope is its limit of resolution. The smallest fluorescence coming from a nanoparticle that the microscope can measure has a size of 170 nm.

Instead, the minimum size of ZnO nanoparticles is 20 nm and of the exosomes is around 100 nm.

The consideration that could be done is that, after the centrifuge, in the pellet there are a lot of exosomes that seem to be empty. But, during the extraction empty exosomes must be centrifuged at 100000 rcf to be pelleted, so, it is possible that a centrifuge at 5000, 7500 or 16870 rcf is enough to pellet these empty exosomes?

Analyzing the percentage of exosomes coupled in the previous chapter, it is possible to see that they are very low and rarely they overcome the 50%.

Probably the empty exosomes in the pellet come from two different causes.

The first one is that, during the centrifugation step, some heavy nanoparticles which are going down drag also some small exosome vesicles.

The second hypothesis is that some of these exosomes are not empty but there is a very small amount of ZnO nanoparticle inside (even just one nanoparticle) whose fluorescence cannot reach the limit of resolution of the microscope.

4.3.4 Morphological characterization

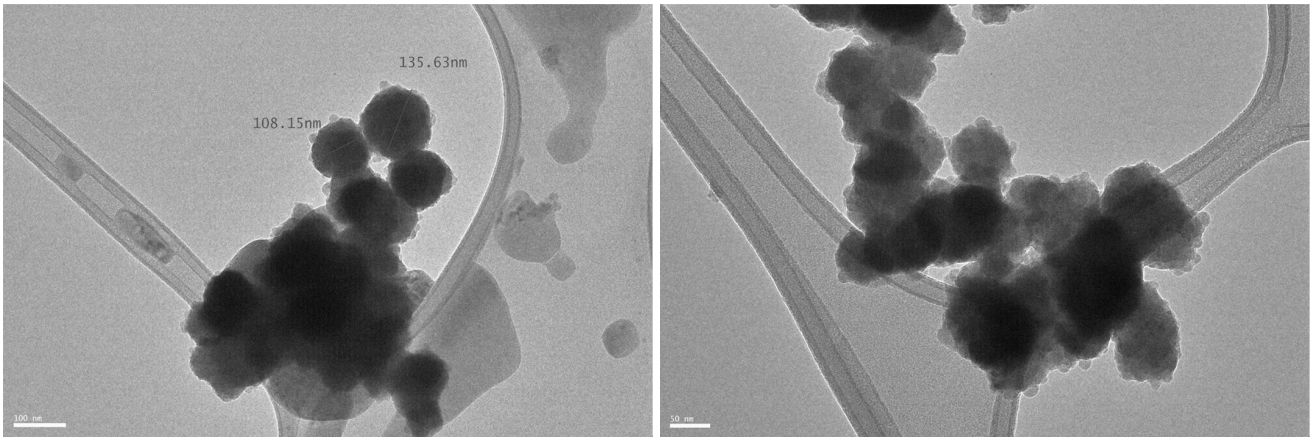

Figure 4.83: TEM image of exosomes

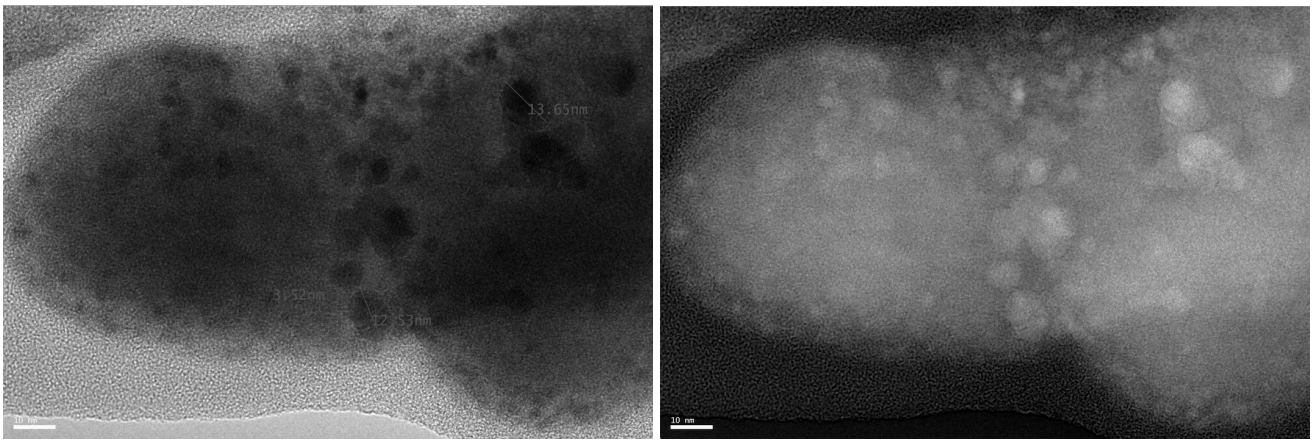

Figure 4.84: TEM (left) and STEM (right) image of TNH 47

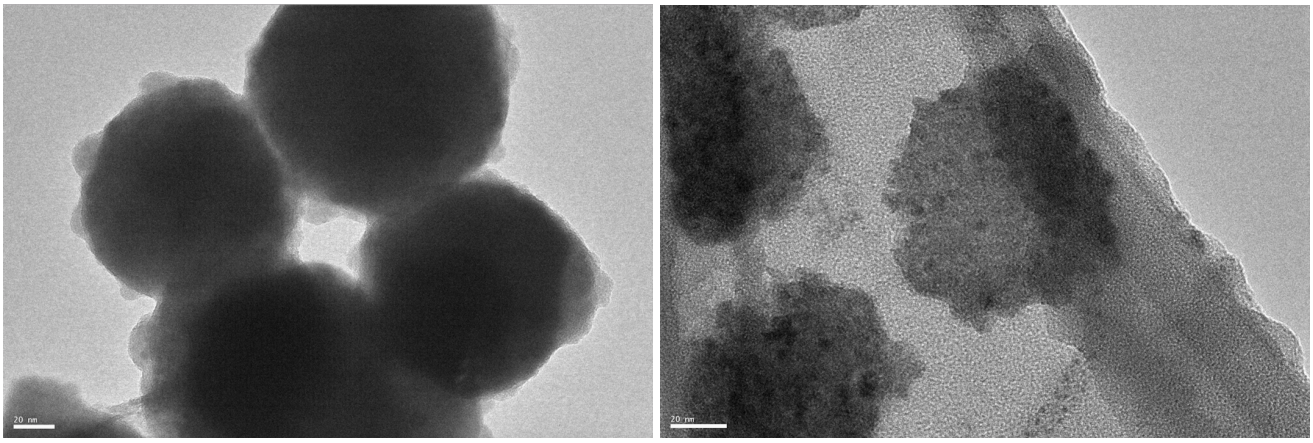

Figure 4.85: Direct comparison of TEM images of exosomes (left) and TNH 47 (right)

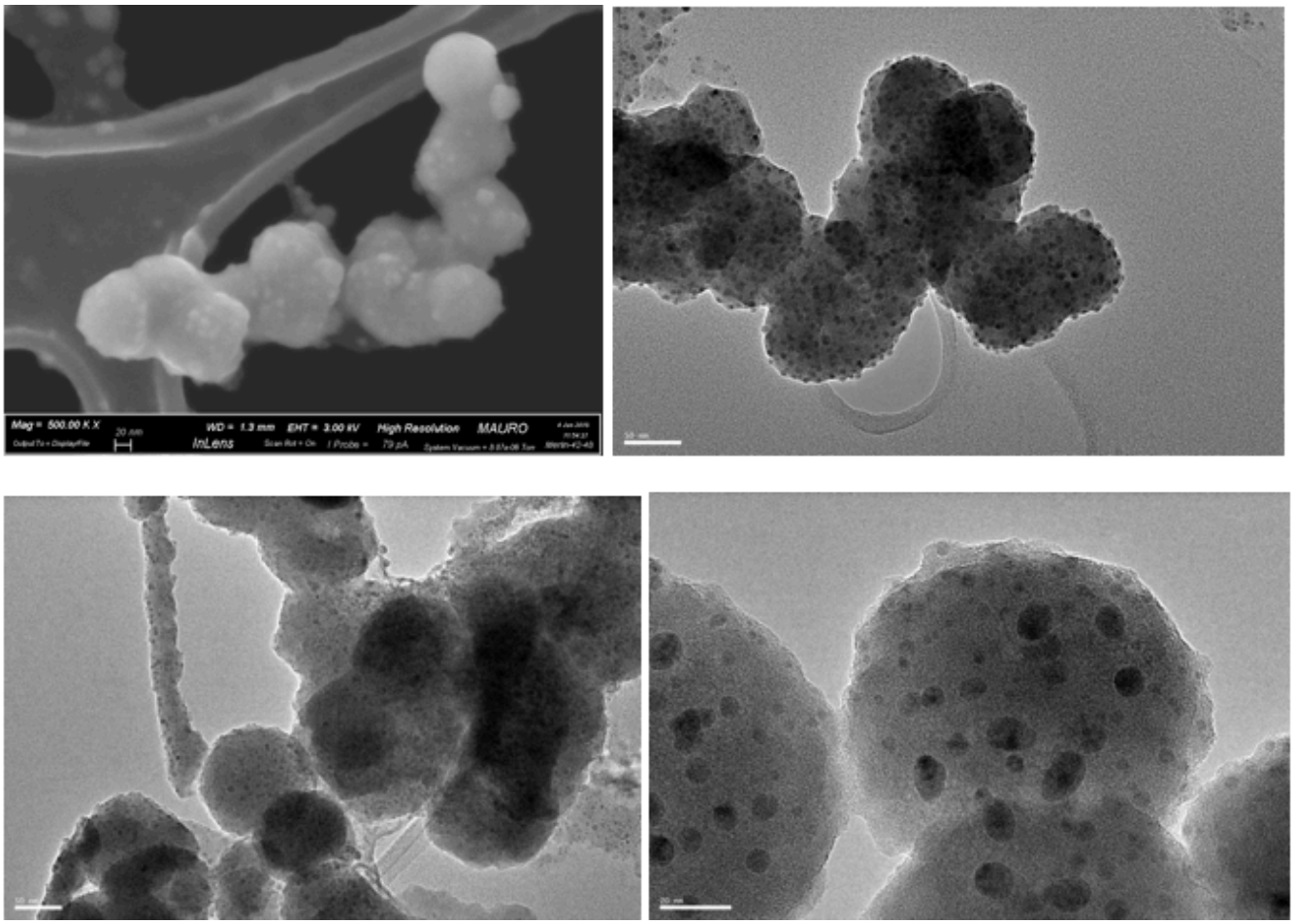

Figure 4.86: Other TEM images of TNH 20, 25

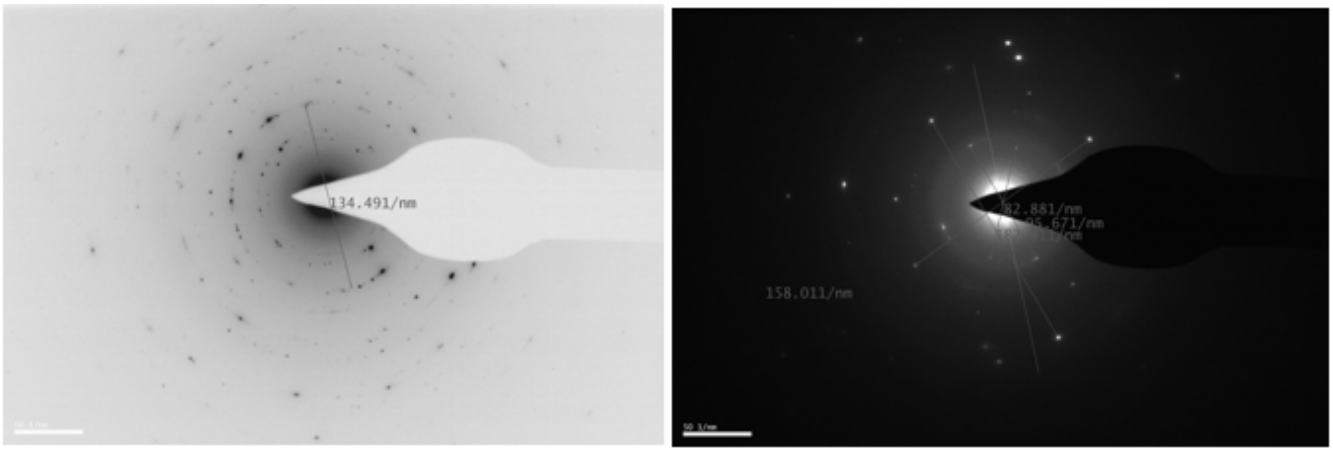

Figure 4.87: Electron diffraction pattern of TNH 20

It is possible to compare the morphology of exosomes (Figure 4.83) to the one of TNH (Figure 4.84 and Figure 4.86) or directly in Figure 4.85.

Exosomes appear as rounded shape empty vesicles with sizes around 100 nm.

In TNH there are darker spots inside the exosomes. The analysis of the dimensions of these spots suggests that they could be considered ZnO nanoparticles. Furthermore, the elemental analysis (EDS) of

TNH underlines the presence of Zn, whereas this element is not detected through elemental analysis related to the pristine exosomes. Similarly, the electron diffraction pattern carried out on the TNH is reported in Figure 4.87 and shows the typical d-spacing belonging to ZnO crystalline structure together with crystalline salts belonging to the dispersing media (physiologic solution). This exact pattern is not observed in the pristine exosome related one, only showing diffraction spots belonging to the physiological buffer salts.

4.3.5 Optimal coupling conditions

Table 16: coupling parameters

Optimal coupling parameters	
Mixing method	Orbital shaker, 200-250 rpm
Temperature	37 °C
Time	90 minutes each run
Volume	100 µl

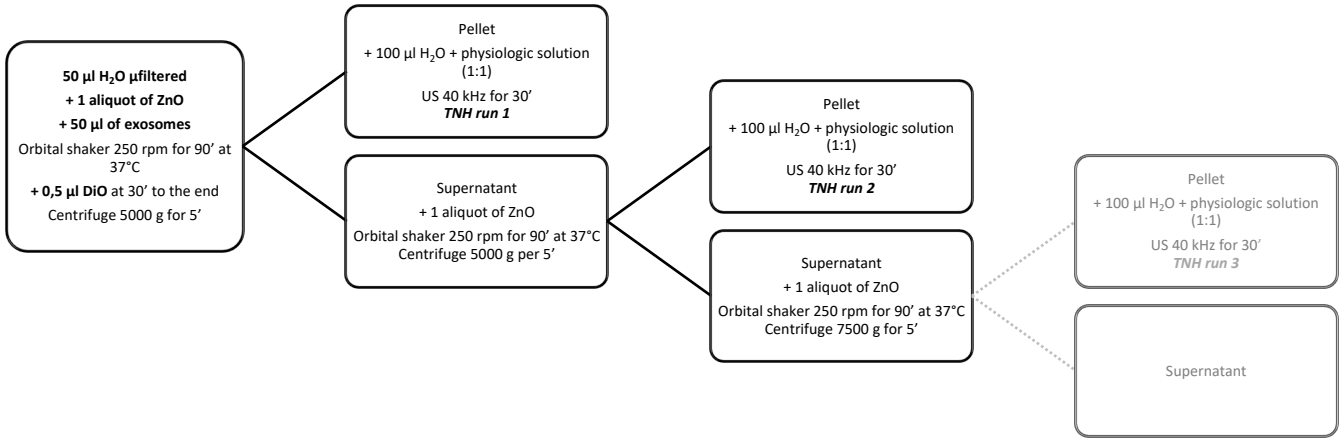

Figure 4.88: Coupling steps

4.4 Calcein release

The aim of this method is to evaluate if the ZnO is internalized inside the exosomes or not. The main idea is that if ZnO is inside exosomes calcein can not be released in water, since it is a cell membrane-impermeable dye and therefore we hypothesize that it would be also hindered to diffuse across the exosome membrane.

First of all, the solution of calcein itself is measured, to record how much time calcein employs to diffuse through the dialysis membrane and saturate the water below.

As shown in Figure 4.89, calcein saturates water in less than 15 minutes.

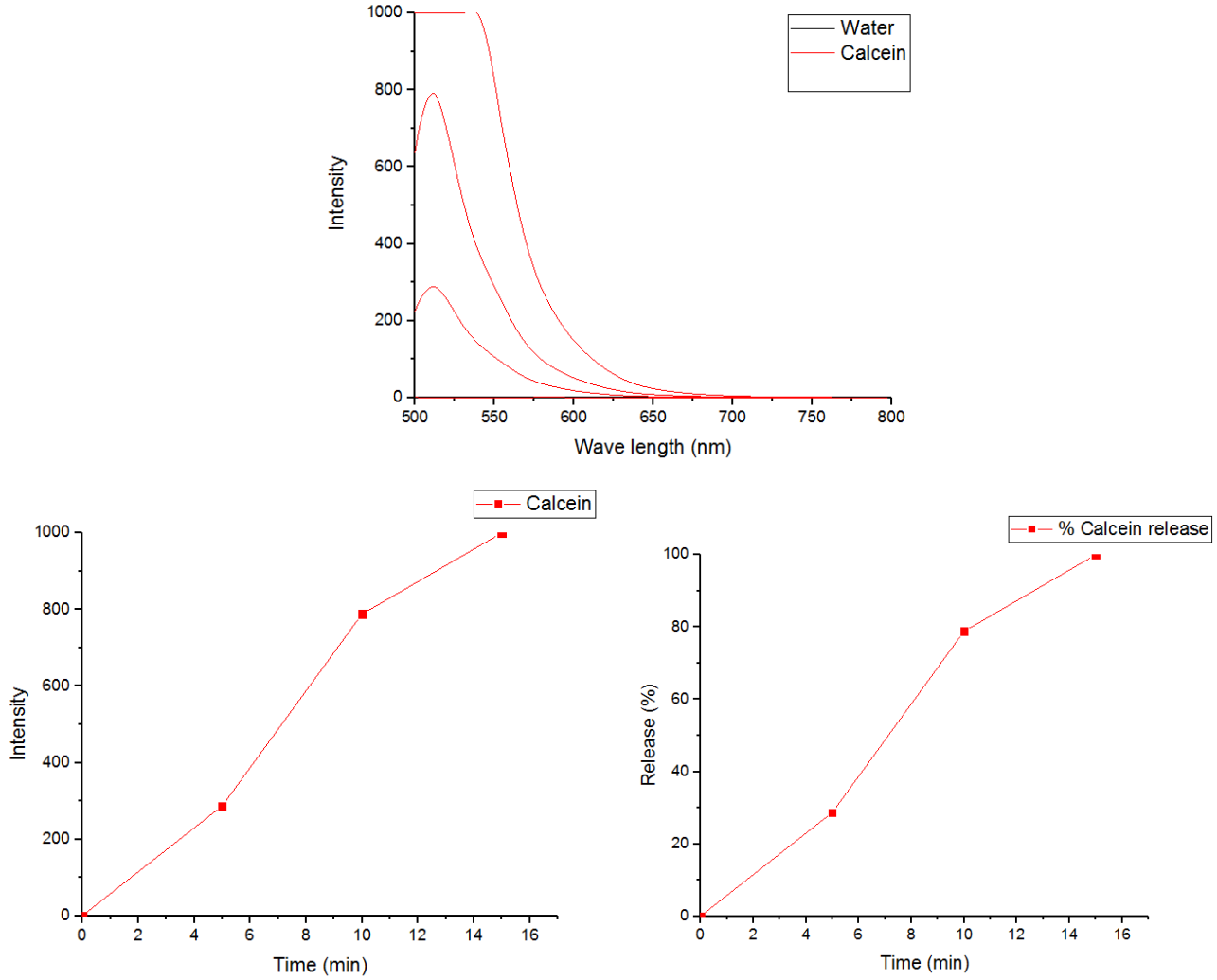

Figure 4.89: Calcein release from the solution of calcein

After that, a test of permeability of the membrane is made: it is carried out to ensure that the ZnO nanoparticles labelled with Atto550 dye (covalently attached to the ZnO surface) does not cross the dialysis membrane.

The curve in red in Figure 4.90 represents the fluorescence of ZnO labelled with Atto550 dispersed in water, while the other curves are the fluorescence of NPs-Atto550 separated from water through a dialysis membrane. It is possible to see that there is no release of Nps-atto550 from the dialysis membrane, proving an efficient confinement of the NPs and the correct selection of the dialysis membrane cut-off.

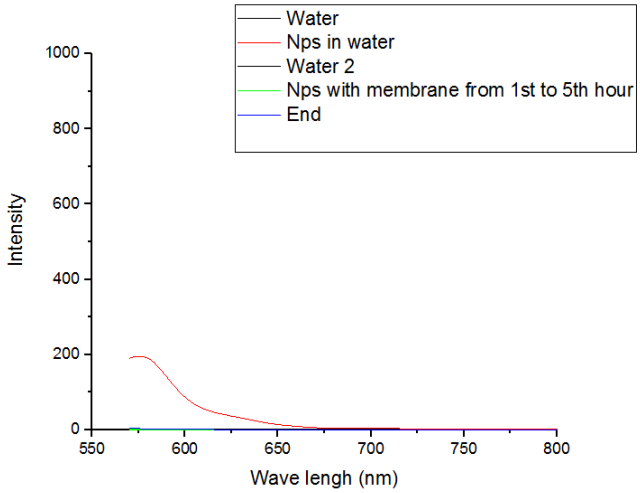

Figure 4.90: Release of atto550

Then a test of release of calcein from ZnO nanoparticles is carried out.

In Figure 4.91 is shown the evolution of the release of calcein adsorbed on the ZnO nanoparticles, without the use of the lipidic membrane. It reaches the saturation immediately after shaking the cuvette.

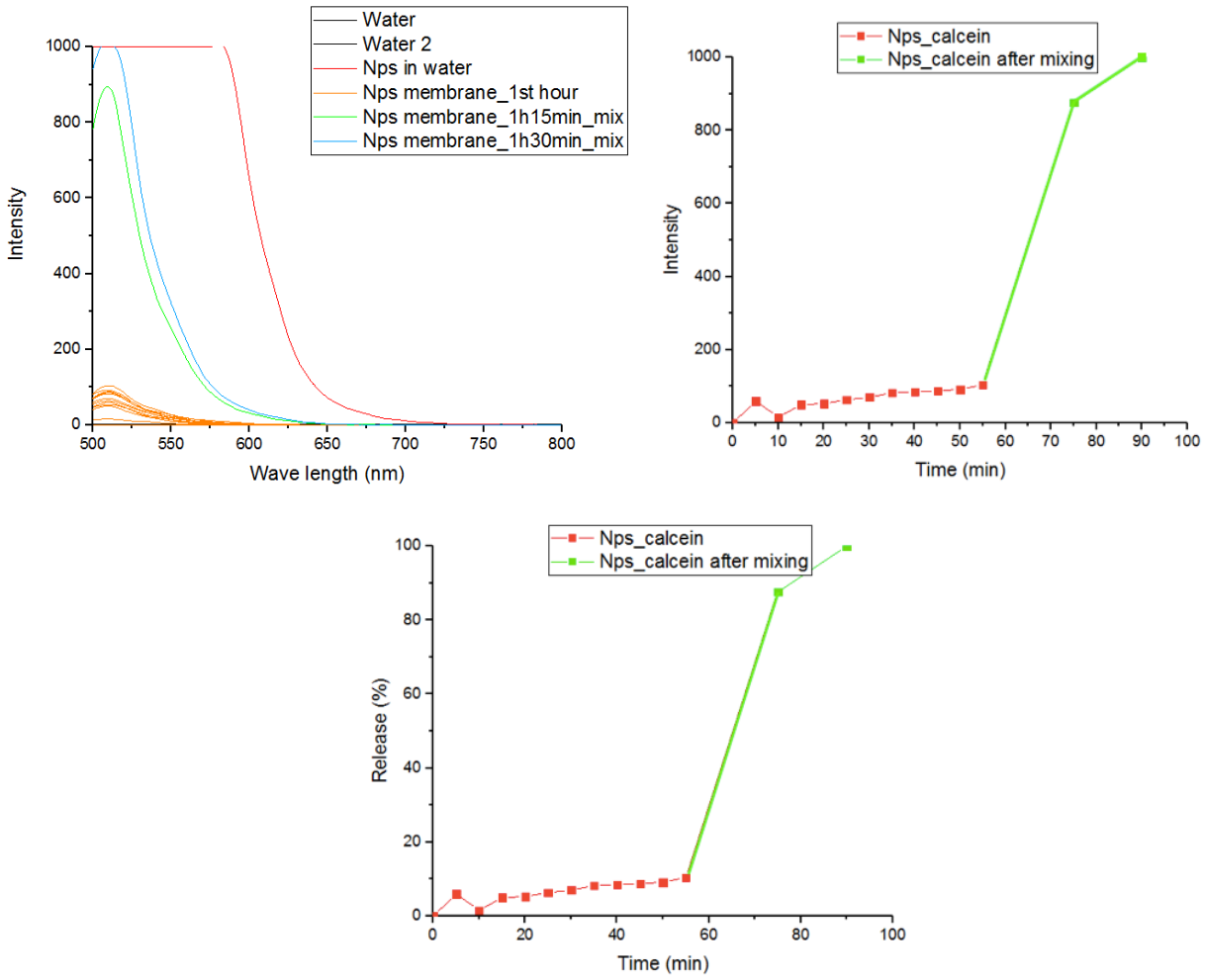

Figure 4.91: Calcein release from a solution of ZnO nanoparticles labelled with calcein

Before using exosomes, three tests with DOPC are carried out. The use of DOPC is because they are less expensive and can be used for predictive behaviour. As shown in Figure 4.92, the saturation of water is not reached until ethanol is added and the lipid membranes disassembled. Anyway, there is an increasing trend in the release of calcein. This is probably due to two different facts. The first one is that there could be some free calcein in the solution because only one washing step is carried out during the preparation. It is not possible however to increase the number of washing steps because calcein is bonded in a very weak way, so with many centrifugations it could detach from the ZnO nanoparticles, furthermore many centrifuges could then damage the membrane of lipids. The second reason is that the coupling never reaches the 100%, so there are probably some ZnO nanoparticles without coating that are able to freely release calcein.

Another proof of the successful coupling is the remarkable increase of the release percentage when ethanol is added and membranes disassembled.

In support of this claim there is also a reference in literature, in [51] where it is possible to see that the release of calcein from liposomes has the same trend of these experiments.

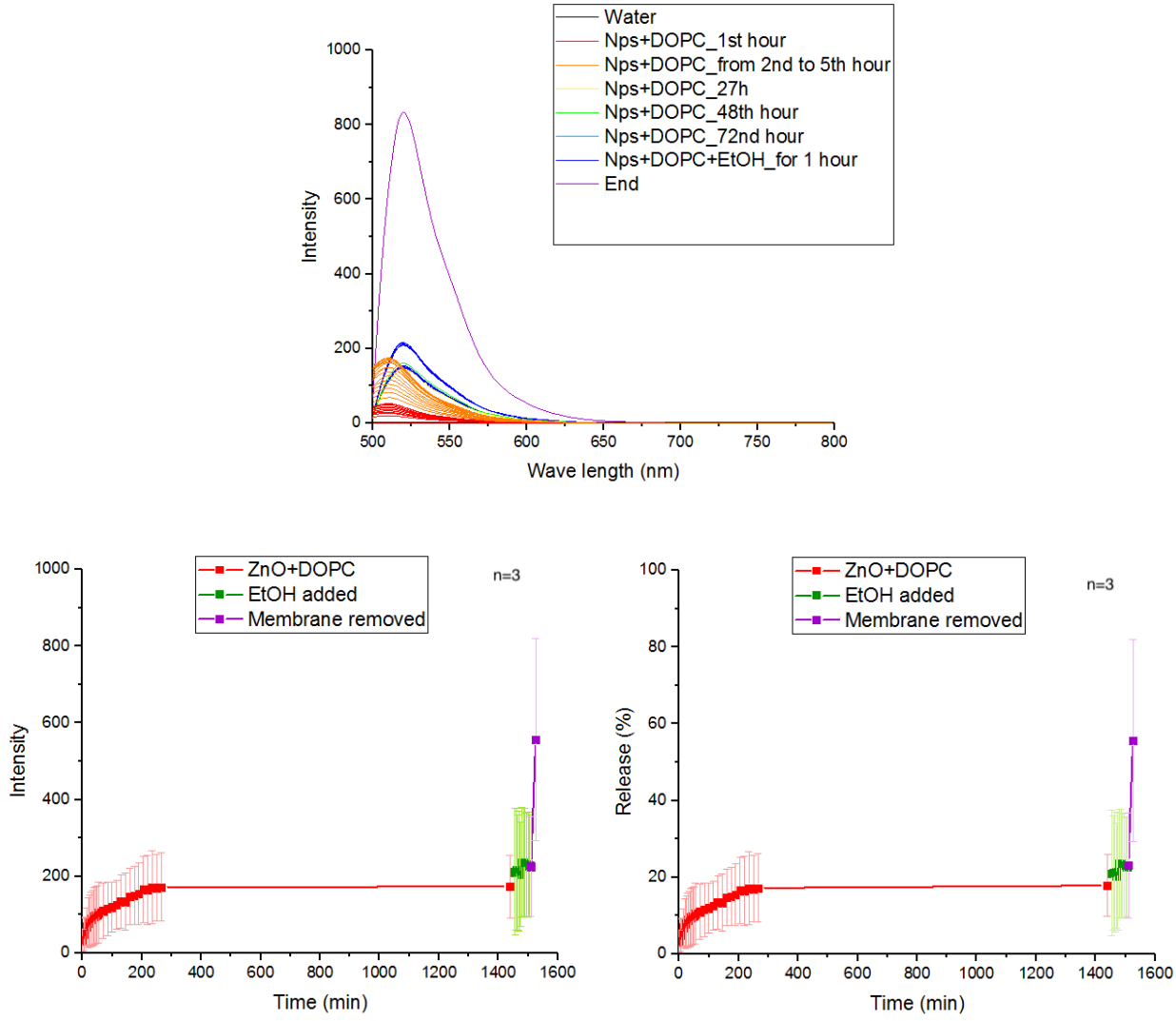

Figure 4.92: Release of calcein from the solution of ZnO coated with DOPC

A similar behaviour could be done for the release of calcein when using the TNH with exosomes. In Figure 4.93 there is the same evolution of the release of calcein. However, the situation for exosomes is a little bit different. The release has a first burst reaching a value of 10%, lower than the burst obtained for the liposomes. However, there is not a dramatic change of fluorescence intensity and thus of calcein release after the disassembling of the lipid bilayer. It can be that the coupling percentage between ZnO-calcein and exososmes is lower than between ZnO-calcein and DOPC and there is more free ZnO in solution which releases calcein since the very beginning.

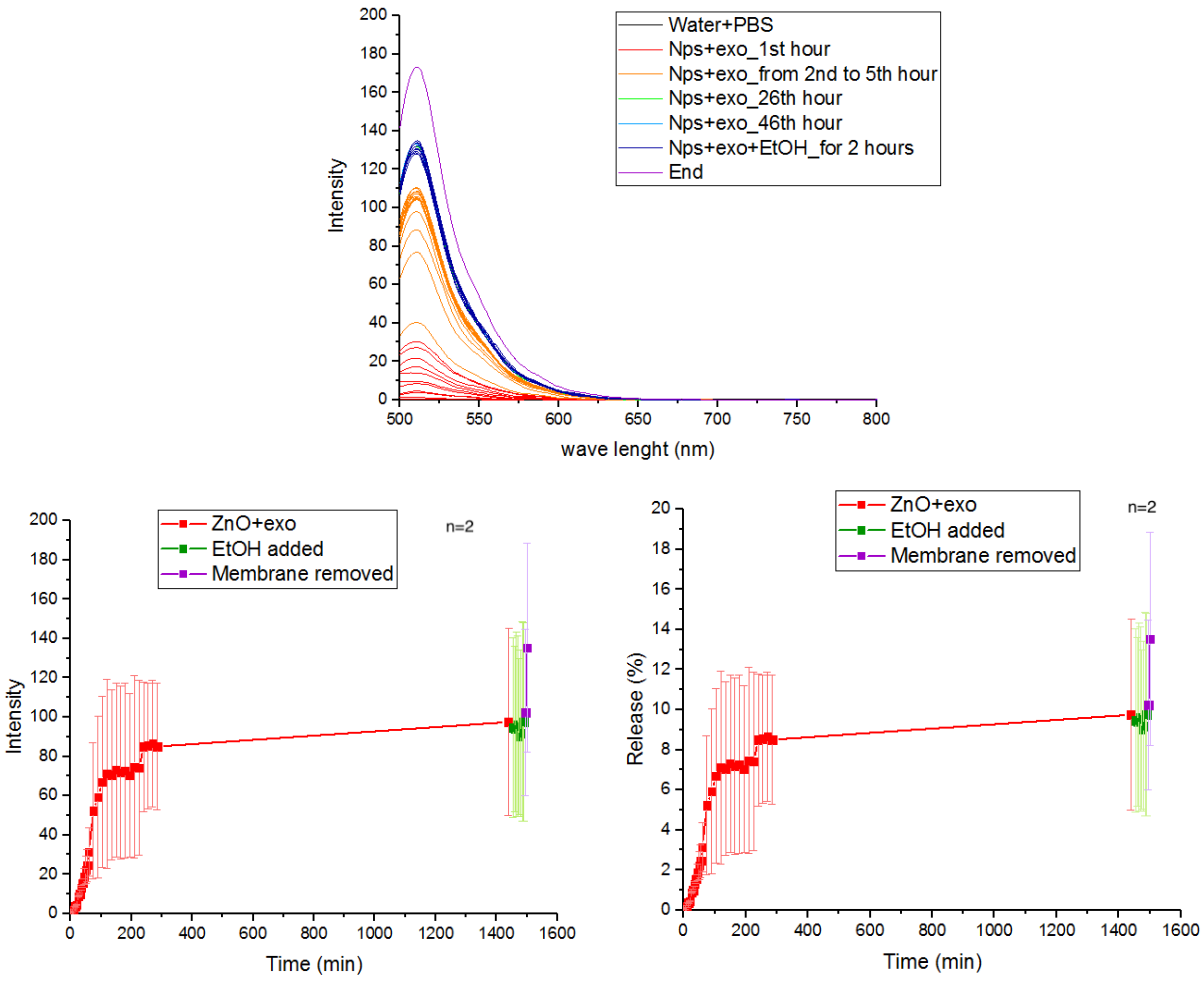

Figure 4.93: Calcein release from the solution of ZnO coated with exosomes

This method of evaluation of the internalization is not suitable for exosomes. As much the coupling percentage is far from from 100%, as many free nanoparticles of ZnO there are in solution that can release calcein. In addition, exosomes membranes are much more complex that the DOPC ones, they present, ligands, proteins and other biological components that could alter the response to the addition of ethanol. In fact, when ethanol is added and the membrane removed in DOPC the calcein released is remarkably increased, from a 20 to a 60%. In exosomes there is not a clear change of trend, after the ethanol addition the calcein released switches from a 10% to a 12%. This could be explained by the ability of ethanol to fix biological compounds and, since the exosomes membranes are very different from the DOPC ones because they contain proteins and other biological components, when it is added to the solution, it has

fixed the exosomes to the dialysis membrane, so calcein is entrapped in these fixed constructs and it can not be released even after the membrane removal.

4.5 Mesoporous Silica Nanoparticles

4.5.1 Transmission Electron Microscopy (TEM)

Figure 4.94 shows the peculiar morphology of mesoporous MCM-41, functionalized with amino groups and labelled with rhodamine. The synthesis produces nanoparticles with a uniform size in the range of 30-300 nm minimizing their self-aggregation. MCM-41 nanoparticles have an irregular geometry, they have a spheroidal, hexagonal or ellipsoidal shape. The nanoparticles are mesoporous and the removal of the surfactant leads to cylindrical mesopores organized in a two-dimensional hexagonal symmetry. Pores have a dimension of 3-4 nm and they allow the load of nanoparticles of drugs with the right dimension and charge.

The staining with PTA has the aim to underline if the surfactant has been completely extracted. Figure 4.94 shows that the inner parts of the nanoparticles and the pores are empty, without darker spots, so there are no residual of surfactant.

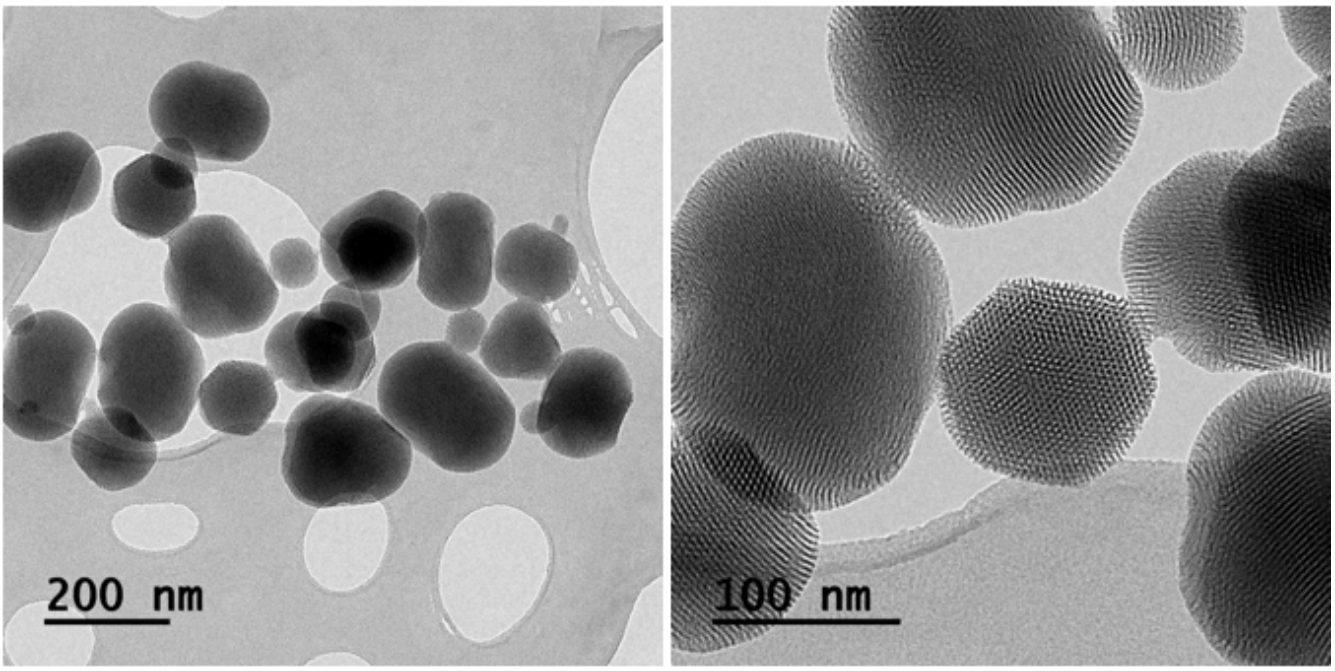

Figure 4.94: MCM-41

4.5.2 DLS and Z-potential

In Figure 4.95, the black curve represents the average result of the DLS of MCM-41 nanoparticles dispersed in ethanol. Most of them has a dimension around 200 nm and they are very well dispersed inside the solution, probably thanks to the repulsion between the negative charges of the nanoparticles. The red curve is the DLS average result of MCM-41 nanoparticles in PBS. The situation is very different

from the one in ethanol. There is not only one peak for the average size, but there are two different peaks, the first one around 200 nm, while the second indicates a size greater than 1 µm. The double distribution of the curve means that the nanoparticles are aggregating inside the solution of PBS. The aggregation between the nanoparticles, when dispersed in PBS, could be caused by the relatively high ionic strength of the solution which could affect the behaviour of the nanoparticles.

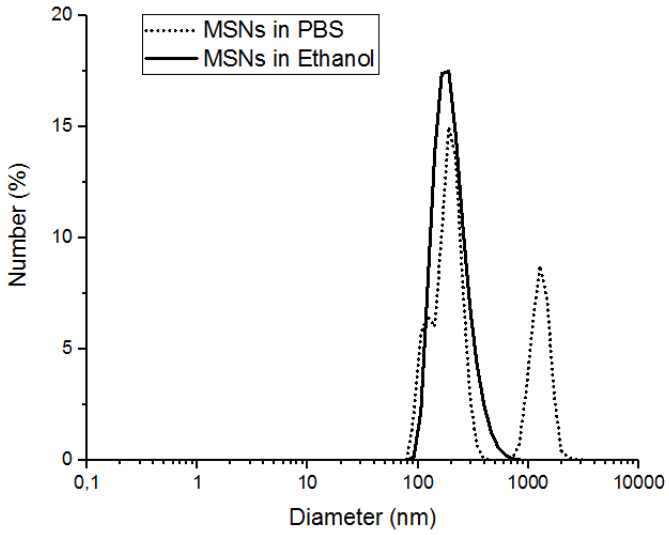

Figure 4.95: DLS measurements of MCM-41 in ethanol and in PBS

The measurement of the Z-potential remains unchanged with a value of -10.6 mV.

4.5.3 Thermogravimetry

Figure 4.96 reports the result obtained with the thermogravimetric analysis. It represents the weight loss in percentage during the whole process. At high temperature mesoporous silica is not degraded, while al the organic residue (after the surfactant removal) is burnt. The only organic material that could be present inside the nanoparticles is the surfactant. The difference in weight before and after the process represents the surfactant not removed during the extraction in the synthesis. Good quality nanoparticles must have a weight loss between 5 and 10%.

In the graph is it can be seen that there is a 6-7% of surfactant left, so this is a good result and MSNs can be used without further extraction steps.

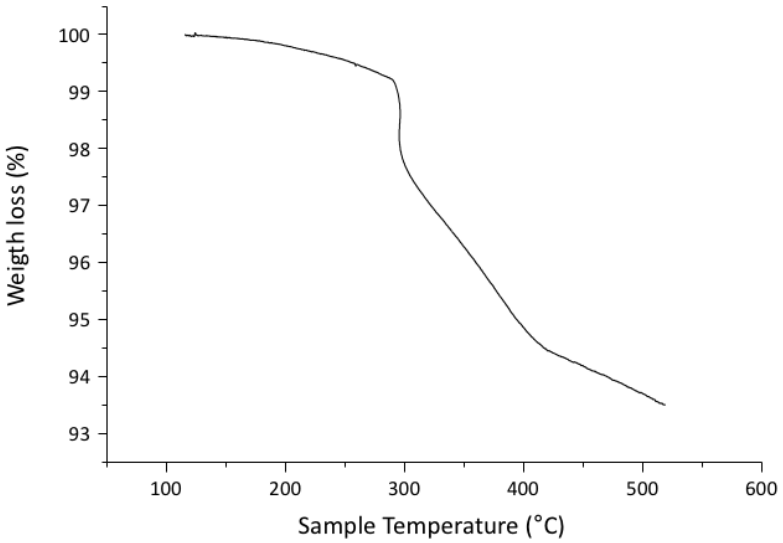

Figure 4.96: Thermogravimetric result

4.5.4 IR analysis

In Figure 4.97, the results obtained by the IR analysis of MSNs labelled with rhodamine are reported.

The graph shows the characteristic band of the siloxane group (-Si-O-Si-) at 1060 cm^{-1}, whereas the bands at 955 and 795 cm^{-1} represent the -Si-OH and -Si-O, respectively [52].

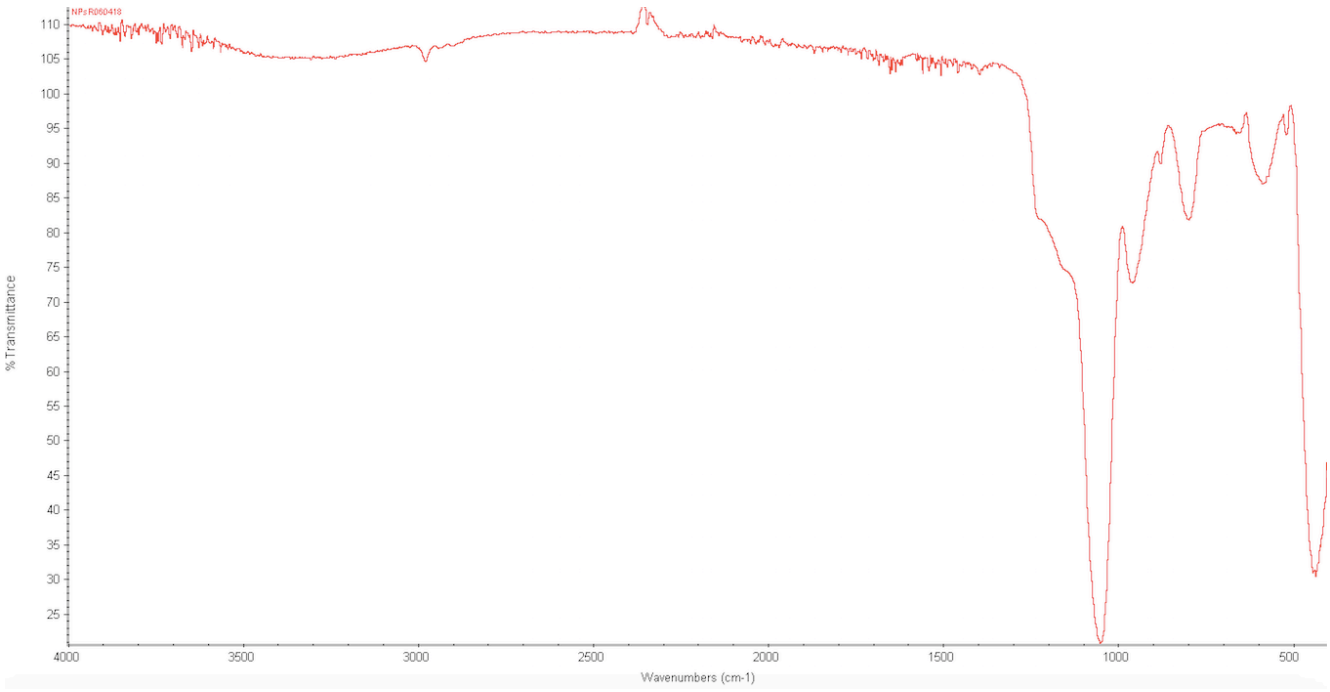

Figure 4.97: IR analysis of MCM-41 nanopaticles

4.6 Coupling mesoporous silica with exosomes

4.6.1 DLS and Z-potential

This method of characterization gives the possibility to compare the sizes and the Z-potential of the nanoparticles naked and covered with the exosomes. The differences between the results of the nanoparticles and the nanoparticles covered by exosomes are a proof that the coupling occurred.

Table 17: Values from the Z-potential measurements

Sample	Z-potential (mV)
MSN	**-10.6**
MSN+EXO 1 run1	-9.64
MSN+EXO 1 run2	-7.62
MSN+EXO 2 run1	-7.61
MSN+EXO 2 run2	-6.69
Exosome from FBS	**-9.53**

The values obtained from the Z-potential measurements of the MCM-41 samples coated with exosomes are directly compared with the one obtained from the naked MCM-41 sample and with the exosomes from FBS. Nevertheless, the results from exosomes and MSNs by themselves are too similar to draw reliable conclusions.

Other interesting results come from the DLS measurements. As shown in Figure 4.98, the size distribution of the coated nanoparticles in PBS is more regular than the one of the nanoparticles naked, the first one has only one size distribution peak around 200 nm, while the naked MCM-41 presents several peaks with bigger dimensions. This could be considered as a proof of the coating that changes the behaviour of MCM-41 nanoparticles in PBS.

Another consideration needs to be done because the exosomes used for these two couplings are derived from fetal bovine serum. This means that, besides the exosomes, there are also a lot of extracellular vesicles, apoptotic bodies and serum proteins. In particular, the last constituents, serum proteins, could establish a competition with exosomes in coating the nanoparticles. In this way, proteins, as well as exosomes, enhance the stability of the MSNs in PBS and it is not possible to discriminate the nature of the coating with this method. This problem is typical only of the exosomes from FBS, it does not occur in exosomes derived from cells.

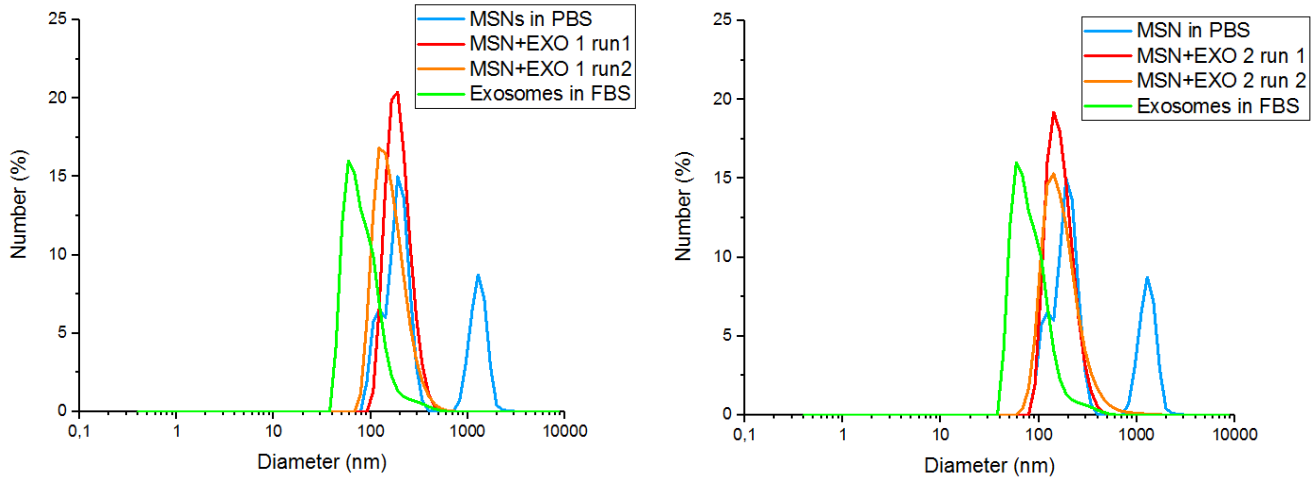

Figure 4.98: DLS measurements of MSN+EXO 1 and MSN+EXO 2

4.6.2 Transmission Electron Microscopy (TEM)

TEM images are acquired with exosomes stained with PTA, so they appear in a darker colour than the inorganic parts. In Figure 4.99 and Figure 4.100 there are some MCM-41 nanoparticles coated with an organic part. It is possible to see under the coating the oriented pores of the nanoparticles and outside a layer of an organic material.

In the nanoparticles of Figure 4.99 the outer layers could be constituted by either lipid bilayers from exosomes and by proteins because the exosomes used for the coupling derived from FBS. In contrast, the layers of Figure 4.100 are made most probably by exosomes and other extracellular vesicles, since they are directly extracted from KB cells.

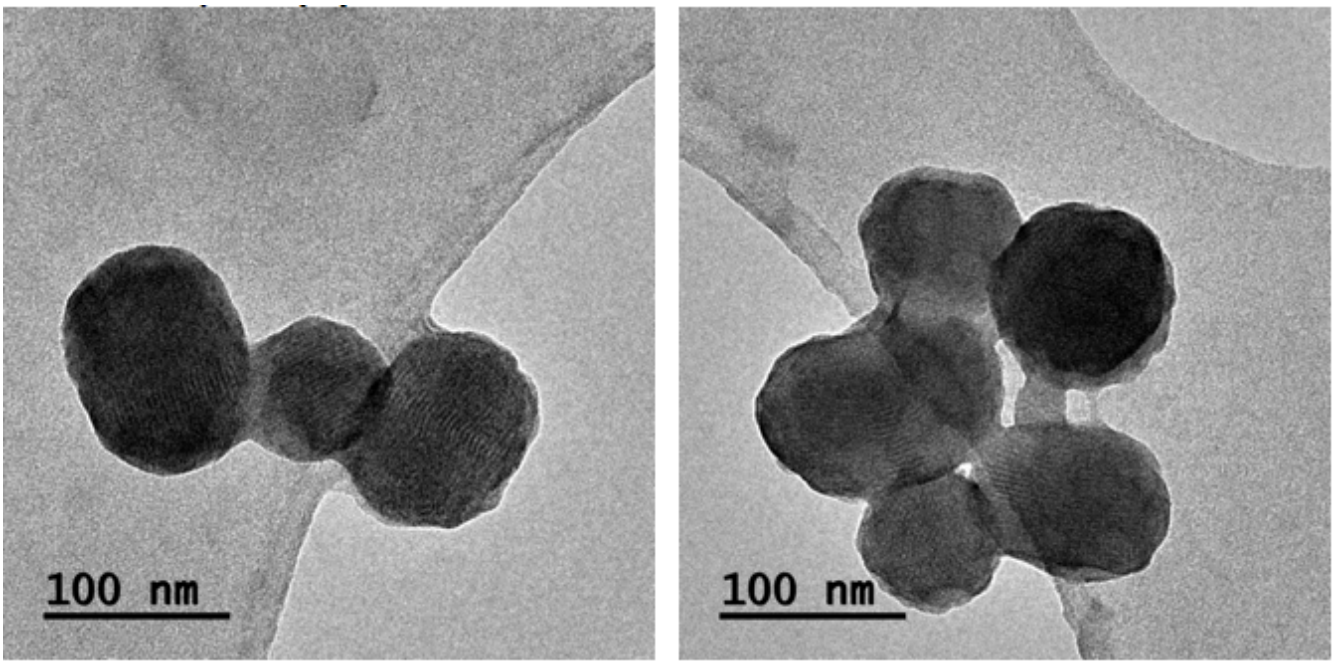

Figure 4.99: MSN+EXO 1 on the left side and MSN+EXO 2 on the right side

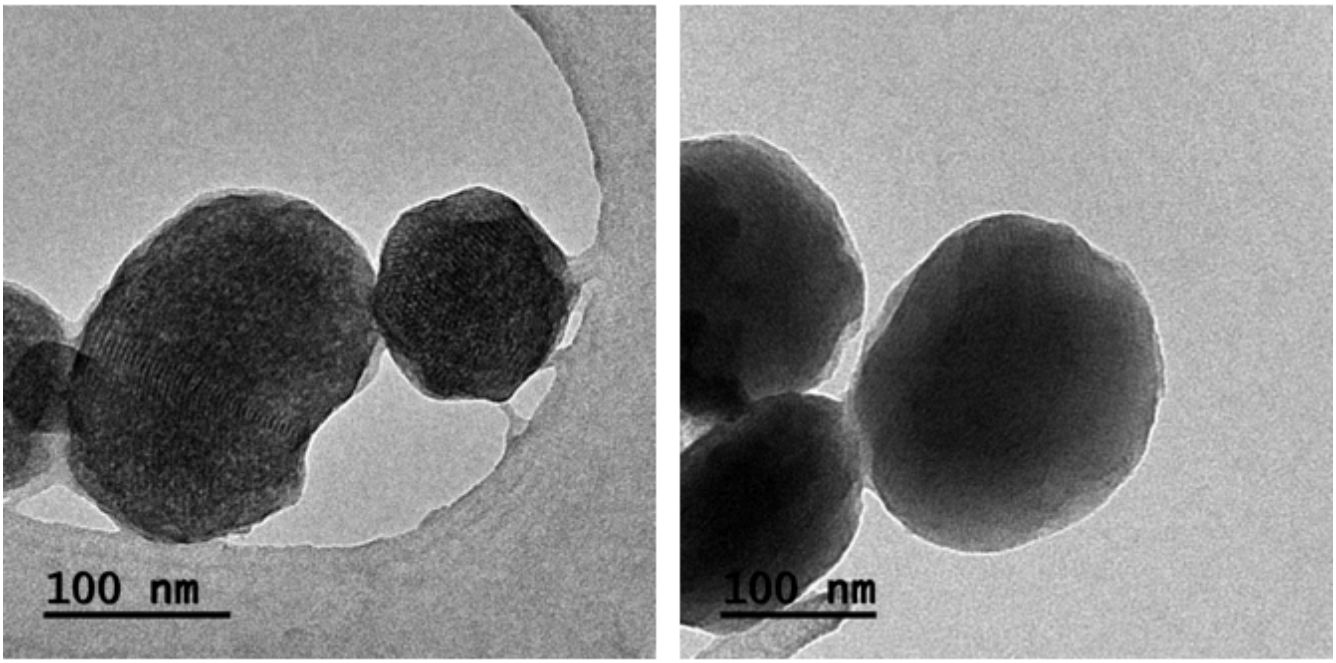

Figure 4.100: MSN+EXO 5 on the left and MSN+EXO on the right

4.6.3 Internalization and release of fluorescein inside HeLa cells

This characterization method is useful to demonstrate the internalization of the MCM-41 nanoparticles coated with exosomes inside the cells and, at the same time, proving the stability of the outer lipid layer until the nanoconstruct is uptaken.

The uptake of MSNs inside the cells is checked observing the colocalization between the red channel (derived from the Rhodamine covalently labelling the MCM-41 nanoparticles), the green channel, representing the fluorescein cargo (only physically adsorbed inside the mesopores) and the bright field channel of the cells. The fourth image is an overlay of these three channels to underline the possible colocalization of the components, see figures below.

The MSNs are loaded with fluorescein, then they are covered with exosomes in order to retain fluorescein inside the pores. The expectation is that the fluorescein remains inside the pores until the nanoconstruct is internalized inside a cell and the phospholipidic layer is disassembled releasing the cargo, for example because of the fusion with the plasma membrane of the cancer cells. For these experiments, exosomes derived from KB cancer cells were used and the two coupling methods 1 and 2 are compared.

In Figure 4.101 the uptake of MSN+EXO 6 (prepared using coupling method 1) after an incubation of two hours with HeLA cells is analysed. Fluorescein is almost totally contained inside the carriers because there is a good colocalization between the red and the green channel. The resolution of the microscope does not allow to determine if the nanoparticles are inside or outside the cells, moreover, it could be useful to observe the cells with a Z-stack analysis in order to evaluate if MSNs are located.

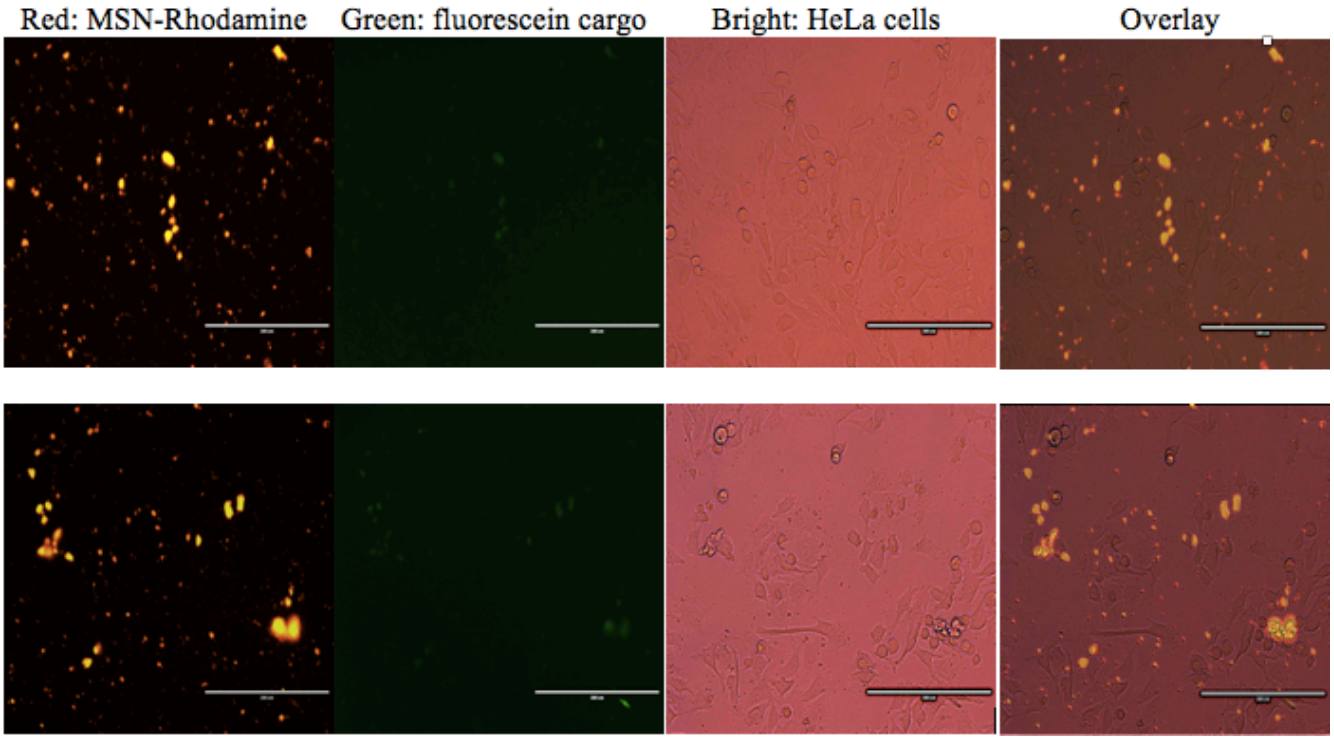

Figure 4.101:Internaization and release of flourescein inside HeLa cells from MSN+EXO 6 after 2 hours. Scale bar: 200 µm.

In Figure 4.102 In Figure 4.102 the internalization of MSN+EXO 8 (prepared using the coupling method 2) after two hours of incubation with HeLa cells is shown. There is more or less the same situation of the sample above with the retaining of fluorescein inside the nanoparticles and the uptake in progress.

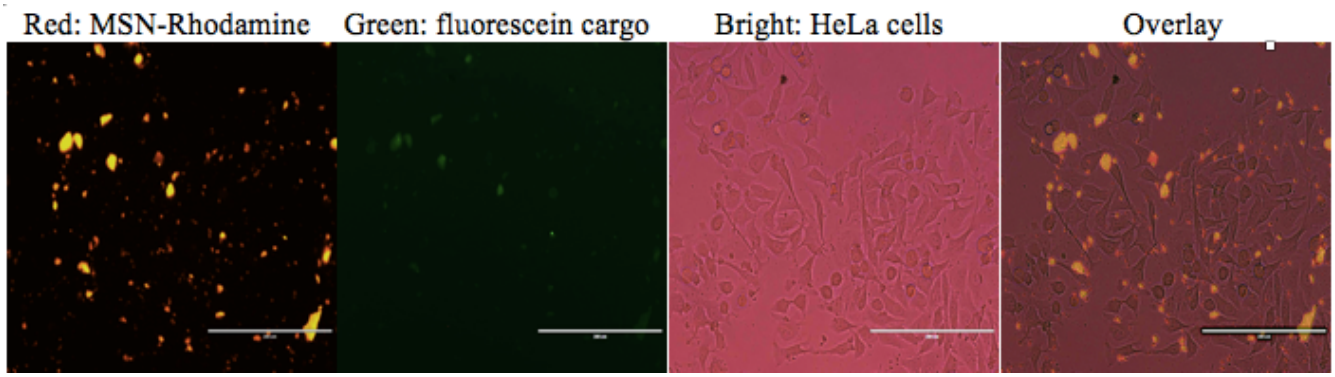

Figure 4.102:Internaization and release of flourescein inside HeLa cells from MSN+EXO 8 after 2 hours. Scale bar: 200 µm.

In Figure 4.103 the medium containing MSN+EXO 6 is left for the uptake until 24 hours.

As told above, the resolution of the microscope does not allow to analyze cells one by one and with the Z-stacks to better evaluate the internalization of MSNs inside the cells and the fluorescein release.

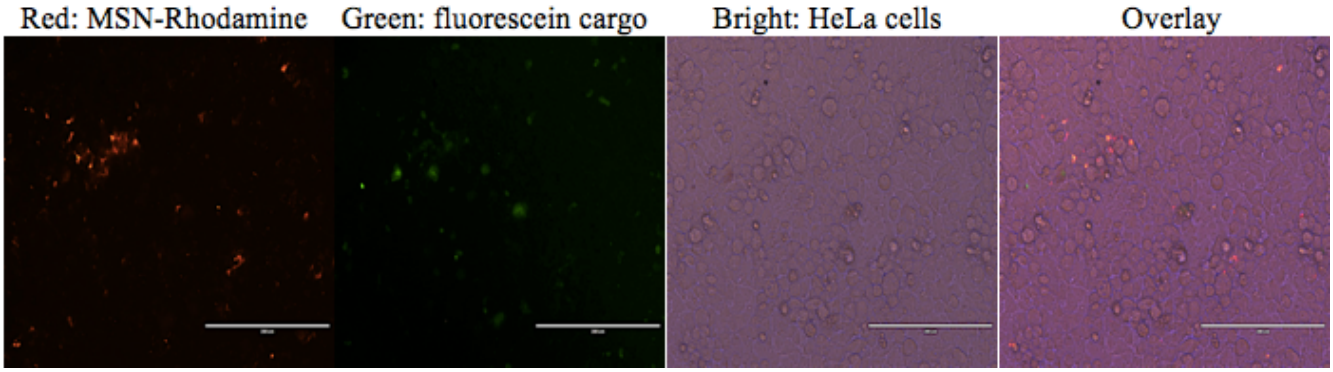

Figure 4.103:Internaization and release of flourescein inside HeLa cells from MSN+EXO 6 after 24 hours. Scale bar: 200 µm.

In Figure 4.104 there is the same treatment described above with MSN+EXO 8. The difference between this and the previous sample is that fluorescein is almost totally released outside the cells. There are no spots localized inside the cells, but there is a widespread fluorescence in all the sample. This means that probably the coating with this method (protocol 2) is less stable in medium than the one made with protocol 1 and so the outer layer is disassembled and fluorescein released before the uptake.

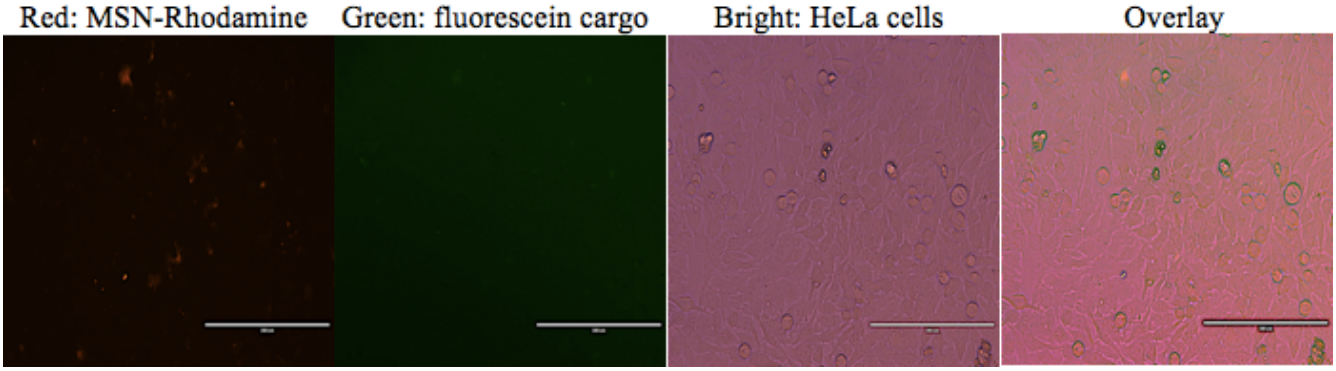

Figure 4.104:Internaization and release of flourescein inside HeLa cells from MSN+EXO 8 after 24 hours. Scale bar: 200 µm.

4.6.4 Flow Cytometry

The preparation of the samples removes all the nanoparticles not internalized by the cells, so the flow cytometry allows to evaluate the percentage of cells that has engulfed fluorescent nanoparticles. For this experiment, MSM-41 nanoparticels were labelled covalently with fluorescein and used as such or coated with exosomes according to the coupling method 1 (MSN-EXO 9) or to the coupling method 2 (MSN-EXO 10).

In the first experiment, as shown in Figure 4.105, the percentages of recorded fluorescent events are very low and there is no remarkably difference between the internalization of nanoparticles coated with exosomes and naked nanoparticles. The analysis was obtained as an average of 3 measurement of the same test.

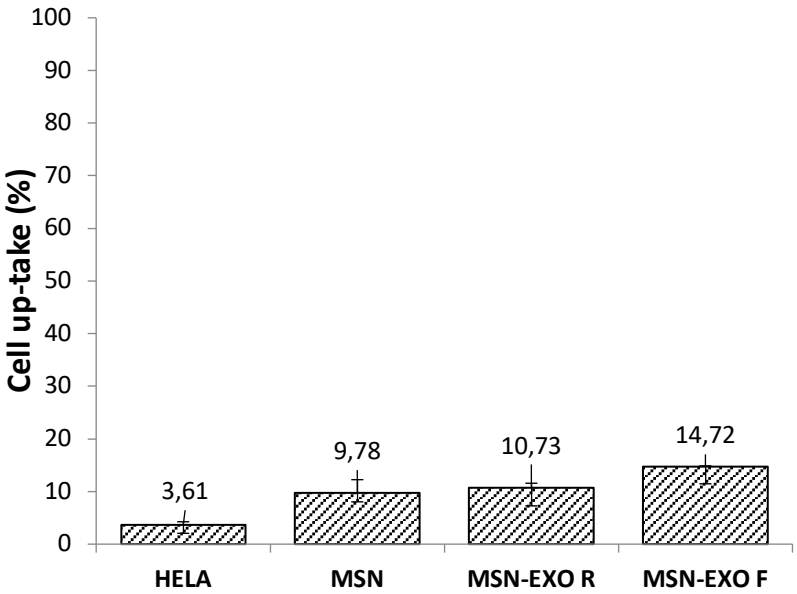

Figure 4.105: Graph reporting the percentage of cells that have internalized fluorescent nanoparticles analyzed by flow cytometry technique. First experiment

The second experiment, in Figure 4.106, shows some interesting data. The percentages are very different from the previous experiment, the internalization is more pronounced for both the exosome-coated nanoparticles with respect to the naked nanoparticles. The analysis was obtained as an average of three measurement of the same test.

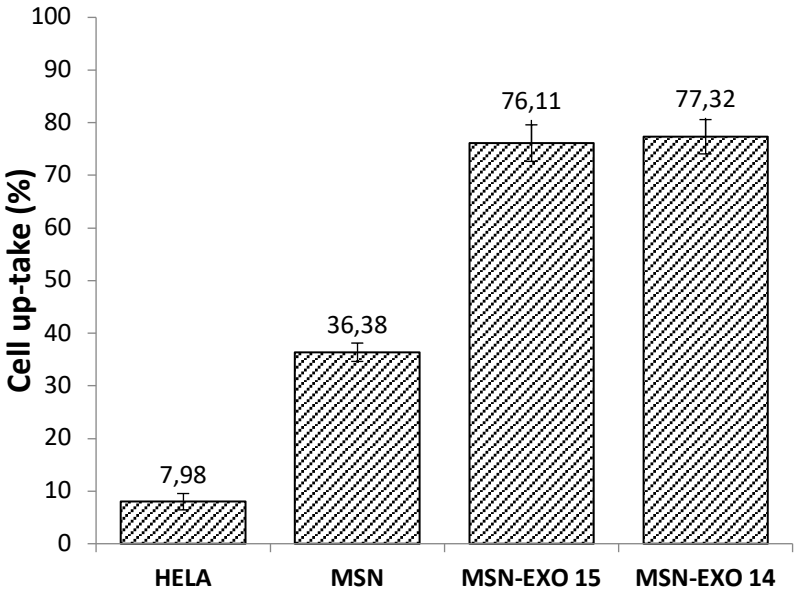

Figure 4.106: Graph reporting the percentage of cells that have internalized fluorescent nanoparticles analyzed by flow cytometry technique. Second experiment

The difference of uptake of fluorescent nanoparticles by HeLa cells is due to the different source of exosomes. For the first experiment, exosomes derived from KB cells have been used, while in the second case, the exosomes are derived from HeLa cells. Probably the uptake in the second case is enhanced by

the fact that the exosomes and the cells in which they must be internalized derive from the same cell lineage.

4.6.5 Stability

The results from the DLS are elaborated to create two graphs that can underline the evolution of the nanoparticle size distribution in solutions over a period of 10 days.

In Figure 4.107 is reported the evolution of the solution with the nanoparticles of mesoporous silica in water and PBS with a ratio 1:1. It can be observed that as soon as the water-PBS solution are added, MSNs, that usually are well dispersed in ethanol, starts to aggregate immediately. This trend is maintained for the first 7 days, MSNs form aggregate larger and larger. On the 7th day there is an inversion of this tendency: in the curves there are two peaks, one is around 1 μm and it represents the aggregates of MSNs, the other one indicates very small sizes, around 30 nm, and it is caused by the MSNs that in PBS are going to be degraded.

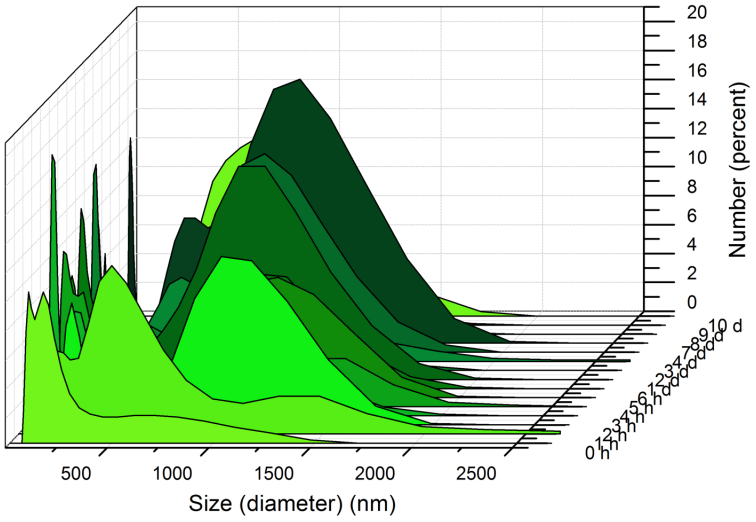

Figure 4.107: Graph with the evolution in time of the solution of MSNs naked

In Figure 4.108 there is the evolution of the solution with MSN+EXO 11. It is very stable during all the period of 10 days, and the sizes are maintained around 200 nm. This means that there is something which prevents the aggregation of MSNs and keep them suspended in the solution.

The stabilization of the nanoparticles could be operated by the exosome coating, or other extracellular vesicles, as well as a protein corona. This multiple possibility is due to the fact the exosomes used for the coupling are derived from FBS, which is rich of proteins.

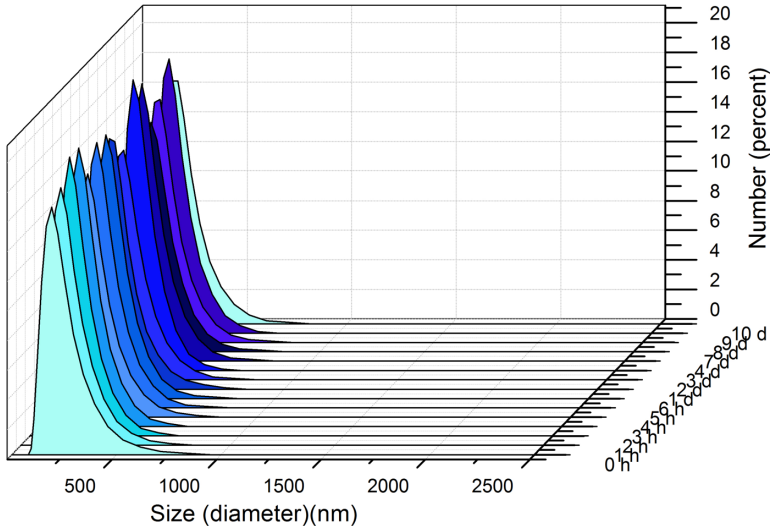

Figure 4.108: Graph with the evolution in time of the solution of MSN+EXO 11

Anyway, it is clear that, in the second sample, there is a coating of something around the nanoparticles which prevents the aggregation of MSNs and that protects them from the degradation by the PBS. It is realistic supposing that the coverage is provided both by exosomes and proteins.

The second experiment is a counterpart of the first one.

In Figure 4.109 there are the two pictures of the cuvettes taken at time 0 and after 24 hours. The pictures of the first six hours are not reported because there are no remarkable differences with the one at time 0. After 24 hours it is possible to see an increase of the fluorescence at the bottom of the cuvette containing naked MSNs. This is exactly the same result obtained from the DLS experiment. The nanoparticles by themselves create large aggregates and they precipitate at the bottom, while the solution with the exosome-coated nanoparticles remain very well dispersed in solution.

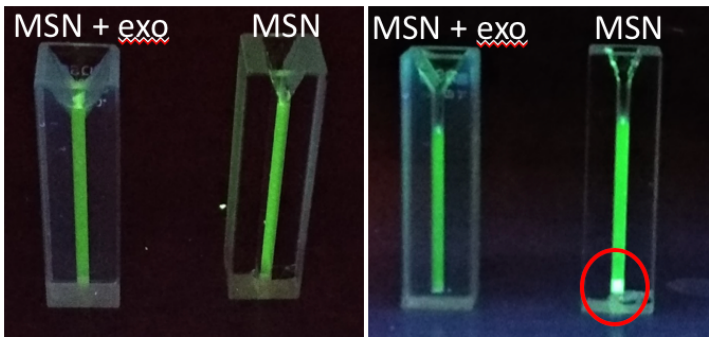

Figure 4.109: The first picture is taken at time 0, the second after 24 hours

4.6.6 Confocal microscopy

Confocal microscopy has the capacity to reach the bottom of the cell layer in order to evaluate if the nanoparticles are engulfed or not.

The cell nuclei are stained with DAPI (blue), MSNs are labelled with rhodamine (red) and exosomes (derived from HeLA cancer cells) with DiO (green).

In Figure 4.110 there are the Z-stacks images of the naked MSNs internalized by the cells. In Figure 4.111 and Figure 4.112 are reported three different z-stacks at the confocal microscope of the same cell region.

The images show that the naked MSNs are aggregated in the cell culture medium and not internalized inside the cells.

In the images of MSN+EXO 12, instead, some nanoparticles are internalized inside the cells, while the others are located very close to them. It is also possible to observe a good co-localization of the MSN in red with the exososmes in green.

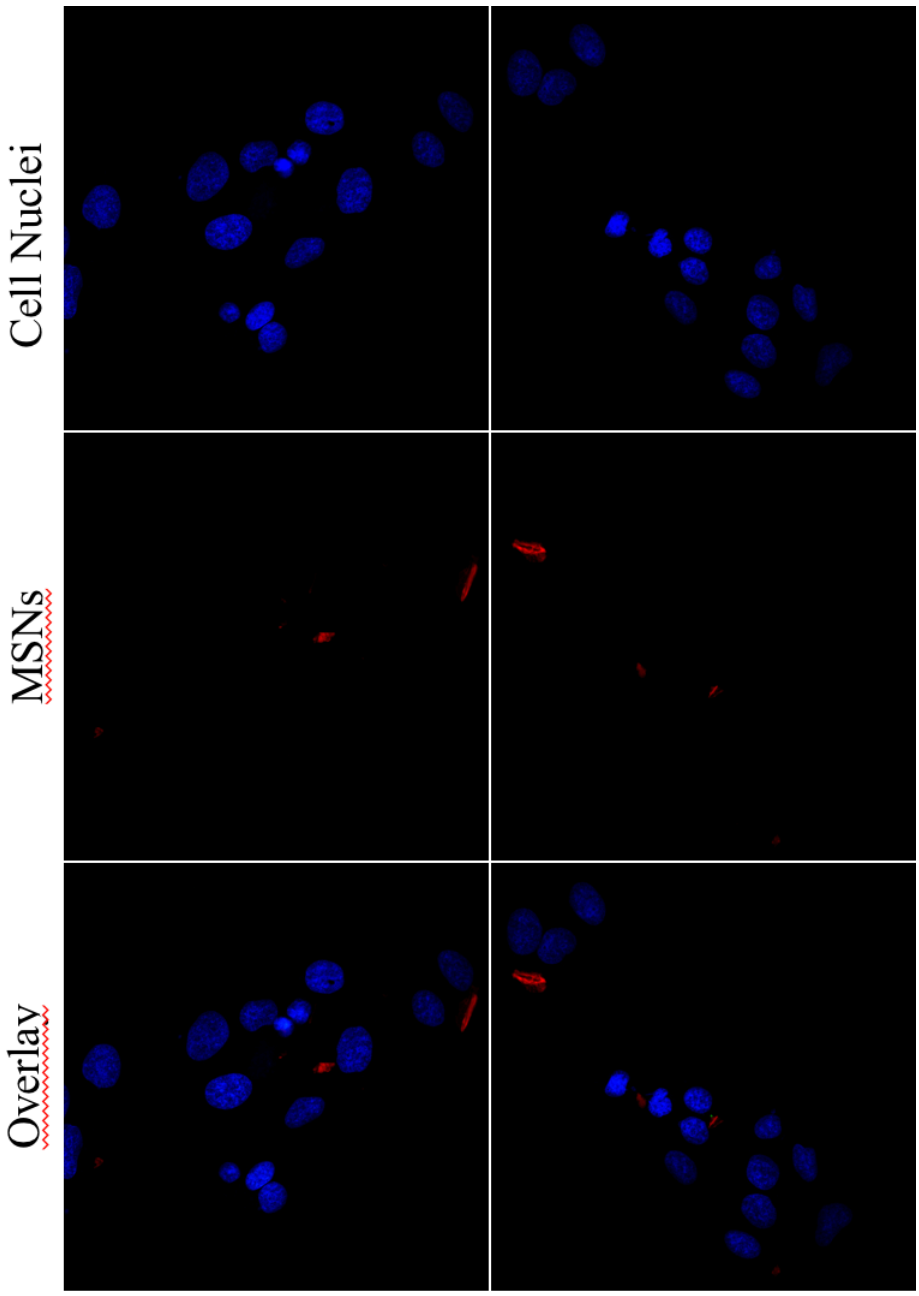

Figure 4.110: Images made with the confocal microscope of the sample with naked MSNs only.

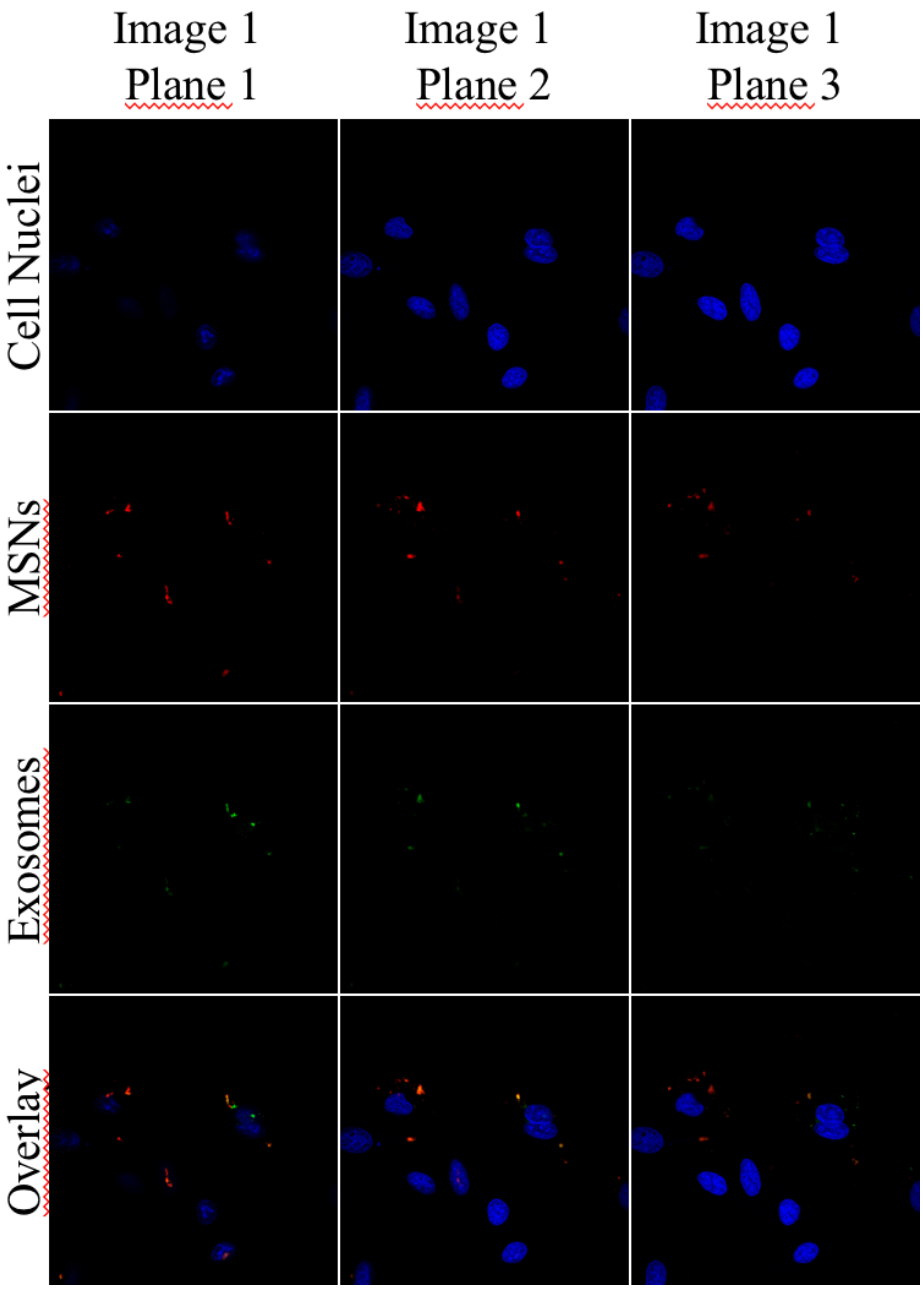

Figure 4.111: Different z-stacks of the same image recorded with the confocal microscope using MSN+EXO 12.

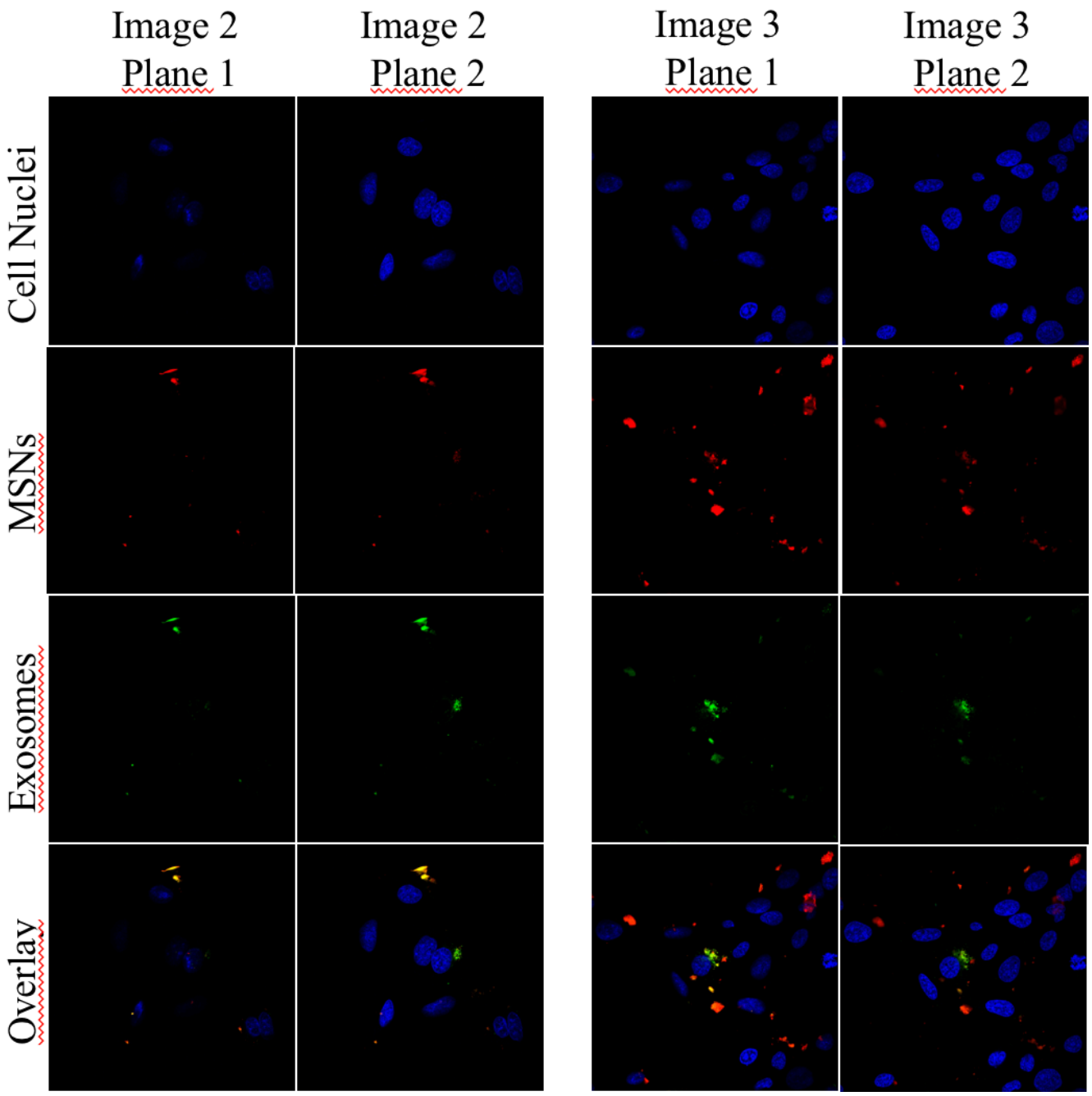

Figure 4.112 Two z-stacks of two images recorded with the confocal microscope using MSN+EXO 12.

4.6.7 Fluorescein release in transwell

Figure 4.113 represents the curve of fluorescein release from MSNs naked and covered by exosomes. The results are the opposite than the expectations. The expected result is that fluorescein release is higher in naked nanoparticles than in MSN+EXO because the coverage of exosomes retains fluorescein inside the pores. On the contrary the MSNs covered by exosomes have a higher release than the naked ones.

It is possible to make some hypothesis to explain these results that do not exclude each other. The most reliable one is that mesoporous silica are not completely covered by the lipid membrane, but there are some naked zones from where fluorescein can be released. The second hypothesis is that, since the measurement is carried out in PBS, naked MSNs create big aggregates, so the fluorescein of the inner nanoparticles is not released, instead MSNs covered by exosomes aggregate less so they have a larger contact surface with the PBS for the fluorescein release. The third one is that, since the naked MSNs undergo the same coupling process of MSN+EXO but without exosomes, the major part of the fluorescein is released during the coupling. In support of this last hypothesis there is the fact that after 48 hours, more or less, a plateau is reached, and the one of the naked MSN is significantly lower than the one of MSN+EXO. The most reliable explanation is that most of the fluorescein has been released during the coupling process.

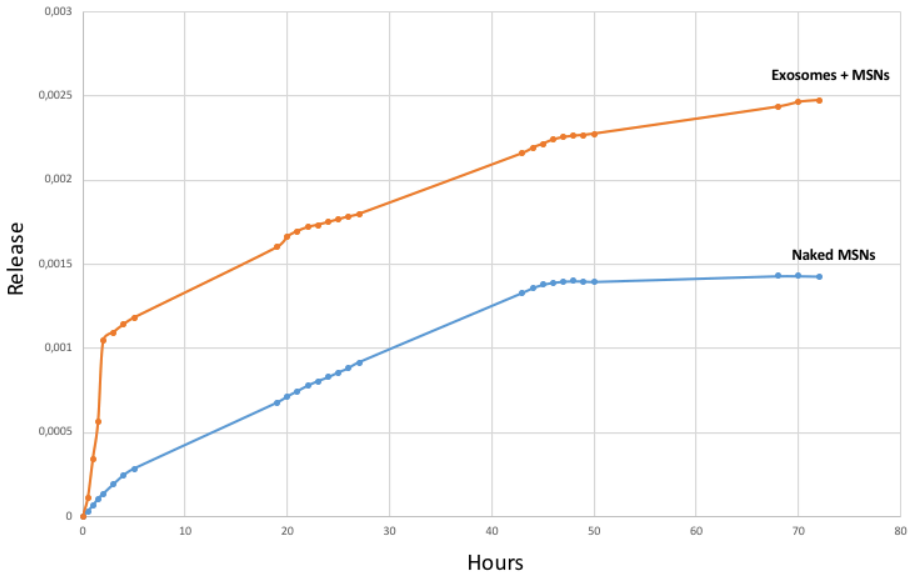

Figure 4.113: Fluorescein release

5 Conclusions

In the last decade, nanotechnologies have led great improvements to medicine, developing new therapeutic techniques, more efficient, patient specific and with less adverse side effects than the conventional methods.

An important field of application is the anticancer therapy, where current therapies are mostly ineffective, especially for metastatic tumors. The most broadly used cancer treatment is chemotherapy, which requires high doses of drugs to be administered systemically which damage not only the cancerous cells, but also the healthy ones with the related known adverse side effects.

Nanomedicine has intervened in this field to reduce the dose for an effective treatment without causing undesired effects to the rest of the body.

The nanomaterials studied in the last years for this application have led to promising results. Their limited size (< 200 nm), combined with their intrinsic chemical and physical properties, allows them to interact directly with the cells at the same scale of most biological properties, moreover, they can exploit the peculiar pathophysiological conditions of the tumors to penetrate inside the damaged cells and cause their death.

The most studied systems for cancer drug delivery are the nanocarriers, among which a prominent role is played by mesoporous silica nanoparticles. MSNs do not possess intrinsic antitumoral activities, but they are attractive for other reasons. First of all, they have a huge surface area and pore volume which can be used to store inside the nanoparticle a large amount of drug, in addition the peculiar pore size allows to load molecules with specific dimensions. Moreover, they can be easily functionalized with various and different chemical or biological components, that play the triple role to retain the drug inside the pores, facilitate the internalization in the target cells and mediate the drug release. After they have carried out their role, MSNs are degraded by the metabolism of the cells in non-toxic products.

Besides these nanocarriers, in the last decade, there has been an increasing interest in nanoparticles with intrinsic antitumor properties. They do not need a drug to exert a toxic effect in tumors, but they have an intrinsic activity or activated with external stimuli which damages the cancerous cells. Among this type of nanoparticles there is the zinc oxide. ZnO has acquired an increasing interest by the researchers due to its properties. The most important one is the capacity of ZnO nanoparticles to exert a toxic activity preferably against cancerous cells, saving the healthy ones. These nanoparticles accumulate in the tumor thanks to the EPR effect and then they act releasing ROS, with the help of an external stimulation through ultrasounds. ROS create an oxidative stress in the cell which leads to its death. ZnO nanoparticles can be functionalized to better reach their target cells reducing the circulation time in the bloodstream.

In this thesis both ZnO nanoparticles and MSNs are covered by a phospholipid bilayer, exosomes, derived from living cells. This coverage allows to increase their stability in physiological environment and drive them towards their target facilitating also the internalization in cancerous cells.

ZnO nanoparticles cover by exosomes lead to the formation of a construct called TNH (TrojaNanoHorse) which is broadly studied in this work. In particular, the coupling process between exosomes and ZnO is systematically studied by varying different parameters to obtain the best coupling

percentage possible. ZnO nanoparticles and exosomes, properly labelled with different fluorescent dyes, are analyzed through a fluorescent microscope and then the microscope software counts how many nanoparticles are colocalized with the extracellular vesicles. In addition, some TEM analysis are carried out to evaluate the morphology of the TNH, also comparing it with exosomes and nanoparticles by themselves.

Instead, the coupling with MSNs and exosomes are only evaluated with cellular tests. Tests of internalization, stability and cargoes release are carried out, leading to discordant results. The MSNs coated with exosomes seems to be internalized inside the cells, especially for those of the same lineage of exosomes extraction, but the cargoes seem not to be retained inside the pores. For what concern the stability, MSNs covered by exosomes are very stable for several days, but it has to be further investigated if this is due to the exosomes coating or only to a protein corona formed around the nanoparticles which prevents the aggregation each other.

TNH seem to be a very promising nanoconstruct for cancer treatment. This thesis work could be a starting point to further investigation on these nanoparticles about cytotoxicity, stability in physiological environment and uptake. Eventually, the outer phospholipid membrane can be functionalized with some ligands, proteins, receptors or antibodies, complementary to the overexpressed proteins on cancer cells, which are able to quickly drive the nanoparticles towards their target and facilitate the uptake into the tumor.

MSNs coated by exosomes are promising as well as the TNHs with ZnO. Further experiments to evaluate the coupling efficiency and the retain of the molecules inside the pores have to be carried out, followed by internalization and stability tests. They can be functionalized in the same way of TNH, enhancing the release of their cargo inside the cancer cells, preventing any adverse effect for healthy cells.

In conclusion, this thesis work has carried out many tests on these nanoconstructs and the results obtained are very encouraging for further studies on both ZnO and MSNs coated with exosomes.

6 Bibliography

[1] E. Pérez-Herrero and A. Fernández-Medarde, "Advanced targeted therapies in cancer: Drug nanocarriers, the future of chemotherapy," *Eur. J. Pharm. Biopharm.*, vol. 93, pp. 52–79, 2015.

[2] S. Senapati, A. K. Mahanta, S. Kumar, and P. Maiti, "Controlled drug delivery vehicles for cancer treatment and their performance," *Signal Transduct. Target. Ther.*, vol. 3, no. 1, p. 7, 2018.

[3] A. Wicki, D. Witzigmann, V. Balasubramanian, and J. Huwyler, "Nanomedicine in cancer therapy: Challenges, opportunities, and clinical applications," *J. Control. Release*, vol. 200, pp. 138–157, 2015.

[4] X. Xu, W. Ho, X. Zhang, N. Bertrand, and O. Farokhzad, "Cancer nanomedicine: From targeted delivery to combination therapy," *Trends Mol. Med.*, vol. 21, no. 4, pp. 223–232, 2015.

[5] M. Vinardell and M. Mitjans, "Antitumor Activities of Metal Oxide Nanoparticles," *Nanomaterials*, vol. 5, no. 2, pp. 1004–1021, 2015.

[6] J. W. Rasmussen, E. Martinez, P. Louka, and D. G. Wingett, "Zinc oxide nanoparticles for selective destruction of tumor cells and potential for drug delivery applications," *Expert Opin. Drug Deliv.*, vol. 7, no. 9, pp. 1063–1077, 2010.

[7] W. Song *et al.*, "Role of the dissolved zinc ion and reactive oxygen species in cytotoxicity of ZnO nanoparticles," *Toxicol. Lett.*, vol. 199, no. 3, pp. 389–397, 2010.

[8] M. Javed Akhtar, M. Ahamed, S. Kumar, M. Majeed Khan, J. Ahmad, and S. A. Alrokayan, "Zinc oxide nanoparticles selectively induce apoptosis in human cancer cells through reactive oxygen species," *Int. J. Nanomedicine*, vol. 7, pp. 845–857, 2012.

[9] Z. Li, S. Tan, S. Li, Q. Shen, and K. Wang, "Cancer drug delivery in the nano era: An overview and perspectives (Review)," *Oncol. Rep.*, vol. 38, no. 2, pp. 611–624, 2017.

[10] B. Bahrami *et al.*, "Nanoparticles and targeted drug delivery in cancer therapy," *Immunol. Lett.*, vol. 190, no. July, pp. 64–83, 2017.

[11] Y. Min, J. M. Caster, M. J. Eblan, and A. Z. Wang, "Clinical Translation of Nanomedicine," *Chem. Rev.*, vol. 115, no. 19, pp. 11147–11190, 2015.

[12] A. Nel, "Toxic Potential of Materials," *Science (80-.).*, vol. 311, no. 5726, pp. 622–627, 2007.

[13] F. Baino *et al.*, "Fe-doped sol-gel glasses and glass-ceramics for magnetic hyperthermia," *Materials (Basel).*, vol. 11, no. 1, 2018.

[14] G. Canavese *et al.*, "Nanoparticle-assisted ultrasound: A special focus on sonodynamic therapy against cancer," *Chem. Eng. J.*, vol. 340, no. January, pp. 155–172, 2018.

[15] D. Liu, F. Yang, F. Xiong, and N. Gu, "The smart drug delivery system and its clinical potential," *Theranostics*, vol. 6, no. 9, pp. 1306–1323, 2016.

[16] I. Brigger, C. Dubernet, and P. Couvreur, "Nanoparticles in cancer therapy and diagnosis," *Adv. Drug Deliv. Rev.*, vol. 64, no. SUPPL., pp. 24–36, 2012.

[17] M. P. Zaborowski, L. Balaj, X. O. Breakefield, and C. P. Lai, "Extracellular Vesicles: Composition, Biological Relevance, and Methods of Study," *Bioscience*, vol. 65, no. 8, pp. 783–797, 2015.

[18] H. Kalra, G. P. C. Drummen, and S. Mathivanan, "Focus on extracellular vesicles: Introducing the next small big thing," *Int. J. Mol. Sci.*, vol. 17, no. 2, 2016.

[19] D. S. Sutaria, M. Badawi, M. A. Phelps, and T. D. Schmittgen, "Achieving the Promise of Therapeutic Extracellular Vesicles: The Devil is in Details of Therapeutic Loading," *Pharm. Res.*, vol. 34, no. 5, pp. 1053–1066, 2017.

[20] J. R. Edgar, "Q & A : What are exosomes , exactly ?," *BMC Biol.*, pp. 1–7, 2016.

[21] C. Théry, A. Clayton, S. Amigorena, G. Raposo, and A. Clayton, "Isolation and Characterization of Exosomes from Cell Culture Supernatants," *Curr. Protoc. Cell Biol.*, vol. Chapter 3, pp. 1–29,

2006.
[22] J. Gao, “Exosomes as Novel Bio-Carriers for Gene and Drug Delivery,” vol. 521, pp. 167–175, 2017.
[23] D. Ha, N. Yang, and V. Nadithe, “Exosomes as therapeutic drug carriers and delivery vehicles across biological membranes: current perspectives and future challenges,” *Acta Pharm. Sin. B*, vol. 6, no. 4, pp. 287–296, 2016.
[24] E. V. Batrakova and M. S. Kim, “Development and regulation of exosome-based therapy products,” *Wiley Interdiscip. Rev. Nanomedicine Nanobiotechnology*, vol. 8, no. 5, pp. 744–757, 2016.
[25] J. Lï¿½tvall *et al.*, “Minimal experimental requirements for definition of extracellular vesicles and their functions: A position statement from the International Society for Extracellular Vesicles,” *J. Extracell. Vesicles*, vol. 3, no. 1, 2014.
[26] X. Luan, K. Sansanaphongpricha, I. Myers, H. Chen, H. Yuan, and D. Sun, “Engineering exosomes as refined biological nanoplatforms for drug delivery,” *Acta Pharmacol. Sin.*, vol. 38, no. 6, pp. 754–763, 2017.
[27] X. Zhuang *et al.*, “Treatment of brain inflammatory diseases by delivering exosome encapsulated anti-inflammatory drugs from the nasal region to the brain,” *Mol. Ther.*, vol. 19, no. 10, pp. 1769–1779, 2011.
[28] Y. Tian *et al.*, “A doxorubicin delivery platform using engineered natural membrane vesicle exosomes for targeted tumor therapy,” *Biomaterials*, vol. 35, no. 7, pp. 2383–2390, 2014.
[29] M. S. Kim *et al.*, “Development of exosome-encapsulated paclitaxel to overcome MDR in cancer cells,” *Nanomedicine Nanotechnology, Biol. Med.*, vol. 12, no. 3, pp. 655–664, 2016.
[30] M. Laurenti, S. Stassi, G. Canavese, and V. Cauda, “Surface Engineering of Nanostructured ZnO Surfaces,” *Adv. Mater. Interfaces*, vol. 4, no. 2, 2017.
[31] M. Niederberger, “Nonaqueous Sol – Gel Routes to Metal Oxide Nanoparticles,” *Acc. Chem. Res.*, vol. 40, no. 9, pp. 793–800, 2007.
[32] V. Cauda *et al.*, *Handbook of Nanomaterials Properties*. 2014.
[33] J. Zhou, N. Xu, and Z. L. Wang, “Dissolving behavior and stability of ZnO wires in biofluids: A study on biodegradability and biocompatibility of ZnO nanostructures,” *Adv. Mater.*, vol. 18, no. 18, pp. 2432–2435, 2006.
[34] K. A. Mccall, C.-C. Huang, and C. A. Fierke, “Zinc and Health: Current Status and Future Directions Function and Mechanism of Zinc Metalloenzymes 1,” *J. Nutr*, vol. 130, no. July, pp. 1437–1446, 2000.
[35] H. Tapiero and K. D. Tew, “Trace elements in human physiology and pathology: Zinc and metallothioneins,” *Biomed. Pharmacother.*, vol. 57, no. 9, pp. 399–411, 2003.
[36] G. Bisht and S. Rayamajhi, “ZnO Nanoparticles: A Promising Anticancer Agent,” *Nanobiomedicine*, vol. 3, p. 9, 2016.
[37] D. Beyersmann, “Homeostasis and cellular functions of zinc,” *Materwiss. Werksttech.*, vol. 33, no. 12, pp. 764–769, 2002.
[38] C. Hanley *et al.*, “Preferential killing of cancer cells and activated human T cells using ZnO nanoparticles,” *Nanotechnology*, vol. 19, no. 29, 2008.
[39] L. Racca *et al.*, “Zinc Oxide Nanostructures in Biomedicine,” *Smart Nanoparticles Biomed.*, pp. 171–187, Jan. 2018.
[40] M. Vallet-Regi, A. Rámila, R. P. Del Real, and J. Pérez-Pariente, “A new property of MCM-41: Drug delivery system,” *Chem. Mater.*, vol. 13, no. 2, pp. 308–311, 2001.
[41] M. Manzano and M. Vallet-Regí, “Mesoporous silica nanoparticles in nanomedicine applications,” *J. Mater. Sci. Mater. Med.*, vol. 29, no. 5, 2018.
[42] F. Hoffmann, M. Cornelius, J. Morell, and M. Fröba, “Silica-based mesoporous organic-inorganic

hybrid materials," *Angew. Chemie - Int. Ed.*, vol. 45, no. 20, pp. 3216–3251, 2006.
[43] M. Manzano, M. Colilla, and M. Vallet-Regí, "Drug delivery from ordered mesoporous matrices," *Expert Opin. Drug Deliv.*, vol. 6, no. 12, pp. 1383–1400, 2009.
[44] A. Baeza, M. Manzano, M. Colilla, and M. Vallet-Regí, "Recent advances in mesoporous silica nanoparticles for antitumor therapy: Our contribution," *Biomater. Sci.*, vol. 4, no. 5, pp. 803–813, 2016.
[45] M. Manzano and M. Vallet-Regí, "New developments in ordered mesoporous materials for drug delivery," *J. Mater. Chem.*, vol. 20, no. 27, pp. 5593–5604, 2010.
[46] Y. Zhao, X. Sun, G. Zhang, B. G. Trewyn, I. I. Slowing, and V. S. Y. Lin, "Interaction of mesoporous silica nanoparticles with human red blood cell membranes: Size and surface effects," *ACS Nano*, vol. 5, no. 2, pp. 1366–1375, 2011.
[47] B. Carr and M. Wright, "Nanoparticle Tracking Analysis Nanoparticle Tracking Analysis," vol. 44, no. 0, pp. 3–5, 2012.
[48] B. Dumontel *et al.*, "Enhanced biostability and cellular uptake of zinc oxide nanocrystals shielded with a phospholipid bilayer," *J. Mater. Chem. B*, vol. 5, no. 44, pp. 8799–8813, 2017.
[49] J. L. Paris, P. D. La Torre, M. Manzano, M. V. Cabañas, A. I. Flores, and M. Vallet-Regí, "Decidua-derived mesenchymal stem cells as carriers of mesoporous silica nanoparticles. in vitro and in vivo evaluation on mammary tumors," *Acta Biomater.*, vol. 33, pp. 275–282, 2016.
[50] A. Baeza, A. Noureddine, P. N. Durfee, K. S. Butler, J. O. Agola, and C. Je, "Multifunctional Protocells for Enhanced Penetration in 3D Extracellular Tumoral Matrices," 2018.
[51] K. Zeng *et al.*, "Lipid-coated ZnO nanoparticles as lymphatic-targeted drug carriers: study on cell-specific toxicity in vitro and lymphatic targeting in vivo," *J. Mater. Chem. B*, vol. 3, no. 26, pp. 5249–5260, 2015.
[52] M. Villegas *et al.*, "Lysine-Grafted MCM-41 Silica as an Antibacterial Biomaterial," *Bioengineering*, vol. 4, no. 4, p. 80, 2017.